UNIVERSITÀ degli STUDI di CATANIA
Dipartimento di Agricoltura, Alimentazione e Ambiente
Di3A

UNIVERSITÀ DEGLI STUDI DI CATANIA

Agricultural, Food and Environmental Science

XXXVIII Cycle

Exploitation of probiotic strains with targeting cholesterol reduction for the formulation of functional foods

Gianluigi Agolino

Advisor:
Prof. Cinzia Lucia Randazzo

Co-advisor:
Prof. Cinzia Caggia

Coordinator:
Prof. Antonio Biondi

Ph. D. attended during 2022/2025

Acknowledgments

This PhD thesis is the results of many collaborations, for which I will always be grateful and proud. Thanks for your constant support and encouragement.
I would like to express my sincerely thanks to my supervisor Prof. Cinzia Randazzo, for giving me this incredible opportunity to undertake my PhD. I am grateful for believing in this project, deepen my knowledge of the subject, and gain incredible experiences throughout my PhD journey.
Thanks to my co-advisor Prof. Cinzia Caggia for the support and availability during this work.
Many thanks to my PhD coordinator, Prof. Antonio Biondi, for his guidance over these three years and for enriching my path with meaningful training experiences, and workshops.

I extended my warmly thank to all the people, past and present, who have worked in the Food Microbiology laboratory, for their fundamental role and constant presence during these four years.
I would like to sincerely thanks Alessandra for being a supportive guide and constant point of reference for my colleagues and me in laboratory. Thanks to my outstanding colleagues (as well as friends) Georgiana, Irene and Gloria. I am very grateful to share this PhD experience together, characterized by work, mutual support, and also by funny moments. Thanks also to all my colleagues which I share this path during the years. A special mention to Amanda, thanks to be a true guide for me everyday (both professionally and personally), and to believe in me. I have learned a lot from here and every suggestion and help is fundamental when we work together. I am grateful to consider her not only a colleague but also a real friend.

During my experiences outside the laboratory, I have met and worked with many people, to whom I am truly thankful. I would like to express

my gratitude to Prof. Lisa Solieri for hosting me in her laboratory at the University of Modena and Reggio Emilia. Thanks to her to be essential in my professional growth, by sharing with me scientific knowledge and for continuous support and help for the realization of my goals. I would like to sincerely thank my special colleagues Chiara and Marianna for the opportunity to work and spend time together, as well as all the colleagues at 'Kennedy' for the moments we enjoyed in Reggio Emilia. I would also thank Prof. Davide Tagliazucchi and Dr. Alice Cattivelli of the University of Modena and Reggio Emilia for their collaboration and contributing to the experimental analyses and articles drafting.

I would like to thank Prof. Reetta Satokari for welcoming in her laboratory at the University of Helsinki and giving me the opportunity continue to my research through the acquisition of new techniques and gaining different perspective of my project. Thanks also to Dr. Kaisa Hiippala for her suggestions and for supporting me during laboratory activities.

Index

Thesis outline **29**

Chapter 1 ..... **1**

1 Bile salt hydrolase: The complexity behind its mechanisms in relation to lowering-cholesterol lactobacilli probiotics 1

Graphical abstract **2**

Abstract **2**

1.1 Introduction **4**

1.2 From primary to secondary bile acids: An overview 8

1.3 From primary to secondary bile acids: An overview 14

1.3.1 BSH and host cholesterol homeostasis 15

1.3.2 BSH and gut bacteria homeostasis 19

1.4 From BSH to hypocholesterolemic action through probiotics **21**

1.4.1 *Lactiplantibacillus plantarum* 30

1.4.2 *Lacticaseibacillus rhamnosus* and *Lacticaseibacillus casei* 31

1.4.3 *Limosilactobacillus fermentum* and *Limosilactobacillus reuteri* 32

1.4.4 *Lactobacillus acidophilus* 34

1.4.5 *Lactobacillus johnsonii* 36

1.5 Lactobacilli *bsh* genes distribution and relationship with cholesterol-lowering activity **37**

1.6 Conclusions and future perspective **40**

Author contributions **41**

Declaration of competing interest **41**

References **41**

Chapter 2 ..... **42**

2 Genomic mining and characterization of two novel *Lacticaseibacillus rhamnosus* probiotic candidates with Bile salt hydrolase activity **42**

Graphical abstract **43**

Abstract **43**

2.1 Introduction **45**

2.2 Material and Methods **48**

2.2.1 Reagents 48

2.2.2 Bacterial strains and culture conditions 48

2.2.3 Genomic sequencing, annotation, and comparative genome analysis 48

2.2.4 Taxonomic identification and phylogenomics 49

2.2.5 Safety and genome stability analyses 50

2.2.6 *In silico* analysis of bsh gene candidates 51

2.2.7 Penicillin V susceptibility 82

2.2.8 Growth curve assay 82

2.2.9 RNA extraction, retro-transcription, and gene expression analysis 83

2.2.10 Semi-quantitative analysis in UHPLC/HR-MS 87

2.2.11 Statistical analysis 88

2.3 Results **89**

2.3.1 Genome sequencing 89

2.3.2 Strain identification 91

2.3.3 Annotation and comparative genome analysis 96

2.3.4 Safety assessment 102

2.3.5 Genome stability 102

2.3.6 Identification and phylogenetic analysis of *bsh* gene candidates 114

2.3.7 Penicillin V susceptibility results 120

2.3.8 Growth curve, bile salt deconjugation activity, and *bsh* gene expression analysis in presence of BAs mixture 121

2.4 Discussion 126

2.5 Conclusions 134

Author contributions 136

Funding 136

Data availability statement 136

Acknowledgments 136

References 137

***Chapter 3* 120**

3 Bile salt hydrolase activity in the food-derived strain *Levilactobacillus brevis* M3R3: genomic and functional characterization 120

Graphical abstract 121

Abstract 121

3.1 Introduction 123

3.2 Material and Methods 125

3.2.1 Bacterial strain and culture conditions 125

3.2.2 Bile salt tolerance assay 126

3.2.3 Growth curve assay 126

3.2.4 UHPLC/HR-MS analysis 127

3.2.5 Genome sequencing 128

3.2.6 Gene prediction and functional annotation 129

3.2.7 Taxonomic identification and comparative genomics 129

3.2.8 Safety, genome stability, and search for probiotic-related traits 156

3.2.9 *In silico* analysis bsh gene candidates 157

3.2.10 RT-PCR assay 157

3.2.11 Penicillin V MIC determination 159

3.2.12 Statistical analysis 159

3.3 Results and Discussion 160

3.3.1 Inhibitory effect of individual bile salts 160
3.3.2 Growth kinetics and deconjugation activity under exposure to individual conjugated bile salts 162
3.3.3 Growth kinetics and deconjugation activity under bile salt mixture exposure 167
3.3.4 General genomic features and taxonomic evaluation 171
3.3.5 Comparative genomics 183
3.3.6 Biosafety Assesment and genome stability evaluation 187
3.3.7 Search for probiotic-related functional traits 192
3.3.8 Identification of *bsh* gene candidates and RT-PCR assay 196
3.3.9 Antibiotic susceptibility 200

3.4 Conclusions 201

Author contributions 203

Funding 203

Data availability 203

Conflict of interest 203

References 204

***Chapter 4* 217**

4 Gastrointestinal survivability of a BSH-positive *Lacticaseibacillus rhamnosus* VB4 strain and its effects on bile acid deconjugation in a dynamic *in vitro* gut model 217

Graphical abstract 218

Abstract 218

4.1 Introduction 220

4.2 Material and Methods 222
4.2.1 BSH-positive *L. rhamnosus* VB4 strain 222
4.2.2 SHIME® Experiment set-up 222

4.2.3 Detection of viability by culture-dependent method 226
4.2.4 Detection gene expression of BSH-positive VB4 strain 227
4.2.5 Detection of BAs from SHIME samples..... 229
4.2.6 Statistical analysis 230
4.3 Results 231
4.3.1 *L. rhamnosus* VB4 strain viability in stomach/small intestine 231
4.3.2 *Bsh* gene detection through qPCR analysis..... 233
4.3.3 Semi-quantitative analysis of BAs in small intestine and colon 235
4.4 Discussion 240
4.5 Conclusions 243
Author contributions 245
Funding 245
Institutional review board statement 245
Acknowledgment 245
Conflict of interest 246
References 246
***Chapter 5* 251**
5 Probiotic strains with Bile Salt Hydrolase activity reduce micellar cholesterol uptake in Caco-2 cells 251
Graphical abstract 252
Abstract 252
5.1 Introduction 254
5.2 Material and Methods 256
5.2.1 Bacterial strains and culture conditions 256
5.2.2 Lactobacilli *in vitro* cholesterol assimilation activity

257
5.2.3 Caco-2 cell cultures 258
5.2.4 Adhesion ability test to Caco-2 cell 258
5.2.5 Preparation of cholesterol micellar solution 259
5.2.6 Caco-2 cell cholesterol uptake assay 260
5.2.7 Statistical analysis 261
5.3 Results 261
5.3.1 Cholesterol assimilation capability of lactobacilli strains 261
5.3.2 Adhesion to intestinal epithelial cells Caco-2 262
5.3.3 Cholesterol uptake by Caco-2 cells 263
5.4 Discussion 265
5.5 Conclusions 267
References 268
***Chapter 6* 273**
6 General discussion and conclusions 273
References 279
7 Annexes: Scientific Curriculum 283
7.1 Research and Professional Experience 283
7.2 Education and Professional qualifications 284
7.3 Membership and Ids 284
7.4 Scientific contributions 285
7.5 Conference proceedings 286
7.6 Training in national or international universities and/or research institutions 288
7.7 Attended Workshop, Courses, Seminars 289
7.7.1 Attended Workshop 289
7.7.2 Attended Courses 289
7.7.3 Attended Seminars 290

7.8 Teaching activities 291

Table Index

Table 1.1 - Overview of main positive and negative effects by microbial BSH activity on host health 18
Table 1.2 - Overview of the main BSH-positive lactobacilli strains with potential cholesterol-lowering activity. 22
Table 2.1 - List of proteins as query for BLASTp search of *bsh* genes in VB4 and VB1 genomes. 81
Table 2.2 - Primer used in this study. 86
Table 2.3 - General features of *L. rhamnosus* VB4 and VB1 genome assemblies. 91
Table 2.4 - Digital DNA-DNA Hybridization (dDDH) values of strains VB4 and VB1 compared with other *Lacticaseibacillus* strain. 94
Table 2.5 - Contigs matching prophage regions and predominant phage sequences predicted in VB4 and VB1 genomes. 104
Table 2.6 - *Cas* gene in VB4 genome. Contigs without *cas* gene were omitted for brevity. 107
Table 2.7 - CRISPR regions in VB4 genome, Contigs without CRISPR regions were omitted for brevity. 108
Table 2.8 - *Cas* genes in VB1 genome. Contigs without *cas* gene were omitted for brevity. 110
Table 2.9 - CRISPR regions in VB1 genome. Contigs without CRISPR regions were omitted for brevity. 112
Table 2.10 - Genome assemblies used for ANI matrix calculation. 116
Table 3.1 - *Levilactobacillus brevis* reference genome used in this study. 132
Table 3.2 - Primer used in this study. 158
Table 3.3 - Effects of different concentrations of individual BSs on the growth of *Levilactobacillus brevis* M3R3 strain. Log_{10} CFU/mL values were measured after 24 h of exposition to conjugated BSs relative to the control (MRS without BSs). Data are the mean of at least three replicates. Statistically significant differences compared

with the control were determined by one-way ANOVA (p<0.05) and are indicated with different letters. Abbreviations: TDCA (taurodeoxycholic acid), TCA (taurocholic acid), GDCA (glycodeoxycholic acid), GCA (glycocholic acid), and na, not applicable. 161
Table 3.4 – Summary of the best models used to fit growth curves of *Levilactobacillus brevis* M3R3 strain. Best-fit models were choosen using AIC (implementing in Grofit)..... 166
Table 3.5 - Assembly and annotation of *Levilactobacillus brevis* M3R3 genome. 172
Table 3.6 - Overview of *cas* gene clusters and CRISPR regions in *Levilactobacillus brevis* M3R3 genome..... 175
Table 3.7 – Matrix of ANIm values. 177
Table 3.8 - Digital DNA-DNA Hybridization (dDDH) values of strain M3R3 compared with other species, as calculated with Formula 2 (identities / HSP length). 181
Table 3.9 - Biosafety evaluations implemented in ProbioMinServer. 189
Table 3.10 - Putative prophage regions predicted in *Levilactobacillus brevis* M3R3 using Phigaro. 190
Table 3.11 - Prediction of metabolite biosynthetic gene clusters (BGCs) carried out in *Levilactobacillus brevis* M3R3 with antiSMASH. 195
Table 4.1 - Conjugated bile acids (BAs) detection in control and VB4-inoculated samples, under upper GIT SHIME® system. Glycocholic acid (GDCA), taurocholic acid (TCA), glycodeoxycholic acid (GDCA), and taurodeoxycholic acid (TDCA) in dudenum, jejunum, ileum, and colon (T_{16h} and T_{24h}). reported values are expressed as AUP ± SD..... 239

Figure Index

Figure 1.1 - Main molecular mechanisms underpinning cholesterol homeostasis control by gut microbiota. (A) Short chain fatty acids (SCFAs)-mediated inhibition of fat storage and cholesterol biosynthesis. SCFAs acts as ligands that bind to activate peroxisome proliferation-activated receptors (PPARs), which controls the transcription and translate of angiopoietin-like protein 4 and, ultimately, reduces fat storage. Butyrate inhibits the activity of 3-hydroxy-3-methyl-glutaryl-conezyme A (HMG-CoA) reductase, the rate-limiting step in the mevalonate pathways. (B) Assimilation of cholesterol molecule on microbial cell surface. (C) Conversion of cholesterol to coprostanol and its excretion by stool. (D) Increase of secondary bile acids (BAs) pool via bile salt hydrolase (BSH) activity. 8

Figure 1.2 - Centrality of BAs metabolism in gastro-intestinal tract and enterohepatic circulation. Bile acids (BAs) (cholic acid and chenodeoxycholic acid) are synthesized from cholesterol in the liver via classical pathway or by the alternative pathway and then conjugated with glycine and/or taurine (*de novo* synthesis). Conjugated BAs. In large intestine, microbial bile acid-inducible (bai) operon converted cholic and chenodeoxycholic acid in deoxycholic and lithocholic acid. Approximately 95% of BAs are resorbed and transported in liver via enterohepatic circulation, some of these directly converted into intestine in conjugated BAs, and the remaining part excreted by feces. 11

Figure 3.3 - Bile Salt Hydrolase (BSH) structure. The αββα-fold core structure of microbial choloylglycine hydrolase and catalytic site (Cys2). 15

Figure 4.4 - Relationship between diet, the intestinal microbiota, BSH activity, and probiotic formulations. Effectiveness of BSH-positive probiotics in counteracting hypercholesterolemia depends on

quadrangular relationship between diet, intestinal microbiome, chosen probiotic bacteria, and pharmacological parameters (kind of probiotic-driving formulation, dose, duration of the treatment). Abbreviation: TC, total cholesterol; CVD, cardio-vascular disease. 30
Figure 2.1 - Circular graphical representation of the *Lacticaseibacillus rhamnosus* strains VB4 (A) and VB1 (B) contigs obtained using Proksee (https://proksee.ca; accessed on 13 January 2024). The black central circle shows the scale expressed in megabases. Moving inward, the two outer violet circles show forward- and reverse-strand CDSs, respectively. Some genes are shown on the outer violet circle with the Proksee's default. In CDSs circles, tRNAs are shown as orange arrows, rRNAs are represented as light blue arrows, tmRNA is displayed as a red arrow, and CRISPR sequences are reported as light green arrows adjacent to each other. The next circle shows the GC content and GC skew as dark blue and dark green and pink, respectively. The represented genomic order of contigs is arbitrary. 90
Figure 2.2 - Phylogenetic analysis of 16S rRNA gene sequences of *Lacticaseibacillus* species. The tree was inferred using the Neighbor-Joining method (Saitou & Nei, 1987) and the Kimura's two-parameter model Kimura, 1980) with Mega XI software (Tamura et al., 2021). Strains VB4 and VB1 are shown in bold, while the sequences of reference strains were from the NCBI RefSeq database. A discrete Gamma distribution (shape parameter = 5) was used to model evolutionary rate variation among sites. Bootstrap values are indicated at branch points based on 1,000 replications. The trees are drawn in scale, with branch length measured in the number of substitutions per site. Bar represents 0.01 substitutions per nucleotide position. The tree was rooted using the branch leading to four outgroup species *E. faecalis*, *W. coagulans*, *B. subtilis*, and *B. vallismortis*. The tree was visualized with iTOL (Letunic & Bork, 2019)..... 92
Figure 2.3 - Heatmap of the average nucleotide identity (ANI) values of 28 *Lacticaseibacillus* strains. The colored squares, designate the strain relatedness based on their ANI values (red color > the threshold

value of 95%; dark and light blue < the threshold values of 95%. .. 96
Figure 2.4 - Distribution of KEGG orthology (KO) categories of identified protein-coding genes in the *Lacticaseibacillus rhamnosus* VB4 (A) and VB1 (B) genomes, respectively..... 99
Figure 2.5 - Pan-genome analysis of *Lacticaseibacillus rhamnosus* strains VB4 and VB1. The strains were compared to *L. rhamnosus* strains Lc705 (ASM2652), GR-1 (ASM2466559), and GG (ASM2847508) using PanExplorer (last accessed on 15 May 2024). (A) Distribution of COG functional groups in VB4 and VB1 genomes. (B) Core-genes proportion and strain-specific genes; (C) distribution of strain-specific genes according to the *L. rhamnosus* pan-genome analysis; and (D) distance tree generated by hierarchical clustering from presence/absence binary matrix of accessory gene clusters among the members of *L rhamnosus* dataset. Genes are colored if present in the genome..... 100
Figure 2.6 - Number of unique genes in *Lacticaseibacillus rhamnosus* strains VB4 and VB1 assigned in COG functional categories. COGs of the *L. rhamnosus* VB4 strain are represented as green bars whereas COGs if the *L. rhamnosus* VB1 strain are displayed as pink bars. COG categories are abbreviated as follows: J; translation, ribosomal structure, and biogenesis; K, transcription; L, replication recombination, and repair; D, cell cycle control, cell division, and chromosome partitioning; V, defense mechanisms; T, signal transduction mechanisms; M, cell wall/membrane/envelop biogenesis; U, intracellular trafficking and vesicular transport; O, post-translational modification, protein turnover, and chaperons; C, transport and metabolism; F, nucleotide transport and metabolism; H, coenzyme transport and metabolism; I, lipid transport and metabolism; P, inorganic transport and metabolism; R, general functional prediction only; and S, function unknown. 101
Figure 2.7 - Organization of the main prophage regions in VB4 (A) and VB1 (A) genome. 103
Figure 2.8 - Distribution of mobile genetic elements in *Lacticaseibacillus rhamnosus* VB4 (A) and VB1 (B) genomes. Major

categories considered were IE, integration/excision; RRR, replication/recombination/repair; P, phage; STD, stability/transfer/defense; and T, transfer. 105
Figure 2.9 - Multiple amino acid sequence alignment of 10 BSHs proteins selected from Table 2.10. 115
Figure 2.10 - Phylogenetic tree of BSH and PVA proteins. The alignments of 96 bacterial proteins were performed with NCBI COBALT (Grishin, 1995; Kahm et al., 2010). The resulting phylogeny was visualized as a phylogenetic tree using iTOL (Letunic & Bork, 2019). Red labels indicate PVA proteins. 120
Figure 2.11 - Growth curves of VB4 and VB1 strains in presence of 1% (w/v) BAs mixture (green) compared with control growth conditions (MRS medium; blue). Growth was monitored over the time as mean of OD_{600nm} values in three different biological replicates. Bars (when visible) indicate standard deviation (SD) values of OD_{600nm} measurements. The curves were fitted by non-linear Gompertz model and plotted using v.8.00 software (San Diego, CA, USA, https://www.graphpad.com/). 122
Figure 2.12 - Growth and deconjugation ability of *Lacticaseibacillus rhamnosus* VB4 and VB1 strains in the presence of a BAs mixture (Oxgall). Kinetic parameters lag phase (λ, expressed in h) (A), maximum growth rate (μ, expressed as h^{-1}) (B), and maximum cell density (A expressed as OD_{600nm}) (C) were computed in MRS and MRS supplemented with BAs 1% (*w/v*) by Grofit package (version 1.1.1-1). Residual unconjugated percentages (%) of GCA, GDCA, GCDCA, TCA, TDCA, and TCDCA were estimated in supernatants collected during late stationary phase (D). Significant differences were calculated with two-way ANOVA and indicated with asterisks, as follows: ***, $p \leq 0.001$; **** $p \leq 0.0001$ (two-way ANOVA). Plotted with GraphPad Prism v.8.00 software (San Diego, CA, USA). Abbreviations: GCA, glycocholic acid; GDCA, glycodeoxycholic acid; GCDCA, glycochenoceoxycholic acid; TCA, taurocholic acid; TDCA, taurodeoxycholic acid, and TCDCA, taurochenodeoxycholic acid. 123

Figure 2.13 - End-point RT-PCR targeting *bsh* gene in BAs-stressed (MRS medium supplemented with 1% (w/v) BAs) and non-stressed (MRS medium) stationary cells of *Lacticaseibacillus rhamnosus* VB4 (A) and VB1 (B), respectively. Three independent replicates, numbered from R1 to R3, were used. +/- RT indicates addition of reverse transcriptase to the cDNA synthesis reaction. The expected PCR product length was established for each amplicon by using 100 bp DNA Gene Ruler Plus as molecular weight marker. For each RT-PCR reaction gDNA was used as positive control. 16S rRNA gene PCR reactions used as control were omitted. Abbreviations: M, molecular-weight size marker; NTC, negative control. 125
Figure 2.14 - Expression profile of *bsh* gene in *Lacticaseibacillus rhamnosus* VB4 and VB1 in MRS (control condition) and MRS supplemented with 1% (w/v) BAs mixture. Significant differences were calculated with a Student's *t*-test and indicated with asterisks, as follow: **** $p \leq 0.0001$. The bar graph was plotted with GraphPad Prism v.8.00 software (San Diego, CA, USA). 126
Figure 3.1 - Representative growth kinetics of *Levilactobacillus brevis* strain M3R3 in MRS medium supplemented with 1.0% (w/v) of each individual bile salt (BS), compared with the control condition (MRS only). Optical density at 600 nm (OD_{600}) was recorded over time. Each condition was tested in three independent biological replicates. Growth curves were modeled using the Grofit package in the R environment, applying both parametric (black) and spline-based (red) methods. Black and red dotted lines indicate the intercepts corresponding to the maximum growth rate (h^{-1}) calculated by the parametric and spline-based approaches, respectively. The vertical green line marks the sampling point used for supernatant collection for UHPLC/HR-MS analysis. Abbreviations: TDCA, taurodeoxycholic acid; TCA, taurocholic acid; GDCA, glycodeoxycholic acid; GCA, glycocholic acid. 164
Figure 3.2 - Growth kinetics parameters and bile salts deconjugation ability of *Levilactobacillus brevis* M3R3 in the presence of 1.0 % (w/v) of individual bile salts (TDCA, TCA, GDCA and GCA)

compared with the control condition (MRS medium). Kinetics parameters, such as (A) maximum growth rate (μ, h^{-1}), (B) lag phase (λ, h), and (C) maximum cell density (A, OD_{600nm}), were estimated using Grofit package. (D) Deconjugation ability expressed as the percentage of residual conjugated bile salt (TDCA, TCA, GDCA, or GCA) quantified in cell-free supernatants collected during the late stationary phase. Significant differences were calculated with one-way ANOVA and indicated with different letters. Graphs are visualized with GraphPad Prism v10.3.1 software (San Diego, CA, USA). Abbreviations: TDCA, taurodeoxycholic acid; TCA, taurocholic acid; GDCA, glycodeoxycholic acid; and GCA, glycocholic acid. 165
Figure 3.3 - Representative growth curves of *Levilactobacillus brevis* strain M3R3 in presence of 1.0 % (*w/v*) bile salts (BSs) mixture (B) compared with the control condition (A; MRS medium). Optical density at 600 nm (OD_{600}) was recorded over time. Each condition was tested in three independent biological replicates. Growth curves were modeled using the Grofit package in the R environment, applying both parametric (black) and spline-based (red) methods. Black and red dotted lines indicate the intercepts corresponding to the maximum growth rate (h^{-1}) calculated by the parametric and spline-based approaches, respectively. The vertical green line marks the sampling point used for supernatant and cells collection for UHPLC/HR-MS analysis and RNA extraction, respectively. 168
Figure 3.4 - Growth kinetics parameters and bile salts deconjugation ability of *Levilactobacillus brevis* M3R3 in the presence of 1.0 % (w/v) of bile salts (BSs) mixture compared with the control condition (MRS medium). Kinetics parameters, such as (A) maximum growth rate (μ, h^{-1}), (B) lag phase (λ, h), and (C) maximum cell density (A, OD_{600nm}), were estimated using Grofit package. Significant differences in growth kinetics parameters were calculated between control and stress conditions with a two-tailed *t*-test and indicated with different letters, $p \leq 0.01$. (d) Deconjugation ability expressed as the percentage of residual conjugated bile salt (TDCA, TCA, GDCA, or GCA) quantified in cell-free supernatants collected during the late

stationary phase. Significant differences among residual compound percentages were calculated with one-way ANOVA and indicated with different letters. Graphs are visualized with GraphPad Prism v10.3.1 software (San Diego, CA, USA). Abbreviations: TCDCA, taurochenodeoxycholic acid TDCA, taurodeoxycholic acid; TCA, taurocholic acid; GCDCA, glycochenodeoxycholic acid; GDCA, glycodeoxycholic acid; and GCA, glycocholic acid. 170
Figure 3.5 - Circular graphical representations of the *Levilactobacillus brevis* M3R3 strain contigs obtained using Proksee (https://proksee.ca; last accessed 13 February 2025). Starting from the outermost ring: Ring 1: PHASTEST, Ring 2: Phigaro, Ring 3: CRISPRCasFinder Annotation (+), Ring 4: Bakta Annotation (+), Ring 5: Prokka Annotation (+), Ring 6: mobileOG-db Annotation (+), Ring 7: CARD RGI Results (+), Rings 8 to 10: ORFs (+3,+2,+1), Ring 11: Features (+), Backbone (Contigs), Ring 13: Features (-), Rings 14 to 16: ORFs (-1,-2,-3), Ring 17: GC Content, Ring 18: GC Skew, Ring 19: CARD RGI Results (-), Ring 20: mobileOG-db Annotation (-), Ring 21: Prokka Annotation (-), Ring 22: Bakta Annotation (-), Ring 23: CRISPRCasFinder Annotation (-)..... 172
Figure 3.6 - Distribution of KEGG orthology (KO) categories of identified protein-coding genes in the *Levilactobacillus brevis* M3R3 genome. 174
Figure 3.7 - Phylogenetic analyses inferring the taxonomical position of *L. brevis* M3R3. (A) 16S rRNA gene-based phylogeny constructed using Neighbor-Joining (NJ) algorithm. (B) Phylogenomic tree constructed using GBDP distances derived from the genomes of TYGS type strains most closely related to L. brevis M3R3..... 176
Figure 3.8 - Maximum-likelihood phylogenetic tree of 175 *Levilactobacillus brevis* strains built on core SNP alignments (3059 SNP found with snippy multi v4.6.0). Branch colors indicate isolation sources: yellow, fermented vegetables; light blue, animal and human gut; red, alcoholic fermented beverages; green, dairy products; grey, unknown, respectively. Clusters A, B, and C are indicated. The tree was visualized using iTOL v7 (Letunic & Bork, 2019). 185

Figure 3.9 - Comparative genomic analysis of *Levilactobacillus brevis* M3R3 and nine conspecific strains. (A) Upset plot showing shared orthogroups of *L. brevis* strains (n=10). (B) Percentage distribution of core, dispensable, singleton genes. (C) KEGG Orthology (KO) annotation of singletons across the ten *L. brevis* genomes. 186
Figure 3.10 - Distribution of mobile genetic elements in *Levilactobacillus brevis* M3R3 genome. Major categories considered were IE, integration/excision; RRR, replication/recombination/repair; P, phage; STD, stability/transfer/defense; and T, transfer. 192
Figure 3.12 - Biosynthetic gene clusters (BGCs) in the genome of *Levilactobacillus brevis* M3R3 predicted by antiSMASH. Candidate clusters were stringently filtered and grouped into families. Arrows are color-coded according to the enzyme family of the predicted product, with gene annotations shown below each arrow. One candidate cluster overlapped with or showed similarity to ribosomally synthesized and post-translationally modified peptide (RiPP) BGCs. Representative clusters included a type III polyketide synthase (T3PKS) region, a terpene precursor region, and a class IV lanthipeptide cluster. 194
Figure 3.13 - Fast minimum evolution tree of 79 putative linear amide C-N hydrolase proteins from *Levilacactobacillus brevis*. Seventy-six linear amide C-N hydrolase proteins of *L. brevis* were retrieved from, whereas three linear amide C-N hydrolase proteins (in bold) were found in *L. brevis* M3R3 genome. Seven PVA (red) and one BSH (purple) proteins were used as control. Sequences were aligned using the COBALT tool with default parameters, while Grishin model was used to infer evolutionary distances. Labels represent protein ID. Clusters I, II, and III are depicted in green, blue, and yellow, respectively. The image was created using the interactive tree of life (iTOL) (Letunic & Bork, 2019). 199
Figure 3.14 - RT-PCR assay targeting the *pva*, *bsh_2A*, and *bsh_3A* genes in *Levilactobacillus brevis* M3R3 strain cells grown on MRS medium supplemented with 1% (*w/v*) BSs mixtures. MRS medium

without any supplementation was used as control. The figure depicts amplified cDNAs, gDNA amplification was used as a positive PCR control. Abbreviations—M: molecular weight marker; N: negative control..... 200
Figure 4.1 - Overview of the SHIME® system setup. The stomach/small intestine (St/SI) reactor connected in series to the colon (C) reactor. The unit was designed for both VB4-inoculated samples (left) and control samples (right). In addition, a workflow is shown describing the incubation steps and times performed and the collection of intestinal and colon fraction samples. St/SI, stomach/small intestine; VB4, *L. rhamnosus* VB4 strain. 226
Figure 4.2 - Survival of *Lacticaseibacillus rhamnosus* VB4 in Stomach/Small Intestine compartments. Viable counts were enumerated on agar plate. Data are expressed as average ± SD of the three independent biological replicates. Results are expressed as mean ± SD of $\log_{10}$ CFU/mL. Data were analysed using ANOVA One-way with Tukey's post-hoc test. The horizontal red line indicates the starting cell density of the VB4 strain (9 $\log_{10}$ unit). $^{a–b}$ Different superscript letters indicate significant differences within samples at different GI fractions (at $p < 0.05$). 232
Figure 4.3 - Transcriptional profiles of *bsh* and *HKG* genes in SHIME® samples. (A) Gene expression of *bsh* and *HKG* genes in VB4-inoculated sample, along upper GIT. (B) *bsh* gene expression in colonic fraction, at 0, 16 and 24 sampling times, of VB4-inoculated and control samples. (C) *HKG* gene expression in colonic fraction, at 0, 16 and 24 sampling times, of VB4-inoculated and control samples. Results are expressed as mean ± SD of $\log_{10}$ copies qPCR. Data were analysed using ANOVA One-way with Tukey's post-hoc test. $^{a–c}$ The different superscript letters indicate significant differences within the same sample over time at $p < 0.05$. $^{A–B}$ The different superscript letters within the sampling time indicate significant differences between the two treated and control theses at $p < 0.05$. *Bsh*, bile salt hydrolase gene; GIT, gastrointestinal tract; *HKG*, housekeeping gene; qPCR, quantitative PCR; VB4, *L. rhamnosus* VB4 strain..... 234

Figure 4.4 - Conjugated BAs in the small intestine. Glycocholic acid (GCA); Taurocholic acid (TCA); Glycodeoxycholic acid (GDCA); Taurodeoxycholic acid (TDCA). Blue bars indicated duodenum samples, jejunum was identified by red bars, while green bars represent ileum. AUP means area under the peak and is an average of at least three replicates. Significant differences were established by two-way ANOVA using Dunnett's post-hoc test ($p < 0.05$). * The superscript asterisks symbol indicates significant differences between inoculated and control samples at the same time at $p < 0.05$. # The hash symbol indicates significant differences within the same sample over time at $p < 0.05$. VB4, *L. rhamnosus* VB4 strain. 236
Figure 4.5 - Conjugated BAs in the colon. Glycocholic acid (GCA); Taurocholic acid (TCA); Glycodeoxycholic acid (GDCA); Taurodeoxycholic acid (TDCA). Semi-transparent blue and red bars identified the different sampling time of colon samples, at 16 and 24 h, respectively. Two-way ANOVA using Dunnett's post-hoc test was performed to assess the BAs profile changes after VB4 administration and BAs type. AUP means area under the peak (n = 3). * The superscript asterisks symbol indicates significant differences between inoculated and control samples at the same time at $p < 0.05$. # The hash symbol indicates significant differences within the same sample over time at $p < 0.05$. VB4, *L. rhamnosus* VB4 strain 238
Figure 5.1 - *In vitro* cholesterol assimilation activity of *L. rhamnosus* VB1, *L. rhamnosus* VB4, *L. brevis* M3R3 in MRS-CHO media, expressed as % of cholesterol assimilation by bacterial cells 262
Figure 5.2 - Adhesion to human intestinal epithelium cells (Caco-2) exhibited by *L. rhamnosus* VB1, *L. rhamnosus* VB4, and *L. brevis* M3R3. Results are expressed as percentage of the added bacterial cells. Data represent the mean ± standard deviation (SD) from a representative experiment performed in six replicates. Statistical significance is indicated with letters ($p < 0.05$). 263
Figure 5.3 - Cholesterol uptake ability of lactobacilli strains. (A) Binding of radiolabeled cholesterol from micellar solution in *L. rhamnosus* VB1, *L. rhamnosus* VB4, and *L. brevis* M3R3 compared

with *L. rhamnosus* GG as reference strains. The results are expressed as percentage of cholesterol uptake in bacterial cells and the error bas indicated SD. (B) Cholesterol uptake in differentiated Caco-2 cells after 5 h of exposure to lipid micelles, following 2 h of pre-incubation with the tested strains (included *L. rhamnosus* GG as a reference strain) compared with Caco-2 cells without prior treatment with bacteria. Data are expressed as percentage of relative cholesterol uptake by the Caco-2 cells. All the results are expressed in mean ± SD, and statistical significance between all the samples was indicated with letters (a, b, c, d) ($p < 0.05$)..... 264

Research highlights

- BSH activity is a pivotal probiotic trait, integrating gut microbiota function into lipid metabolic pathway;
- Genomic and functional study of two human-derived *L. rhamnosus* strains (VB4 and VB1) revealed their BSH activity, the presence and the different distribution of *bsh* gene;
- The BSH functionality of *L. brevis* M3R3 strain was revealed through genome sequencing, BSH assays, and bile acid deconjugation test;
- The VB4 strains survivability, bile acid modulation, and transcriptomic responses was depicted during the simulated gastrointestinal transit by using the SHIME® gut model;
- BSH-positive probiotic strains (VB1, VB4, and M3R3) reduce micellar cholesterol uptake in intestinal Caco-2 cells.

Abstract

The bile salt hydrolase (BSH) activity has emerged as a key probiotic trait linking gut microbiota functionality with host lipid metabolism and cardiovascular health. BSH is an enzyme which catalyzed the deconjugation of bile acids (BAs), which play a pivotal role in maintenance of host cholesterol homeostasis. *Lactobacillus* species are widely acknowledged as central BSH-active probiotics, by enhancing gastrointestinal strain survivability, as well as contributing to cholesterol-lowering activity.

This thesis investigated the genomic, phenotypic, and functional properties of three BSH-positive candidates, *Lacticaseibacillus rhamnosus* VB1, *Lacticaseibacillus rhamnosus* VB4, and *Levilactobacillus brevis* M3R3, from human and food sources.

Probiogenomic and phenotypic analyses revealed strain-specific genetic features related to BAs tolerance and deconjugation capacity in all the three investigated strains. Both human isolates *L. rhamnosus* VB1 and VB4 strains carried a single copy of the *bsh* gene, most likely underpinning their BSH potential. Among them, VB4 exhibited greater resistance to BAs condition and a higher deconjugation ability. Interestingly, VB1 displayed higher *bsh* expression than VB4 at stationary phase under BAs stress. *L. brevis* M3R3, isolated from sourdough, possessed two distinct *bsh* genes potentially contributing to BSH activity. This genetic feature supported a strong BAs deconjugation capacity and enhanced adaptability under bile salt conditions.

Given its strong role in bile acid (BAs) deconjugation, strain VB4 was further investigated using the in vitro SHIME® model. Culture-dependent analyses confirmed its survival throughout the simulated digestive process. Moreover, gene expression and metabolomic profiling revealed an effective modulation of BA pools during intestinal transit, particularly in the colon phase, where interactions with the resident microbiota amplified the observed

changes following VB4 administration.

In parallel, functional assays were performed to evaluate the role of the three selected strains in cholesterol metabolism. Data demonstrated their capacity to assimilate cholesterol and to reduce micellar cholesterol uptake by Caco-2 cells, with VB1 showing the strongest adhesion and cholesterol-lowering efficiency, followed by VB4 and M3R3.

Overall, these findings identify VB1 and VB4, together with M3R3, as promising BSH-positive strains with cholesterol-lowering potential. Their detailed characterization—through probiogenomic analyses, dynamic gut models, and host-cell assays—provides a solid framework for the development of next-generation probiotics aimed at regulating lipid homeostasis.

Keywords: bile salt hydrolase, lactobacilli, probiotic strains, cholesterol-lowering activity, bile acids deconjugation, probiogenomic, gut microbiota

Riassunto

L'attività di idrolasi dei sali biliari (BSH) è riconosciuta come una caratteristica probiotica fondamentale, che collega la funzionalità del microbiota intestinale al metabolismo lipidico dell'ospite e alla salute cardiovascolare. La BSH è un enzima che catalizza la deconiugazione degli acidi biliari (BA), i quali svolgono un ruolo cruciale nel mantenimento dell'omeostasi del colesterolo nell'ospite. I lattobacilli sono una specie batterica ampiamente riconosciuta tra i principali probiotici con attività BSH, capaci di migliorare la loro sopravvivenza nel tratto gastrointestinale, oltre che a contribuire alla riduzione del colesterolo. Questa tesi ha esaminato in dettaglio gli aspetti genomici, fenotipici e funzionali di tre ceppi BSH-positivi: *Lacticaseibacillus rhamnosus* VB1, *Lacticaseibacillus rhamnosus* VB4 e *Levilactobacillus brevis* M3R3, di origine umana e alimentare.

Le analisi probiogenomiche e fenotipiche hanno rivelato caratteristiche genetiche ceppo specifiche, associate alla tolleranza ai BAs e alla capacità di deconiugazione in tutti e tre i ceppi studiati. Negli isolati umani *L. rhamnosus* VB1 e VB4 è stata riscontrata la presenza di una singola copia del gene *bsh*, riconducibile al loro potenziale BSH. Tra i due, VB4 ha mostrato una maggiore resistenza in presenza dei BAs e una più elevata capacità di deconiugazione. *L. brevis* M3R3, isolato da lievito madre, possiede due distinti geni *bsh* potenzialmente coinvolti nell'attività BSH, supportato da una robusta deconiugazione dei BAs e una crescita adattativa in presenza di sali biliari.

Per via della sua spiccata deconiugazione dei BAs, VB4 è stato ulteriormente studiato utilizzando il modello *in vitro* SHIME®, dimostrando la persistenza del ceppo durante il processo digestivo simulato, a livello gastrico e intestinale, mediante metodi coltura-dipendenti. Inoltre, sono state condotte analisi di espressione genica e metabolomiche, che hanno indicato una modulazione efficace dei pool di BA durante il transito intestinale fino alla fase colica, dove l'interazione con il microbiota residente ha ulteriormente contribuito

ai cambiamenti osservati in seguito alla somministrazione di VB4.

In parallelo, sono stati condotti saggi funzionali per valutarne il coinvolgimento nel metabolismo del colesterolo. I risultati hanno confermato la capacità dei tre ceppi selezionati di assimilare colesterolo e ridurre l'assorbimento micellare di colesterolo da parte delle cellule Caco-2, con VB1 che ha mostrato la più elevata adesione ed efficienza ipocolesterolemizzante, seguito da VB4 e M3R3.

Complessivamente, questi risultati identificano VB1 e VB4, insieme a M3R3, come potenziali ceppi BSH-positivi con attività di riduzione del colesterolo. Grazie a un approccio integrato che combina screening probiogenomico, modelli intestinali dinamici e saggi cellulari, è stato possibile delineare un quadro di riferimento utile allo sviluppo di probiotici avanzati destinati alla regolazione dell'omeostasi lipidica.

Parole chiave: idrolasi dei sali biliari, lattobacilli, ceppi probiotici, attività di riduzione del colesterolo, deconiugazione degli acidi biliari, probiogenomica, microbiota intestinale

Thesis outline

This thesis gives contributes to the current scientific research on development of novel probiotic strain to use for the formulation of an innovative functional food. In the last years, there was a growing interest from both market and consumers in functional foods, products that, in addition to their nutritional value, are capable to enhance their health-promoting activity by using beneficial agents as probiotics.

Recent advances in the probiotic field have been focused on their capacity to regulate plasma cholesterol levels, making them as promising alternative to pharmacological strategies in preventing and managing mild hypercholesterolemia. The administration of well-characterized probiotic strains represents a scientifically supported strategy in modulating lipid metabolism through multiple mechanisms. The bile salt hydrolase (BSH) activity is considered one of the key pathways by which gut bacteria exert cholesterol-lowering effects. BSH catalyzes the deconjugation of bile acids (BAs), reducing their absorption in the enterohepatic circulation and enhancing their fecal excretion. Although the molecular and regulatory mechanisms of BSH are not fully clarified, several scientific evidence supports the strong correlation between BSH activity and the blood cholesterol level reduction, to the extent to consider it as a key probiotic function in modulating cholesterol levels. BSH activity is well-documented among established probiotic genera, with the highest prevalence observed in *Lactobacillus* genus (recently re-classified into multiple genera) which are recognized for their higher safety profile as QPS (Qualified Presumption as Safety) status strain, and long-standing used for both food and clinical applications.

This thesis critically aims to investigate and validate a novel BSH-positive probiotic candidate. Following a preliminary screening, the most promising strains were subjected to genetic and biochemical analyses to confirm the presence of *bsh*-like genes and their BAs deconjugation capacity.

The thesis is structured into six chapters, based on distinct

scientific contributions developed and explored at different and complementary stages of the research work. An overview of the objective and content of each chapter are outlined as follow:

- **Chapter 1:** ***Bile salt hydrolase: The complexity behind its mechanism in relation to lowering cholesterol lactobacilli probiotic*** – this first chapter consists of an extensive literature review offering an update of the recent findings on the role of BSH activity, with a focus on the cholesterol-lowering potential. Particular attention is given to the complex interactions between BAs and the gut microbiota, emphasizing *Lactobacillus* species. The chapter also aims to contextualize BSH activity as a key probiotic trait in lactobacilli, highlighting its relevance within the broader framework of host-microbiota metabolic regulation.
- **Chapter 2:** ***Genome mining and characterization of two novel Lacticaseibacillus rhamnosus probiotic candidates with Bile Salt Hydrolase activity*** – this chapter consists in the genomic and functional analysis of two *Lacticaseibacillus rhamnosus* strain named VB4 and VB1, from human origin, investigated for their probiotic potential as BAs modulators. The study includes genome analysis to identify *bsh* genes and genetic traits associated with probiotic properties. Phenotypically, *in vitro* evaluations of BSH activity and BAs tolerance were performed, including also transcriptional differences between the two strains.
- **Chapter 3:** ***Bile Salt Hydrolase Activity in the Food-Derived Strain Levilactobacillus brevis M3R3: Genomic and Functional Characterization*** – it consists of the characterization of the *Levilactobacillus brevis* M3R3, isolated from sourdough, to evaluate its probiotic potential related to BSH activity. The study aimed to evaluate the BSH potential through *in vitro* assays in order to demonstrate the BAs deconjugation and growth performance under BAs exposure, as well as *bsh* gene expression profile. Whole-genome sequencing was also performed to assess the strain's safety and to identify features

linked to probiotic functionality, with particular attention to the presence and phylogenetic classification of *bsh* genes.

- **Chapter 4:** ***Gastrointestinal survivability of a BSH-positive Lacticaseibacillus rhamnosus VB4 strain and its effect on bile acid deconjugation in a dynamic in vitro gut model*** – this contribution aims to investigate the viability and functionality of the *Lacticaseibacillus rhamonsus* VB4 strain, previously explored for its BSH ability. The strain was further characterized for its BSH potential under simulated gastrointestinal condition using the *in vitro* SHIME® (Simulator of the Human Intestinal Microbial Ecosystem) model, integrating BAs profiling and transcriptomic analysis to assess its functional response and tolerance throughout the digestive environment.
- **Chapter 5**: ***Probiotic strains with Bile Salt Hydrolase activity reduce micellar cholesterol uptake in Caco-2 cells*** – this study provides a preliminary contribution to the hypothetical relationship between the BSH activity and the cholesterol-lowering potential of the under-study lactobacilli. The strains were subjected to *in vitro* assays employing intestinal epithelial cell lines, which served as a model to evaluate bacterial interaction with the host epithelium, in order to evaluate the cholesterol uptake during micelles exposure.
- **Chapter 6:** ***General discussion and conclusion*** – the final chapter is focused the main findings obtained across the different research activities conducted during the present Ph.D. path, providing clear evidence of the overall scenario regarding the potential of BSH-positive probiotics in cholesterol-lowering applications, and future proposal on the administration of a functional food with beneficial activity.

Chapter 1

1 Bile salt hydrolase: The complexity behind its mechanisms in relation to lowering-cholesterol lactobacilli probiotics

Gianluigi Agolino[1], Alessandra Pino[1,2], Amanda Vaccalluzzo[1], Marianna Cristofolini[3], Lisa Solieri[3,*], Cinzia Caggia[1,2], and Cinzia Lucia Randazzo[1,2,**]

[1]Department of Agriculture, Food and Environment (Di3A), University of Catania, Via Santa Sofia 100, 95123 Catania, Italy
[2]Probioetna SRL, Spin off of University of Catania, Via Santa Sofia 100, 95123 Catania, Italy
[3]Department of Life Sciences, University of Modena and Reggio Emilia, Via Amendola, 2-Pad. Besta, 42100 Reggio Emilia, Italy

*Corresponding author: lisa.solieri@unimore.it (L. Solieri)
**Corresponding author: cinzia.randazzo@unict.it (C.L. Randazzo)

Published in Journal of Functional Food, *2024, 120, 106357*
DOI: https://doi.org/10.1016/j.jff.2024.106357

Graphical abstract

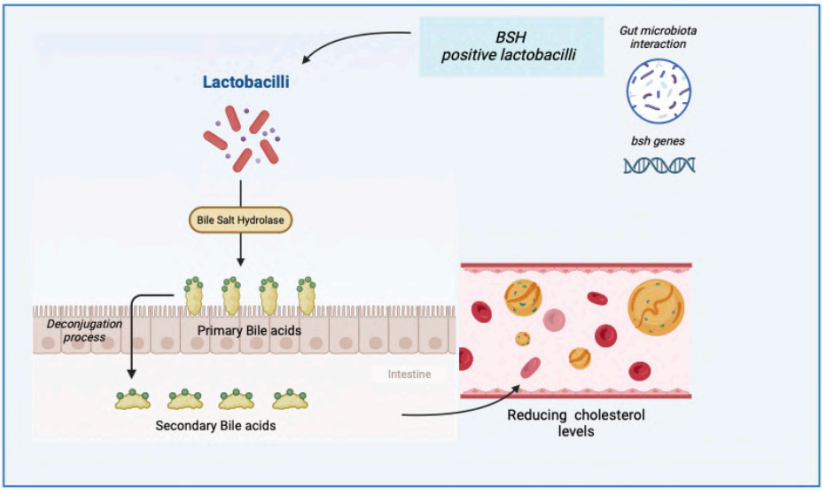

Abstract

Bile Salt Hydrolase (BSH) is a bacterial enzyme (EC 3.5.1.24) that initiates the crucial deconjugation of bile acids (BAs), a process necessary for their transformation into secondary BAs by gut microbes. Recent advance has delved deeper into BAs, recognizing them as endocrine molecules capable of modulating lipid and sugar metabolism in the host.

In this review, we elucidate how this wealth of research has broadened our understanding about the intricate mechanisms between BAs and the gut microbiota beyond BSH, underlying the hypocholesterolemic effects of probiotic lactobacilli. We highlight the

expanded range of various species lactobacilli with proven cholesterol-lowering activity both in vitro and in vivo associated with BSH activity. In addition, a summary of genomic and metagenomic studies investigating *bsh* genes in both gut microbiota and lactobacilli is provided, to be used as an additional tool for the selection of a potential lactobacilli probiotic.

Keywords: probiotic; lactobacilli; bile acids; bile salt hydrolase; hypercholesterolemia

1.1 Introduction

Globally, hypercholesterolemia represents an important risk factor for cardio-vascular disease (CVDs), causing 2.6 million deaths and 29.7 million disability-adjusted life years (DALYS) (World Health Organization, 2024). At this regard, cholesterol plays a crucial role in maintaining human physiological homeostasis, influencing the fluidity of biological membranes and the permeability of the barrier between cells and the external environment. Cholesterol acts as a precursor for steroid hormones, bile salts, fats, and lipophilic vitamins, and is involved in various brain functions (Goedecke & Fernández-Hernando, 2012).

The multifaceted contribution of cholesterol to diverse biological processes makes necessary to tightly regulate the concentration in the human body through a delicate balance between input and output pathways (Klaassen & Aleksunes, 2010; Li et al., 2021; Payne & Hales, 204; van der Wulp et al., 2013). Most of the human cholesterol (80% of total cholesterol) is synthesized in hepatic tissue and extrahepatic cells via the mevalonate pathway, starting from acetyl-CoA. The remaining portion, known as dietary cholesterol, is introduced through the consumption of fatty foods, which undergo metabolism and transportation via lipoproteins, subsequently distributed to various body districts through the bloodstream (Schade et al., 2020).

Regarding output pathways, free cholesterol can be either excreted into bile or converted into bile acids (BAs). Additionally, cholesterol can reach the intestinal lumen through non-biliary transepithelial cholesterol efflux (TICE) (Luo et al., 2020). The ingestion, absorption, synthesis, and excretion of cholesterol are

intricately linked to lipoprotein trafficking. Cholesterol is secreted into circulation in very low-density lipoprotein (VLDL) from the liver, and its removal from the bloodstream involved the uptake of low-density lipoprotein (LDL) by the LDL receptor. The transport of cholesterol from perihelial tissues to the liver occurs through high-density lipoproteins (HDL) particles via the process of reverse cholesterol transport (Nemes et al., 2016).

Over the years, a growing body of literature consistently indicated that alteration in these intricate regulatory mechanisms can result in elevated levels of serum cholesterol in the circulatory system, in a condition known as hypercholesterolemia. This condition has been persistently linked to an increased risk of developing cardiovascular disease (CVDs), manifesting as atherosclerosis, heart failure, or hypertension (Amarenco et al., 2020; Mortense & Nordestgaard, 2020).

Diet rich in unsaturated fats and polygenic predisposition are significant contributors to the development of hypercholesterolemia (Bhatnagar et al., 2008).

In addition to the diet and genetic factors, recent studies have highlighted the significance impact of the gastro-intestinal tract (GIT) microbiota on the body's cholesterol levels (Brown & Hazen, 2018). Moreover, dysbiosis of the gut microbiota has been observed in variour CVDs (Tang et al., 2017; Vourakis et al., 2021). For example, patients with coronary artery disease exhibit an increase in *Lactobacillus*, *Streptococcus*, *Escherichia*, *Shigella*, and *Enterococcus* species in the gut, coupled with a reduction in taxa known to enhance gut barrier function, such as *Faecalibacterium* spp. and *Bacteroides fragilis* (Tang et al., 2017; Witkowski et al., 2020).

Similarly, individuals at high risk for stroke show a decrease in butyrate-producing bacteria (Ahmad et al., 2019).

The gut microbiota influences serum cholesterol levels through carious molecular patterns, which can be categorized into four modes of action (Olas, 2020; Pandey et al., 2015) (Figure 1.1). Firstly, short-chain fatty acids (SCFAs), the primary by-product of gut microbiota catabolism, can reduce blood lipids by inhibiting hepatic cholesterol synthesis or redirecting plasma cholesterol towards the liver. Secondly, microbial surface proteins can bind exogenous cholesterol synthesis or phosphatidylcholine vesicle, incorporating cholesterol into the bacterial cell for increased resistance to environmental cues (Ishimwe et al., 2015). Alternatively, certain intestinal taxa can convert cholesterol into coprostanol, a metabolite with lover intestinal absorption capacity than cholesterol, easily eliminated through feces (Juste & Gérard, 2021; Kenny et al., 2020; Reis et al., 2017). Lastly, gut microbiota modifies primary BAs, the end-products of cholesterol metabolism, into secondary BAs, escaping enterohepatic recirculation and being eliminated through stool (Yntema et al., 2023). The conversion of cholesterol into free BAs is predominantly mediated by microbes with Bile Salt Hydrolase (BSH) activity, which is considered pivotal for exerting a serum cholesterol-lowering effect and preventing hypercholesterolemia (Bourgin et al., 2021; Jones et al., 2013).

Over the years, intervention strategies centered on gut microbiota modulation, such as prebiotics and probiotics, have been proposed to treat and prevent hypercholesterolemia alongside pharmacological interventions. Specifically, probiotic strains exhibiting cholesterol-lowering activity have successfully been

employed to address hypercholesterolemic conditions (Vourakis et al., 2021), and functional food containing probiotics with cholesterol-lowering activity as adjunct cultures have gained wide acceptance among consumers (Shehata et al., 2016). The International Scientific Association for Probiotics and Prebiotics defines probiotics as "live microorganisms that, when administered in adequate amounts, confer a health benefit on the host" (Hill et al., 2014). According to the World Health Organization (WHO), BSH activity is included among probiotic bacteria (Singhal et al., 2019).

The aim of this review is to offer a thorough examination of the impact of BSH activity of probiotic species on cholesterol homeostasis, with a focus on lactobacilli. We firstly highlight recent advances in understanding how gut microbiota and the associated BSH activities shape BAs pool. Then we underline this knowledge enables to improve the usage of biotherapeutics like probiotic BSH-competent lactobacilli, to directly modulate BAs pool and/or to modify the microbiota suitable to metabolize primary BAs into secondary BAs.

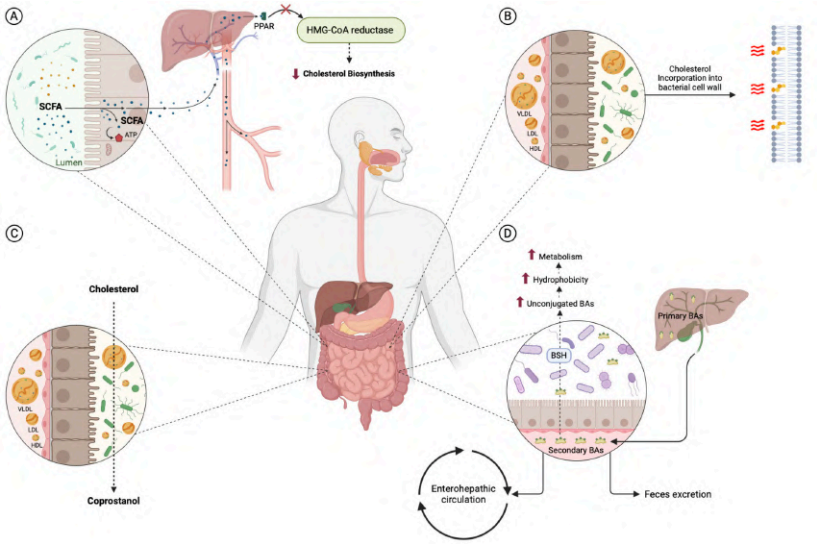

Figure 1.1 - Main molecular mechanisms underpinning cholesterol homeostasis control by gut microbiota. (A) Short chain fatty acids (SCFAs)-mediated inhibition of fat storage and cholesterol biosynthesis. SCFAs acts as ligands that bind to activate peroxisome proliferation-activated receptors (PPARs), which controls the transcription and translate of angiopoietin-like protein 4 and, ultimately, reduces fat storage. Butyrate inhibits the activity of 3-hydroxy-3-methyl-glutaryl-conezyme A (HMG-CoA) reductase, the rate-limiting step in the mevalonate pathways. (B) Assimilation of cholesterol molecule on microbial cell surface. (C) Conversion of cholesterol to coprostanol and its excretion by stool. (D) Increase of secondary bile acids (BAs) pool via bile salt hydrolase (BSH) activity.

1.2 *From primary to secondary bile acids: An overview*

Human primary BAs, mainly chenodeoxycholic acid (CDCA) and cholic acid (CA), are amphipathic steroid molecules produced starting from cholesterol in the liver hepatocytes and subsequently

conjugated to glycine (predominantly in humans) or taurine (mainly in rodents) to form bile salts, which are stored in the gallbladder, Conjugation improves BAs solubility and reduces the potential damage of the cell membrane. Once secreted into the small intestine, conjugated BAs act as detergent molecules and contribute to th solubilization of dietary fats and lipid soluble vitamins assuring their absorption through the small intestine and colon. Approximately 95% primary bile salts are submitted to the active re-uptake from the distal small intestine via the apical sodium dependent bile acid transported (ASBT) (the so-called enterohepatic circulation) (Al-Dury & Marschall, 2018).

The remaining 5% of BAs (~0.3-0.6 g of bile acid per day) eludes enterohepatic recirculation and reaches the distal small and large intestine where deconjugation by BSH-positive microbes occurs. Deconjugated BAs reach the colon and undergo many other microbial transformations resulting into secondary BAs. Secondary BAs can be passively recycled through the large intestine wall and into the blood-stream, where they join other BAs up taken by enterohepatic circulation. Alternatively, they can be excreted by stool. The most abundant microbial-derived secondary BAs in humans include lithocholic acid (LCA) and deoxycholic acid (DCA), derived from CA and CDCA (Ghaffarzadegan et al., 2019; Poland & Flynn, 2021). Conventionally, colonic bacteria are known to catalyze three main reactions on cholesterol core of deconjugated BAs, namely dihydroxylation, dehydrogenation, and epimerization, which chemically expand the diversity and the overall hydrophobicity of the resulting secondary BAs pool (Gérard, 2013; Ridlon et al., 2014). Dihydroxylation of the C7 hydroxy of CA and CDCA, converts BAs

to the major secondary BAs, DCA and LCA, respectively. This reaction is catalyzed in the caecum and colon mainly by *Clostridium* bacteria with the bile acid-induced (*bai*) operon. Recent application of metabolomics technique has considerably increased the complexity of secondary BAs pool as well as the pattern of microbial-catalyzed reactions. Furthermore, gut microbiota was also proved to conjugate primary and secondary BAs at C24 carbonyl both *in vivo* (Quinn et al., 2020) and *in vitro* (Lucas et al., 2021) producing microbial-derived conjugated BA (MCBA) (Figure 1.2). The most important producers of MCBA are *Bifidobacterium*, *Bacteroides*, and *Enterococcus* spp. (Lucas et al., 2021).

In addition to lipid absorption, microbially metabolized secondary BAs mediate the crosstalk between human and microbial cells and affect the overall host cholesterol homeostasis. As direct consequence of deconjugation, secondary BAs are more prone to fecal secretion than the primary BAs. Feces elimination redirects new cholesterol units to be used for the *de novo* primary BAs biosynthesis, leading to a serum cholesterol-lowering effect (Long et al., 2017). When secondary BAs reach the systemic circulation, they act as endocrine molecules and activate BA-mediated pathways involved in host metabolic processes, including lipid and glucose metabolism, energy expenditure, and systemic inflammation (Shapiro et al., 2018) (Figure 1.2).

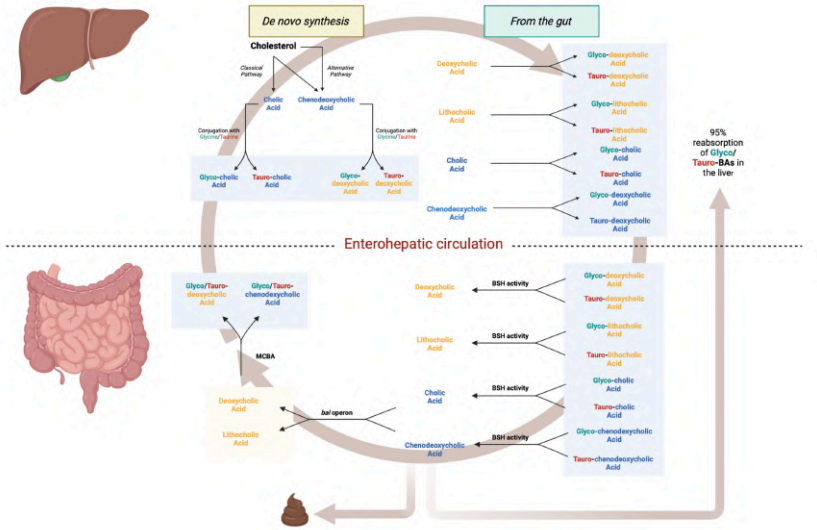

Figure 1.2 - Centrality of BAs metabolism in gastro-intestinal tract and enterohepatic circulation. Bile acids (BAs) (cholic acid and chenodeoxycholic acid) are synthesized from cholesterol in the liver via classical pathway or by the alternative pathway and then conjugated with glycine and/or taurine (*de novo* synthesis). Conjugated BAs. In large intestine, microbial bile acid-inducible (bai) operon converted cholic and chenodeoxycholic acid in deoxycholic and lithocholic acid. Approximately 95% of BAs are resorbed and transported in liver via enterohepatic circulation, some of these directly converted into intestine in conjugated BAs, and the remaining part excreted by feces.

BAs are agonistic/antagonistic for several receptors involved in host energy homeostasis, such as Farnesoid X Receptor (FXR), Takeda G-protein Receptor 5 (TGR5), Pregnane X receptor (PXR) and Vitamin D Receptor (VDR) (Wahlström et al., 2016). The degree of activity and the modulation action depend upon chemistry of

secondary BAs and organ in which receptors are activated. For instance, deconjugated BAs bind better the FXR compared to the glycine- and taurine-conjugated counterparts and, among deconjugated BAs, CDCA is the most potent agonist for FXR. FXR is a bile nuclear receptor expressed in liver, intestine, kidney and adrenal, which has the functional role to repress BAs synthesis in the liver, regulate BAs cycling in enterohepatic tissues, and maintain constant BAs concentrations in body. BA-mediated modulation of FXR reduces cholesterol synthesis, decrease cholesterol absorbance, and enhances disposal of cholesterol in feces in several works (Caron et al., 2013; Chand et al., 2017; Geng and Lin, 2016; Hartman et al., 2009; Li et al., 2013). FXR agonism also reduces hepatic gluconeogenesis and glycolysis and increases glycogen synthesis while playing an anti-inflammatory role during liver injury. Bacterial BSH deconjugate the FXR antagonist tauro-β-muricholic acid, permitting hepatic FXR to inhibit lipogenesis and cholesterol metabolism, thereby suppressing weight gain and lowering serum cholesterol and triglyceride levels (Joyce et al., 2014).

TGR5 is another bile acid receptors involved in host metabolism, widely distributed in different organs (gallbladder, liver, lungs, spleen and intestine) and tissues (bone marrow, adipose and muscle tissue). TGR5 activation depends on binding to the secondary bile acids LCA and DCA (Pols et al., 2011; Thomas et al., 2009; Wahlström et al., 2016). The scientific evidence demonstrated experimental aspects on its involvement on metabolic disorder (Pols et al., 2011; Thomas et al., 2009). Specifically, TGR5 activating several metabolic pathways in response to BAs interaction, improving the glucose homeostasis inducing gut GLP-1 (glucagon-like peptide-

1) release, regulating the basal metabolism and increasing energy expenditure in brown adipose tissue. Additionally, it is involved in inflammatory response in hepatic cells, as evidence of reduction of pro-inflammatory cytokines in macrophage (Kuppfer cells), suggesting TGR5 as potential immunosuppressive reducing cholestasis and liver damage (Keitel et al., 2008; Thomas et al., 2009; Wahlström et al., 2016).

BAs receptor PXR causing the activation of hepatic enzyme, demonstrating its potential involvement in BAs alternative pathway and detoxification (Chand et al., 2017; Guo et al., 2003), in this regard, PXR acts as a physiological sensor of secondary BAs, specifically binding LCA, in order to mitigate their toxic effect (Guo et al., 2003; Kliewer & Wilson, 2002). Several studies highlighted its involvement in other metabolism, such as lipid and glucose metabolism. Furthermore, its agonistic effect on many metabolic substances made it possible to hypothesize its role in the prevention and treatment of various diseases (including biliary cholestasis and xenobiotic protections), suggesting PXR as a target for different drugs (Adachi et al., 2005; Kliewer & Wilson, 2002; Lv et al; 2022).

Also, VDR acts as a receptor for LCA, modulating liver and intestinal detoxification by secondary BAs. The structure-function of this receptor was analyzed in order to understand its double nature to bind xenobiotics such as LCA, as well as the calcemic hormone 1α,25-dihydroxyvitamin D_3 (1,25$(OH)_2D_3$) involved in skeletal and calcium homeostasis (Haussler et al., 2011). According to Adachi et al. (2005) the receptor changing its conformation in binding 1,25$(OH)_2D_3$ or LCA, exerting a different response in the various biological processes. Concerning this, LCA ligand resulting weaker than 1,25$(OH)_2D_3$ by

increasing 30-times VDR activation compared to PXR receptors. The strong potential of this interaction should be useful to elucidate more functions on VDR.

Despite of this scientific evidence, the complete mechanisms underpinning the complex interplay between BAs and human receptors are still poorly understood.

1.3 From primary to secondary bile acids: An overview

Bile Salt Hydrolase (BSH) (EC 3.5.1.24) is a microbial choloylglycine hydrolase belonging to the N-terminal nucleophilic (Ntn) superfamily which catalyzes the first critical deconjugation reaction required for the subsequent microbial-catalyzed BAs biotransformation (Linhorst & Lübke, 2022). The Ntn superfamily is characterized by the catalytic mechanisms which involves a nucleophilic attack by the N-terminal residue on the substrate carbonyl carbon residue is located within the characteristic αββα-fold core structure on Ntn hydrolases and serves as a nucleophile and a proton donor (Figure 1.3). The N-terminal amino group serves as the proton acceptor and activates the nucleophilic thiol group of the cysteine side chain, which is responsible for the hydrolysis of host-synthesized conjugated BAs in their deconjugated forms with the concomitant release of glycine and taurine (Bourgin et al., 2021, Geng & Lin, 2016; Jones et al., 2008; Ridlon et al., 2014). This reaction acts as a 'gatekeeper' for subsequent microbial-catalyzed BAs transformation that turn deconjugated BAs into secondary BAs (Figure 1.2). Consequently, BSH-positive bacteria are considered key player in host cholesterol metabolism.

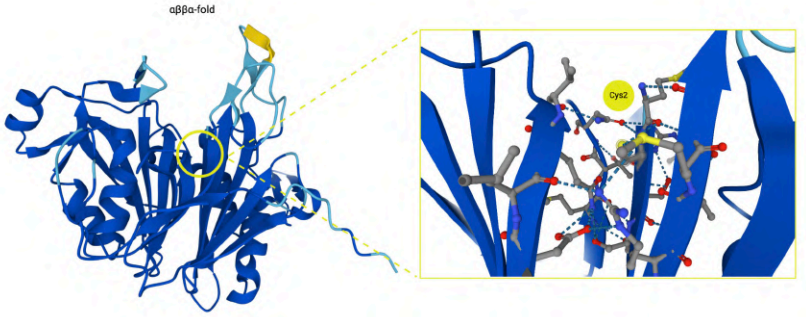

Figure 3.3 - Bile Salt Hydrolase (BSH) structure. The αββα-fold core structure of microbial choloylglycine hydrolase and catalytic site (Cys2).

1.3.1 BSH and host cholesterol homeostasis

BSH activity appears to be common in gut microbes and is more widespread in Grap-positive that in Gram-negative bacteria. It has been demonstrated that the major gut phyla such as *Lactobacillus*, *Bifidobacterium*, *Enterococcus*, and *Clostridium* spp. are BSH competent (Begley et al., 2006; Chand et al., 2017; Long et al., 2017; Ridlon et al., 2016). BHS activity has been also documented in other Gram-positive bacteria such *Listeria monocytogenes* (Bourgin et al., 2021; Chand et al., 2017; Long et al., 2017), and in Gram-negative bacteria including *Xanthomonas maltophilia* (Chand et al., 2017; Dean et al., 2002; Long et al., 2017), *Brucella abortus* (Chand et al., 2017), and *Bacteroides* spp. (Bourgin et al., 2021; Chand et al., 2017). Differences among bacteria BSH have been described based on of their preferential activity towards either glycine-conjugated or taurine-conjugated BAs (Foley & O'Flaherty et al., 2021). Microbial BSHs are also active towards MCBA (Foley & O'Flaherty et al., 2021).

Dysregulation in BSH activity has been directly implicated in

cholesterol homeostasis alterations, such as CVDs (Feng et al., 2015; Kaur et al., 2011; Lau et al., 2017; Manolis et al., 2022; Nesci et al., 2023; Novakovic et al., 2020) and obesity (Joyce et al., 2014), as well as in cancer (Ma et al., 2018) and inflammatory bowel disease (IBD) (Chassard et al., 2012; Lavelle & Sokol, 2020; Principi et al., 2018). Recently, BSH has been demonstrated to reduce *C. difficile* spore germination and growth *in vitro* and colonization in pre-clinical *in vivo* models of *C. difficile* infection (CDI) (Foley et al., 2023). Dysbiosis and antibiotic usages have been reported to modify microbial BSH activity. For instance, antibiotic usage depletes BSH, increasing conjugated BAs and decreasing secondary BAs (Theriot et al., 2014).

Different mechanisms link microbial BSH activity to host cholesterol homeostasis. Increase in BSH activity enhances the pool of hydrophobic deconjugated BAs which escape the active absorption via ABST, favoring the conversion into secondary BAs by colonic bacteria (Ridlon, 2020). As reported above, BSH activities strongly impact the secondary BAs pool which in turn modulate lipid and glucose metabolism via the interaction with several receptors involved in mechanisms regulating host energy harvest. Congruently, mice overexpressing BSH exhibited a significant reduction in host weight gain, plasma cholesterol, and liver triglycerides (Joyce et al., 2014) Furthermore, increase pool of secondary BAs more prone to feces elimination than conjugated BAs biosynthesis, leading to a serum cholesterol-lowering effect (Long et al., 2017). Increased BSH activity may also reduce the absorption of dietary cholesterol as deconjugated BAs are less effective that conjugated counterparts in the solubilization and absorption of lipids.

In addition to hypocholesterolemic activity and further positive

action, possible detrimental effects have been related to BSH-mediated deconjugation of BAs (Table 1.1). Deconjugated BAs have lower emulsifying capacity than the conjugated BAs, thus an increase in deconjugated BAs is often associated with malabsorption of lipids, causing steatorrhea in humans (Kim & Lee, 2005) and growth depression in chickens (Knarreborg et al., 2002). As BSH activity helps bacteria against the toxic effect on conjugated BAs, pathogenic bacteria with BSH activity can display higher ability to colonize gut than pathogenic bacteria without BSH. Therefore, increased BSH activity has been related to establishment of various intestinal pathogens such as *L. monocitogenes* and *B. abortus* (Dussurget et a., 2002), whilst a reduction of conjugated BAs could promote microbial alteration in GIT (Chand et al., 2017; Choi et al., 2015; Marchesini et al., 2011; Thanissery et al., 2017). In addition, it was also proved that changing in BAs composition can compromised gut motility, potentially leading to either slowed or accelerated transit times through GIT (Ridlon et al., 2016). Moreover, high level of free secondary BAs has been related to DNA damage and ROS-associated oxidative stress in epithelia intestinal cells, which can contribute to the onset of colon-rectal cancer (Begley et al., 2006; Choi et al., 2015; Ishimwe et al., 2015). As consequence, secondary BAs such as DCA and LCA are more carcinogenic than primary BAs (Jia et al., 2020). Finally, patients that have obstructed biliary ducts caused by gallstone formation frequently have a high-level of secondary BAs, suggesting that alterations in the concentrations of BAs may results in bile being supersaturated with cholesterol (Begley et al., 2006; Veysey et al., 1999). Previous studies were also focused on the signaling effect of BAs in pathological and physiological bone homeostasis, increasing

knowledge about the gut-bones axis (Cho et al., 2013; Xiang et al., 2023). At neurological level, the physiological functions and molecular implications of bile acids in the central nervous system remain largely unknown. However, recent studies highlighted the role of BAs as a signal molecule in modulation of gut-brain axis and regulation of neurological disorders, such as Alzheimer's and Parkinson's disease (Mahmoudian Dehkordi et al., 2019; Monteiro-Cardoso et al., 2021; Mulak, 2021).

Table 1.1 - Overview of main positive and negative effects by microbial BSH activity on host health

Healthy effects	**References**
Prevention of hypercholesterolemia (cholesterol-lowering effect)	Begley et al., 2006; Bourgin et al., 2021; Jones et al., 2013; Kriaa et al., 2019; Wang et al., 2019
Control of weight gain in obesity and metabolic syndrome	Bourgin et al., 2021: Geng and Lin, 2016; Joyce et al., 2014; Li et al., 2013; Parséus et al., 2017
Production of short-chain fatty acids	Chand et al., 2017; Hernández-Gòmez et al., 2021; Tsai et al., 2014
Reduction of Inflammatory Bowel Disease (IBDs)	Gadaleta et al., 2022; Geng and Lin, 2016
Bile acid sequestrants and the treatment of type-2 diabetes mellitus	Bustos et al., 2018; Hansen et al., 2014
Immune homeostasis effect	Foley et al., 2019; Geng and Lin, 2016; Inagaki et al., 2006; Joyce et al., 2014
Controlling circadian rhythms	Foley et al., 2019; Gadaleta et al., 2022; Geng and Lin, 2016; Govindarajan et al., 2016; Joyce et al., 2014; Yao et al., 2018;
Positive regulation of bones homeostasis	Cho et al., 2013; Xiang et al., 2023
Regulation of neurological and neurodegenerative disorders	Ackerman and Gerhard, 2016; Monteiro-Cardoso et al., 2021; Mulak, 2021
Side effects	**References**
Persistence of pathogens	Marchesini et al., 2011; Thanissery et al., 2017

Lipid malabsorption and variation in BAs profile	Bustos et al., 2018; Geng and Lin, 2016; Joyce et al., 2014; Kim and Lee, 2005
Colon-rectal cancer (carcinogenesis)	Begley et al., 2006; Bustos et al., 2018; Gadaleta et al., 2022; Geng and Lin, 2016; Ishimwe et al., 2015; Marteau et al., 1995; Nagengast et al., 1995; Ou et al., 2013; Pazzi et al., 1997; Venneman and van Erpecum, 2010
Formation of gallstone, obstruction of biliary ducts	Begley et al., 2006; Veysey et al., 1999
Imbalance of gut microbiota	Chand et al., 2017
Compromises gut motility	Ridlon et al., 2016

1.3.2 BSH and gut bacteria homeostasis

While microbes can shape chemical diversity and functionality of enterohepatic BAs pools, BAs pools can in turn have direct and indirect effects on the gut microbial community, influencing fitness and host colonization (Islam et al., 2011). BAs mainly promote dissipation of the transmembrane electrical potential ($\Delta\Psi$) and intracellular acidification. In some bacteria BAs induce oxidative damage to DNA and RNA, and protein misfolding. Historically it was proposed that the primary role of BSH in gut bacteria is the reduction of the toxicity of conjugated BAs and the promotion of microbial viability (Chand et al., 2017; De Smet et al., 1995; Guzior &Quinn, 2021). Numerous studies have noted that conjugated forms of BAs are more effective at compromising bacterial membrane integrity than deconjugated forms, as reviewed by Begley et al., (2006). However, a recent study using Gram-positive lactobacilli partially disagrees this notion as some BAs were found to be more toxic to the bacterium after deconjugation (Foley & O'Flaherty et al., 2021). Another evolutive advantage of BSH is that free amino acids like taurine or glycine could

serve as potential energy sources, facilitating bile detoxification and providing a nutritional benefit to BSH-active bacteria over BSH-inactive bacteria. Glycine, for instance, can be catabolized to ammonia and carbon dioxide, while taurine is metabolized to ammonia, carbon dioxide and sulfate (Begley et al., 2006; Ridlon et al., 2016).

Among conjugated BAs, glyco-conjugated ones exhibit greater toxicity than taurine-conjugated BAs, particularly under low pH conditions (Begley et al., 2006; Chand et al., 2017; Kim et al., 2004; Pavlović et al., 2012). Conventionally, bacterial BSHs have been described to preferentially catalyze the deconjugation of glycol-conjugated BAs compared to taurine-conjugated forms, mitigating toxicity (Begley et al., 2006; De Smet et al., 1995). The small size and minimal steric hindrance of glycine, compared to the steric hindrance of taurine, may contribute to the higher substrate preference of BSH for glycine-conjugates over taurine-conjugates (Sjövall et al., 2010). More recently, Foley er al., (2023) demonstrated that lactobacilli BSH can have different substrate specificity, depending upon structural loop near o catalytic site. BSH substrate specificity can affect *Lactobacillus* growth in a conjugation-dependent manner and could explain why many lactobacilli encode multiple BSHs. An expanded repertoire of BSH with different substrate specificity can confer selective advances in gut and has been considered a signature of gut adaptation (Foley et al., 2023; Yao et al., 2018). Studies on the distribution of *bsh* genes in lactobacilli from different niches proved that *bsh* genes were not ubiquitous in lactobacilli and that BSH-positive lactobacilli were strongly correlated with a vertebrate-adapted lifestyle (Liang et al., 2018; O'Flaherty et al., 2018). Recently a metagenomic survey of BSH protein sequences in human microbiota

significantly expanded our knowledge on BSH genetics. In detail, BSHs were classified in 7 phylotypes, with lactobacilli BSHs belonging to BSH-T3 phylotype. This kind of BSH was found only in lactobacilli and exhibited the highest enzyme activity (Song et al., 2023).

1.4 From BSH to hypocholesterolemic action through probiotics

The growing demand for natural remedies has prompted the exploration of non-pharmacological strategies to address hypercholesterolemia. A significant fraction of the population affected by hypercholesterolemia relies on statins to inhibit cholesterol synthesis and prevent intestinal absorption. However, prolonged use of, these drugs is often associated with side effects (Tian et al., 2022), such as cardio-vascular events (caused by hemorrhagic stroke and diabetes), myopathy, muscular pain, skeletal symptoms, neuro-cognitive disease, liver and renal dysfunctions (Collins et al., 2016; Ramkumar et al., 2016; Thompson et al., 2016). Indeed, the use of these is not recommended for individuals with mild hypercholesterolemia and at risk of premature CVD, for whom dietary interventions are recommended, with reduction of saturated fat intake and, more recently, the adoption of probiotics. Several studies have shown BSH-positive probiotics can be a supplements or replacement in individuals with hypercholesterolemia. The best-studied BSH-active probiotic strains from human and non-human origins, that exhibited experimentally validated cholesterol-lowering activity in vivo are lactobacilli belonging to the species *Limosilactobacillus reuteri* (basionym *Lactobacillus reuteri*), *Lactiplantibacillus*

plantarum (baionym *Lactobacillus plantarum*), *Lacticaseibacillus casei* (basionym *Lactobacillus casei*), *Lactobacillus acidophilus*, *Lacticaseibacillus rhamnosus* (basionym *Lactobacillus rhamnosus*), *Lactobacillus gasseri*, *Lactobacillus jhonsonii*, *Lactobacillus salivarius*, and *Limosilactobacillus fermentum* (baionym *Lactobacillus fermentum*) (Table 1.2). Furthermore, BSH-positive bifidobacteria, such as *Bifidobacterium longum*, *Bifidobacterium bifidum*, *Bifidobacterium adolescentis* and *Bifidobacterium animalis*, were reported to significantly reduce circulating cholesterol (Bordoni et al., 2013; De Smet et al., 1994; Huang et al., 2019; Li, 2012; Tanaka et al., 1999). Even if BSH has been extensively studied in lactobacilli, recent studies proved that *bsh* genes are not ubiquitous among lactobacilli, with *bsh*-encoding lactobacilli correlating with a vertebrate-adapted lifestyle (Liang et al., 2018; O'Flaherty et al., 2018).

Table 1.2 - Overview of the main BSH-positive lactobacilli strains with potential cholesterol-lowering activity.

	Lactiplantibacillus plantarum			
	Strain number	**Isolation source**	**Main results**	**References**
Human origin	Lp21 Lp91	Human feces	↑ BSH activity ↓ Total Cholesterol levels ↓ LDL-Cholesterol levels ↑ HDL-Cholesterol levels	Kumar et al., 2011, 2012
	CHOL-200	Human feces	↑ BSH activity ↑ *in vitro* Cholesterol activity ↓ Total Cholesterol levels ↓ LDL-Cholesterol levels ↑ HDL-Cholesterol levels	Frappier et al., 2022

	PH40	Infant feces	↓ Total Cholesterol levels ↓Tryglicerides levels	Nguyen et al., 2007
	CK 102	Infant feces	↑ BSH activity	Patel et al., 2010
	TGCM15 TGCM33	Thai fermented food	↑ BSH activity ↑ *in vitro* Cholesterol activity	Sirilun et al., 2010
Food origin	KLDS 1.0344	Chinese fermented milk	↑ BSH activity ↓ LDL-Cholesterol levels	Guo et al., 2019
	Lp09 Lp45	Kefir grains	↓ Total Cholesterol levels ↓ LDL-Cholesterol levels ↓ Tryglicerides levels ↑ Fecal BAs levels	Huang et al., 2013
	BBE7	Pickle	↑ BSH activity ↑ *in vitro* Cholesterol activity	Dong et al., 2012
	X15	Yogurt	↑ BSH activity ↓ Total Cholesterol levels ↓ Tryglicerides levels	Liu et al., 2021

Lactobacillus acidophilus

	Strain type	**Isolation source**	**Main results**	**References**
Human origin	CL1285	Human feces	↑ BSH activity ↑ *in vitro* Cholesterol activity ↓ Total Cholesterol levels ↓ LDL-Cholesterol levels ↑ HDL:Cholesterol ratio	Frappier et al., 2022
Food origin	BFE6126 BFE6160 BFE6127 BFE6056	Fermented milk	↑ BSH activity ↑ *in vitro* Cholesterol activity	Mathara et al., 2008; Patel et al., 2010

Lacticaseibacillus casei

	Strain type	**Isolation source**	**Main results**	**References**
Food origin	J57	Pulque	↑ BSH activity ↑ survival in GIT	González-Vázquez et al., 2015
	F0822	Fermented milk	↑ BSH activity ↓ Total Cholesterol levels	Guo et al., 2018

			↓ LDL-Cholesterol levels	
	AG AP	Fermented milk	↑ BSH activity ↑ *in vitro* Cholesterol activity	Widodo et al., 2021

Limosilactobacillus fermentum

	Strain type	**Isolation source**	**Main results**	**References**
Human origin	NCDO934	Infant intestine	↑ BSH activity	Kumar et al., 2013
Food origin	MTCC 8711	Yogurt	↑ BSH activity ↑ *in vitro* Cholesterol activity	Jayashree et al., 2014
	Y57	Lassi/Yogurt	↑ BSH activity ↑ *in vitro* Cholesterol activity ↓ LDL-Cholesterol levels ↑ HDL-Cholesterol levels	Zafar et al., 2022

Lacticaseibacillus rhamnosus

	Strain type	**Isolation source**	**Main results**	**References**
Human origin	E9	Infant feces	↑ BSH activity	Kaya et al, 2017
Food origin	FM9	Lassi/Yogurt	↑ BSH activity ↑ *in vitro* Cholesterol activity ↓ LDL-Cholesterol levels ↑ HDL-Cholesterol levels	Zafar et al., 2022

Lactobacillus johnsonii

	Strain type	**Isolation source**	**Main results**	**References**

Animal origin	334	Ileal tissue of pig	↑ BSH activity ↓ LDL-cholesterol levels	Zhu et al., 2022

Limosilactobacillus reuteri

	Strain type	**Isolation source**	**Main results**	**References**
Animal origin		Pig feces	↓ Total Cholesterol levels ↓ LDL-Cholesterol levels	De Smet et al., 1998

↑ *increase*; ↓ *decrease*

The principal mechanism underpinning the hypocholesterolemic impact is the BSH activity and the inclusion of the *bsh* gene has traditionally been seen as favorable characteristics in probiotics. This genetic trait equips probiotics to flourish within GIT environment, effectively contributing to the reduction of serum cholesterol level. Numerous studies have predominantly delved into the correlation between BSH enzyme activity and the *in vitro* potential for cholesterol reduction. Klaver and van der Meer (1993) established a significant link between the cholesterol-lowering effects of bifidobacteria and lactobacilli and their BSH activities. Tanaka et al. (2000) conducted an extensive investigation into the distribution of the *bsh* gene and BSH activity across more than 300 species, encompassing genera like *Bifidobacterium* and *Lactobacillus*, as well as specific species such as *Lactococcus lactis*, *Leuconostoc mesenteroides*, and *Streptococcus termophilus*. Miremadi et al., (2014) explored the cholesterol reduction capabilities of 14 strains of lactobacilli and bifidobacteria, highlighting that *L. acidophilus* CSCC 2400 and *B. longum* CSCC 5022 significantly hydrolyzed glycine- or taurine-conjugated BAs owing to their heightened BSH activity.

While Walker and Gilliland (1993) reported that *L. acidophilus* strains secrete BSH to deconjugate BAs, Dambekodi and Gilliland (1998) found no clear correlation between in vitro cholesterol reduction and the extent of BAs deconjugation. These partial inconsistencies suggest that, beyond BSH, other mechanisms may play a role in the cholesterol-lowering effects of probiotics.

One direct cholesterol-lowering mechanism involved the capability of probiotic strains such as *L. delbrueckii* subsp. *bulgaricus*, *L. acidophilus*. *L. helveticus*, and *L. casei* to bind cholesterol to the cell surface through interactions with peptidoglycan. Additionally, these strains can convert cholesterol into coprostanol through cholesterol reductase activity (Ahire et al., 2012; Lye et al., 2010). Lactobacilli probiotics can also indirectly lower blood cholesterol by fermenting prebiotics, increasing the production of SCFAs. These SCFAs inhibit hepatic cholesterol synthesis, resulting in a reduction of blood lipids (Ashaolu et al., 2021) (Figure 1.4).

Given that not only BSH-positive probiotics exhibit cholesterol lowering effects, but it also imperative to conduct studies using animal models and human trials to establish a positive correlation between BSH activity and the hypocholesterolemic effect *in vivo*.

Sridevi et al. (2009) demonstrated that the oral administration of immobilized BSH enzymes from *L. buchneri* significantly reduced both triglycerides and serum cholesterol in a rodent model of hypercholesterolemia. Kim et al. (2017) validated the hypocholesterolemic effects of a probiotic mixture (*L. reuteri* and *L. plantarum*, along with *B. longum*, *B. lactis*, and *B. breve*) on diet-induced hypercholesterolemic rats. Similarly, probiotic lactobacilli overexpressing the *bsh* gene hindered cholesterol absorption and

accelerated cholesterol transportation in diet-induced hypercholesterolemic rats (Wang et al., 2019).

In a placebo-controlled, randomized study, Ooi and Liong (2010) reported that administering a symbiotic capsule containing a BSH-active strain of *L. gasseri* with inulin led to significant reductions in total cholesterol and LDL-cholesterol compared to the placebo group. Similar outcomes were observed with yogurt containing microencapsulated *L. reuteri* NCMIB 30242 (Jones et al., 2012a). Furthermore, in a randomized, double-blinded study on hypercholesterolemic subjects, capsules containing BSH-positive *L. reuteri* NCMIB 30242 resulted in higher plasma deconjugated BAs levels, but lower total cholesterol, LDL-cholesterol, and non-HDL-cholesterol levels compared to the placebo group (Jones et al., 2012b). Notably, *L. reuteri* NCMIB 30242 was the first probiotic strain marketed (commercially known as Cardioviva®, or LCR®) for cholesterol-reducing purposes based on BSH and BAs deconjugation mechanisms (Lee et al., 2023; Martoni et al., 2015).

In another clinical trial, the consumption of yogurt containing *L. reuteri* CRL 1098 significantly decreased total circulating cholesterol and LDL-cholesterol levels, while HDL and triglyceride levels remained unchanged (Malpeli et al., 2015). Niamah et al. (2017) also observed that soy milk fermented by a probiotic starter consisting of *S. termophilus*, *L. acidophilus*, and *B. bifidum* decreased cholesterol and triglyceride levels compared to the control. More recently, Keleszade et al. (2022) reported that the use of *L. plantarum* 13110402 (LP_{LDL}®), a commercialized probiotic bacterium mainly known for its BSH activity, significantly reduced total cholesterol levels in hypercholesterolemic subjects, administered with probiotic capsules,

compared to the placebo group.

Positive correlation between BSH activity and the lowering of cholesterol levels have also been demonstrated through meta-analyses. A recent meta-analysis by Mo et al. (2019) supported the use of probiotics to significantly reduce total cholesterol and LDL-cholesterol in hypercholesterolemic adults. Similarly, a meta-analysis of 30 randomized controlled trials found that probiotics reduced total cholesterol and LDL levels compared to the placebo by 7.8 mg/ml and 7.3 mg/dl, respectively (Wang et al., 2018). According to this meta-analysis, a combination of *B. lactis* and *L. acidophilus*, VSL #3, and *L. plantarum* are among the most effective probiotics for lowering total cholesterol. Among probiotic lactobacilli, the most substantial reduction in total cholesterol was observed with *L. plantarum*, while the most significant reduction in LDL was noted with *L. plantarum* and *L. reuteri* (Wu et al., 2017).

Despite the positive evidence described above, clinical studies supporting probiotic-mediated hypocholesterolemic effects are considered too weak to endorse probiotics as an alternative biotherapy to improve blood lipid profiles. Heterogeneities in cohort composition, intervention duration, dose, and probiotic supplementation make *in vivo* studies poorly comparable, and meta-analyses inconsistent (Khalesi et al., 2019). Moreover, various inter-individual factors affect subject' responsiveness to the hypocholesterolemic action of probiotics. In an 18-week double-blinded, placebo-controlled study in adults with metabolic deregulations, Wastyk et al. (2023) revealed that a specific probiotic impacted aspects of metabolic disorders in a diet-dependent manner. Compared to the control group, only a subset of 10 out of 26 participants who received a probiotic cocktail containing

three probiotic strains exhibited a decrease in triglyceride concentration. This high level of inter-individual variation suggests that the efficacy of probiotics in counteracting hypercholesterolemia could depend on several factors beyond BSH activity. The intricate relationship between diet, intestinal microbiota, probiotics, and therapy (dose, intervention duration, and formulations) requires an in-deep characterization to optimize effectiveness of BSH-positive probiotics in lowering cholesterol (Figure 1.4). Based on these considerations, precision therapy should overcome the limitations of the current "one-size-fits-all therapy" approach (Suez et al., 2019).

Some studies have reported the potential use of a strain-specific replacement therapy in combating hypercholesterolemia, correlated with the most studied probiotics with BSH-ability (Ali et al., 2022; Sudum et al., 2019; Tsai et al., 2014).

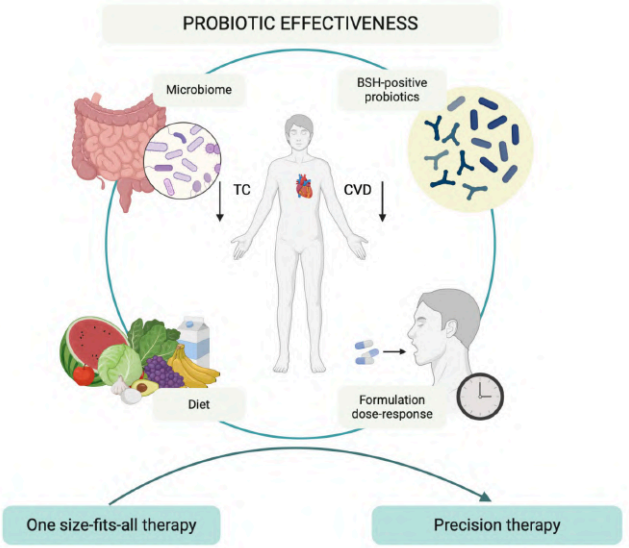

Figure 4.4 - Relationship between diet, the intestinal microbiota, BSH activity, and probiotic formulations. Effectiveness of BSH-positive probiotics in counteracting hypercholesterolemia depends on quadrangular relationship between diet, intestinal microbiome, chosen probiotic bacteria, and pharmacological parameters (kind of probiotic-driving formulation, dose, duration of the treatment). Abbreviation: TC, total cholesterol; CVD, cardio-vascular disease.

1.4.1 Lactiplantibacillus plantarum

As previous mentioned, *L. plantarum* stands out as one of the most extensively studied probiotic species with documented BSH activity and cholesterol-lowering properties (De Smet et al., 1994; Dong et al., 2012; Guo et al., 2019; Liu et al., 2021). The *in vitro* evidence supporting the cholesterol-lowering potential of *L. plantarum* has been substantiated by *in vivo* studies. In a research

endeavor conducted by Huang et al. (2013), various BSH-positive strains of *L. plantarum* isolated from kefir were investigated for their hypocholesterolemic effects in an animal model fed with a cholesterol-rich diet. Among the kefir-derived strains, *L. plantarum* Lp09 and Lp45 showed the strongest BSH activity. Notably, Lp09 displayed superior survivability intervals compared to Lp45. When hypocholesterolemic rats were supplemented with Lp09 and Lp45, the treatment effectively reduced total cholesterol, triglycerides, and LDL-cholesterol compared to placebo group. Furthermore, Lp09 demonstrated the additional benefit on increasing fecal bile salt concentrations, a crucial contributing to the reduction of serum cholesterol.

1.4.2 Lacticaseibacillus rhamnosus and Lacticaseibacillus casei

Numerous studies have provided compelling evidence that several strains belonging to *Lacticaseibacillus* group exert hypocholesterolemic effect *in vitro* and *in vivo* and have correlated this hypocholesterolemic effect to BSH activity. For instance, in a recent investigation by Zafar et al. (2022), BSH activity leading to cholesterol reduction was unequivocally demonstrated for *L. rhamnosus* strain FM9 isolated from fermented milk. The experimental design encompassed various diet groups monitored for a period of 30 days, including rats fed a diet rich in fat with a high cholesterol content (HFCD), a group treated with statins on a high-fat diet (SDHF), and eight groups fed a high-fat diet supplemented with potential probiotic strains the pre-selected based on BSH activity *in vitro*. The collected data revealed that among pre-selected strains, *L. rhamnosus* FM9 has an anti-obesity effect and an impact on the

regulation of serum lipid profiles in rats comparable to statins.

Also, Tsai et al., (2014) demonstrated that PROBIOS-23 containing *L. rhamnosus*, as well as *B. adolescentis* and *P. acidilactici* significantly reduced serum total cholesterol, triglycerides, and LDL-cholesterol in hypercholesterolemic hamsters.

Similarity, *L. casei* member of the *Lacticaseibacillus* group, underwent investigation for its potential in reducing cholesterol levels, by BSH mechanism. In an experimental study, also conducted in hamster, the consumption of *L. casei*-fermented milk. Proving the fundamental role of BSH activity in hypercholesterolemia subjects. Remarkably, the administration of wild-type *L. casei* F0822 fermented milk compared with *bsh*-deleted mutant in high-fat-diet hamsters, shown a significant capacity to reduce the total cholesterol and non-HDL cholesterol serum level, and a reduction of esterified cholesterol and total cholesterol into hepatic cells. Finally, a daily enhancing fecal BAs extraction, provided evidence of a major BSH involvement on hypercholesterolemic effect, compared with other potential mechanisms, such as cholesterol integration on bacterial cell membrane mediated by S-Layer Protein (SLP) (Guo et al., 2018).

1.4.3 *Limosilactobacillus fermentum* and *Limosilactobacillus reuteri*

L. fermentum, a widely distributed bacterium found in both food and human gut, is extensively utilized in food products due to its significant biotechnological and health-promoting properties (Zhao et al., 2022). Over the years, various studies have highlighted the cholesterol-lowering potential of *L. fermentum* often linked to its BSH activity (Asan-Ozusaglam & Gunyakti, 2018; Lye et al., 2017; Pan et

al., 2011; Pereira er al., 2003). In the study reported above, Zafar et al., (2022) demonstrated that *L. fermentum* BSH-positive strain Y57 was effective like *L. rhamnosus* in lowering cholesterol in animal model. In a study conducted by Palaniyandi et al. (2020), *L. fermentum* MJM60397, isolated from Indian cow milk curd, was characterized as a potential probiotic strain with hypocholesterolemic effects. The study included analyses to assess resistance to GIT conditions, adhesion to Caco-2 cells, BSH activity, and *in vitro* cholesterol-lowering activity. In an *in vivo* experiment with male mice on a high-cholesterol diet, significant reductions in LDL-cholesterol levels in serum and liver were observed in groups administered with *L. fermentum* MJM60397 and *L. acidophilus* ATCC 43121 compared to the control group. Interestingly, fecal samples showed elevated bile salts levels, in MJM60397 groups compared to the control and ATCC 43121 groups. These results indicated that *L. fermentum* MJM60397 exhibit a strong cholesterol-lowering effect, justified by the increase of BAs deconjugation and the reduction of bile absorption. Decrease of bile absorption induced liver bile synthesis from cholesterol, that leads in lower serum LDL-cholesterol levels. Gene expression analysis in the liver revealed the overexpression of the LDL-receptor gene in the MJM60397 group, supporting how supplementation with BSH positive probiotic promotes BAs secretion by feces (Palaniyandi et al., 2020).

L. reuteri, a member of the *Limosilactobacillus* group, is. Well-established probiotic species, especially known for their ability to produced ‘reuterin’, a complex multi-components anti-microbial compound, recognize as health-promoting agent (Mu et al., 2018; Sun et al., 2022). *L. reuteri* recognized as a potential probiotic for

mitigating various CVDs (Koppinger et al., 2020; Liu et al., 2023). Seminal study of Taranto et al. (2020) emphasized the *L. reuteri* ability to reduce endogenous cholesterol by persisting in the GIT and maintaining microbiota balance, providing protective effects against CVDs. The close association between cholesterol-lowering ability and BSH activity in *L. reuteri* has been consistently demonstrated in multiple experiments (Bustos et al., 2016; De Boever et al., 2000; Martoni et al., 2015). Notably, *L. reuteri* has been proven to reduce cholesterol absorption rate *in vitro* and also *in vivo* (Bustos et al., 2016; Jones et al., 2012a; Koppinger et al., 2020; Liu et al., 2023). Tomaro-Duchesneau et al. (2014) demonstrated, in an *in vitro* gut condition experiments that *L. reuteri* NCMIB 701089 assimilates at least 67% of cholesterol. In a randomized clinical trial (Jones et al., 2012a), microencapsulated *L. reuteri* was administered to 127 healthy hypercholesterolemic subjects which were monitored over 9-week period. As result, subjects supplemented with *L. reuteri* NCMIB 30242 exhibited significant reduction in total cholesterol LDL-cholesterol, HDL-cholesterol, and apoB-100 levels compared to the placebo group, while triglycerides and HDL-cholesterol remained unchanged.

1.4.4 Lactobacillus acidophilus

Lactobacillus acidophilus strains generally exhibit a strong and well-characterized BSH activity and are frequently employed as BSH-positive controls in various studies (Horackova et al., 2020; Khare & Gaur, 2020; Liong & Shah, 2005; Walker and Gilliland, 1993). Over the years, numerous L. acidophilus strains have been identified as probiotics exhibiting cholesterol-lowering activity in addition to other

beneficial function, such as preservation of gut homeostasis, regulation of immune response, lactose-tolerance, gastro-intestinal cancer prevention, as well as CVDs regression (Gao et al., 2022). Among there, *L. acidophilus* NCFM (binti Khan et al., 2022; Gilliland & Walker, 1990), *L. acidophilus* ATCC 43121 (Corzo & Gilliland, 1999), and *L. acidophilus* ATCC 314 (Tomaro-Duchesneau et al., 2014) play direct or indirect roles in combating hypercholesterolemia.

The BSH-positive *L. acidophilus* strain NCFM exhibited in vitro cholesterol assimilation and potential control of blood cholesterol levels (Gao et al., 2022; Gilliland & Walker, 1990; McAuliffe et al., 2005). Recent human studies involving supplementation with *L. acidophilus* NCFM, either alone or in combination with other probiotics or prebiotics, aimed to evaluate previously observed *in vitro* conditions in *L. acidophilus* NCFM consumers (binti Khan et al., 2022). This study was conducted on a hypercholesterolemic adult population over an 8-week period and included various treatment groups such as inulin-treated, dietary fiber-treated (β- glucan). *L. acidophilus* NCFM group (20×10^9 CFU/ml), and a symbiotic group (combination of *L. acidophilus* NCFM, *Bifidobacterium lactis* Bi-07, and prebiotic). The blood lipid profile exhibited positive responses in the *L. acidophilus* probiotic groups as well as in the inulin/ β- glucan groups. Specifically, the NCFM group showed excellent total cholesterol levels in the blood lipid profile, along with a moderate enhancement of HDL-cholesterol and triglyceride levels. However, limited evidence was observed regarding the symbiotic formulation's impact on the lipid profile after administration.

According to Corzo and Gilliland (1999), *L. acidophilus* ATCC

43121 is a BSH-positive strain more prone to deconjugated glycocholate sodium salt rather that taurocholate sodium salt. Especially, at neutral pH values (pH 6.5) like those found in small intestine. This condition is optimal for potential probiotic strains with BSH activity in the small intestine. De Rodas et al. (1996) used hypercholesterolemia-induced pigs as animal model to successfully demonstrate the hypocholesterolemic effect of *L. acidophilus* ATCC 43121. Similarly, Park et al., (2007) also provided evidence supporting the cholesterol-lowering effect of *L. acidophilus* ATCC 43121 in clinical studies with hypercholesterolemic rats. The same study cited above for the hypercholesterolemic effect of *L. fermentum* MJM60397, proved that *L. acidophilus* ATCC 43121 also significantly reduced LDL-cholesterol levels in serum and liver in male mice submitted to high cholesterol diet (Palaniyandi et al., 2020).

Lastly, *L. acidophilus* ATCC 314 has been described to exert hypocholesterolemic effect through various mechanisms, such as conversion of cholesterol into coprostanol, the integration of free-cholesterol molecules into the bacterial cell membrane, and BSH activity (Lye et al., 2010). However, a more recent screening of different *L. acidophilus* strains carried out by Horackova et al. (2020) indicated that *L. acidophilus* ATCC 314 is BHS-negative as confirmed by in vitro assay and the lack of any *bsh* genes.

1.4.5 Lactobacillus johnsonii

Recently, the significant role of *Lactobacillus johnsonii* is regulating serum cholesterol levels has been demonstrated. The BSH property of *L. johnsonii* 334 plays a crucial role in cholesterol-lowering activity and seems involved FXR-mediated mechanisms

(DiMarzio et al., 2017; Yang &Wu, 2022). Zhu et al. (2022) constructed recombinant mice. Expressing a heterologous *bsh* gene from *L. johnsonii* 334 to investigate how BSH enzyme can modulate FXR-controlled signaling pathways. Recombinant mice and mice fed with *L. johnsonii* 334 showed similar decreased levels of total cholesterol, triglycerides, and LDL-cholesterol group. Accordingly, a high percentage of deconjugated bile salts was found in recombinant mice compared to the control condition. This evidence supported the correlation between the presence of the heterologous *bsh* gene and hypocholesterolemic effects. FXR-encoding gene were found upregulated in mice supplemented with *L. johnsonii* 334 and in recombinant mice overexpressing *L. johnsonii* 334 *bsh* gene but not in control group. These findings supported the involvement of FXR-mediated pathways in cholesterol reduction and the link between these FXR-mediated pathways and the probiotic BSH activity.

1.5 *Lactobacilli bsh genes distribution and relationship with cholesterol-lowering activity*

Molecular effectors of probiotic functionalities should be deeply understood to rationally select novel probiotic candidates and move from the currently adopted "one-size-fits-all therapy" approach to precision biotherapeutics. The presence of *bsh* gene is really considered a selection criterion for probiotic candidates with cholesterol-lowering effect. As reported above, *bsh* gene is considered pivotal in foundations in potential probiotic strains are crucial for comprehending the mechanisms of interaction between bacteria and their host (McAuliffe et al., 2005). Over the years, the critical impact of BSH activity in the gut microbial community has been

demonstrated, offering a fresh perspective on *Lactobacillus* spp. and a high-throughput method for selectin potential probiotic strains. Due to their essential role in BAs hydrolyzation and the identification of bacteria that possess and express the *bsh* gene. This correlation reflects in the regulation of host physiology and disease conditions (Chand et al., 2017; Kumar et al., 2006; Núnez-Sánchez et al., 2022; Song et al., 2019). Horizontal gene transfer (HGT) is suggested for acquisition of *bsh* genes, with the *bsh* locus located in different genetic regions, associated with bacterial chromosome, as well as transposable elements (plasmids or transposons). However, there is no strong evidence supporting HGT of *bsh* genes in GIT microbes (Claesson et al., 2006; Geng & Lin, 2016). These genes are regulated and organized differently in various species and genera, often included in an operon, and the transcript can be either monocistronic or polycistronic (Pavlović et al., 2012; Ridlon et al., 2006). *Lactiplantibacillus plantarum*, a long-used probiotic, is genetically characterized by four conserved copies of *bsh genes (bsh1*, *bsh2*, *bsh3*, and *bsh4*) (Ertükmen et al., 2023; Lambert et al., 2008; Ren et al., 2011; Song et al., 2019; Wang et al., 2021). Functional analysis in *L. plantarum* WCFS1 confirmed the role of the BSH enzyme and its involvement in BAs deconjugation in the small intestine. *Bsh1* was found to be directly involved in glycocholic acid bile tolerance, with *bsh2*, *bsh3*, and *bsh4* being extremely conserved and associated with fundamental physiological roles. The extensive conservation suggests an early acquisition of these genes during species evolution. Using the CRISPR-Cas9 system, a recent study on *L. plantarum* AR113 confirmed the association between the *bsh* gene and BSH activity, with *bsh1* identified as the main responsible for the greater BSH

activity. Additionally, *bsh1* and *bsh3* were considered key genes in bile salt tolerance, showing substrate preference against glycol-conjugated BAs (Lambert et al., 2008; Wang et al., 2021). In *L. acidophilus*, two genes, *bshA* and *bshB*, with distinct substrate specifically, have been identified (Horackova et al., 2020; Lambert et al., 2008; McAulifee et al., 2005; Patel et al., 2010). A preliminary screening in *L. acidophilus* NCFM revealed the presence and putative roles of these two genes, with *bshA* involved in glyco-conjugated BAs steroid nucleus tolerance and *bshB* showed 57% similarity with *bshA*, indicating its potential role in encoding different substrate. The similarity between *bsh1* in *L. plantarum* and *bshA* and *bshB* in *L. acidophilus* suggests the involvement of both genes in enzyme production (Lambert et al., 2008; Pavlović et al., 2012). Phenotypic studies with *bsh* mutants revealed the roles of BshA and BshB against specific substrates, with BshA active against conjugated BA steroid nucleus and BshB dependent on taurine BA-structure (McAuliffe et al 2005). *L. johnsonii* expresses BSH activity, encoding two antigenically different isoforms, BSHα and BSHβ, identified as part of a single operon (Elkins et al., 2001; Pavlović et al., 2012). Further studies are needed to establish a connection between the *bsh* gene and cholesterol-lowering activity in *L. johnsonii*. In *L. fermentum*, the presence of *bsh1* and *bsh2* genes has been demonstrated, with functional analyses confirming their BSH properties and cholesterol reduction under *in vitro* conditions (Jayashree et al., 2014; Kumar et al., 2013). Genome sequence analysis of *L. fermentum* MTC8711 revealed the presence of these genes, and their cloning assimilation after 24 h, maintained up to 96 h. the presence and the genetic arrangement in *Lactobacillus* probiotic strain is highly variable.

Certain species with BSH ability, existing in single copy as well as multiple copies. Among this *Limosilactobacillus reuteri* (Bustos et al., 2015) and *Lacticaseibacillus rhamnosus* (Kaya et al., 2017), which supported bile detoxification and BAs deconjugation, with a preferential way in glyco-conjugated compared with tauro-conjugate, to explain come physiological conditions.

1.6 Conclusions and future perspective

The use of BSH-positive lactobacilli to prevent CVDs and other disorder involving bile acid metabolism is well-documented. BSH activity is one of the mechanisms through which probiotics lower cholesterol, making them potential candidates for integrative or recovery biotherapy to reduce the risk of CVDs. However, contrasting data on the effectiveness of these probiotic strains indicate that the correlation between BSH activity and hypocholesterolemic effects in strain-dependent. Therefore, understanding the mechanisms by which probiotic strains regulate bile acid metabolism is crucial to enhance their therapeutic potential. Most molecular effectors involved in these mechanisms are still unknown, and possible synergistic or antagonistic interactions with BSH with different specifies can modulate bile acid profiles differently and, consequently, have varying cholesterol-lowering effects. Additionally, bile acid patterns vary significantly between individuals and are influenced by diet, medication use, and other factors.

In conclusion, elucidating the mechanisms by which bile acids regulate gut microbiome structure through omics approaches and dynamics GI tract simulators could provide strategies for lowering blood cholesterol and insights for enhancing cardiovascular health.

Author contributions

Gianluigi Agolino: Writing– original draft, Data curation. Alessandra Pino: Writing– review & editing. Amanda Vaccalluzzo: Writing– original draft. Marianna Cristofolini: Data curation. Lisa Solieri: Writing– review & editing. Cinzia Caggia: Supervision, Funding acquisition. Cinzia Lucia Randazzo: Supervision, Funding acquisition.

Declaration of competing interest

The authors declare the following financial interests/personal relationships which may be considered as potential competing interests: Alessandra Pino, Cinzia Caggia, and Cinzia Lucia Randazzo declare that they are members of ProBioEtna, a spinoff of the University of Catania, Italy. In addition, the authors declare that they do not have any personal, financial, professional, political, or legal interests with a significant chance of interfering with the performance of their ethical or legal duties.

References

1. Ackerman, H. D., & Gerhard, G. S. (2016). Bile Acids in Neurodegenerative Disorders. *Frontiers in aging neuroscience*, *8*, Article 263. https://doi.org/10.3389/fnagi.2016.00263.
2. Adachi, R., Honma, Y., Masuno, H., Kawana, K., Shimomura, I., Yamada, S., & Makishima, M. (2005). Selective activation of vitamin D receptor by lithocholic acid acetate, a bile acid derivative. *Journal of lipid research*, *46*(1), 46–57. https://doi.org/10.1194/jlr.M400294-JLR200.
3. Ahire, J. J., Bhat, A. A., Thakare, J. M., Pawar, P. B., Zope, D. G., Jain, R. M., & Chaudhari, B. L. (2012). Cholesterol assimilation and biotransformation by *Lactobacillus helveticus*. *Biotechnology letters*, *34*(1), 103–107. https://doi.org/10.1007/s10529-011-0733-2.

4. Ahmad, A. F., Dwivedi, G., O'Gara, F., Caparros-Martin, J., & Ward, N. C. (2019). The gut microbiome and cardiovascular disease: current knowledge and clinical potential. *American journal of physiology. Heart and circulatory physiology*, *317*(5), H923–H938. https://doi.org/10.1152/ajpheart.00376.2019.
5. Ali, S. M., Salem, F. E., Aboulwafa, M. M., & Shawky, R. M. (2022). Hypolipidemic activity of lactic acid bacteria: Adjunct therapy for potential probiotics. *PloS one*, *17*(6), e0269953. https://doi.org/10.1371/journal.pone.0269953.
6. Al-Dury, S., & Marschall, H. U. (2018). Ileal Bile Acid Transporter Inhibition for the Treatment of Chronic Constipation, Cholestatic Pruritus, and NASH. *Frontiers in pharmacology*, *9*, 931. https://doi.org/10.3389/fphar.2018.00931.
7. Amarenco, P., Kim, J. S., Labreuche, J., Charles, H., Abtan, J., Béjot, Y., Cabrejo, L., Cha, J. K., Ducrocq, G., Giroud, M., Guidoux, C., Hobeanu, C., Kim, Y. J., Lapergue, B., Lavallée, P. C., Lee, B. C., Lee, K. B., Leys, D., Mahagne, M. H., Meseguer, E., … Treat Stroke to Target Investigators (2020). A Comparison of Two LDL Cholesterol Targets after Ischemic Stroke. *The New England journal of medicine*, *382*(1), 9. https://doi.org/10.1056/NEJMoa1910355.
8. Asan-Ozusaglam, M., & Gunyakti, A. (2018). *Lactobacillus fermentum* strains from human breast milk with probiotic properties and cholesterol-lowering effects. *Food science and biotechnology*, *28*(2), 501–509. https://doi.org/10.1007/s10068-018-0494-y.
9. Ashaolu, T. J., Ashaolu, J. O., & Adeyeye, S. A. O. (2021). Fermentation of prebiotics by human colonic microbiota *in vitro* and short-chain fatty acids production: a critical review. *Journal of applied microbiology*, *130*(3), 677–687. https://doi.org/10.1111/jam.14843.
10. Begley, M., Hill, C., & Gahan, C. G. (2006). Bile salt hydrolase activity in probiotics. *Applied and environmental microbiology*, *72*(3), 1729–1738. https://doi.org/10.1128/AEM.72.3.1729-1738.2006.
11. Bhatnagar, D., Soran, H., & Durrington, P. N. (2008). Hypercholesterolaemia and its management. *BMJ (Clinical research ed.)*, *337*, a993. https://doi.org/10.1136/bmj.a993.

12. binti Khan, F. I., Ooi, Y. B., Tan, L. L., Azmi, Z., & Matanjun, P. (2022). *Lactobacillus acidophilus* NCFM, Inulin, and Oat Bran Reduce TC and LDL-C in Adults with Hypercholesterolaemia. *Borneo Journal of Medical Sciences (BJMS)*, *16*(2), 31-46. https://doi.org/10.51200/bjms.v16i2.3338.
13. Bordoni, A., Amaretti, A., Leonardi, A., Boschetti, E., Danesi, F., Matteuzzi, D., Roncaglia, L., Raimondi, S., & Rossi, M. (2013). Cholesterol-lowering probiotics: *in vitro* selection and *in vivo* testing of bifidobacteria. *Applied microbiology and biotechnology*, *97*(18), 8273–8281. https://doi.org/10.1007/s00253-013-5088-2.
14. Bourgin, M., Kriaa, A., Mkaouar, H., Mariaule, V., Jablaoui, A., Maguin, E., & Rhimi, M. (2021). Bile Salt Hydrolases: At the Crossroads of Microbiota and Human Health. *Microorganisms*, *9*(6), 1122. https://doi.org/10.3390/microorganisms9061122.
15. Brown, J. M., & Hazen, S. L. (2018). Microbial modulation of cardiovascular disease. *Nature reviews. Microbiology*, *16*(3), 171–181. https://doi.org/10.1038/nrmicro.2017.149.
16. Bustos, A. Y., de Valdez, G. F., Raya, R., de Almeida, A. M., Fadda, S., & Taranto, M. P. (2015). Proteomic analysis of the probiotic *Lactobacillus reuteri* CRL1098 reveals novel tolerance biomarkers to bile acid-induced stress. *Food Research International*, *77*, 599-607. https://doi.org/10.1016/j.foodres.2015.10.001.
17. Bustos, A. Y., Font, G. M., Raya, R. R., & Taranto, M. P. (2016). Genetic characterization and gene expression of bile salt hydrolase (*bsh*) from *Lactobacillus reuteri* CRL 1098, a probiotic strain. http://dx.doi.org/10.19070/2577-4336-160001.
18. Bustos, A. Y., Font de Valdez, G., Fadda, S., & Taranto, M. P. (2018). New insights into bacterial bile resistance mechanisms: the role of bile salt hydrolase and its impact on human health. *Food research international (Ottawa, Ont.)*, *112*, 250–262. https://doi.org/10.1016/j.foodres.2018.06.035.
19. Caron, S., Huaman Samanez, C., Dehondt, H., Ploton, M., Briand, O., Lien, F., Dorchies, E., Dumont, J., Postic, C., Cariou, B., Lefebvre, P., & Staels, B. (2013). Farnesoid X receptor inhibits the transcriptional activity of carbohydrate response element binding protein in human

hepatocytes. *Molecular and cellular biology*, *33*(11), 2202–2211. https://doi.org/10.1128/MCB.01004-12.

20. Chand, D., Avinash, V. S., Yadav, Y., Pundle, A. V., Suresh, C. G., & Ramasamy, S. (2017a). Molecular features of bile salt hydrolases and relevance in human health. *Biochimica et biophysica acta. General subjects*, *1861*(1 Pt A), 2981–2991. https://doi.org/10.1016/j.bbagen.2016.09.024.
21. Chassard, C., Dapoigny, M., Scott, K. P., Crouzet, L., Del'homme, C., Marquet, P., Martin, J. C., Pickering, G., Ardid, D., Eschalier, A., Dubray, C., Flint, H. J., & Bernalier-Donadille, A. (2012). Functional dysbiosis within the gut microbiota of patients with constipated-irritable bowel syndrome. *Alimentary pharmacology & therapeutics*, *35*(7), 828–838. https://doi.org/10.1111/j.1365-2036.2012.05007.x.
22. Cho, S. W., An, J. H., Park, H., Yang, J. Y., Choi, H. J., Kim, S. W., Park, Y. J., Kim, S. Y., Yim, M., Baek, W. Y., Kim, J. E., & Shin, C. S. (2013). Positive regulation of osteogenesis by bile acid through FXR. *Journal of bone and mineral research : the official journal of the American Society for Bone and Mineral Research*, *28*(10), 2109–2121. https://doi.org/10.1002/jbmr.1961.
23. Choi, S. B., Lew, L. C., Yeo, S. K., Nair Parvathy, S., & Liong, M. T. (2015). Probiotics and the BSH-related cholesterol lowering mechanism: a Jekyll and Hyde scenario. *Critical reviews in biotechnology*, *35*(3), 392–401. https://doi.org/10.3109/07388551.2014.889077.
24. Claesson, M. J., Li, Y., Leahy, S., Canchaya, C., van Pijkeren, J. P., Cerdeño-Tárraga, A. M., Parkhill, J., Flynn, S., O'Sullivan, G. C., Collins, J. K., Higgins, D., Shanahan, F., Fitzgerald, G. F., van Sinderen, D., & O'Toole, P. W. (2006). Multireplicon genome architecture of *Lactobacillus salivarius*. *Proceedings of the National Academy of Sciences of the United States of America*, *103*(17), 6718–6723. https://doi.org/10.1073/pnas.0511060103.
25. Collins, R., Reith, C., Emberson, J., Armitage, J., Baigent, C., Blackwell, L., Blumenthal, R., Danesh, J., Smith, G. D., DeMets, D., Evans, S., Law, M., MacMahon, S., Martin, S., Neal, B., Poulter, N., Preiss, D., Ridker, P., Roberts, I., Rodgers, A., … Peto, R. (2016). Interpretation of the evidence for the efficacy and safety of statin therapy. *Lancet*

(London, England), *388*(10059), 2532–2561. https://doi.org/10.1016/S0140-6736(16)31357-5.

26. Corzo, G., & Gilliland, S. E. (1999). Bile salt hydrolase activity of three strains of *Lactobacillus acidophilus*. *Journal of dairy science*, *82*(3), 472–480. https://doi.org/10.3168/jds.S0022-0302(99)75256-2.
27. Dambekodi, P. C., & Gilliland, S. E. (1998). Incorporation of cholesterol into the cellular membrane of *Bifidobacterium longum*. *Journal of dairy science*, *81*(7), 1818–1824. https://doi.org/10.3168/jds.S0022-0302(98)75751-0.
28. De Boever, P., Wouters, R., Verschaeve, L., Berckmans, P., Schoeters, G., & Verstraete, W. (2000). Protective effect of the bile salt hydrolase-active *Lactobacillus reuteri* against bile salt cytotoxicity. *Applied microbiology and biotechnology*, *53*(6), 709–714. https://doi.org/10.1007/s002530000330.
29. De Rodas, B. Z., Gilliland, S. E., & Maxwell, C. V. (1996). Hypocholesterolemic action of *Lactobacillus acidophilus* ATCC 43121 and calcium in swine with hypercholesterolemia induced by diet. *Journal of dairy science*, *79*(12), 2121–2128. https://doi.org/10.3168/jds.S0022-0302(96)76586-4.
30. De Smet, I., De Boever, P., & Verstraete, W. (1998). Cholesterol lowering in pigs through enhanced bacterial bile salt hydrolase activity. *The British journal of nutrition*, *79*(2), 185–194. https://doi.org/10.1079/bjn19980030.
31. De Smet, I. D., Hoorde, L. V., Saeyer, N. D., Woestyne, M. V., & Verstraete, W. (1994). In vitro study of bile salt hydrolase (BSH) activity of BSH isogenic *Lactobacillus plantarum* 80 strains and estimation of cholesterol lowering through enhanced BSH activity. *Microbial ecology in health and disease*, *7*(6), 315-329. https://doi.org/10.3109/08910609409141371.
32. De Smet, I., Van Hoorde, L., Vande Woestyne, M., Christiaens, H., & Verstraete, W. (1995). Significance of bile salt hydrolytic activities of lactobacilli. *The Journal of applied bacteriology*, *79*(3), 292–301. https://doi.org/10.1111/j.1365-2672.1995.tb03140.x.
33. Dean, M., Cervellati, C., Casanova, E., Squerzanti, M., Lanzara, V., Medici, A., Polverino De Laureto, P., & Bergamini, C. M. (2002).

Characterization of cholylglycine hydrolase from a bile-adapted strain of *Xanthomonas maltophilia* and its application for quantitative hydrolysis of conjugated bile salts. *Applied and environmental microbiology*, *68*(6), 3126–3128. https://doi.org/10.1128/AEM.68.6.3126-3128.2002.

34. DiMarzio, M., Rusconi, B., Yennawar, N. H., Eppinger, M., Patterson, A. D., & Dudley, E. G. (2017). Identification of a mouse *Lactobacillus johnsonii* strain with deconjugase activity against the FXR antagonist T-β-MCA. *PloS one*, *12*(9), e0183564. https://doi.org/10.1371/journal.pone.0183564.
35. Dong, Z., Zhang, J., Lee, B., Li, H., Du, G., & Chen, J. (2012). A bile salt hydrolase gene of *Lactobacillus plantarum* BBE7 with high cholesterol-removing activity. *European Food Research and Technology*, *235*, 419-427. https://doi.org/10.1007/s00217-012-1769-9.
36. Dussurget, O., Cabanes, D., Dehoux, P., Lecuit, M., Buchrieser, C., Glaser, P., Cossart, P., & European Listeria Genome Consortium (2002). *Listeria monocytogenes* bile salt hydrolase is a PrfA-regulated virulence factor involved in the intestinal and hepatic phases of listeriosis. *Molecular microbiology*, *45*(4), 1095–1106 https://doi.org/10.1046/j.1365-2958.2002.03080.x.
37. Elkins, C. A., Moser, S. A., & Savage, D. C. (2001). Genes encoding bile salt hydrolases and conjugated bile salt transporters in *Lactobacillus johnsonii* 100-100 and other *Lactobacillus* species. *Microbiology (Reading, England)*, *147*(Pt 12), 3403–3412. https://doi.org/10.1099/00221287-147-12-3403.
38. Ertürkmen, P., Fırıncıoğulları, B., & Öner, Z. (2023). The Expression Levels of Genes Responsible for the Enzymatic Activity of Bile Salt Hydrolase (BSH) and the Relationship of Cholesterol Assimilation in *L. plantarum* and *L. paracasei*. *Current microbiology*, *80*(6), 205. https://doi.org/10.1007/s00284-023-03311-2.
39. Feng, Q., Liang, S., Jia, H., Stadlmayr, A., Tang, L., Lan, Z., Zhang, D., Xia, H., Xu, X., Jie, Z., Su, L., Li, X., Li, X., Li, J., Xiao, L., Huber-Schönauer, U., Niederseer, D., Xu, X., Al-Aama, J. Y., Yang, H., … Wang, J. (2015). Gut microbiome development along the colorectal adenoma-carcinoma sequence. *Nature communications*, *6*, 6528. https://doi.org/10.1038/ncomms7528.

40. Foley, M. H., O'Flaherty, S., Allen, G., Rivera, A. J., Stewart, A. K., Barrangou, R., & Theriot, C. M. (2021). *Lactobacillus* bile salt hydrolase substrate specificity governs bacterial fitness and host colonization. *Proceedings of the National Academy of Sciences of the United States of America*, *118*(6), e2017709118. https://doi.org/10.1073/pnas.2017709118.
41. Foley, M. H., O'Flaherty, S., Barrangou, R., & Theriot, C. M. (2019). Bile salt hydrolases: Gatekeepers of bile acid metabolism and host-microbiome crosstalk in the gastrointestinal tract. *PLoS pathogens*, *15*(3), e1007581. https://doi.org/10.1371/journal.ppat.1007581.
42. Foley, M. H., Walker, M. E., Stewart, A. K., O'Flaherty, S., Gentry, E. C., Patel, S., Beaty, V. V., Allen, G., Pan, M., Simpson, J. B., Perkins, C., Vanhoy, M. E., Dougherty, M. K., McGill, S. K., Gulati, A. S., Dorrestein, P. C., Baker, E. S., Redinbo, M. R., Barrangou, R., & Theriot, C. M. (2023). Bile salt hydrolases shape the bile acid landscape and restrict *Clostridioides difficile* growth in the murine gut. *Nature microbiology*, *8*(4), 611–628. https://doi.org/10.1038/s41564-023-01337-7.
43. Frappier, M., Auclair, J., Bouasker, S., Gunaratnam, S., Diarra, C., & Millette, M. (2022). Screening and Characterization of Some Lactobacillaceae for Detection of Cholesterol-Lowering Activities. *Probiotics and antimicrobial proteins*, *14*(5), 873–883. https://doi.org/10.1007/s12602-022-09959-9Gao, H., Li, X., Chen, X., Hai, D., Wei, C., Zhang, L., & Li, P. (2022). The Functional Roles of *Lactobacillus acidophilus* in Different Physiological and Pathological Processes. *Journal of microbiology and biotechnology*, *32*(10), 1226–1233. https://doi.org/10.4014/jmb.2205.05041.
44. Geng, W., & Lin, J. (2016). Bacterial bile salt hydrolase: an intestinal microbiome target for enhanced animal health. *Animal health research reviews*, *17*(2), 148–158. https://doi.org/10.1017/S1466252316000153.
45. Gérard P. (2013). Metabolism of cholesterol and bile acids by the gut microbiota. *Pathogens (Basel, Switzerland)*, *3*(1), 14–24. https://doi.org/10.3390/pathogens3010014.

46. Ghaffarzadegan, T., Essén, S., Verbrugghe, P., Marungruang, N., Hållenius, F. F., Nyman, M., & Sandahl, M. (2019). Determination of free and conjugated bile acids in serum of Apoe(-/-) mice fed different lingonberry fractions by UHPLC-MS. *Scientific reports*, *9*(1), 3800. https://doi.org/10.1038/s41598-019-40272-8.
47. Gilliland, S. E., & Walker, D. K. (1990). Factors to consider when selecting a culture of *Lactobacillus acidophilus* as a dietary adjunct to produce a hypocholesterolemic effect in humans. *Journal of dairy science*, *73*(4), 905–911. https://doi.org/10.3168/jds.S0022-0302(90)78747-4.
48. Goedeke, L., & Fernández-Hernando, C. (2012). Regulation of cholesterol homeostasis. *Cellular and molecular life sciences: CMLS*, *69*(6), 915–930. https://doi.org/10.1007/s00018-011-0857-5.
49. González-Vázquez, R., Azaola-Espinosa, A., Mayorga-Reyes, L., Reyes-Nava, L. A., Shah, N. P., & Rivera-Espinoza, Y. (2015). Isolation, Identification and Partial Characterization of a Lactobacillus casei Strain with Bile Salt Hydrolase Activity from Pulque. *Probiotics and antimicrobial proteins*, *7*(4), 242–248. https://doi.org/10.1007/s12602-015-9202-x.
50. Govindarajan, K., MacSharry, J., Casey, P. G., Shanahan, F., Joyce, S. A., & Gahan, C. G. (2016). Unconjugated Bile Acids Influence Expression of Circadian Genes: A Potential Mechanism for Microbe-Host Crosstalk. *PloS one*, *11*(12), e0167319. https://doi.org/10.1371/journal.pone.0167319 .
51. Guo, G. L., Lambert, G., Negishi, M., Ward, J. M., Brewer, H. B., Jr, Kliewer, S. A., Gonzalez, F. J., & Sinal, C. J. (2003). Complementary roles of farnesoid X receptor, pregnane X receptor, and constitutive androstane receptor in protection against bile acid toxicity. *The Journal of biological chemistry*, *278*(46), 45062–45071. https://doi.org/10.1074/jbc.M307145200.
52. Guo, L., Wang, L., Liu, F., Li, B., Tang, Y., Yu, S., Zhang, D., & Huo, G. (2019). Effect of bile salt hydrolase-active *Lactobacillus plantarum* KLDS 1.0344 on cholesterol metabolism in rats fed a high-cholesterol diet. *Journal of functional foods*, *61*, 103497. https://doi.org/10.1016/j.jff.2019.103497.

53. Guo, C. F., Zhang, S., Yuan, Y. H., Li, J. Y., & Yue, T. L. (2018). Bile Salt Hydrolase and S-Layer Protein are the Key Factors Affecting the Hypocholesterolemic Activity of *Lactobacillus casei*-Fermented Milk in Hamsters. *Molecular nutrition & food research*, *62*(24), e1800728. https://doi.org/10.1002/mnfr.201800728.
54. Guzior, D. V., & Quinn, R. A. (2021). Review: microbial transformations of human bile acids. *Microbiome*, *9*(1), 140. https://doi.org/10.1186/s40168-021-01101-1.
55. Hansen, M., Sonne, D. P., & Knop, F. K. (2014). Bile acid sequestrants: glucose-lowering mechanisms and efficacy in type 2 diabetes. *Current diabetes reports*, *14*(5), 482. https://doi.org/10.1007/s11892-014-0482-4.
56. Hartman, H. B., Gardell, S. J., Petucci, C. J., Wang, S., Krueger, J. A., & Evans, M. J. (2009). Activation of farnesoid X receptor prevents atherosclerotic lesion formation in LDLR-/- and apoE-/- mice. *Journal of lipid research*, *50*(6), 1090–1100. https://doi.org/10.1194/jlr.M800619-JLR200.
57. Haussler, M. R., Jurutka, P. W., Mizwicki, M., & Norman, A. W. (2011). Vitamin D receptor (VDR)-mediated actions of 1α,25(OH)$_2$vitamin D$_3$: genomic and non-genomic mechanisms. *Best practice & research. Clinical endocrinology & metabolism*, *25*(4), 543–559. https://doi.org/10.1016/j.beem.2011.05.010.
58. Hernández-Gómez, J. G., López-Bonilla, A., Trejo-Tapia, G., Ávila-Reyes, S. V., Jiménez-Aparicio, A. R., & Hernández-Sánchez, H. (2021). *In Vitro* Bile Salt Hydrolase (BSH) Activity Screening of Different Probiotic Microorganisms. *Foods (Basel, Switzerland)*, *10*(3), 674. https://doi.org/10.3390/foods10030674.
59. Hill, C., Guarner, F., Reid, G., Gibson, G. R., Merenstein, D. J., Pot, B., Morelli, L., Canani, R. B., Flint, H. J., Salminen, S., Calder, P. C., & Sanders, M. E. (2014). Expert consensus document. The International Scientific Association for Probiotics and Prebiotics consensus statement on the scope and appropriate use of the term probiotic. *Nature reviews. Gastroenterology & hepatology*, *11*(8), 506–514. https://doi.org/10.1038/nrgastro.2014.66.

60. Horackova, S., Vesela, K., Klojdova, I., Bercikova, M., & Plockova, M. (2020). Bile salt hydrolase activity, growth characteristics and surface properties in *Lactobacillus acidophilus*. *European Food Research and Technology*, *246*, 1627-1636. https://doi.org/10.1007/s00217-020-03518-8.
61. Huang, C. H., Ho, C. Y., Chen, C. T., Hsu, H. F., & Lin, Y. H. (2019). Probiotic BSH Activity and Anti-Obesity Potential of *Lactobacillus plantarum* Strain TCI378 Isolated from Korean Kimchi. *Preventive nutrition and food science*, *24*(4), 434–441. https://doi.org/10.3746/pnf.2019.24.4.434.
62. Huang, Y., Wang, X., Wang, J., Wu, F., Sui, Y., Yang, L., & Wang, Z. (2013). *Lactobacillus plantarum* strains as potential probiotic cultures with cholesterol-lowering activity. *Journal of dairy science*, *96*(5), 2746–2753. https://doi.org/10.3168/jds.2012-6123.
63. Inagaki, T., Moschetta, A., Lee, Y. K., Peng, L., Zhao, G., Downes, M., Yu, R. T., Shelton, J. M., Richardson, J. A., Repa, J. J., Mangelsdorf, D. J., & Kliewer, S. A. (2006). Regulation of antibacterial defense in the small intestine by the nuclear bile acid receptor. *Proceedings of the National Academy of Sciences of the United States of America*, *103*(10), 3920–3925. https://doi.org/10.1073/pnas.0509592103.
64. Ishimwe, N., Daliri, E. B., Lee, B. H., Fang, F., & Du, G. (2015). The perspective on cholesterol-lowering mechanisms of probiotics. *Molecular nutrition & food research*, *59*(1), 94–105. https://doi.org/10.1002/mnfr.201400548.
65. Islam, K. B., Fukiya, S., Hagio, M., Fujii, N., Ishizuka, S., Ooka, T., Ogura, Y., Hayashi, T., & Yokota, A. (2011). Bile acid is a host factor that regulates the composition of the cecal microbiota in rats. *Gastroenterology*, *141*(5), 1773–1781. https://doi.org/10.1053/j.gastro.2011.07.046.
66. Jayashree, S., Pooja, S., Pushpanathan, M., Rajendhran, J., & Gunasekaran, P. (2014). Identification and characterization of bile salt hydrolase genes from the genome of *Lactobacillus fermentum* MTCC 8711. *Applied biochemistry and biotechnology*, *174*(2), 855–866. https://doi.org/10.1007/s12010-014-1118-5.

67. Jia, B., Park, D., Hahn, Y., & Jeon, C. O. (2020). Metagenomic analysis of the human microbiome reveals the association between the abundance of gut bile salt hydrolases and host health. *Gut microbes*, *11*(5), 1300–1313. https://doi.org/10.1080/19490976.2020.1748261.
68. Jones, B. V., Begley, M., Hill, C., Gahan, C. G., & Marchesi, J. R. (2008). Functional and comparative metagenomic analysis of bile salt hydrolase activity in the human gut microbiome. *Proceedings of the National Academy of Sciences of the United States of America*, *105*(36), 13580–13585. https://doi.org/10.1073/pnas.0804437105.
69. Jones, M. L., Martoni, C. J., Parent, M., & Prakash, S. (2012a). Cholesterol-lowering efficacy of a microencapsulated bile salt hydrolase-active *Lactobacillus reuteri* NCIMB 30242 yoghurt formulation in hypercholesterolaemic adults. *The British journal of nutrition*, *107*(10), 1505–1513. https://doi.org/10.1017/S0007114511004703.
70. Jones, M. L., Martoni, C. J., & Prakash, S. (2012b). Cholesterol lowering and inhibition of sterol absorption by *Lactobacillus reuteri* NCIMB 30242: a randomized controlled trial. *European journal of clinical nutrition*, *66*(11), 1234–1241. https://doi.org/10.1038/ejcn.2012.126.
71. Jones, M. L., Tomaro-Duchesneau, C., Martoni, C. J., & Prakash, S. (2013). Cholesterol lowering with bile salt hydrolase-active probiotic bacteria, mechanism of action, clinical evidence, and future direction for heart health applications. *Expert opinion on biological therapy*, *13*(5), 631–642. https://doi.org/10.1517/14712598.2013.758706.
72. Joyce, S. A., MacSharry, J., Casey, P. G., Kinsella, M., Murphy, E. F., Shanahan, F., Hill, C., & Gahan, C. G. (2014). Regulation of host weight gain and lipid metabolism by bacterial bile acid modification in the gut. *Proceedings of the National Academy of Sciences of the United States of America*, *111*(20), 7421–7426. https://doi.org/10.1073/pnas.1323599111.
73. Juste, C., & Gérard, P. (2021). Cholesterol-to-Coprostanol Conversion by the Gut Microbiota: What We Know, Suspect, and Ignore. *Microorganisms*, *9*(9), 1881. https://doi.org/10.3390/microorganisms9091881.

74. Kaur, N., Chen, C. C., Luther, J., & Kao, J. Y. (2011). Intestinal dysbiosis in inflammatory bowel disease. *Gut microbes*, *2*(4), 211–216. https://doi.org/10.4161/gmic.2.4.17863.
75. Kaya, Y., Kök, M. Ş., & Öztürk, M. (2017). Molecular cloning, expression and characterization of bile salt hydrolase from *Lactobacillus rhamnosus* E9 strain. *Food Biotechnology*, *31*(2), 128-140. https://doi.org/10.1080/08905436.2017.1303778.
76. Keitel, V., Donner, M., Winandy, S., Kubitz, R., & Häussinger, D. (2008). Expression and function of the bile acid receptor TGR5 in Kupffer cells. *Biochemical and biophysical research communications*, *372*(1), 78–84. https://doi.org/10.1016/j.bbrc.2008.04.171.
77. Keleszade, E., Kolida, S., & Costabile, A. (2022). The cholesterol lowering efficacy of *Lactobacillus plantarum* ECGC 13110402 in hypercholesterolemic adults: a double-blind, randomized, placebo controlled, pilot human intervention study. *Journal of Functional Foods*, *89*, 104939. https://doi.org/10.1016/j.jff.2022.104939.
78. Kenny, D. J., Plichta, D. R., Shungin, D., Koppel, N., Hall, A. B., Fu, B., Vasan, R. S., Shaw, S. Y., Vlamakis, H., Balskus, E. P., & Xavier, R. J. (2020). Cholesterol Metabolism by Uncultured Human Gut Bacteria Influences Host Cholesterol Level. *Cell host & microbe*, *28*(2), 245–257.e6. https://doi.org/10.1016/j.chom.2020.05.013.
79. Khalesi, S., Bellissimo, N., Vandelanotte, C., Williams, S., Stanley, D., & Irwin, C. (2019). A review of probiotic supplementation in healthy adults: helpful or hype? *European journal of clinical nutrition*, *73*(1), 24-37. https://doi.org/10.1038/s41430-018-0135-9.
80. Khare, A., & Gaur, S. (2020). Cholesterol-Lowering Effects of *Lactobacillus* Species. *Current microbiology*, *77*(4), 638–644. https://doi.org/10.1007/s00284-020-01903-w.
81. Kim, G. B., & Lee, B. H. (2005). Biochemical and molecular insights into bile salt hydrolase in the gastrointestinal microflora-a review. *Asian-australasian journal of animal sciences*, *18*(10), 1505-1512. https://doi.org/10.5713/ajas.2005.1505.
82. Kim, S. J., Park, S. H., Sin, H. S., Jang, S. H., Lee, S. W., Kim, S. Y., Kwon, B., Yu, K. Y., Kim, S. Y., & Yang, D. K. (2017).

Hypocholesterolemic Effects of Probiotic Mixture on Diet-Induced Hypercholesterolemic Rats. *Nutrients*, *9*(3), 293. https://doi.org/10.3390/nu9030293.

83. Kim, G. B., Yi, S. H., & Lee, B. H. (2004). Purification and characterization of three different types of bile salt hydrolases from *Bifidobacterium* strains. *Journal of dairy science*, *87*(2), 258–266. https://doi.org/10.3168/jds.S0022-0302(04)73164-1.
84. Klaassen, C. D., & Aleksunes, L. M. (2010). Xenobiotic, bile acid, and cholesterol transporters: function and regulation. *Pharmacological reviews*, *62*(1), 1–96. https://doi.org/10.1124/pr.109.002014.
85. Klaver, F. A., & van der Meer, R. (1993). The assumed assimilation of cholesterol by Lactobacilli and *Bifidobacterium bifidum* is due to their bile salt-deconjugating activity. *Applied and environmental microbiology*, *59*(4), 1120–1124. https://doi.org/10.1128/aem.59.4.1120-1124.1993.
86. Kliewer, S. A., & Willson, T. M. (2002). Regulation of xenobiotic and bile acid metabolism by the nuclear pregnane X receptor. *Journal of lipid research*, *43*(3), 359–364. https://doi.org/10.1016/S0022-2275(20)30141-3.
87. Knarreborg, A., Engberg, R. M., Jensen, S. K., & Jensen, B. B. (2002). Quantitative determination of bile salt hydrolase activity in bacteria isolated from the small intestine of chickens. *Applied and environmental microbiology*, *68*(12), 6425–6428. https://doi.org/10.1128/AEM.68.12.6425-6428.2002.
88. Koppinger, M. P., Lopez-Pier, M. A., Skaria, R., Harris, P. R., & Konhilas, J. P. (2020). *Lactobacillus reuteri* attenuates cardiac injury without lowering cholesterol in low-density lipoprotein receptor-deficient mice fed standard chow. *American journal of physiology. Heart and circulatory physiology*, *319*(1), H32–H41. https://doi.org/10.1152/ajpheart.00569.2019.
89. Kriaa, A., Bourgin, M., Potiron, A., Mkaouar, H., Jablaoui, A., Gérard, P., Maguin, E., & Rhimi, M. (2019). Microbial impact on cholesterol and bile acid metabolism: current status and future prospects. *Journal of lipid research*, *60*(2), 323–332. https://doi.org/10.1194/jlr.R088989.

90. Kumar, R. S., Brannigan, J. A., Prabhune, A. A., Pundle, A. V., Dodson, G. G., Dodson, E. J., & Suresh, C. G. (2006). Structural and functional analysis of a conjugated bile salt hydrolase from Bifidobacterium longum reveals an evolutionary relationship with penicillin V acylase. *The Journal of biological chemistry*, *281*(43), 32516–32525. https://doi.org/10.1074/jbc.M604172200.
91. Kumar, R., Grover, S., & Batish, V. K. (2011). Hypocholesterolaemic effect of dietary inclusion of two putative probiotic bile salt hydrolase-producing *Lactobacillus plantarum* strains in Sprague-Dawley rats. *The British journal of nutrition*, *105*(4), 561–573. https://doi.org/10.1017/S0007114510003740.
92. Kumar, R., Grover, S., & Batish, V. K. (2012). Bile Salt Hydrolase (Bsh) Activity Screening of Lactobacilli: In Vitro Selection of Indigenous *Lactobacillus* Strains with Potential Bile Salt Hydrolysing and Cholesterol-Lowering Ability. *Probiotics and antimicrobial proteins*, *4*(3), 162–172. https://doi.org/10.1007/s12602-012-9101-3.
93. Kumar, R., Rajkumar, H., Kumar, M., Varikuti, S. R., Athimamula, R., Shujauddin, M., Ramagoni, R., & Kondapalli, N. (2013). Molecular cloning, characterization and heterologous expression of bile salt hydrolase (Bsh) from *Lactobacillus fermentum* NCDO394. *Molecular biology reports*, *40*(8), 5057–5066. https://doi.org/10.1007/s11033-013-2607-2.
94. Lambert, J. M., Bongers, R. S., de Vos, W. M., & Kleerebezem, M. (2008). Functional analysis of four bile salt hydrolase and penicillin acylase family members in *Lactobacillus plantarum* WCFS1. *Applied and environmental microbiology*, *74*(15), 4719–4726. https://doi.org/10.1128/AEM.00137-08.
95. Lau, K., Srivatsav, V., Rizwan, A., Nashed, A., Liu, R., Shen, R., & Akhtar, M. (2017). Bridging the Gap between Gut Microbial Dysbiosis and Cardiovascular Diseases. *Nutrients*, *9*(8), 859. https://doi.org/10.3390/nu9080859.
96. Lavelle, A., & Sokol, H. (2020). Gut microbiota-derived metabolites as key actors in inflammatory bowel disease. *Nature reviews. Gastroenterology & hepatology*, *17*(4), 223–237. https://doi.org/10.1038/s41575-019-0258-z.

97. Lee, M., Park, J., Kim, O. K., Kim, D., Han, M. J., Kim, S. H., Kim, T. H., & Lee, J. (2023). *Lactobacillus reuteri* NCIMB 30242 (LRC) Inhibits Cholesterol Synthesis and Stimulates Cholesterol Excretion in Animal and Cell Models. *Journal of medicinal food*, *26*(8), 529–539. https://doi.org/10.1089/jmf.2022.K.0137.
98. Li, G. (2012). Intestinal probiotics: interactions with bile salts and reduction of cholesterol. *Procedia Environmental Sciences*, *12*, 1180-1186. https://doi.org/10.1016/j.proenv.2012.01.405.
99. Li, F., Jiang, C., Krausz, K. W., Li, Y., Albert, I., Hao, H., Fabre, K. M., Mitchell, J. B., Patterson, A. D., & Gonzalez, F. J. (2013). Microbiome remodelling leads to inhibition of intestinal farnesoid X receptor signalling and decreased obesity. *Nature communications*, *4*, 2384. https://doi.org/10.1038/ncomms3384.
100. Li, H., Yu, X. H., Ou, X., Ouyang, X. P., & Tang, C. K. (2021). Hepatic cholesterol transport and its role in non-alcoholic fatty liver disease and atherosclerosis. *Progress in lipid research*, *83*, 101109. https://doi.org/10.1016/j.plipres.2021.101109.
101. Liang, L., Yi, Y., Lv, Y., Qian, J., Lei, X., & Zhang, G. (2018). A Comprehensive Genome Survey Provides Novel Insights into Bile Salt Hydrolase (BSH) in *Lactobacillaceae*. *Molecules (Basel, Switzerland)*, *23*(5), 1157. https://doi.org/10.3390/molecules23051157.
102. Linhorst, A., & Lübke, T. (2022). The Human Ntn-Hydrolase Superfamily: Structure, Functions and Perspectives. *Cells*, *11*(10), 1592. https://doi.org/10.3390/cells11101592.
103. Liong, M. T., & Shah, N. P. (2005). Bile salt deconjugation ability, bile salt hydrolase activity and cholesterol co-precipitation ability of lactobacilli strains. *International Dairy Journal*, *15*(4), 391-398. https://doi.org/10.1016/j.idairyj.2004.08.007.
104. Liu, Y., Zheng, S., Cui, J., Guo, T., & Zhang, J. (2021). Effect of bile salt hydrolase-active Lactobacillus plantarum Y15 on high cholesterol diet induced hypercholesterolemic mice. *CyTA-Journal of Food*, *19*(1), 408-417. https://doi.org/10.1080/19476337.2021.1914176.
105. Liu, J., Zhu, R., Song, J., Sohaib, M., Wang, S., Mao, J., Qi, J., Xiong, X., Zhou, W., & Guo, L. (2023). *Limosilactobacillus reuteri* consumption significantly reduces the total cholesterol concentration

without affecting other cardiovascular disease risk factors in adults: A systematic review and meta-analysis. *Nutrition research (New York, N.Y.)*, *117*, 1–14. https://doi.org/10.1016/j.nutres.2023.06.004.

106. Long, S. L., Gahan, C. G. M., & Joyce, S. A. (2017). Interactions between gut bacteria and bile in health and disease. *Molecular aspects of medicine*, *56*, 54–65. https://doi.org/10.1016/j.mam.2017.06.002.
107. Lucas, L. N., Barrett, K., Kerby, R. L., Zhang, Q., Cattaneo, L. E., Stevenson, D., Rey, F. E., & Amador-Noguez, D. (2021). Dominant Bacterial Phyla from the Human Gut Show Widespread Ability To Transform and Conjugate Bile Acids. *mSystems*, e0080521. Advance online publication. https://doi.org/10.1128/mSystems.00805-21.
108. Luo, J., Yang, H., & Song, B. L. (2020). Mechanisms and regulation of cholesterol homeostasis. *Nature reviews. Molecular cell biology*, *21*(4), 225–245. https://doi.org/10.1038/s41580-019-0190-7.
109. Lv, Y., Luo, Y. Y., Ren, H. W., Li, C. J., Xiang, Z. X., & Luan, Z. L. (2022). The role of pregnane X receptor (PXR) in substance metabolism. *Frontiers in endocrinology*, *13*, 959902. https://doi.org/10.3389/fendo.2022.959902.
110. Lye, H. S., Kato, T., Low, W. Y., Taylor, T. D., Prakash, T., Lew, L. C., Ohno, H., & Liong, M. T. (2017). *Lactobacillus fermentum* FTDC 8312 combats hypercholesterolemia via alteration of gut microbiota. *Journal of biotechnology*, *262*, 75–83. https://doi.org/10.1016/j.jbiotec.2017.09.007.
111. Lye, H. S., Rusul, G., & Liong, M. T. (2010). Removal of cholesterol by lactobacilli via incorporation and conversion to coprostanol. *Journal of dairy science*, *93*(4), 1383–1392. https://doi.org/10.3168/jds.2009-2574.
112. Ma, C., Han, M., Heinrich, B., Fu, Q., Zhang, Q., Sandhu, M., Agdashian, D., Terabe, M., Berzofsky, J. A., Fako, V., Ritz, T., Longerich, T., Theriot, C. M., McCulloch, J. A., Roy, S., Yuan, W., Thovarai, V., Sen, S. K., Ruchirawat, M., Korangy, F., … Greten, T. F. (2018). Gut microbiome-mediated bile acid metabolism regulates liver cancer via NKT cells. *Science (New York, N.Y.)*, *360*(6391), eaan5931. https://doi.org/10.1126/science.aan5931.
113. Mahmoudian Dehkordi, S., Arnold, M., Nho, K., Ahmad, S., Jia, W., Xie, G., Louie, G., Kueider-Paisley, A., Moseley, M. A., Thompson, J.

W., St John Williams, L., Tenenbaum, J. D., Blach, C., Baillie, R., Han, X., Bhattacharyya, S., Toledo, J. B., Schafferer, S., Klein, S., Koal, T., … Alzheimer's Disease Neuroimaging Initiative and the Alzheimer Disease Metabolomics Consortium (2019). Altered bile acid profile associates with cognitive impairment in Alzheimer's disease-An emerging role for gut microbiome. *Alzheimer's & dementia : the journal of the Alzheimer's Association*, *15*(1), 76–92. https://doi.org/10.1016/j.jalz.2018.07.217.

114. Malpeli, A., Taranto, M. P., Cravero, R. C., Tavella, M., Fasano, M. V., Vicentin, D., Ferraris, G., Magrini, G., Hébert, E., Font de Valdez, G., Varea, A. M., Tavella, J. M., & González, H. F. (2015). Effect of daily consumption of *Lactobacillus reuteri* CRL 1098 on cholesterol reduction in hypercholesterolemic subjects. *Food and Nutrition Sciences*, *6*. http://dx.doi.org/10.4236/fns.2015.617163.
115. Manolis, A. A., Manolis, T. A., Melita, H., & Manolis, A. S. (2022). Gut Microbiota and Cardiovascular Disease: Symbiosis Versus Dysbiosis. *Current medicinal chemistry*, *29*(23), 4050–4077. https://doi.org/10.2174/0929867328666211213112949.
116. Marchesini, M. I., Connolly, J., Delpino, M. V., Baldi, P. C., Mujer, C. V., DelVecchio, V. G., & Comerci, D. J. (2011). *Brucella abortus* choloylglycine hydrolase affects cell envelope composition and host cell internalization. *PloS one*, *6*(12), e28480. https://doi.org/10.1371/journal.pone.0028480.
117. Marteau, P., Gerhardt, M. F., Myara, A., Bouvier, E., & Rambaud J. C. (1995). Metabolism of bile salts by alimentary bacteria during transit in the human small intestine. *Microbial Ecology in Health and Disease, 8(4)*, 151–157. https://doi.org/10.3109/08910609509140093.
118. Martoni, C. J., Labbé, A., Ganopolsky, J. G., Prakash, S., & Jone M. L. (2015). Changes in bile acids, FGF-19 and sterol absorption in response to bile salt hydrolase active *L. reuteri* NCIMB 30242. *Gut microbes*, *6*(1), 57–65. https://doi.org/10.1080/19490976.2015.1005474.
119. Mathara, J. M., Schillinger, U., Guigas, C., Franz, C., Kutima, P. M., Mbugua, S. K., Shin, H. K., & Holzapfel, W. H. (2008). Functional characteristics of *Lactobacillus* spp. from traditional Maasai fermented

milk products in Kenya. *International journal of food microbiology*, *126*(1-2), 57–64. https://doi.org/10.1016/j.ijfoodmicro.2008.04.027.

120. McAuliffe, O., Cano, R. J., & Klaenhammer, T. R. (2005). Genetic analysis of two bile salt hydrolase activities in *Lactobacillus acidophilus* NCFM. *Applied and environmental microbiology*, *71*(8), 4925–4929. https://doi.org/10.1128/AEM.71.8.4925-4929.2005.
121. Miremadi, F., Ayyash, M., Sherkat, F., & Stojanovska, L. (2014). Cholesterol reduction mechanisms and fatty acid composition of cellular membranes of probiotic Lactobacilli and *Bifidobacteria*. *Journal of Functional Foods*, *9*, 295-305. https://doi.org/10.1016/j.jff.2014.05.002.
122. Mo, R., Zhang, X., & Yang, Y. (2019). Effect of probiotics on lipid profiles in hypercholesterolaemic adults: A meta-analysis of randomized controlled trials. *Medicina clinica*, *152*(12), 473–481. https://doi.org/10.1016/j.medcli.2018.09.007.
123. Monteiro-Cardoso, V. F., Corlianò, M., & Singaraja, R. R. (2021). Bile Acids: A Communication Channel in the Gut-Brain Axis. *Neuromolecular medicine*, *23*(1), 99–117. https://doi.org/10.1007/s12017-020-08625-z.
124. Mortensen, M. B., & Nordestgaard, B. G. (2020). Elevated LDL cholesterol and increased risk of myocardial infarction and atherosclerotic cardiovascular disease in individuals aged 70-100 years: a contemporary primary prevention cohort. *Lancet (London, England)*, *396*(10263), 1644–1652. https://doi.org/10.1016/S0140-6736(20)32233-9.
125. Mu, Q., Tavella, V. J., & Luo, X. M. (2018). Role of *Lactobacillus reuteri* in Human Health and Diseases. *Frontiers in microbiology*, *9*, 757. https://doi.org/10.3389/fmicb.2018.00757.
126. Mulak A. (2021). Bile Acids as Key Modulators of the Brain-Gut-Microbiota Axis in Alzheimer's Disease. *Journal of Alzheimer's disease : JAD*, *84*(2), 461–477. https://doi.org/10.3233/JAD-210608.
127. Nagengast, F. M., Grubben, M. J., & van Munster, I. P. (1995). Role of bile acids in colorectal carcinogenesis. *European journal of cancer (Oxford, England: 1990)*, *31A*(7-8), 1067–1070. https://doi.org/10.1016/0959-8049(95)00216-6.

128. Nemes, K., Åberg, F., Gylling, H., & Isoniemi, H. (2016). Cholesterol metabolism in cholestatic liver disease and liver transplantation: From molecular mechanisms to clinical implications. *World journal of hepatology*, *8*(22), 924–932. https://doi.org/10.4254/wjh.v8.i22.924.
129. Nesci, A., Carnuccio, C., Ruggieri, V., D'Alessandro, A., Di Giorgio, A., Santoro, L., Gasbarrini, A., Santoliquido, A., & Ponziani, F. R. (2023). Gut Microbiota and Cardiovascular Disease: Evidence on the Metabolic and Inflammatory Background of a Complex Relationship. *International journal of molecular sciences*, *24*(10), 9087. https://doi.org/10.3390/ijms24109087.
130. Nguyen, T. D., Kang, J. H., & Lee, M. S. (2007). Characterization of *Lactobacillus plantarum* PH04, a potential probiotic bacterium with cholesterol-lowering effects. *International journal of food microbiology*, *113*(3), 358–361. https://doi.org/10.1016/j.ijfoodmicro.2006.08.015Niamah, A. K., Sahi, A. A., & Al-Sharifi, A. S. N. (2017). Effect of Feeding Soy Milk Fermented by Probiotic Bacteria on Some Blood Criteria and Weight of Experimental Animals. *Probiotics and antimicrobial proteins*, *9*(3), 284–291. https://doi.org/10.1007/s12602-017-9265-y.
131. Niamah, A. K., Sahu, A. A., & Al-Sharifi, A. S. N. (2017). Effect of the feeding soy milk fermented by probiotic bacteria o some dlood criteria and weight of experimental animals. *Probiotics and Antimicrobial Proteins, 9(3),* 284-291. https://doi.org/10.1007/s12602-017-9265-y.
132. Novakovic, M., Rout, A., Kingsley, T., Kirchoff, R., Singh, A., Verma, V., Kant, R., & Chaudhary, R. (2020). Role of gut microbiota in cardiovascular diseases. *World journal of cardiology*, *12*(4), 110–122. https://doi.org/10.4330/wjc.v12.i4.110.
133. Núñez-Sánchez, M. A., Herisson, F. M., Keane, J. M., García-González, N., Rossini, V., Pinhiero, J., Daly, J., Bustamante-Garrido, M., Hueston, C. M., Patel, S., Canela, N., Herrero, P., Claesson, M. J., Melgar, S., Nally, K., Caplice, N. M., & Gahan, C. G. M. (2022). Microbial bile salt hydrolase activity influences gene expression profiles and gastrointestinal maturation in infant mice. *Gut microbes*, *14*(1), 2149023. https://doi.org/10.1080/19490976.2022.2149023.

134. O'Flaherty, S., Briner Crawley, A., Theriot, C. M., & Barrangou, R. (2018). The *Lactobacillus* bile salt hyrdrolase repertoire reveals niche-specific adaptation. *mSphere, 21*(24), Article 9737. https://doi.org/10.1128/mSphere.00140-18.
135. Olas B. (2020). Probiotics, Prebiotics and Synbiotics-A Promising Strategy in Prevention and Treatment of Cardiovascular Diseases? *International journal of molecular sciences*, *21*(24), 9737. https://doi.org/10.3390/ijms21249737.
136. Ooi, L. G., & Liong, M. T. (2010). Cholesterol-lowering effects of probiotics and prebiotics: a review of *in vivo* and *in vitro* findings. *International journal of molecular sciences*, *11*(6), 2499–2522. https://doi.org/10.3390/ijms11062499.
137. Ou, J., Carbonero, F., Zoetland, E. G., DeLany, J. P., Wang, M., Newton, K., Gaskis, H. R., & O'Keefe, S. J. (2013). Diet, microbiota, and microbial metabolites in colon cancer risk in rural Africans and African Americans. *The American Journal of Clinical Nutrition, 98*(1), 111-120. https://doi.org/10.3945/ajcn.112.056689.
138. Palaniyandi, S. A., Damodharan, K., Suh, J. W., & Yang, S. H. (2020). Probiotic Characterization of Cholesterol-Lowering *Lactobacillus fermentum* MJM60397. *Probiotics and antimicrobial proteins*, *12*(3), 1161–1172. https://doi.org/10.1007/s12602-019-09585-y.
139. Pan, D. D., Zeng, X. Q., & Yan, Y. T. (2011). Characterisation of *Lactobacillus fermentum* SM-7 isolated from koumiss, a potential probiotic bacterium with cholesterol-lowering effects. *Journal of the science of food and agriculture*, *91*(3), 512–518. https://doi.org/10.1002/jsfa.4214.
140. Pandey, K. R., Naik, S. R., & Vakil, B. V. (2015). Probiotics, prebiotics and synbiotics- a review. *Journal of food science and technology*, *52*(12), 7577–7587. https://doi.org/10.1007/s13197-015-1921-1.
141. Park, Y. H., Kim, J. G., Shin, Y. W., Kim, S. H., & Whang, K. Y. (2007). Effect of dietary inclusion of *Lactobacillus acidophilus* ATCC 43121 on cholesterol metabolism in rats. *Journal of microbiology and biotechnology*, *17*(4), 655–662. http://dx.doi.org/10.1007/s12602-023-10171-6.

142. Parséus, A., Sommer, N., Sommer, F., Caesar, R., Molinaro, A., Ståhlman, M., Greiner, T. U., Perkins, R., & Bäckhed, F. (2017). Microbiota-induced obesity requires farnesoid X receptor. *Gut*, *66*(3), 429–437. https://doi.org/10.1136/gutjnl-2015-310283.
143. Patel, A. K., Singhania, R. R., Pandey, A., & Chincholkar, S. B. (2010). Probiotic bile salt hydrolase: current developments and perspectives. *Applied biochemistry and biotechnology*, *162*(1), 166–180. https://doi.org/10.1007/s12010-009-8738-1.
144. Pavlović, N., Stankov, K., & Mikov, M. (2012). Probiotics--interactions with bile acids and impact on cholesterol metabolism. *Applied biochemistry and biotechnology*, *168*(7), 1880–1895. https://doi.org/10.1007/s12010-012-9904-4Payne, A. H., & Hales, D. B. (2004). Overview of steroidogenic enzymes in the pathway from cholesterol to active steroid hormones. *Endocrine reviews*, *25*(6), 947–970. https://doi.org/10.1210/er.2003-0030.
145. Payne, A. H, & Hales, D. B. (2004). Overview of steroidogenic enzymes in the pathway from cholesterol to active steroid hormones. *Endocrine Reviews, 25*(6), 947-970. https://doi.org/10.1210/er.2003-0030 .
146. Pazzi, P., Puviani, A. C., Dalla Libera, M., Guerra, G., Ricci, D., Gullini, S., & Ottolenghi, C. (1997). Bile salt-induced cytotoxicity and ursodeoxycholate cytoprotection: in-vitro study in perifused rat hepatocytes. *European journal of gastroenterology & hepatology*, *9*(7), 703–709. https://doi.org/10.1097/00042737-199707000-00011.
147. Pereira, D. I., McCartney, A. L., & Gibson, G. R. (2003). An in vitro study of the probiotic potential of a bile-salt-hydrolyzing *Lactobacillus fermentum* strain, and determination of its cholesterol-lowering properties. *Applied and environmental microbiology*, *69*(8), 4743–4752. https://doi.org/10.1128/AEM.69.8.4743-4752.2003.
148. Poland, J. C., & Flynn, C. R. (2021). Bile Acids, Their Receptors, and the Gut Microbiota. *Physiology (Bethesda, Md.)*, *36*(4), 235–245. https://doi.org/10.1152/physiol.00028.2020.
149. Pols, T. W., Noriega, L. G., Nomura, M., Auwerx, J., & Schoonjans, K. (2011). The bile acid membrane receptor TGR5 as an emerging target in metabolism and inflammation. *Journal of hepatology*, *54*(6), 1263–1272. https://doi.org/10.1016/j.jhep.2010.12.004.

150. Principi, N., Cozzali, R., Farinelli, E., Brusaferro, A., & Esposito, S. (2018). Gut dysbiosis and irritable bowel syndrome: The potential role of probiotics. *The Journal of infection*, *76*(2), 111–120. https://doi.org/10.1016/j.jinf.2017.12.013.
151. Quinn, R. A., Melnik, A. V., Vrbanac, A., Fu, T., Patras, K. A., Christy, M. P., Bodai, Z., Belda-Ferre, P., Tripathi, A., Chung, L. K., Downes, M., Welch, R. D., Quinn, M., Humphrey, G., Panitchpakdi, M., Weldon, K. C., Aksenov, A., da Silva, R., Avila-Pacheco, J., Clish, C., … Dorrestein, P. C. (2020). Global chemical effects of the microbiome include new bile-acid conjugations. *Nature*, *579*(7797), 123–129. https://doi.org/10.1038/s41586-020-2047-9.
152. Ramkumar, S., Raghunath, A., & Raghunath, S. (2016). Statin Therapy: Review of Safety and Potential Side Effects. *Acta Cardiologica Sinica*, *32*(6), 631–639. https://doi.org/10.6515/acs20160611a .
153. Reis, S. A., Conceição, L. L., Rosa, D. D., Siqueira, N. P., & Peluzio, M. C. G. (2017). Mechanisms responsible for the hypocholesterolaemic effect of regular consumption of probiotics. *Nutrition research reviews*, *30*(1), 36–49. https://doi.org/10.1017/S0954422416000226.
154. Ren, J., Sun, K., Wu, Z., Yao, J., & Guo, B. (2011). All 4 bile salt hydrolase proteins are responsible for the hydrolysis activity in *Lactobacillus plantarum* ST-III. *Journal of food science*, *76*(9), M622–M628. https://doi.org/10.1111/j.1750-3841.2011.02431.x.
155. Ridlon J. M. (2020). Conceptualizing the Vertebrate Sterolbiome. *Applied and environmental microbiology*, *86*(16), e00641-20. https://doi.org/10.1128/AEM.00641-20.
156. Ridlon, J. M., Harris, S. C., Bhowmik, S., Kang, D. J., & Hylemon, P. B. (2016). Consequences of bile salt biotransformations by intestinal bacteria. *Gut microbes*, *7*(1), 22–39. https://doi.org/10.1080/19490976.2015.1127483.
157. Ridlon, J. M., Kang, D. J., & Hylemon, P. B. (2006). Bile salt biotransformations by human intestinal bacteria. *Journal of lipid research*, *47*(2), 241–259. https://doi.org/10.1194/jlr.R500013-JLR200.
158. Ridlon, J. M., Kang, D. J., Hylemon, P. B., & Bajaj, J. S. (2014). Bile acids and the gut microbiome. *Current opinion in*

gastroenterology, *30*(3), 332–338. https://doi.org/10.1097/MOG.0000000000000057.

159. Schade, D. S., Shey, L., & Eaton, R. P. (2020). Cholesterol Review: A Metabolically Important Molecule. *Endocrine practice : official journal of the American College of Endocrinology and the American Association of Clinical Endocrinologists*, *26*(12), 1514–1523. https://doi.org/10.4158/EP-2020-0347.
160. Shapiro, H., Kolodziejczyk, A. A., Halstuch, D., & Elinav, E. (2018). Bile acids in glucose metabolism in health and disease. *The Journal of experimental medicine*, *215*(2), 383–396. https://doi.org/10.1084/jem.20171965Shehata M.G., El Sohaimy S.A., Malak A. El-Sahn, Youssef M.M. (2016). Screening of isolated potential probiotic lactic acid bacteria for cholesterol lowering property and bile salt hydrolase activity. *Annals of Agricultural Sciences*, *Volume 61, Issue 1,* Pages 65-75, ISSN 0570-1783. https://doi.org/10.1016/j.aoas.2016.03.001.
161. Shehata, M. G., El Sohaimy, S. A., El-Sahn, M. A., & Youssef, M. M. (2016). Screening of isolated potential probiotic lactic acid bacteria for cholesterol lowering property and bile salt hydrolase activity. *Annals of Agricultural Sciences,* *61*(1), 65-75. https://doi.org/10.1016/j.aoas.2016.03.001.
162. Singhal, N., Maurya, A. K., Mohanty, S., Kumar, M., & Virdi, J. S. (2019). Evaluation of Bile Salt Hydrolases, Cholesterol-Lowering Capabilities, and Probiotic Potential of *Enterococcus faecium* Isolated From Rhizosphere. *Frontiers in microbiology*, *10*, 1567. https://doi.org/10.3389/fmicb.2019.01567.
163. Sirilun, S., Chaiyasut, C., Kantachote, D., & Luxananil, P. (2010). Characterisation of non human origin probiotic *Lactobacillus plantarum* with cholesterol-lowering property. *Afr J Microbiol Res*, *4*(10), 994-1000. https://api.semanticscholar.org/CorpusID:52212894.
164. Sjövall, J., Griffiths, W. J., Setchell, K. D., Mano, N., & Goto, J. (2010). Analysis of bile acids. *Steroid analysis*, 837-966. https://doi.org/10.1016/j.foodres.2009.02.016.
165. Song, Z., Cai, Y., Lao, X., Wang, X., Lin, X., Cui, Y., Kalavagunta, P. K., Liao, J., Jin, L., Shang, J., & Li, J. (2019). Taxonomic profiling and

populational patterns of bacterial bile salt hydrolase (BSH) genes based on worldwide human gut microbiome. *Microbiome*, *7*(1), 9. https://doi.org/10.1186/s40168-019-0628-3.

166. Song, Z., Feng, S., Zhou, X., Song, Z., Li, J., & Li, P. (2023). Taxonomic identification of bile salt hydrolase-encoding lactobacilli: Modulation of the enterohepatic bile acid profile. *iMeta*, *2*(3), e128. https://doi.org/10.1002/imt2.128.
167. Sridevi, N., Vishwe, P., & Prabhune, A. (2009). Hypocholesterolemic effect of bile salt hydrolase from *Lactobacillus buchneri* ATCC 4005. *Food Research International, 42*(4), 516-520. http://dx.doi.org/10.1016/j.foodres.2009.02.016.
168. Sudun, Liu, S., Xiao, C., Peng, C., Liang, L., He, X., Zhao, S., & Zhang, G. (2019). Probiotic strains improve high-fat diet-induced hypercholesterolemia through modulating gut microbiota in ways different from atorvastatin. *Food & function*, *10*(9), 6098–6109. https://doi.org/10.1039/c9fo00444k.
169. Suez, J., Zmora, N., Segal, E., & Elinav, E. (2019). The pros, cons, and many unknowns of probiotics. *Nature medicine*, *25*(5), 716–729. https://doi.org/10.1038/s41591-019-0439-x.
170. Sun, M. C., Hu, Z. Y., Li, D. D., Chen, Y. X., Xi, J. H., & Zhao, C. H. (2022). Application of the Reuterin System as Food Preservative or Health-Promoting Agent: A Critical Review. *Foods (Basel, Switzerland)*, *11*(24), 4000. https://doi.org/10.3390/foods11244000.
171. Tanaka, H., Doesburg, K., Iwasaki, T., & Mierau, I. (1999). Screening of lactic acid bacteria for bile salt hydrolase activity. *Journal of dairy science*, *82*(12), 2530–2535. https://doi.org/10.3168/jds.S0022-0302(99)75506-2.
172. Tanaka, H., Hashiba, H., Kok, J., & Mierau, I. (2000). Bile salt hydrolase of *Bifidobacterium longum*-biochemical and genetic characterization. *Applied and environmental microbiology*, *66*(6), 2502–2512. https://doi.org/10.1128/AEM.66.6.2502-2512.2000.
173. Tang, W. H., Kitai, T., & Hazen, S. L. (2017). Gut microbiota in cardiovascular health and disease. *Circulation Research, 120*(7), 1183-1196. https://doi.org/10.1161/CIRCRESAHA.117.309715.

174. Taranto, M. P., Medici, M., Perdigon, G., Ruiz Holgado, A. P., & Valdez, G. F. (2000). Effect of *Lactobacillus reuteri* on the prevention of hypercholesterolemia in mice. *Journal of dairy science*, *83*(3), 401–403. https://doi.org/10.3168/jds.S0022-0302(00)74895-8.
175. Thanissery, R., Winston, J. A., & Theriot, C. M. (2017). Inhibition of spore germination, growth, and toxin activity of clinically relevant *C. difficile* strains by gut microbiota derived secondary bile acids. *Anaerobe*, *45*, 86–100. https://doi.org/10.1016/j.anaerobe.2017.03.004.
176. Theriot, C. M., Koenigsknecht, M. J., Carlson, P. E., Jr, Hatton, G. E., Nelson, A. M., Li, B., Huffnagle, G. B., Z Li, J., & Young, V. B. (2014). Antibiotic-induced shifts in the mouse gut microbiome and metabolome increase susceptibility to *Clostridium difficile* infection. *Nature communications*, *5*, 3114. https://doi.org/10.1038/ncomms4114.
177. Thomas, C., Gioiello, A., Noriega, L., Strehle, A., Oury, J., Rizzo, G., Macchiarulo, A., Yamamoto, H., Mataki, C., Pruzanski, M., Pellicciari, R., Auwerx, J., & Schoonjans, K. (2009). TGR5-mediated bile acid sensing controls glucose homeostasis. *Cell metabolism*, *10*(3), 167–177. https://doi.org/10.1016/j.cmet.2009.08.001.
178. Thompson, P. D., Panza, G., Zaleski, A., & Taylor, B. (2016). Statin-Associated Side Effects. *Journal of the American College of Cardiology*, *67*(20), 2395–2410. https://doi.org/10.1016/j.jacc.2016.02.071.
179. Tian, L., Liu, R., Zhou, Z., Xu, X., Feng, S., Kushmaro, A., Marks, R. S., Wang, D., & Sun, Q. (2022). Probiotic Characteristics of *Lactiplantibacillus plantarum* N-1 and Its Cholesterol-Lowering Effect in Hypercholesterolemic Rats. *Probiotics and antimicrobial proteins*, *14*(2), 337–348. https://doi.org/10.1007/s12602-021-09886-1.
180. Tomaro-Duchesneau, C., Jones, M. L., Shah, D., Jain, P., Saha, S., & Prakash, S. (2014). Cholesterol assimilation by *Lactobacillus* probiotic bacteria: an *in vitro* investigation. *BioMed research international*, *2014*, 380316. https://doi.org/10.1155/2014/380316.
181. Tsai, C. C., Lin, P. P., Hsieh, Y. M., Zhang, Z. Y., Wu, H. C., & Huang, C. C. (2014). Cholesterol-lowering potentials of lactic acid bacteria based on bile-salt hydrolase activity and effect of potent strains on

cholesterol metabolism in vitro and in vivo. *TheScientificWorldJournal*, *2014*, 690752. https://doi.org/10.1155/2014/690752.

182. van der Wulp, M. Y., Verkade, H. J., & Groen, A. K. (2013). Regulation of cholesterol homeostasis. *Molecular and cellular endocrinology*, *368*(1-2), 1–16. https://doi.org/10.1016/j.mce.2012.06.007.
183. Venneman, N. G., & van Erpecum, K. J. (2010). Pathogenesis of gallstones. *Gastroenterology clinics of North America*, *39*(2), 171–vii. https://doi.org/10.1016/j.gtc.2010.02.010.
184. Veysey, M. J., Thomas, L. A., Mallet, A. I., Jenkins, P. J., Besser, G. M., Wass, J. A., Murphy, G. M., & Dowling, R. H. (1999). Prolonged large bowel transit increases serum deoxycholic acid: a risk factor for octreotide induced gallstones. *Gut*, *44*(5), 675–681. https://doi.org/10.1136/gut.44.5.675.
185. Vourakis, M., Mayer, G., & Rousseau, G. (2021). The Role of Gut Microbiota on Cholesterol Metabolism in Atherosclerosis. *International journal of molecular sciences*, *22*(15), 8074. https://doi.org/10.3390/ijms22158074.
186. Wahlström, A., Sayin, S. I., Marschall, H. U., & Bäckhed, F. (2016). Intestinal Crosstalk between Bile Acids and Microbiota and Its Impact on Host Metabolism. *Cell metabolism*, *24*(1), 41–50. https://doi.org/10.1016/j.cmet.2016.05.005.
187. Walker, D. K., & Gilliland, S. E. (1993). Relationship among bile tolerance, bile salt deconjugation, and assimilation of cholesterol by *Lactobacillus acidophilus*. *Journal of dairy science*, *76*(4), 956–961. https://doi.org/10.3168/jds.s0022-0302(93)77422-6.
188. Wang, L., Guo, M. J., Gao, Q., Yang, J. F., Yang, L., Pang, X. L., & Jiang, X. J. (2018). The effects of probiotics on total cholesterol: A meta-analysis of randomized controlled trials. *Medicine*, *97*(5), e9679. https://doi.org/10.1097/MD.0000000000009679.
189. Wang, G., Huang, W., Xia, Y., Xiong, Z., & Ai, L., (2019). Cholesterol-lowering potentials of *Lactobacillus* strain overexpression of bile salt hydrolase on high cholesterol diet-induced hypercholesterolemic

mice. *Food & function*, *10*(3), 1684–1695. https://doi.org/10.1039/c8fo02181c.

190. Wang, G., Yu, H., Feng, X., Tang, H., Xiong, Z., Xia, Y., Ai L., & Song, X. (2021). Specific bile salt hydrolase genes in *Lactobacillus plantarum* AR113 and relationship with bile salt resistance. *LWT*, *145*, 111208. https://doi.org/10.1016/j.lwt.2021.111208.
191. Wastyk, H. C., Perelman, D., Topf, M., Fragiadakis, G. K., Robinson, J. L., Sonnenburg, J. L., Gardner, C. D., & Sonnenburg, E. D. (2023). Randomized controlled trial demonstrates response to a probiotic intervention for metabolic syndrome that may correspond to diet. *Gut microbes*, *15*(1), 2178794. https://doi.org/10.1080/19490976.2023.2178794.
192. Widodo, W., Fanani, T. H., Fahreza, M. I., & Sukarno, A. S. (2021). Cholesterol assimilation of two probiotic strains of *Lactobacillus casei* used as dairy starter cultures. *Applied Food Biotechnology*, *8*(2), 103-112. https://doi.org/10.22037/afb.v8i2.30661.
193. Witkowski, M., Weeks, T. L., & Hazen, S. L. (2020). Gut Microbiota and Cardiovascular Disease. *Circulation research*, *127*(4), 553–570. https://doi.org/10.1161/CIRCRESAHA.120.316242.
194. World Health Organization. (2024). *Global patient safety report 2024*. World Health Organization. https://www.who.int/data/gho/indicator-metadata-registry/imr-details/3236.
195. Wu, Y., Zhang, Q., Ren, Y., & Ruan, Z. (2017). Effect of probiotic *Lactobacillus* on lipid profile: A systematic review and meta-analysis of randomized, controlled trials. *PloS one*, *12*(6), e0178868. https://doi.org/10.1371/journal.pone.0178868.
196. Xiang, T., Deng, Z., Yang, C., Tan, J., Dou, C., Luo, F., & Chen, Y. (2023). Bile acid metabolism regulatory network orchestrates bone homeostasis. *Pharmacological research*, *196*, 106943. https://doi.org/10.1016/j.phrs.2023.106943.
197. Yang, Y., & Wu, C. (2022). Targeting gut microbial bile salt hydrolase (BSH) by diet supplements: new insights into dietary modulation of human health. *Food & function*, *13*(14), 7409–7422. https://doi.org/10.1039/d2fo01252a.

198. Yao, L., Seaton, S. C., Ndousse-Fetter, S., Adhikari, A. A., DiBenedetto, N., Mina, A. I., Banks, A. S., Bry, L., & Devlin, A. S. (2018). A selective gut bacterial bile salt hydrolase alters host metabolism. *eLife*, *7*, e37182. https://doi.org/10.7554/eLife.37182.
199. Yntema, T., Koonen, D. P. Y., & Kuipers, F. (2023). Emerging Roles of Gut Microbial Modulation of Bile Acid Composition in the Etiology of Cardiovascular Diseases. *Nutrients*, *15*(8), 1850. https://doi.org/10.3390/nu15081850.
200. Zafar, H., Ain, N. U., Alshammari, A., Alghamdi, S., Raja, H., Ali, A., Siddique, A., Tahir, S. D., Akbar, S., Arif, M., Alharbi, M., & Rahman, A. (2022). *Lacticaseibacillus rhamnosus* FM9 and *Limosilactobacillus fermentum* Y57 Are as Effective as Statins at Improving Blood Lipid Profile in High Cholesterol, High-Fat Diet Model in Male Wistar Rats. *Nutrients*, *14*(8), 1654. https://doi.org/10.3390/nu14081654.
201. Zhao, Y., Yu, L., Tian, F., Zhao, J., Zhang, H., Chen, W., Xue, Y., & Zhai, Q. (2022). Environment-Related Genes Analysis of *Limosilactobacillus fermentum* Isolated from Food and Human Gut: Genetic Diversity and Adaption Evolution. *Foods (Basel, Switzerland)*, *11*(19), 3135. https://doi.org/10.3390/foods11193135.
202. Zhu, H., Zhao, F., Zhang, W., Xia, W., Chen, Y., Liu, Y., Fan, Z., Zhang, Y., & Yang, Y. (2022). Cholesterol-lowering effect of bile salt hydrolase from a *Lactobacillus johnsonii* strain mediated by FXR pathway regulation. *Food & function*, *13*(2), 725–736. https://doi.org/10.1039/d1fo03143k

Chapter 2

2 Genomic mining and characterization of two novel *Lacticaseibacillus rhamnosus* probiotic candidates with Bile salt hydrolase activity

Gianluigi Agolino[1], Marianna Cristofolini[2], Amanda Vaccalluzzo[1], Davide Tagliazucchi[2], Alice Cattivelli[2], Alessandra Pino[1,3,*], Cinzia Caggia[1,3], Lisa Solieri[2,**], and Cinzia Lucia Randazzo[1,3]

[1]Department of Agriculture, Food and Environment (Di3A), University of Catania, Via Santa Sofia 100, 95123 Catania, Italy
[2]Department of Life Sciences, University of Modena and Reggio Emilia, Via Amendola, 2-Pad. Besta, 42100 Reggio Emilia, Italy
[3]Probioetna SRL, Spin off of University of Catania, Via Santa Sofia 100, 95123 Catania, Italy

*Corresponding author: alessandra.pino@unimore.it (A. Pino)
**Corresponding author: lisa.solieri@unimore.it (L. Solieri)

Published in *Biomolecules, 2025, 15(1), 86*
DOI: https://doi.org/10.3390/biom15010086

Graphical abstract

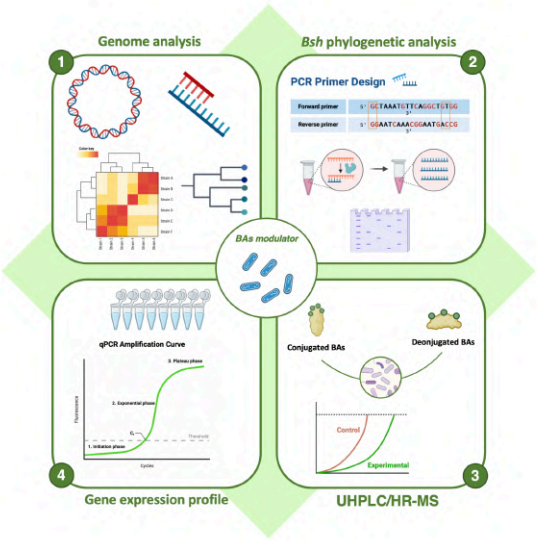

Abstract

Bile salt hydrolase (BSH: EC 3.5.1.24) is the microbial enzyme that catalyzes the conversion of primary bile acids (BAs) into secondary ones, promoting microbial adaptation and modulating several host's biological functions. Probiotics with BSH activity are supposed to survive harsh intestinal conditions and exert a cholesterol-lowering effect. Here, *Lacticaseibacillus rhamnosus* strains (VB4 and VB1), isolated from the vaginal ecosystem, were submitted to a genomic survey, *in vitro* BSH activity, and BAs tolerance assay to unravel their probiotic potential as BAs modulators. The draft

genomes of *L. rhamnosus* VB4 and VB1 strain-specific genes involved in metabolism and transport, as well as in DNA recombination. Each strain harbors a single *bsh* gene, encoding a C-N amide hydrolase, which conserved the essential residues required in the BSH core site. According to the results, compared to VB1, the VB4 strain tolerated better BAs stress and was more active in deconjugation BAs. However, BAs stress increased in the *bsh* gene transcription in the VB1 strain but not in the VB4 strain, suggesting a partially nonlinear relationship between BSH activity and gene expression. In conclusion, despite the complexity if the BSH transcriptional system, the results support the VB4 strain as a promising BAs-deconjugating probiotic candidate.

Keywords: *Lacticaseibacillus rhamnosus*; bile salt hydrolase; bile acid deconjugation; probiotics; bile acids stress

2.1 Introduction

Bile acids (BAs) are versatile signal molecules with endocrine and paracrine functions, mainly involved in uptake of endogenous and dietary lipids (i.e., fatty acids, triglycerides, and cholesterol), as well as fat-soluble vitamins (Bourgin et al., 2021; Bustos et al., 2018). Primary BAs derive from cholesterol in the liver and consist of an amphipathic steroid ring conjugated at the C24 carboxyl group to either glycine or taurine. They reach the small intestine through the common bile duct, where a part of BAs is altered by the gut microbiota (Agolino et al., 2024; Bustos et al., 2018; Mohanty et al., 2024). Conjugated BAs, released into the duodenum, are subjected to several modifications by the gut microbial community (Bourgin et al., 2021; Ridlon & Bajaj, 2015). Bile salt hydrolase (BSH; EC 3.5.1.24) is a cysteine hydrolase belonging to the N-terminal nucleophile (Ntn) hydrolase superfamily, recognized as the crucial enzymatic mediator of gut microbiome-host interactions and BAs-associated biological processes (Bourgin et al., 2021; Lee et al., 2024). This enzyme catalyzes the deconjugation of primary BAs, acting as a 'gatekeeper' for subsequent microbial transformation of the deconjugated forms into secondary BAs (Agolino et al., 2024; Foley et al., 2019; Ridlon & Gaskins, 2024). Over the years, researcher have shown that microbial BSHs shape the host's secondary BAs pool, ultimately regulating host and microbial physiology (Bourgin et al., 2021; Bustos et al., 2018; Dong & Lee, 2018; Foley et al., 2021; Joyce et al., 2014; Yao et al., 2018), but the mechanisms underpinning these effects remain elusive (Agolino et al., 2024; Begley et al., 2006). BSH activity, exerted by microorganisms, is associated with positive effects in regulating lipid absorption and cholesterol metabolism, as well as

in maintaining glucose body balance (Bustos et al., 2018; Dong & Lee, 2018; Foley et al., 2019; Ridlon & Bajaj, 2015). Furthermore, BAs contribute to gut microbiota homeostasis, exhibiting detergent-like antibacterial action, immunomodulatory, and anti-inflammatory effects (Foley et al., 2019). Historically, BSH has been proposed to support the colonization and survivability of bacteria into the human intestine, thanks to their role in bile detoxification (Begley et al., 2006; Bustos et al., 2018) but contrasting evidence on this action has been recently collected (Foley et al., 2021; Moser and Savage, 2001). Generally, BSH activity has been listed as a desirable probiotic feature, according to World Health Organization (WHO) selection criteria (da Silva et al., 2024). BSH activity is constitutively expressed in the major gut microbial families such as *Lactobacillaceae*, *Bifidobacteriaceae*, *Enterococcaceae*, *Enterobacteriaceae*, and *Clostridiaceae* (Bourgin et al., 2021; Ridlon & Gaskins, 2024). Among BSH-encoding bacteria, lactobacilli have been documented to strongly contribute to the majority of the total BSH activity *in vivo* (Song et al., 2023) and their ability to deconjugate BAs is generally associated to the overall cholesterol-lowering effect *in vivo* (Begley et al., 2006). In lactobacilli genomes the number of paralogous *bsh* genes varies in relation to species, strains, and lifestyle (O'Flaherty et al., 2018; Song et al., 2023). For instance, *Lactobacillus acidophilus* ATCC 4796, *Lactobacillus gasseri* ATCC 33323, and *Limosilactobacillus fermentum* MTCC 8711 encode two *bsh* genes (Foley et al., 2021; Jayashree et al., 2014; McAuliffe et al., 2005), while *Lactiplantibacillus plantarum* WCFS1 four *bsh* genes (Lambert et al., 2008). *Lactobacillaceae* BSHs are also highly variable in substrate preferences with consequences on lactobacilli survival and

host colonization (Foley et al., 2021; O'Flaherty et al., 2018).

Lacticaseibacillus rhamnosus is a nomadic species which has been broadly reported as capable of exerting beneficial health effects. This species has a Qualified Presumption of Safety (QPS) status and is naturally present in the gastrointestinal tract, in vaginal microbiota, and in fermented food (Capurso, 2019). Since the description of *L. rhamnosus* GG in 1989, many other *L. rhamnosus* strains with beneficial properties on human health have been fully characterized and classified as probiotics (Rossi et al., 2022). Many of them have been proven to possess cholesterol-lowering activity, often associated with BSH activity and the presence of putative *bsh* genes (Hernández-Gómez et al., 2021; Kaya et al., 2017; Park et al., 2021; Zafar et al., 2022). However, the role of the *bsh* gene in *L. rhamnosus* BSH activity has been not deeply investigated. Specifically, the *L. rhamnosus* genome generally contains one single copy of the *bsh* gene (Agolino et al., 2024), but recently the classification of this gene has been questioned in *L. rhamnosus*. Song et al. (2023), divided lactobacilli BSHs in four phylotypes and assigned *L. rhamnosus* BSH to the phylotype BSH-T0, while O'Flaherty et al. (2018) identified the putative BSH-encoding gene of *L. rhamnosus* GG as homologous to penicillin V acylase (PVA), another member of Ntn hydrolase superfamily strongly related to BSH.

The present study aimed to comprehensively analyze the genomes of two human-derived *L. rhamnosus* candidate, previously selected for their *in vitro* ability to deconjugate BAs. In order to better understand how their genetic structure was related to this ability, a transcriptional study on the putative BSH-encoding gene candidates was coupled to growth assays and in vitro screening for BA

conjugating activity by LC-MS/MS.

2.2 Material and Methods

2.2.1 Reagents

Unless otherwise specified, the media were purchased from Oxoid (Basingstoke, Hampshire, UK), whereas the reagents were obtained from Sigma-Aldrich (St. Louis, MO, USA). Anaerobic systems and molecular biology reagents were bought from Thermo Fisher Scientific (Waltham, MA, USA). The BMR Genomics (Padova, Italy) supplied oligonucleotides and performed the Sanger sequencing services.

2.2.2 Bacterial strains and culture conditions

Lacticaseibacillus rhamnosus strains, used in the present study, belonged to the microbial culture collection of ProBioEtna srl, Spin Off of the University of Catania, Italy. The strains, preserved at −80 °C in de Man, Rogosa and Sharpe (MRS) medium (pH 6.5) containing 25% (*v*/*v*) of glycerol, were routinely propagated in MRS medium, supplemented with 1.5% (*w*/*v*) agar when required, and incubated at 37 °C for 24 h

2.2.3 Genomic sequencing, annotation, and comparative genome analysis

The DNA extraction was carried out through the QIAcube (Qiagen, Germantown MD, USA) automated extraction system using the DNeasy® UltraClean® Microbial Kit (Qiagen, Germantown MD, USA), according to the manufacturer's instructions for Gram-positive bacteria. The concentration and purity of the DNA were evaluated

using a NanoDrop ND-1000 spectrophotometer (Thermo Fisher Scientific, Waltham, MA, USA). For the whole-genome sequencing, the gDNA integrity was assessed by agarose gel electrophoresis and the purity was checked by a spectrophotometer, according to an OD_{260}/OD_{280} ratio of 1.8–2.0, and an OD_{260}/OD_{230} ratio of 2.0–2.2 was used for the whole-genome sequencing. Synbiotec srl (Camerino, Italy) performed both the library preparation and genome sequencing. Briefly, the genomes were sequenced with the Illumina MiSeq Sequencing System, using the proprietary V3 reagents kit, producing 2 × 150 bp paired-end reads. The raw reads were trimmed with Trimmomatic version 0.39 (Bolger et al., 2015) and *de novo* assembly was performed with Unicycler version 0.5.0 (Wick et al., 2017). The genome quality was evaluated with the software BUSCO version 5.5.0 Seppey et al., 2019) using lactobacillales_odb10 (v2020-03-06) as the lineage dataset. The genome annotation was performed with BAKTA v. 1.7.0 (Schwengers et al., 2021). Customized graphical maps of genomes were achieved through the Proksee Server version 1.1.2 (Grant et al., 2023) using the annotation file in GenBank format (gbk). The KEGG functional annotation was performed by BLASTKOALA version 3.0 (Kanehisa et al., 2016). The comparative genome analysis was carried out with PanExplorer v2.0 web-based tool (Dereeper et al., 2022). Three reference genomes included in the analysis were chosen from experimentally validated *L. rhamnosus* probiotics, such as strains Lc705 (FM179323.1), GR-1 (CP102542.1), and GG (CP031290.1).

2.2.4 Taxonomic identification and phylogenomics

The 16S rRNA gene was used for the initial species

identification. Similarities of the 16S rRNA genes to the NCBI RefSeq database (O'Leary et al., 2016) were searched using the nucleotide basic local alignment search tool available at NCBI (accessed on 1 June 2024). The Muscle program (Edgar, 2004) and the Neighbor-joining method (Saitou and Nei, 1987) were used to align the sequences and to perform the phylogenetic tree analysis, with the bootstrap test of 1000 replicates by MEGA11 (Tamura et al., 2021), respectively. The evolutionary distances in the units of the number of base substitutions per site were computed using the Kimura 2-parameter method (Kimura, 1980). To draw the resulting phylogenetic tree, the Interactive Tree Of Life (iTOL version 7) was used (Letunic and Bork, 2019). A cutoff of 98.7% 16S rRNA gene similarity was applied for the species attribution (Stackebrandt, 2006). *Weizmannia coagulans*, *Bacillus subtilis*, *Bacillus vallismortis*, and *Enterococcus faecalis* were included in the analysis as outgroup species (Ventura et al., 2009).

2.2.5 Safety and genome stability analyses

The presence of prophages and virulence genes was detected and mapped with Phigaro v2.3.0 (Starikova et al., 2009) and VirulenceFinder 2.0 (Malberg Tetzschner et al., 2020), respectively. Antimicrobial resistance (AMR) genes were searched through CARD v4.0 (Alcock et al., 2003) and ResFinder v4.3.2 (Bortolaia et al., 2020) tools. Putative plasmids were identified using the PlasmidFinder v2.1 database (https://cge.food.dtu.dk/services/PlasmidFinder/, accessed on 1 December 2024) according to the following screening criteria: a 95% identity threshold and minimum coverage of 60% (Carattoli & Hasman, 2020). CRISPR (Clustered Regularly Interspaced Short

Palindromic Repeats) arrays and their corresponding Cas proteins were pinpointed by employing CRISPRCasFinder v2.2 (Couvin et al., 2018). The presence of mobile element genes was examined using BLASTX searches against the comprehensive the mobileOG-db database v1.1.3 (Brown et al., 2022) with >90% identity and >90% coverage, respectively.

2.2.6 In silico analysis of bsh gene candidates

The amino acid sequences of the previously characterized *bsh* genes were used as queries to search *bsh* gene candidates in genome sequences of strains VB4 and VB1 through the BLASTp tool (https://blast.ncbi.nlm.nih.gov/Blast.cgi, 2 February 2024) (**Table 2.1**) Candidate *bsh* genes in VB4 and VB1 genomes were then aligned using the Constraint-Based Alignment Tool (COBALT) (Papadopoulos & Agarwala, 2007) with 88 Refseq amino acid sequences annotated as *bsh* or putative *bsh* proteins from lactobacilli species and 6 amino acid sequences annotated as PVA proteins and chosen according to O'Flaherty et al. (2018) and Daly et al. (2021). When required, sequence alignments were visualized with Jalview v2.11.4.0 (Waterhouse et al., 2009). A phylogenetic tree was constructed with the Fast Minimum evolution tree method (Desper & Gascuel, 2004). The evolutionary distance between sequences was modeled according to Grishin (Grishin, 1995) with the maximum allowed fraction of mismatched bases set up to 0.85. The resulting tree was visualized with iTOL (Letunic & Bork, 2019).

Table 2.1 - List of proteins as query for BLASTp search of *bsh* genes in VB4 and VB1 genomes.

Accession number	Locus tag	Old locus tag	Coordinates	Encoded Protein	Source Organism	Reference
NC_004567.2	LP_RS14790	lp_0067	3.154.512..3.155.486	Bile salt hydrolase 1 (WP_011102211.1)	*Lactiplantibacillus plantarum* WCFS1	Lambert et al., 2008
NC_004567.2	LP_RS00270	lp_0067	64.823..65.839	Bile salt hydrolase 2 (WP_011100864.1)		
NC_004567.2	LP_RS10935	lp_2572	2.290.117..2.291.070	Bile salt hydrolase 3 (WP_011101831.1)		
NC_004567.2	PL_RS14050	lp_3362	2.987.554..2.988.540	Bile salt hydrolase 4 (WP_003643511.1)		
CP156988.1	ABG771_04540	-	869290..870252	Bile salt hydrolase A (XBE42563.1)	*Lactobacillus acidophilus* NCK1909	Foley et al., 2023
CP156988.1	ABG771_05415	-	1058236..1059213	Bile salt hydrolase B (XBE40978.1)		
NC_008530.1	LGAS_RS00260	LGAS_0054	70380..69430	Bile salt hydrolase A (7SVF)	*Lactobacillus gasseri* ATCC	
NC_008530.1	LGAS_RS04710	LGAS_0959	960746..961723	Bile salt hydrolase B (7SVH)		
ASM1924v3	LCAZH_RS02445	LCAZH_0447	448786..449802	ACC93573.1 (WP_003583296.1)	*Lacticaseibacillus paracasei* Zhang	Zhang et al., 2009
ANQ47241.1	-	-	-	-	*Lacticaseibacillus rhamnosus* E9	Kaya et al., 2017

2.2.7 Penicillin V susceptibility

The microdilution broth method was used for the determination of the Minimum Inhibitory Concentration (MIC) value of penicillin V (PenV), based on international methodologies ISO 10932/IDF 233 (2010) for the discrimination of antibiotic susceptibility referred to lactobacilli. According to that, a bacterial suspension of each strain was standardized to 1 McFarland (3.0×10^8 CFU/mL) and diluted 1:100 (final concentration of 3.0×10^6 CFU/mL). The experiment was performed in 96-well plates filled with 140 µL of serial two-fold dilution of penicillin V (128–0.25 µL/mg) in double-concentrated LSM broth (90% Isosensitest and 10% MRS broth; Oxoid) and 10 µL of the diluted bacterial suspension. The plates were incubated under anaerobic conditions at 37 °C for 48 h. According to the MIC cut-off values, the tested strains were classified as resistant or susceptible to the tested antibiotic, in accordance with EFSA guidelines (2018).

2.2.8 Growth curve assay

The growth assays were performed in 100 mL screw-top flasks (Corning, Acton, MA, USA) filled with 45 mL of MRS medium containing a 1.0% (*w*/*v*) mixture of BAs or MRS without BAs, as a control, and incubated at 37 °C under static conditions. After pre-culturing each strain in 10 mL of MRS medium, the cells were transferred to each flask at a final concentration of 1.00×10^5 CFU/mL. All the experiments were carried out in triplicates. The samples were aseptically withdrawn for the measurement of absorbance at 600 nm (OD_{600nm}) at least three times a day and, in the stationary growth phase, additional aliquots were taken for

biochemical and gene expression analyses. The resulting growth curves were modelled according to the parametric equations available in Grofit R package (Kahm et al., 2010). A indicated the maximum cell density reached by the culture at the stationary phase of growth (expressed as OD_{600nm}values), μ was the maximum growth rate (expressed as$\cdot h^{-1}$), and λ the length of the latency phase (expressed in h). For the mass spectrometry analysis and gene expression analysis, aliquots were taken when the OD_{600nm} values were constant for three consecutive measurements. In detail, the samples for the mass spectrometry analysis were centrifuged at 12,000× *g* for 10 min (4 °C), and the supernatants were immediately stored at −80 °C after 0.22 μm filtration. For the gene expression analysis, a volume of cell suspensions corresponding to 2.0×10^8 CFU was centrifuged at 12,000× *g* for 10 min (4 °C), and the resulting pellet was washed with DEPC-treated ddH_2O and immediately stored at −80 °C.

2.2.9 RNA extraction, retro-transcription, and gene expression analysis

RNA extraction was carried out using the Zymo Direct-zol RNA MiniPrep kit (R2071, Zymo Research, Irvine, CA, USA) and applying few modifications to the manufacturer's instructions. Briefly, after adding up to 700 μL of the Tri reagent, the mechanical lysis of cells was achieved using a Vortex Genie 2 instrument (Mo Bio Laboratories Carlsbad, CA, USA) by performing two rounds of 20 min at the highest speed alternating with 3 min on ice. The quantity of total RNA was measured spectrophotometrically using a Nanodrop Nd 1000 system (Nanodrop Technologies, Wilmington, DE, USA) and only samples determined to have A260/280 absorbance ratios between

1.8 and 2.2 were considered for further analyses. The integrity of the total RNA was evaluated by denaturing gel electrophoresis on a 0.9% (*w*/*v*) agarose gel with formaldehyde (10 mL of 10× 3-morpholinepropane sulfonic acid [MOPS] running buffer) and 18 mL of 37% formaldehyde (12 mol/L) in pH 7.0 1× MOPS running buffer (0.4 mol/L MOPS, 1 mol/L sodium acetate, and 0.01 mol/L EDTA) after the RNA treatment at 65 °C for 10 min. To remove any contamination of gDNA, 1 µg of the RNA sample was treated with dsDNase (EN0771, Thermo Fisher Scientific) (final volume 40 µL) and, thereafter, RNA was reverse transcribed to cDNA at 42 °C for 60 min with random hexamer primers using the RevertAid RT Kit (EP0441; Thermo Fisher Scientific) according to the manufacturer's instructions.

The end-point PCR amplification of the putative *bsh* gene was carried out with a Dream Taq DNA polymerase. RT-PCR of the 16S rRNA gene was used as the positive control and carried out as previously reported (Solieri et al., 2022). RT-qPCR reactions were performed with tenfold-diluted cDNA using the PowerUp SYBR Green Master Mix (A25742; Thermo Fisher Scientific) on a QuantStudio 3 real-time PCR system (Thermo Fisher Scientific, Waltham, MA, USA). Each reaction was prepared in a 20 µL mixture containing 10 µL of the Power SYBR Green master mix, 0.3 µM of each primer with the designated final concentration, and 5 µL of diluted cDNA. The thermal conditions were as follows: 50 °C for 2 min, 95 °C for 2 min, 40 cycles at 95 °C for 15 s, and then at 60 °C for 1 min with fluorescence measurement, and the melt curve stage including 95 °C for 15 s, 60 °C for 1 min, and increasing the temperature step to 95 °C at a rate of 0.15 °C/s. All the primers used

in this study are listed in **Table 2.2**. The expression of the *bsh* gene was normalized to that of the 16S rRNA gene to yield a relative transcript level. Gene expression ratios were calculated using the software tool REST 2009 based on the efficiency-corrected method (Pfaffl et al., 2002). All qPCR reactions were performed in triplicates including the non-template control for each target.

Table 2.2 - Primer used in this study.

PCR assay	Target gene	Primer	Sequence (5'->3')	Length (bp)	Tm	PCR product lenght (bp)
end-point PCR	*bsh*	Bsh_rha_F3	ACGGCTACTTGGAAGACTAAAT	22	62	643
		Bsh_rha_R3	CATTGTAAAGCACGCGGATAC	21	62	
RT-qPCR	*bsh*	Bsh_rha_qF2	GGAATACGGGTGGCATACAA	20	63	136
		Bsh_rha_qR2	CAGGCCAAACATGCCATAAC	20	63	
	16S	16S_F1	GTAGGTGGCAAGCGTTATCC	20	62.8	101
		16S_R1	GATGCGCTTCCTCGGTTAAG	20	63	

2.2.10 Semi-quantitative analysis in UHPLC/HR-MS

An Ultra-High-Performance Liquid Chromatography High-Resolution Mass Spectrometry (UHPLC/HR-MS) analysis was carried out by applying the protocol reported in (Karlov et al., 2023), with minor modifications. The UHPLC Ultimate 3000 module (Thermo Fisher Scientific, San Jose, CA, USA) was used for the chromatographic separation, whereas the tandem mass spectrometry identification and semi-quantitative analysis were carried out through a Q Exactive Hybrid Quadrupole-Orbitrap Mass Spectrometer (Thermo Fisher Scientific, San Jose, CA, USA). After appropriate dilution, 10 µL of the sample were injected in the UHPLC system loaded with a C18 column (Acquity UPLC HSS C18 Reversed phase, 2.1 × 100 mm, 1.8 µm particle size, Waters, Milan, Italy). The used mobile phases were water with 0.1% formic acid (mobile phase A) and acetonitrile with 0.1% formic acid (mobile phase B). The gradient began with 58% of B, and then linearly increased to 75% of B in 10 min. Next, the percentage of mobile phase B was brought to 98% in 1 min and kept for a further 6 min before coming back to the initial conditions. The flow rate was fixed at 0.3 mL/min, and the column temperature was maintained at 45 °C. The negative electrospray conditions were as indicated below: capillary voltage, 2.7 kV; capillary temperature, 320 °C; sheath gas, 40; and auxiliary gas, 30. The MS parameters were resolution, 70,000; AGC target, 3×10^6; maximum IT, 247 ms; and scan range, 100 to 1500 *m*/*z*. MS/MS parameters were as follows: resolution, 17,500; AGC target, 5×10^5; maximum IT, 120 ms; and isolation window, 1 *m*/*z*.

The analyzed samples were MRS medium containing 1.0%

(*w*/*v*) BAs mixture inoculated with the selected strains and incubated as reported in the section 2.2.8. To determine the percentage of the decrease in BAs, a standard solution was prepared containing the mixture of BAs dissolved in MRS at the same concentration of 1.0% (*w*/*v*) as for the inoculated samples.

The relative amount of BAs was determined by integrating the area under the peak (AUP). AUP values were quantified from the extracted ion chromatograms (EIC) calculated for each mass-to-charge ratio of compound (tolerance ± 5 ppm) using the Genesis algorithm function in the Thermo Xcalibur Quantitative Browser.

The percentage of decrease for each BA, namely taurocholate (TCA), taurodeoxycholate (TDCA), taurochenodeoxycholate (TCDCA), glycocholate (GCA), glycodeoxycholate (GDCA), and glycochenodeoxycholate (GCDCA), was calculated as follows:

$$\%\ decrease = 100 - \left[\frac{100 \times (AUP\ of\ BAs\ in\ inoculated\ sample)}{\text{AUP of BAs in standard solution}}\right]$$

2.2.11 Statistical analysis

All the analyses were carried out in triplicates and the data are reported as the mean ± SD. GraphPad Prism v.8.00 was used to generate graphs and to perform statistical analysis. *p*-values were calculated using two-sided Student's *t*-tests, unless stated otherwise. Statistical significance was considered at $p < 0.05$ and the levels of significance were represented as * $p \leq 0.05$, ** $p \leq 0.01$, *** $p \leq 0.001$, and **** $p \leq 0.0001$.

2.3 Results

2.3.1 Genome sequencing

Strains VB4 and VB1 were characterized at the genome level. The reads assembly resulted in 70 contigs, corresponding to a total length of 2,926,936 bp, and in 19 contigs, corresponding to a total of 2,917,389 bp, respectively, for VB4 and VB1 strains. The GC contents were 46.63% and 46.65% for strains VB4 and VB1, respectively, and a clear definition of positive and negative strands were obtained in both cases (**Figure 2.1A, B**). The genomic features of strains VB4 and VB1 are summarized in **Table 2.3**.

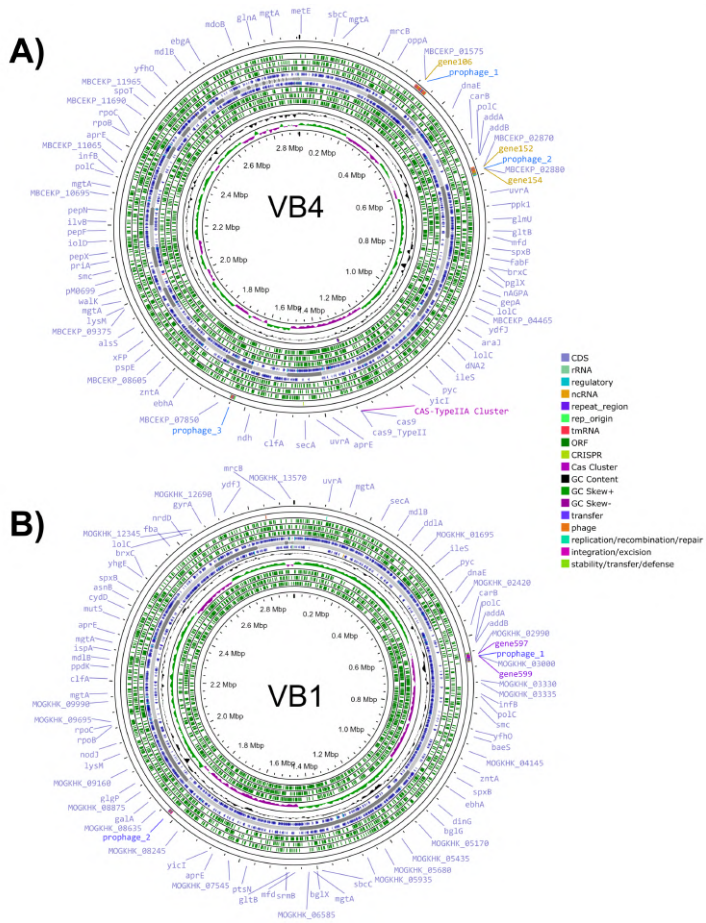

Figure 2.1 - Circular graphical representation of the *Lacticaseibacillus rhamnosus* strains VB4 (A) and VB1 (B) contigs obtained using Proksee (https://proksee.ca; accessed on 13 January 2024). The black central circle shows the scale expressed in megabases. Moving inward, the two outer violet circles show forward- and reverse-strand CDSs, respectively. Some genes are shown on

the outer violet circle with the Proksee's default. In CDSs circles, tRNAs are shown as orange arrows, rRNAs are represented as light blue arrows, tmRNA is displayed as a red arrow, and CRISPR sequences are reported as light green arrows adjacent to each other. The next circle shows the GC content and GC skew as dark blue and dark green and pink, respectively. The represented genomic order of contigs is arbitrary.

Table 2.3 - General features of *L. rhamnosus* VB4 and VB1 genome assemblies.

Features	*L. rhamnosus* VB4	*L. rhamnosus* VB1
Size (bp)	2,926,936	2,917,389
Contigs	70	19
GC (%)	46.63	46.65
N50	111,122	406,064
Largest contig (bp)	222,067	1,025,915
CDS	2,769	2,704
Gene average length (bp)	903	921
tRNA	45	46
rRNA	4	2
tmRNA (ssrA)	1	1
ncRNA	4	7
oriC	1	2

2.3.2 Strain identification

The phylogenetic analysis of 16S rRNA gene sequences showed that strains VB4 and VB1 formed a monophyletic group with reference sequences of *L. rhamnosus* NBRC 3425 and JCM 1136^T (**Figure 2.2**) Accordingly, the calculation of average nucleotide identity (ANI) values showed that strains VB4 and VB1 obtained ANIb values of 97.16% and 99.74% with *L. rhamnosus* DSM 20021^T, both above the threshold for species allocation (95%) (**Figure 2.3**). The TYGS phylogenetic predictions further supported the attribution to the species *L. rhamnosus* based on dDDH values (**Table 2.4**). Based

on ANIb and dDDH values, strain VB4 appeared more related to *L. rhamnosus* GG than strain VB1.

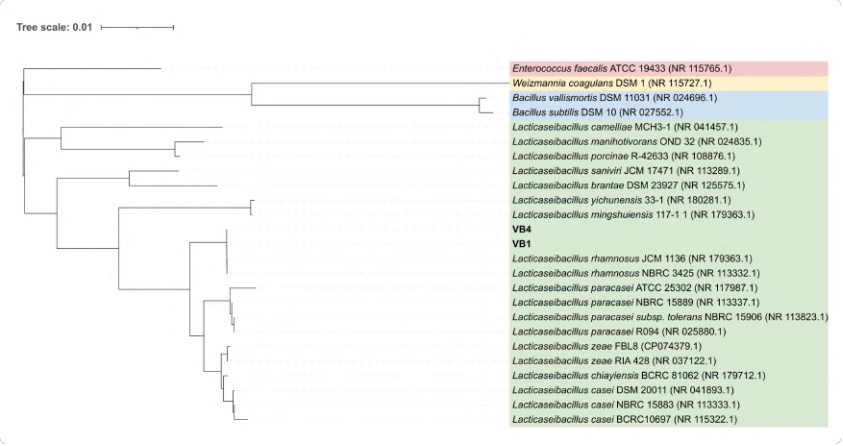

Figure 2.2 - Phylogenetic analysis of 16S rRNA gene sequences of *Lacticaseibacillus* species. The tree was inferred using the Neighbor-Joining method (Saitou & Nei, 1987) and the Kimura's two-parameter model Kimura, 1980) with Mega XI software (Tamura et al., 2021). Strains VB4 and VB1 are shown in bold, while the sequences of reference strains were from the NCBI RefSeq database. A discrete Gamma distribution (shape parameter = 5) was used to model evolutionary rate variation among sites. Bootstrap values are indicated at branch points based on 1,000 replications. The trees are drawn in scale, with branch length measured in the number of substitutions per site. Bar represents 0.01 substitutions per nucleotide position. The tree was rooted using the branch leading to four outgroup species *E. faecalis*, *W. coagulans*, *B. subtilis*, and *B. vallismortis*. The tree was visualized with iTOL (Letunic & Bork, 2019).

Table 2.4 - Digital DNA-DNA Hybridization (dDDH) values of strains VB4 and VB1 compared with other *Lacticaseibacillus* strain.

Query strain	Subject strain	dDDH (d0, in %)	C.I. (d0, in %)	dDDH (d4, in %)	C.I. (d4, in %)	dDDH (d6, in %)	C.I. (d6, in %)	G+C content difference (in %)
VB4	*Lacticaseibacillus rhamnosus* JCM 1136	79,9	[75.9 - 83.3]	76,7	[73.7 - 79.5]	82,2	[78.9 - 85.1]	0,05
VB4	*Lacticaseibacillus casei* ATCC 393	25,2	[21.8 - 28.8]	24,1	[21.8 - 26.6]	23,9	[21.0 - 27.0]	1,25
VB4	*Lacticaseibacillus huelsenbergensis* DSM 115425T	25,4	[22.0 - 29.0]	23,6	[21.3 - 26.1]	23,9	[21.1 - 27.0]	1,3
VB4	*Lacticaseibacillus paracasei* JCM 8130	20,2	[17.0 - 23.8]	23,5	[21.2 - 25.9]	19,7	[17.0 - 22.8]	0,08
VB4	*Lacticaseibacillus zeae* KCTC 3804	25,5	[22.2 - 29.2]	23,3	[21.0 - 25.8]	24	[21.2 - 27.1]	1,12
VB4	*Lacticaseibacillus chiayiensis* BCRC 81062	25,5	[22.1 - 29.1]	22,9	[20.6 - 25.3]	23,9	[21.0 - 27.0]	0,51
VB4	*Lacticaseibacillus casei* DSM 20011	20	[16.8 - 23.6]	22,6	[20.3 - 25.0]	19,5	[16.8 - 22.5]	0,19
VB4	*Lacticaseibacillus paracasei subsp. tolerans* DSM 20258	19,7	[16.5 - 23.3]	22,5	[20.3 - 25.0]	19,2	[16.5 - 22.2]	0,21
VB4	*Lacticaseibacillus paracasei* ATCC 25302	19,8	[16.7 - 23.4]	22,4	[20.1 - 24.8]	19,3	[16.6 - 22.4]	0,12
VB1	*Lacticaseibacillus rhamnosus* JCM 1136	97,8	[96.3 - 98.6]	98,7	[98.0 - 99.1]	98,8	[98.0 - 99.3]	0,03
VB1	*Lacticaseibacillus casei* ATCC 393	25,2	[21.9 - 28.8]	23,9	[21.6 - 26.3]	23,8	[21.0 - 26.9]	1,23
VB1	*Lacticaseibacillus huelsenbergensis* DSM 115425T	25,6	[22.3 - 29.3]	23,3	[21.0 - 25.8]	24,1	[21.2 - 27.2]	1,29

VB1	*Lacticaseibacillus zeae* KCTC 3804	25,1	[21.7 - 28.7]	23,3	[21.0 - 25.7]	23,6	[20.8 - 26.7]	1,1
VB1	*Lacticaseibacillus chiayiensis* BCRC 81062	24,9	[21.6 - 28.6]	22,9	[20.6 - 25.4]	23,5	[20.6 - 26.6]	0,49
VB1	*Lacticaseibacillus paracasei* JCM 8130	19,6	[16.4 - 23.2]	22,2	[19.9 - 24.6]	19,1	[16.4 - 22.1]	0,1
VB1	*Lacticaseibacillus paracasei subsp. tolerans* DSM 20258	19,6	[16.4 - 23.1]	22,1	[19.8 - 24.5]	19,1	[16.4 - 22.1]	0,23
VB1	*Lacticaseibacillus paracasei* ATCC 25302	19,7	[16.5 - 23.3]	22	[19.7 - 24.4]	19,2	[16.5 - 22.2]	0,14
VB1	*Lacticaseibacillus casei* DSM 20011	19,8	[16.6 - 23.4]	21,8	[19.5 - 24.2]	19,3	[16.5 - 22.3]	0,21
VB1	*Lacticaseibacillus mingshuiensis* JCM 33567	12,9	[10.2 - 16.2]	20,4	[18.1 - 22.8]	13,3	[10.9 - 16.0]	8,52

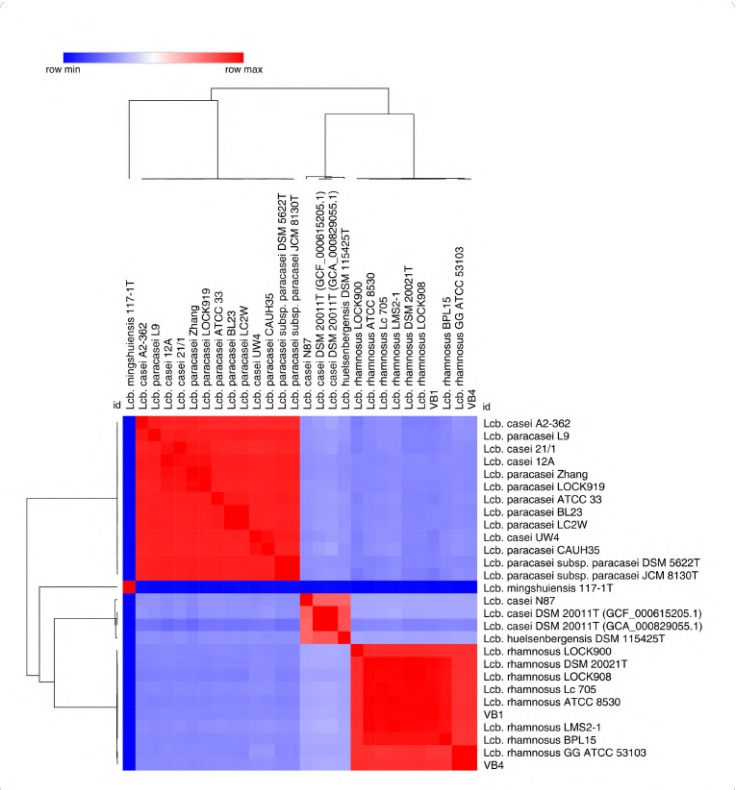

Figure 2.3 - Heatmap of the average nucleotide identity (ANI) values of 28 *Lacticaseibacillus* strains. The colored squares, designate the strain relatedness based on their ANI values (red color > the threshold value of 95%; dark and light blue < the threshold values of 95%.

2.3.3 Annotation and comparative genome analysis

Genome annotation predicted a total of 2,824 and 2,760 genes

in VB4 and VB1 genome assemblies, respectively, including 2769 (VB4) and 2704 (VB1) CDS, 45 (VB4) and 46 (VB1) tRNA, 4 (VB4) and 2 (VB1) rRNA, and 1 (VB4) and 1 (VB1) tmRNA, respectively (**Table 2.3**).

For the VB4 genome, the KEGG functional annotation by BLASTKOALA assigned approximately half of the genes (51.0%, 1413 genes) into 23 different functional categories, mostly related to carbohydrate metabolism (234, 16.57%), protein families: genetic information processing (13.31%), and protein families: signaling and cellular processes (9.91%), among others (**Figure 2.4A**). The KEGG functional annotation of the VB1 genome by BLASTKOALA revealed that 55.5% of the genes were assigned to 23 functional categories with slightly different proportions compared to VB4 (**Figure 2.4B**).

Based on the clusters of orthologous groups (COG), the VB4 and VB1 strains differed in distribution of clusters in COG categories (**Figure 2.5A**). To identify strain-specific genes of *L. rhamnosus* VB4 and VB1, we compared them to the genome sequences of *L. rhamnosus* GG, *L. rhamnosus* GR-1, and *L. rhmanosus* La075. The pan-genome consisted of 3653 COG, containing a core-gene of 58.3% and a strain-specific gene pool of 16.9%. Non-necessary genes, defined as lacking in at least one of the strains, accounted for 24.9% (**Figure 2.5B**) and, together with the strain-specific genes, constituted the accessory genome. The distribution of strain-specific clusters showed that VB4 and VB1 differed in the number of singletons. Specifically, 130 genes were uniquely located in the genome of the *L. rhamnosus* VB4, whereas 50 genes were uniquely assigned in the *L. rhamnosus* VB1 genome (**Figure 2.5C**). The sharing pattern of

accessory COG corroborated the relationships established among the *L. rhamnosus* strains through the ANI analysis and supported that strain VB4 was more related to *L. rhamnosus* GG, and strain VB1 to *L. rhamnosus* GR-1 (**Figure 2.5D**).

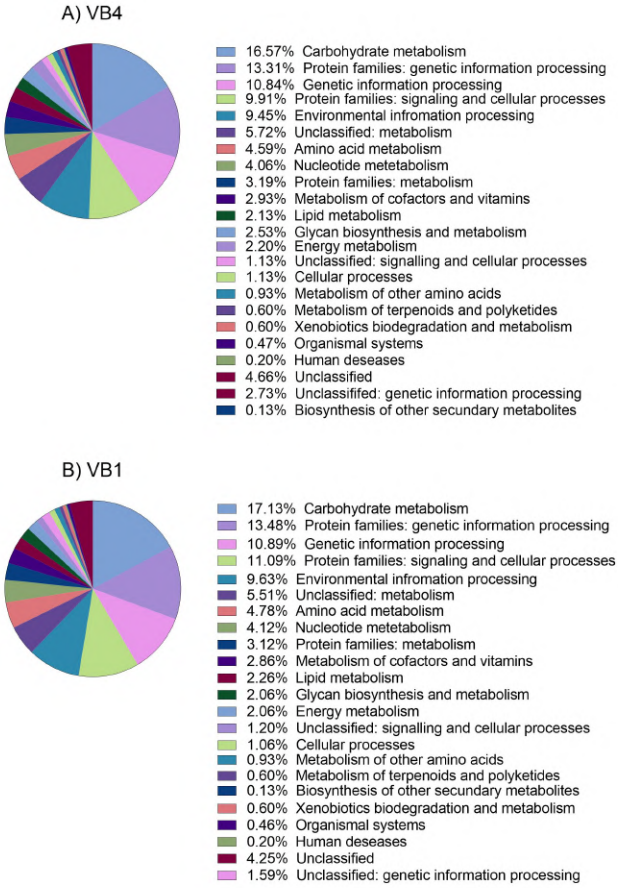

Figure 2.4 - Distribution of KEGG orthology (KO) categories of identified protein-coding genes in the *Lacticaseibacillus rhamnosus* VB4 (A) and VB1 (B) genomes, respectively.

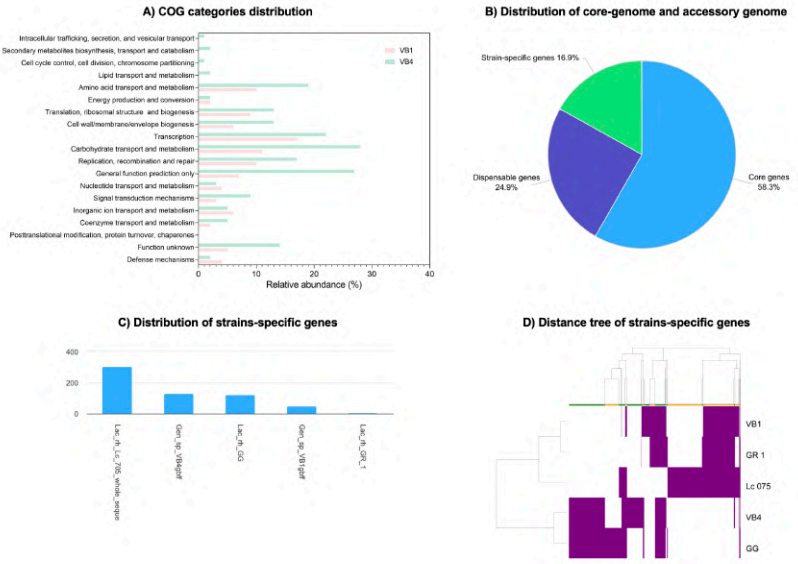

Figure 2.5 - Pan-genome analysis of *Lacticaseibacillus rhamnosus* strains VB4 and VB1. The strains were compared to *L. rhamnosus* strains Lc705 (ASM2652), GR-1 (ASM2466559), and GG (ASM2847508) using PanExplorer (last accessed on 15 May 2024). (A) Distribution of COG functional groups in VB4 and VB1 genomes. (B) Core-genes proportion and strain-specific genes; (C) distribution of strain-specific genes according to the *L. rhamnosus* pan-genome analysis; and (D) distance tree generated by hierarchical clustering from presence/absence binary matrix of accessory gene clusters among the members of *L rhamnosus* dataset. Genes are colored if present in the genome.

The functional analysis of strain-specific genes pointed out that three main COG categories were abundant in VB4 strain-specific genes, namely carbohydrates metabolism and transport (20), amino acid transport and metabolism (12), and cell wall/membrane/envelope

biogenesis (10), but poorly represented in VB1 genome. In VB1 genome strain-specific genes mainly belonged to the categories of transcription (11) and replication, recombination, and repair (7) (**Figure 2.6**).

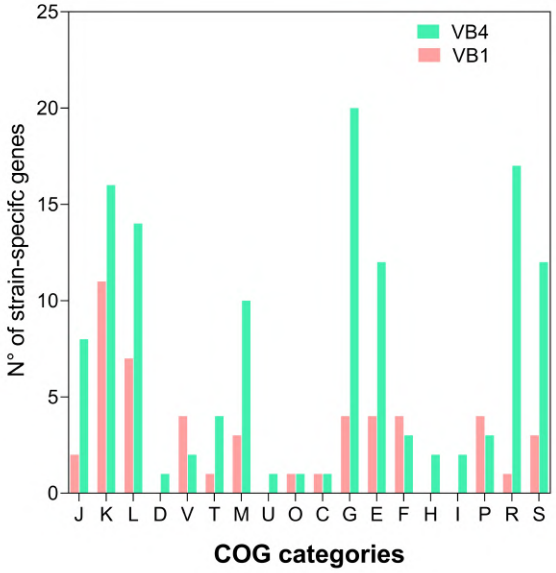

Figure 2.6 - Number of unique genes in *Lacticaseibacillus rhamnosus* strains VB4 and VB1 assigned in COG functional categories. COGs of the *L. rhamnosus* VB4 strain are represented as green bars whereas COGs if the *L. rhamnosus* VB1 strain are displayed as pink bars. COG categories are abbreviated as follows: J; translation, ribosomal structure, and biogenesis; K, transcription; L, replication recombination, and repair; D, cell cycle control, cell division, and chromosome partitioning; V, defense mechanisms; T, signal transduction mechanisms; M, cell wall/membrane/envelop biogenesis; U, intracellular trafficking and vesicular transport; O, post-translational modification, protein turnover, and chaperons; C, transport and metabolism; F, nucleotide transport and metabolism; H,

coenzyme transport and metabolism; I, lipid transport and metabolism; P, inorganic transport and metabolism; R, general functional prediction only; and S, function unknown.

2.3.4 Safety assessment

According to EFSA, the genomes of both VB4 and VB1 strains were checked for the presence of AMR genes by using two independent and maintained databases (EFSA, 2021). Both CARD and ResFinder analyses did not reveal AMR genes in any genome, indicating that *L. rhamnosus* VB4 and VB1 can be considered safe in relation to the potential dissemination of AMR genes. The VirulenceFinder webserver did not render results for any of the strains, while PathogenFinder showed probabilities of being a human pathogen of 0.097 and 0.098 (above 1) for *L. rhamnosus* VB4 and VB1, respectively. These results are in accordance with the QPS status of *L. rhamnosus*.

2.3.5 Genome stability

The presence of plasmid replication initiation proteins in *L. rhamnosus* VB4 and VB1 strains was not revealed by the PlasmidFinder (v2.1), suggesting that both strains do not possess any plasmids. The Phigaro pipeline was used to detect the prophage sequences in the genomes of *L. rhamnosus* VB4 (**Figure 2.7A**) and VB1 (**Figure 2.7B**). Three and two prophage regions were detected in VB4 and VB1 genomes, respectively. In both strains, putative prophage regions belonged to the *Siphoviridae* family (**Table 2.5**). In the VB4 genome, contig 2 harbored a 33.6 kb long prophage region encoding 41 prophage proteins (Figure 2.7A). This region was 100% identical (83% query coverage) to *Caudoviricetes* sp. isolate cttX04

(BK021713.1). In the VB1 genome, the longest prophage region (23.8 kb) was located on contig 1, contained 19 phage proteins, and was 99.85% (query coverage 52%) identical to the previously described *L. rhamnosus* Lc-Nu-like prophage (AY780364.1) (**Figure 2.7B**). The genomes of both VB4 and VB1 strains were checked to delineate regions associated with mobile elements by using the mobileOG-db plugin within Proksee. The analysis confirmed that VB4 has more regions related to mobile elements than VB1, especially integrases and phage-related genes (**Figure 2.8**).

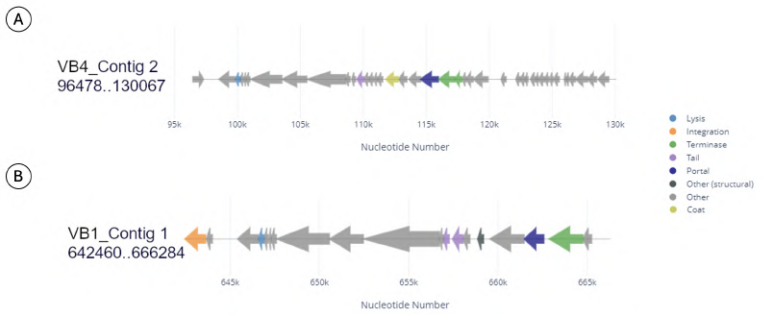

Figure 2.7 - Organization of the main prophage regions in VB4 (A) and VB1 (A) genome.

Table 2.5 - Contigs matching prophage regions and predominant phage sequences predicted in VB4 and VB1 genomes.

Strains	Contigs	Kb	GC%	N° prophage ORFs	Predominant phage	Query coverage (%)	Identity (%)
VB4	2	33.6	46.2	41	*Caudoviricetes* sp. isolate cttX04 (BK021713.1)	83	100
	3	22.3	43.3	10	*Caudoviricetes* sp. isolate ctSOR2 (BK047574.1)	70	100
	12	12.6	45.7	11	*Caudoviricetes* sp. isolate ctRgI1 (BK047375.1)	86	100
VB1	1	23.8	42.7	19	Lc-Nu-like prophage (AY780364.1)	52	99.85
	3	10.2	45.7	10	*Caudoviricetes* sp. isolate ctnST1 (BK026254.1)	97	99.98

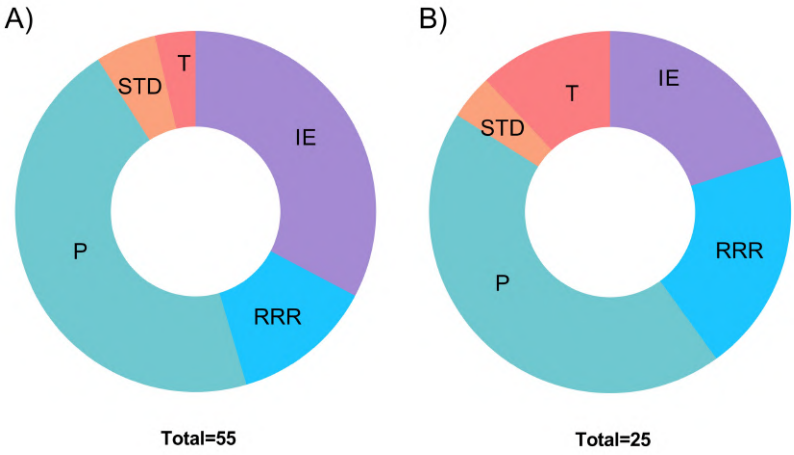

Figure 2.8 - Distribution of mobile genetic elements in *Lacticaseibacillus rhamnosus* VB4 (A) and VB1 (B) genomes. Major categories considered were IE, integration/excision; RRR, replication/recombination/repair; P, phage; STD, stability/transfer/defense; and T, transfer.

The analysis of CRISPR sequences with CRISPRCasFinder indicated that contig 9 of the VB4 genome contains a complete CRISPR–Cas system of type II-A/LsaI1, consisting of four *cas* genes (*cas1*, *cas2*, *cas9*, and *csn2*) and one 1553 bp long CRISPR array containing 23 spacers (**Table 2.6** and **2.7**). BLASTn searches compared all 23 spacers against the phage and plasmid NCBI databases and revealed full or partial matching with several *L. rhamnosus*. Another CRISPR region was detected on contig 10 of the VB4 genome assembly, but without any *cas* genes in the surrounding region. In contrast, the VB1 genome encoded a Cas3 protein on contig

9, typical for a CRISPR-Cas system type I (Makarova et al., 2018) (**Table 2.8**). However, no CRISPR regions were detected near to this ORF, while the only detected CRISPR region was located on contig 1 (coordinates 88741..88886) upstream to the only transposase gene found in the VB1 genome (100% identical to ISLca2 from *L. casei* BL23) (**Table 2.9**).

Table 2.6 - *Cas* gene in VB4 genome. Contigs without *cas* gene were omitted for brevity.

#SequenceID	Cas-type/subtype	Gene status	System	Type	Begin	End	Strand	Other information
contig_9_29	csn2_TypeIIA	mandatory	CAS-TypeIIA	CDS	29106	29786	-	ID=1_29;partial=00;start_type=TTG;rbs_motif=AGGA;rbs_spacer=5-10bp;gc_cont=0.402;conf=100.00;score=78.52;cscore=74.54;sscore=3.97;rscore=10.77;uscore=0.11;tscore=-8.20
contig_9_30	cas2_TypeI-II-III	accessory	CAS	CDS	29783	30088	-	ID=1_30;partial=00;start_type=ATG;rbs_motif=GGAG/GAGG;rbs_spacer=5-10bp;gc_cont=0.438;conf=99.99;score=42.04;cscore=23.07;sscore=18.98;rscore=9.74;uscore=5.52;tscore=3.72
contig_9_31	cas1_TypeII	accessory	CAS-TypeIIU	CDS	30066	30971	-	ID=1_31;partial=00;start_type=ATG;rbs_motif=GGA/GAG/AGG;rbs_spacer=5-10bp;gc_cont=0.447;conf=100.00;score=92.61;cscore=87.24;sscore=5.37;rscore=0.78;uscore=1.52;tscore=3.72
contig_9_32	cas9_TypeII	mandatory	CAS-TypeIIU	CDS	31177	35268	-	ID=1_32;partial=00;start_type=ATG;rbs_motif=GGAGG;rbs_spacer=5-10bp;gc_cont=0.423;conf=99.99;score=524.92;cscore=502.47;sscore=22.45;rscore=16.30;uscore=3.08;tscore=3.72

Table 2.7 - CRISPR regions in VB4 genome, Contigs without CRISPR regions were omitted for brevity.

	VB4	
Sequence	contig_9	contig_10
Sequence_basename	contig_9	contig_10
Duplicated_Spacers	0	0
CRISPR_Id	contig_9_1	contig_10_1
CRISPR_Start	27532	59245
CRISPR_End	29085	59346
CRISPR_Length	1553	101
Potential_Orientation (AT%)	Reverse	Unknown
CRISPRDirection	Unknown	Unknown
Consensus_Repeat	GCTCTTGAACTGATTGATCTGACATCTACCTG AGAC	GGGTAAAACCCTTCCAATCTCCAACTTCATTA TACC
Repeat_ID (CRISPRdb)	Unknown	Unknown
Nb_CRISPRs_with_same_Repeat (CRISPRdb)	0	0
Repeat_Length	36	36
Spacers_Nb	23	1
Mean_size_Spacers	30	30
Standard_Deviation_Spacers	0	0
Nb_Repeats_matching_Consensus	21	2
Ratio_Repeats_match/TotalRepeat	0.875	1
Conservation_Repeats (% identity)	91.6666666666667	100
EBcons_Repeats	97.2307923074907	100
Conservation_Spacers (% identity)	0	100

EBcons_Spacers	0	100
Repeat_Length_plus_mean_size_Spacers	66	66
Ratio_Repeat/mean_Spacers_Length	1.2	1.2
CRISPR_found_in_DB (if sequence IDs are similar)	0	0
Evidence_Level	4	1

Table 2.8 - *Cas* genes in VB1 genome. Contigs without *cas* gene were omitted for brevity.

#SequenceID	Cas-type/subtype	Gene status	System	Type	Begin	End	Strand	Other information
contig_9_38	Cas3_TypeI	forbidden	CAS	CDS	41617	42963	+	ID=1_38;partial=00;start_type=ATG;rbs_motif=AGxAGG/AGGxGG;rbs_spacer=3-4bp;gc_cont=0.491;conf=100.00;score=147.15;cscore=131.40;sscore=15.75;rscore=7.31;uscore=3.24;tscore=3.99

Table 2.9 - CRISPR regions in VB1 genome. Contigs without CRISPR regions were omitted for brevity.

	VB1
Sequence	contig_1
Sequence_basename	contig_1
Duplicated_Spacers	0
CRISPR_Id	contig_1_1
CRISPR_Start	88741
CRISPR_End	88886
CRISPR_Length	145
Potential_Orientation (AT%)	Unknown
CRISPRDirection	Unknown
Consensus_Repeat	GCGTGATGGCCGGTCTTTGGCCATTGCGCCCAAGGTCCTTACA
Repeat_ID (CRISPRdb)	Unknown
Nb_CRISPRs_with_same_Repeat (CRISPRdb)	0
Repeat_Length	43
Spacers_Nb	1
Mean_size_Spacers	60
Standard_Deviation_Spacers	0
Nb_Repeats_matching_Consensus	1
Ratio_Repeats_match/TotalRepeat	0.5
Conservation_Repeats (% identity)	97.6744186046512
EBcons_Repeats	97.6744186046512
Conservation_Spacers (% identity)	100
EBcons_Spacers	100

Repeat_Length_plus_mean_size_Spacers	103
Ratio_Repeat/mean_Spacers_Length	0.716666666666667
CRISPR_found_in_DB (if sequence IDs are similar)	0
Evidence_Level	1

2.3.6 Identification and phylogenetic analysis of bsh gene candidates

In this work, the presence of BSH enzyme-encoding genes in VB4 and VB1 genomes was investigated using the BLASTP tool (https://blast.ncbi.nlm.gov/Blast.cgi; accessed on 2 February 2024) and amino acid sequences of previously characterized *bsh* genes as queries (**Table 2.1**). We found a putative *bsh* gene on contigs 37 and 2 of VB4 and VB1 genome assemblies, respectively. In both strains, the genes were 1017 bp long and encoded two 338 aa long proteins which differed from each other for two aa substitutions, P167L and D169G, respectively. The predicted proteins were members of the choloylglycine hydrolase family and were annotated as linear C-N amide hydrolases (Pfam PF02275) (*E*-value: 4.5×10^{-48}). In addition, they contained residues Cys2, Arg18, Asp21, Asn82, Asn175, and Arg228, which are close in 3D structure, concurring to form the central active site of the BSH enzyme, as shown in **Figure 2.9** (Dong & Lee, 2018).

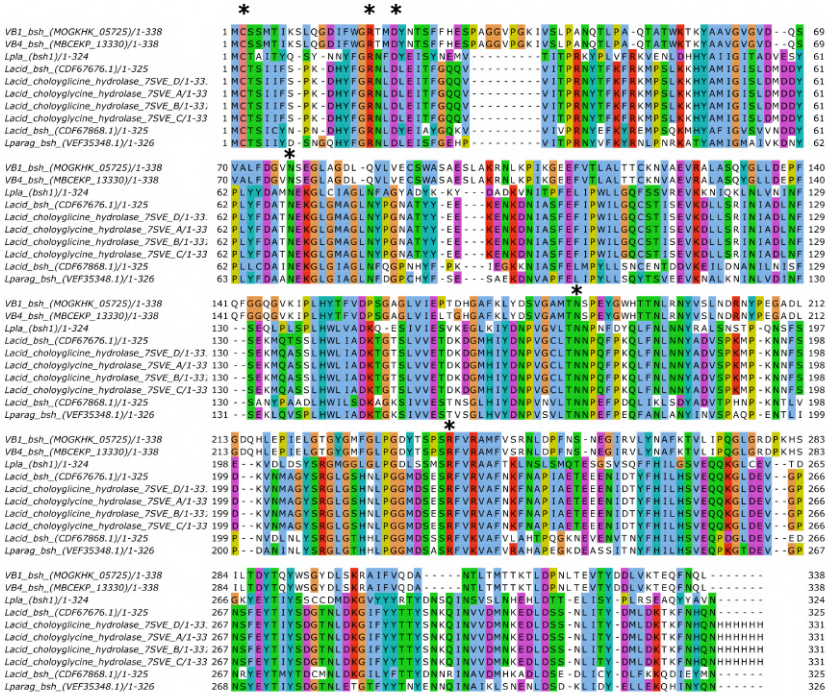

Figure 2.9 - Multiple amino acid sequence alignment of 10 BSHs proteins selected from Table 2.10.

Table 2.10 - Genome assemblies used for ANI matrix calculation.

Specie	Strain	GenBank accession number
Lacticaseibacillus casei	N87	GCA_001013375.1
Lacticaseibacillus casei	DSM 20011 = JCM 1134 = ATCC 393 JCM 1134 [T]	GCA_000829055.1
Lacticaseibacillus casei	DSM 20011 = JCM 1134 = ATCC 393 [T]	GCA_000615205.1
Lacticaseibacillus casei	12A	GCA_000309565.2
Lacticaseibacillus casei	21/1	GCA_000309585.1
Lacticaseibacillus casei	A2-362	GCA_000510825.1
Lacticaseibacillus casei	UW4	GCA_000309745.1
Lacticaseibacillus huelsenbergensis	DSM 115425 [T]	GCA_029726355.1
Lacticaseibacillus mingshuiensis	117-1 [T]	GCA_016861785.1
Lacticaseibacillus paracasei	BL23	GCA_964065205.1
Lacticaseibacillus paracasei	ATCC 334	GCA_000014525.1
Lacticaseibacillus paracasei	L9	GCA_964065205.1
Lacticaseibacillus paracasei	CAUH35	GCA_001191565.1
Lacticaseibacillus paracasei	Zhang	GCA_000019245.3

Lacticaseibacillus paracasei	LOCK919	GCA_000418515.1
Lacticaseibacillus paracasei	LC2W	GCA_000194785.1
Lacticaseibacillus paracasei subsp. *paracasei*	ATCC 25302 = DSM 5622 = JCM 8130 ATCC 25302 [T]	GCA_004354655.1
*Lacticaseibacillus paracasei s*ubsp. *paracasei*	JCM 8130 [T]	GCA_000159495.1
Lacticaseibacillus rhamnosus	ATCC 8530	GCA_000233755.1
Lacticaseibacillus rhamnosus	DSM 20021 = JCM 1136 = NBRC 3425 DSM 20021 [T]	GCA_007990855.1
Lacticaseibacillus rhamnosus	GG ATCC 53103	GCA_000011045.1
Lacticaseibacillus rhamnosus	Lc 705	GCA_000026525.1
Lacticaseibacillus rhamnosus	LOCK900	GCA_000418475.1
Lacticaseibacillus rhamnosus	LOCK908	GCA_000418495.1
Lacticaseibacillus rhamnosus	BPL15	GCA_001368735.1
Lacticaseibacillus rhamnosus	LMS2-1	GCA_000160175.1

The putative BSH proteins of VB4 and VB1 strains were aligned with 88 representative BSH proteins from 18 lactobacilli species and 6 representative PVA proteins through the COBALT alignment tool. The resulting COBALT alignment was used to calculate a phylogenetic tree. As shown in **Figure 7**, 39 BSH proteins from *L. rhamnosus* (including VB4 and VB1) and the closest *Lacticaseibacillus* relatives (namely *Lacticaseibacillus paracasei*, *Lacticaseibacillus casei*, *Lacticaseibacillus zeae*, and *Lacticaseibacillus chyaiensis*) formed a congruent cluster together with the BSH proteins of *L. acidophilus*, *L. plantarum* (locus tag LP_RS14790), *Limosilactibalcillus reuteri*, and *Lactobacillus paragasseri*. In detail, within this cluster, putative BSH proteins clustered in three minor clusters, corresponding to *L. paracasei*, *L. casei* (including the closest relatives *L. zeae* and *L. chayiensis*), and *L. rhamnosus*. BSH proteins from *L. paracasei*, *L. casei*, and *L. rhamnosus* were also related to the PVA proteins from *Lactococcus lactis* and *Lysinibacillus sphaericus*.

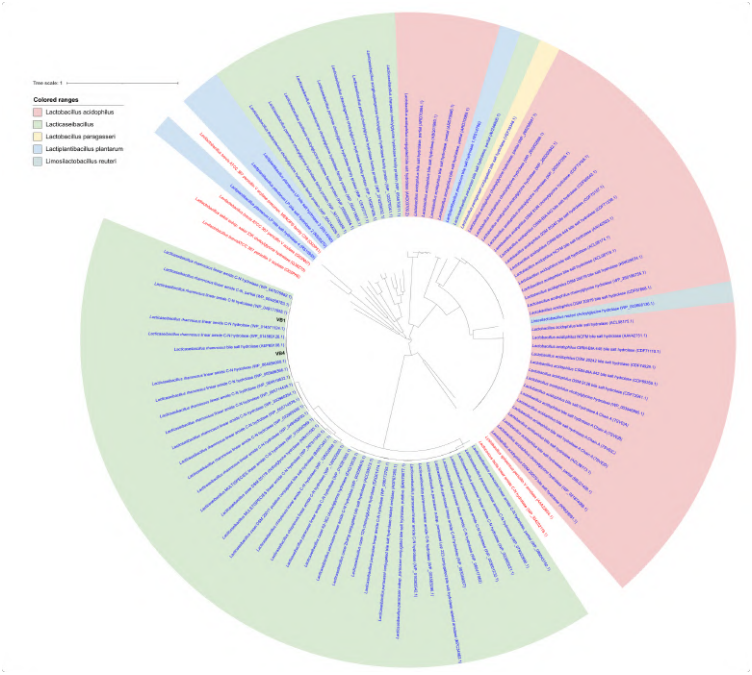

Figure 2.10 - Phylogenetic tree of BSH and PVA proteins. The alignments of 96 bacterial proteins were performed with NCBI COBALT (Grishin, 1995; Kahm et al., 2010). The resulting phylogeny was visualized as a phylogenetic tree using iTOL (Letunic & Bork, 2019). Red labels indicate PVA proteins.

2.3.7 Penicillin V susceptibility results

In order to exclude that predicted BSH proteins in VB4 and VB1 strains can confer PenV tolerance due to a BSH/PVA bifunctional role, the MIC assay was carried out. No visible growth was revealed by testing different PenV dilutions. VB4 and VB1 showed MIC values of 1 µg/mL and 0.5 µg/mL, respectively, and therefore, according to the EFSA breakpoint (4 µg/mL) (Karlov et al.,

2023), they can be considered sensitive to PenV.

2.3.8 Growth curve, bile salt deconjugation activity, and bsh gene expression analysis in presence of BAs mixture

Results of growth curves, in both MRS media with and without 1.0% of BAs, were reported in **Figure 2.11**. According to that, VB4 and VB1 strains differed in growth parameters under the control condition and differently responded to BAs stress (**Figure 2.12**). Under the control condition, the VB1 strain exhibited a long lag phase which significantly decreased in response to the BAs mixture ($p < 0.05$) (**Figure 2.12A**). In contrast, the BAs mixture did not affect the lag phase of strain VB4 ($p > 0.05$). As expected, both strains significantly reduced the μ_{max} and A values in the presence of the BAs mixture compared to the control condition. In addition, the VB4 strain reduced the growth rate and maximum culture density at a lesser extent than VB1 ($p < 0.05$) (**Figure 2.12B, C**).

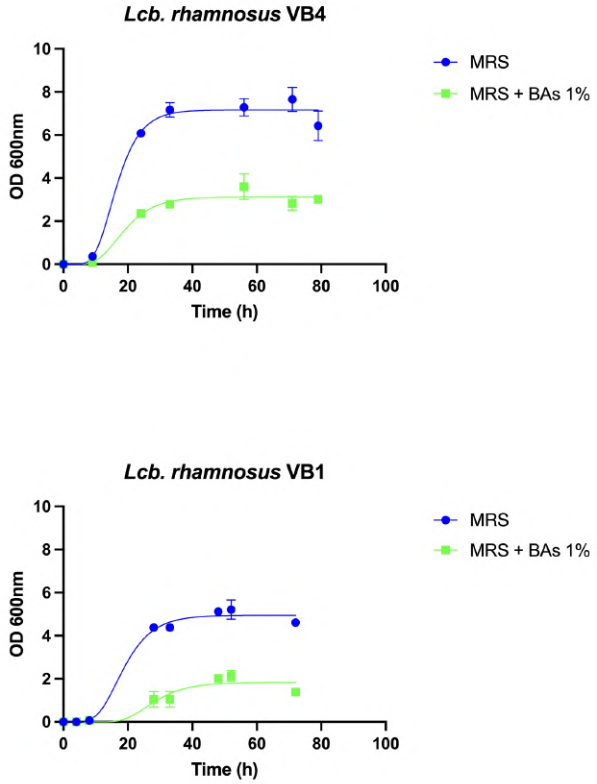

Figure 2.11 - Growth curves of VB4 and VB1 strains in presence of 1% (w/v) BAs mixture (green) compared with control growth conditions (MRS medium; blue). Growth was monitored over the time as mean of OD_{600nm} values in three different biological replicates. Bars (when visible) indicate standard deviation (SD) values of OD_{600nm} measurements. The curves were fitted by non-linear Gompertz model and plotted using v.8.00 software (San Diego, CA, USA, https://www.graphpad.com/).

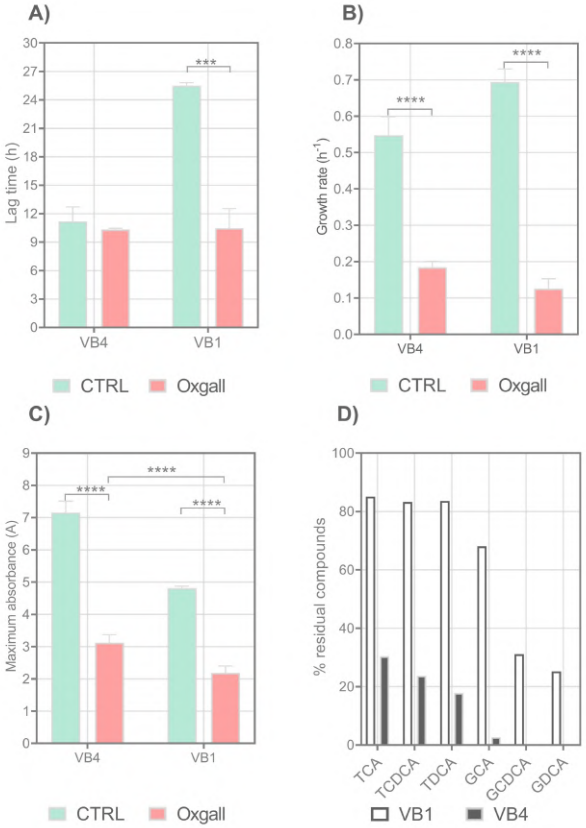

Figure 2.12 - Growth and deconjugation ability of *Lacticaseibacillus rhamnosus* VB4 and VB1 strains in the presence of a BAs mixture (Oxgall). Kinetic parameters lag phase (λ, expressed in h) (A), maximum growth rate (μ, expressed as h^{-1}) (B), and maximum cell density (A expressed as OD_{600nm}) (C) were computed in MRS and MRS supplemented with BAs 1% (*w/v*) by Grofit package (version 1.1.1-1). Residual unconjugated percentages (%) of GCA, GDCA, GCDCA, TCA, TDCA, and TCDCA were estimated in supernatants collected

during late stationary phase (D). Significant differences were calculated with two-way ANOVA and indicated with asterisks, as follows: ***, $p \leq 0.001$; **** $p \leq 0.0001$ (two-way ANOVA). Plotted with GraphPad Prism v.8.00 software (San Diego, CA, USA). Abbreviations: GCA, glycocholic acid; GDCA, glycodeoxycholic acid; GCDCA, glycochenoceoxycholic acid; TCA, taurocholic acid; TDCA, taurodeoxycholic acid, and TCDCA, taurochenodeoxycholic acid.

We examined the BAs deconjugation activity and *bsh* gene expression in VB4 and VB1 cells grown in the presence of a BAs mixture. Concerning BAs deconjugation activity, a UHPLC/HR-MS analysis of supernatants collected at the stationary phase was used to determine the BAs profiles and calculate the percentage of residual unconjugated TCA, TDCA, TCDCA, GCA, GCDA, and GCDCA. As reported in Figure 2.12D, despite the high similarity of putative BSH proteins, strains VB4 and VB1 exhibited significant differences in the ability to deconjugate BAs. In particular, the VB1 strain was active in deconjugating GCDCA and GDCA, leaving only 31.1% and 25.2% of conjugated residual compounds in the medium, respectively. However, the VB1 strain was poorly active in deconjugating GCA (residual percentage of 68.1%) and almost completely inactive in deconjugating the tauro-conjugated BAs. Differently, strain VB4 was found to be able to deconjugate TCA, TDCA, and TCDCA at high extent and was more active than VB1 in deconjugating glyco-conjugated BAs, such as GCDCA, GDCA, and GCA.

Furthermore, the VB4 and VB1 strains also strongly differed in the transcriptional regulation of the *bsh* gene. Preliminarily, we assessed the *bsh* gene transcription by end-point PCR and found that both strains actively transcribed the *bsh* gene both in MRS and MRS supplemented with the BAs mixture (**Figure 2.13**). An RT-qPCR

assay was carried out cells in the stationary phase, showing that while the VB4 strain did not significantly change the *bsh* gene expression in the presence of the BAs mixture compared to MRS alone ($p > 0.05$), the VB1 strain significantly increased the *bsh* gene expression when grown on the BAs mixture ($p < 0.05$) (**Figure 2.14**).

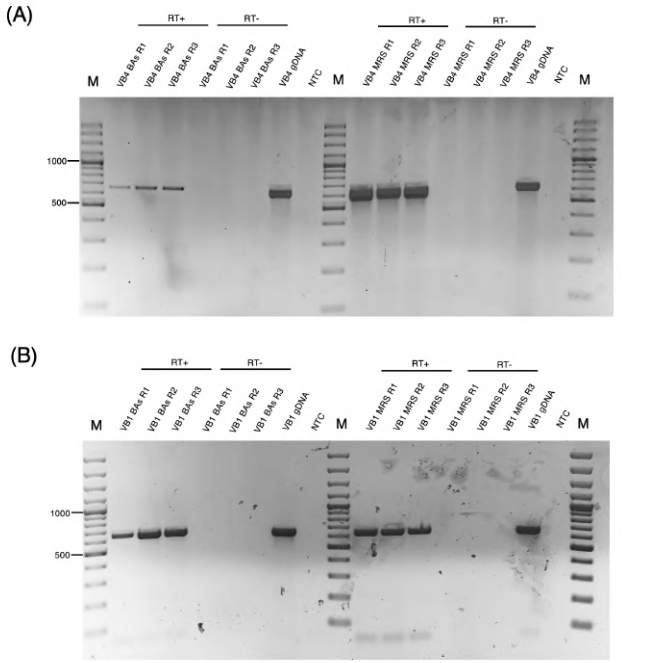

Figure 2.13 - End-point RT-PCR targeting *bsh* gene in BAs-stressed (MRS medium supplemented with 1% (w/v) BAs) and non-stressed (MRS medium) stationary cells of *Lacticaseibacillus rhamnosus* VB4 (A) and VB1 (B), respectively. Three independent replicates, numbered from R1 to R3, were used. +/- RT indicates addition of reverse transcriptase to the cDNA synthesis reaction.

The expected PCR product length was established for each amplicon by using 100 bp DNA Gene Ruler Plus as molecular weight marker. For each RT-PCR reaction gDNA was used as positive control. 16S rRNA gene PCR reactions used as control were omitted. Abbreviations: M, molecular-weight size marker; NTC, negative control.

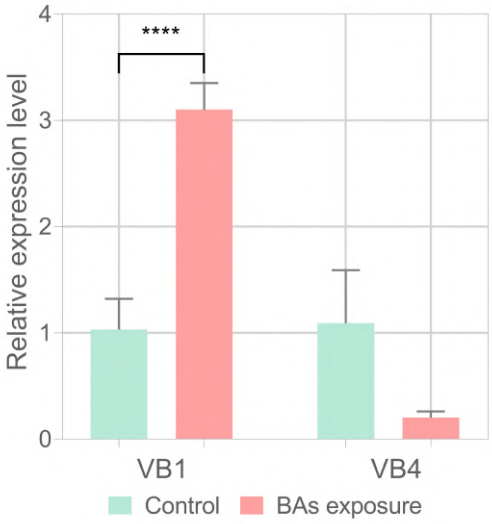

Figure 2.14 - Expression profile of *bsh* gene in *Lacticaseibacillus rhamnosus* VB4 and VB1 in MRS (control condition) and MRS supplemented with 1% (w/v) BAs mixture. Significant differences were calculated with a Student's *t*-test and indicated with asterisks, as follow: **** $p \leq 0.0001$. The bar graph was plotted with GraphPad Prism v.8.00 software (San Diego, CA, USA).

2.4 Discussion

Since 2009, genomics has contributed to conducting accurate genetic studies of probiotic bacteria, establishing genetic characteristics linked to favorable outcomes as well as those possibly

associated with undesirable traits. In combination with *in vitro* and *in vivo* assays, it is considered a robust approach for the discovery and characterization of probiotic strains (Castro-López et al., 2021; Ventura et al., 2009). In this study, we presented the genome sequences of *L. rhamnosus* VB4 and VB1 strains isolated from vaginal samples which have showed a remarkable propensity to deconjugate BAs in a preliminary qualitative direct plate assay. Lactobacilli are considered essential in the vaginal environment where they help maintain the vaginal natural acidic pH, inhibit the growth of potentially harmful microbes, and stabilize the microbial balance (Amabebe & Anuba, 2018). In particular, *L. rhamnosus* strains from vaginal microbiota have been extensively investigated for their probiotic adhesion properties and for the capability to synthesize bacteriocins (Ceapa et al., 2016). However, there are no studies related to the investigation of BSH activity in *L. rhamnosus* strains of vaginal origin.

Safety and genomic stability are essential requirements in probiotics selection. In accordance with regulatory authorities, such as EFSA and FDA, which apply safety guidelines and safety standards on bacterial probiotic strains based on taxonomic classification (EFSA, 2021), it is crucial to accurately determine a new strain's taxonomy before considering its safety and probiotic efficacy. We established unequivocally that VB4 and VB1 strains are *L. rhamnosus* using 16S-rRNA and genome-based phylogenetic analyses. Although many *L. rhamnosus* strains are naturally resistant to vancomycin, this characteristic is an intrinsic phenotype due to the specific structure of cell wall (Tynkkynne et al., 1998). Congruently, the *in silico* analysis and genome annotation did not detect any genetic

determinants for toxigenic activity and AMR in VB4 and VB1 strains, confirming their safe status.

Core- and pan-genes have been widely used to investigate bacterial species evolution and to study intra-strain functional differences within species. In accordance with the evidence of this study, the unique genes of VB4 are likely related to its growing environment and metabolic properties, namely carbohydrates metabolism and transport, amino acid transport and metabolism, and cell wall/membrane/envelope biogenesis. Interestingly, both ANIb and clustering analysis of sharing pattern of accessory COG supported that strain VB4 resembles *L. rhamnosus* GG, a probiotic bacterium with BSH activity isolated from human feces, while VB1 genome is related to *L. rhamnosus* GR-1, a vaginal probiotic bacterium. The probiotic strains *L. rhamnosus* GG and GR-1 have been proved to exert serum cholesterol-lowering activity and to be protective against atherosclerotic plaque formation (Kim et al., 2016; Fang et al., 2019); however, these healthy effects have been not related to BSH activity. *L. rhamnosus* GG and GR-1 strains have been recently included in a pan-genome study which identifies eight phylogroups within *L. rhamnosus* (Dutra-Silva et al., 2023). They resulted to belong to phylotypes 1 and 6, respectively, which mainly differed from each other for genes related to adhesion and bacteriocin production. Indeed, these probiotic traits could be investigated in VB4 and VB1 strains in further studies.

Mobile genetic elements, such as plasmids, prophages, gene islands, and insertion elements, play a major role in horizontal gene transfer in bacteria, driving speciation and functional diversification (Ceapa et al., 2021). The identification of prophages belonging to

the *Siphoviridae* family (currently listed as morphotypes of the *Caudoviricetes* class; Adriaenssens et al., 2020), using a Phigaro analysis, revealed a higher number of phage-related genetic elements in the *L. rhamnosus* strain VB4 than VB1. In particular, *Siphoviridae* prophages are double-stranded prophages largely found in the human intestine virome (Carding et al., 2017), which play a crucial role in bacterial genetic diversity, evolution, and adaptation to changing environments. Previous studies have also documented *Siphoviridae* prophages in *L. rhamnosus* (Durmaz et al., 2008; Happel et al., 2022; Wonglapsuwan et al., 2024) and in other *Lacticaseibacillus* species (da Silva et al., 2022; Mohamed et al., 2023). Interestingly, the Lc-Nu-like prophage, which has been partially found in the VB1 genome, has also been previously detected in other probiotic strains, including *L. rhamnosus* GG (Tuohimaa et al., 2006). It has been proposed that LAB strains containing bacteriophages could have positive impacts on human host (Nanda et al., 2015; Wang et al., 2010). For instance, the expression of prophage functional genes can confer bacterial cell survival advantages in adverse environments (Wang et al., 2010). On the other end, antibiotic resistance genes can be disseminated via phage-mediated transduction. Therefore, it is becoming increasingly evident that prophages should be determined in probiotic genomes for a complete understanding of bacterial physiology, adaptation, and genetic stability.

In addition to prophages, other putative mobile elements, including transposases genes, were found more abundantly in the VB4 genome, compared to the VB1 genome. In addition, the VB4 genome contains a complete type II-A CRISPR–Cas system, which is

relatively widespread across the genus *Lactobacillus* (Panahi et al., 2023). It is expected that CRISPR-positive strains are expected to carry significantly fewer intact prophages than CRISPR-negative strains, as the CRISPR-Cas system acts as anti-phage defense system and inhibits the prophage integration into lactobacilli. However, lactobacilli with a CRISPR-Cas type IIA system, such as *L. rhamnosus* VB4, are more susceptible to temperate phage infections than lactobacilli with a CRISPR-Cas type I/III system (Pei et al., 2021). Consistently, the VB4 strain contains a higher number of phage-related genes than the VB1 strain. In contrast, the VB1 strain contains a lower number of putative genetic mobile elements than VB4 and harbors a type I Cas gene. However, the lack of a CRISPR region around the type I Cas gene raises doubts on the authenticity of the CRISPR-Cas structure in the VB1 genome (Zhang et al., 2017).

Additionally, for the genomic characteristics to be fulfilled, potential probiotics must respond to certain phenotypic activities. At the gastrointestinal level, these microorganisms must be able to deconjugate BAs, which are highly toxic due to their cleansing action. The deconjugation of primary BAs catalyzed by bacteria with the BSH^+ phenotype is considered a pivotal mechanism which assures bacterial fitness and host colonization. Deconjugation products are important precursors of secondary BAs which act as modulators of multiple hosts signaling pathways, mainly involved in body weight maintenance, lipid absorption, and cholesterol metabolism (Agolino et al., 2024). Consequently, dysregulations of secondary BAs are associated with obesity, hypercholesterolemia, cancer, and *Clostridium difficile* infection (Lee et al., 2024). Treatments with BSH-positive probiotics have been shown to increase BSH activity in

the gut and confer multiple health benefits to the host, including the reduction in blood cholesterol levels (Joyce et al., 2014). Therefore, the identification of genes within probiotic genomes involved in BAs deconjugation activity is crucial for discovering new probiotics with BA-modulating properties and potential cholesterol-lowering effects. Even though oral administrations of probiotic lactobacilli have been proven to reduce blood cholesterol levels in animals and humans, the link between bacterial BSH activity and the resulting cholesterol-lowering effect remains poorly understood (Agolino et al., 2024). Similarly, the data supporting the role of BSH in reducing BAs toxicity and assuring bacterial cells with BAs tolerance are contrasting (Begley et al, 2006; Foley et al., 2023; Moser et al., 2001). Furthermore, in some probiotic species, such as *L. rhamnosus*, BSH proteins are highly homologous to PVA and are classified under a single family in various public domain databases, including the CBAH family in Pfam, the Ntn-CGH-like family in CDD, and the C59 family in MEROPS (Daly et al., 2021), leading to possible errors in gene annotation. Recently, the presence of the 'true' *bsh* gene has been questioned for some probiotic species, including *L. rhamnosus* (O'Flaherty et al., 2018). Our results revealed that the VB4 and VB1 strains displayed a distinct BAs deconjugation phenotype without exhibiting any tolerance to PenV. The observed BSH activity is consistent with the presence of the predicted *bsh* gene in the genome, as the only genetic determinants. Remarkably, the BSH protein of strain VB4 was identical in length and amino acid sequence to a *L. rhamnosus* BSH protein which has been experimentally validated by heterologous expression in *E. coli* (AEP69108.1) (Kaya et al., 2018). We cannot exclude that the predicted BSH proteins of

the VB4 and VB1 strains could be active on acyl-homoserine lactones, but, if present, this activity should not contribute to any antibiotic resistance. Similarly, Lambert et al. (2008) reported that *bsh2*, *bsh3*, and *bsh4* genes of *Lactiplantibacillus plantarum* WCFS1 encode BSH enzymes active both towards bile salts and two types of acyl-homoserine lactones, without significantly contributing to PenV tolerance. On the other hand, BSH enzyme of *L. gasseri* JCM 5343^T was demonstrated to degrade both BAs and PenV (Kusada et al., 2022), suggesting that BSH activity and PenV tolerance should be both evaluated in BSH^+ probiotic screening.

Although the search for the *bsh* gene is the first step in screening BSH^+ probiotic candidates, the proposed approach, which integrates genomics and metabolomics, has shown that the high similarity in the sequences of BSH proteins results in neither the same tolerance to BAs nor the same BSH activity in *L. rhamnosus* VB4 and VB1. Indeed, concentrations of BAs slightly higher than the estimated average bile concentration in the human gastrointestinal tract (Corzo & Gilliland, 1999) significantly reduced the lag phase of the VB1 strain but compromised its growth rate compared to the VB4 strain, suggesting a greater tolerance of the latter. Furthermore, strain VB1 exhibited a remarkable glyco-specific deconjugation activity, a phenotype expected for BSH^+ lactobacilli. Like strain VB1, *L. rhamnosus* strain GG is poorly active against TCA and TDCA (Hernández-Gómez et al., 2021). The glycine preference of lactobacilli BSH may be due to the higher abundance of glycine-conjugated BAs in human bile and the proposed higher toxicity of these to taurine-conjugated BAs (Corzo & Gilliland, 1999; Prete et al., 2020). However, Foley and coworkers (2021) showed that

deconjugated BAs, such as CA, CDCA, and DCA, are more toxic to species *L. acidophilus* and *L. gasseri*, suggesting that conjugated/deconjugated BA–bacterial interaction is more complex than that previously assumed. Similarly, Prete et al. (2020) reported that BSH-mediated conversion to more hydrophobic moieties may reduce bacterial growth.

Unlike VB1, *L. rhamnosus* VB4 strains are also active on tauro-conjugated BAs. The ability to cleave the amide bond between the taurine and steroid moiety has been described in *L. johnsonii* and *L. gasseri* species (Dong & Lee, 2018). Here, it was hypothesized that the BSH activity of the VB4 strain towards taurine-conjugated BAs could have an interesting effect in modulating secondary BAs. Taurine is the limiting factor in bacterial bile acid amidates (BBAAs) synthesis by colonic microbiota (Rimal et al., 2024). Probiotics with BSH activity on tauro-conjugated BAs could positively affect BBAAs levels.

BSH proteins of the VB4 and VB1 strains are almost identical, thus the observed difference in BSH activities towards glyco- or tauro-conjugated BA substrates could reflect differences in tolerance to the resulting deconjugated moieties rather than differences in the substrate affinity of the BSH enzymes. Furthermore, the VB4 strain exhibited more BAs-deconjugating activity than VB1 but did not increase the *bsh* gene transcription under BAs exposition, supporting that the strains also differ in *bsh* gene transcriptional regulation. Previous works reported that the exposure of *L. salivarius* and *L. acidophilus* BSH-active strains to bile did not induce the *bsh* gene expression (Foley et al., 2021; Pfeiler et al., 2007). Similarly, Lambert and coworkers (2008) reported that the expression of the

four *bsh* genes is not induced in the *L. plantarum* WCFS1 strain by exposure to porcine bile, while Bron et al. (2006) found that only the *bsh1* gene is strongly upregulated by BAs in this strain. Recently, a transcriptomic study confirmed that all four *bsh* genes are downregulated in *L. plantarum* grown under BAs stress (Chen et al., 2024). The lack of correlation between the observed enzymatic activity and the transcriptional regulation of the *bsh* gene in strains VB4 and VB1 could suggest that the BSH+ phenotype involves more gene pathways than the mere BSH activity and that these gene pathways could be different in both tested strains. The presence of conjugated BAs changes the pathways responsible for membrane organization and permeability in *Bifidobacterium longum* (Sánchez et al., 2005), while exposure to GCA impacts the expression of genes encoding cell surface proteins and transport proteins in *L. acidophilus* (Foley et al., 2021). These results suggest that the ability to eliminate the BAs outside the cell is a key factor in decreasing the detergent effect of deconjugated BAs and assuring a BSH+ phenotype. A time-line transcriptomic analysis coupled with the BA-profiling by metabolomics could help to elucidate this point in the VB4 and VB1 strains in future.

2.5 Conclusions

Probiotics can be one of the promising therapeutic tools for manipulating a host's BAs profile. The results shown in the present work demonstrated that the VB4 and VB1 strains have very similar BSH proteins but different BSH activity, suggesting that they probably differ in the detoxification system of the resulting unconjugated BAs. Combining bacterial genomics and metagenomic approaches, we

demonstrated that strain VB4 is a promising BAs-modulating probiotic candidate and that BSH active phenotype is a complex trait which probably depends on different factors other than the presence of *bsh* gene in *L. rhamnosus* vaginal strains.

This work was conducted in collaboration with the University of Modena and Reggio Emilia, under the supervision of Professors Lisa Solieri and Davide Tagliazucchi, with the contribution of Dr. Marianna Cristofolini and Alice Cattivelli, during a research and training period within the doctoral project at the Department of Life Sciences.

Author contributions

Writing—original draft preparation, G.A. and L.S.; writing—review and editing, M.C., A.V., D.T., A.C., A.P., C.C. and C.L.R.; data curation, G.A., A.V., D.T., A.P., L.S. and C.L.R.; formal analysis, G.A., M.C., D.T., A.C., A.P. and L.S.; investigation, D.T., A.P., C.C., L.S. and C.L.R.; methodology, D.T., A.P., L.S. and C.L.R.; conceptualization, A.P., L.S. and C.L.R.; software, L.S.; visualization, L.S.; and funding acquisition, A.P., L.S. and C.L.R. All authors have read and agreed to the published version of the manuscript.

Funding

The authors acknowledge the support of the NBFC to University of Modena and Reggio Emilia, funded by the Italian Ministry of University and Research, PNRR, Missione 4 Componente 2, "Dalla ricerca all'impresa", Investimento 1.4, Project CN00000033. The funders had no role in study design, data collection and analysis, decision to publish, or preparation of the manuscript.

Data availability statement

UHPLC/HR-MS data will be made available on request. Raw reads of *L. rhamnosus* VB1 and VB4 genomes have been deposited at the NCBI Sequence Read Archive (SRA) under the accession numbers PRJNA1139681 and PRJNA1139679, respectively.

Acknowledgments

The authors acknowledge the Fondazione Cassa di Risparmio di Modena for funding the UPLC-ESI-Q Exactive Hybrid Quadrupole-Orbitrap Mass Spectrometer system at the Centro Interdipartimentale Grandi Strumenti (CIGS). The authors acknowledge the project PIAno di inCEntivi per la RIcerca di Ateneo 2020/2022—Linea di Intervento 3 "Starting Grant".

Project Title “Selezione di probiotici con attività idrolasica dei sali biliari (BSH) per la salute umana”, ProBSH.

References

1. Adriaenssens, E. M., Sullivan, M. B., Knezevic, P., van Zyl, L. J., Sarkar, B. L., Dutilh, B. E., Alfenas-Zerbini, P., Łobocka, M., Tong, Y., Brister, J. R., Moreno Switt, A. I., Klumpp, J., Aziz, R. K., Barylski, J., Uchiyama, J., Edwards, R. A., Kropinski, A. M., Petty, N. K., Clokie, M. R. J., Kushkina, A. I., … Krupovic, M. (2020). Taxonomy of prokaryotic viruses: 2018-2019 update from the ICTV Bacterial and Archaeal Viruses Subcommittee. *Archives of virology*, *165*(5), 1253–1260. https://doi.org/10.1007/s00705-020-04577-8.
2. Agolino, G., Pino, A., Vaccalluzzo, A., Cristofolini, M., Solieri, L., Caggia, C., & Randazzo, C. L. (2024). Bile salt hydrolase: The complexity behind its mechanism in relation to lowering-cholesterol lactobacilli probiotics. *Journal of Functional Foods*, *120*, 106357. https://doi.org/10.1016/j.jff.2024.106357.
3. Alcock, B. P., Huynh, W., Chalil, R., Smith, K. W., Raphenya, A. R., Wlodarski, M. A., Edalatmand, A., Petkau, A., Syed, S. A., Tsang, K. K., Baker, S. J. C., Dave, M., McCarthy, M. C., Mukiri, K. M., Nasir, J. A., Golbon, B., Imtiaz, H., Jiang, X., Kaur, K., Kwong, M., … McArthur, A. G. (2023). CARD 2023: expanded curation, support for machine learning, and resistome prediction at the Comprehensive Antibiotic Resistance Database. *Nucleic acids research*, *51*(D1), D690–D699. https://doi.org/10.1093/nar/gkac920.
4. Amabebe, E., & Anumba, D. O. C. (2018). The Vaginal Microenvironment: The Physiologic Role of *Lactobacilli*. *Frontiers in medicine*, *5*, 181. https://doi.org/10.3389/fmed.2018.001.
5. Begley, M., Hill, C., & Gahan, C. G. (2006). Bile salt hydrolase activity in probiotics. *Applied and environmental microbiology*, *72*(3), 1729–1738. https://doi.org/10.1128/AEM.72.3.1729-1738.2006.
6. Bolger, A. M., Lohse, M., & Usadel, B. (2014). Trimmomatic: a flexible trimmer for Illumina sequence data. *Bioinformatics (Oxford, England)*, *30*(15), 2114–2120. https://doi.org/10.1093/bioinformatics/btu170.

7. Bortolaia, V., Kaas, R. S., Ruppe, E., Roberts, M. C., Schwarz, S., Cattoir, V., Philippon, A., Allesoe, R. L., Rebelo, A. R., Florensa, A. F., Fagelhauer, L., Chakraborty, T., Neumann, B., Werner, G., Bender, J. K., Stingl, K., Nguyen, M., Coppens, J., Xavier, B. B., Malhotra-Kumar, S., … Aarestrup, F. M. (2020). ResFinder 4.0 for predictions of phenotypes from genotypes. *The Journal of antimicrobial chemotherapy*, *75*(12), 3491–3500. https://doi.org/10.1093/jac/dkaa345.
8. Bourgin, M., Kriaa, A., Mkaouar, H., Mariaule, V., Jablaoui, A., Maguin, E., & Rhimi, M. (2021). Bile Salt Hydrolases: At the Crossroads of Microbiota and Human Health. *Microorganisms*, *9*(6), 1122. https://doi.org/10.3390/microorganisms9061122.
9. Bron, P. A., Molenaar, D., de Vos, W. M., & Kleerebezem, M. (2006). DNA micro-array-based identification of bile-responsive genes in Lactobacillus plantarum. *Journal of applied microbiology*, *100*(4), 728–738. https://doi.org/10.1111/j.1365-2672.2006.02891.x.
10. Brown, C. L., Mullet, J., Hindi, F., Stoll, J. E., Gupta, S., Choi, M., Keenum, I., Vikesland, P., Pruden, A., & Zhang, L. (2022). mobileOG-db: a Manually Curated Database of Protein Families Mediating the Life Cycle of Bacterial Mobile Genetic Elements. *Applied and environmental microbiology*, *88*(18), e0099122. https://doi.org/10.1128/aem.00991-22.
11. Bustos, A. Y., Font de Valdez, G., Fadda, S., & Taranto, M. P. (2018). New insights into bacterial bile resistance mechanisms: the role of bile salt hydrolase and its impact on human health. *Food research international (Ottawa, Ont.)*, *112*, 250–262. https://doi.org/10.1016/j.foodres.2018.06.035.
12. Capurso L. (2019). Thirty Years of *Lactobacillus rhamnosus* GG: A Review. *Journal of clinical gastroenterology*, *53 Suppl 1*, S1–S41. https://doi.org/10.1097/MCG.0000000000001170.
13. Carattoli, A., & Hasman, H. (2020). PlasmidFinder and In Silico pMLST: Identification and Typing of Plasmid Replicons in Whole-Genome Sequencing (WGS). *Methods in molecular biology (Clifton, N.J.)*, *2075*, 285–294. https://doi.org/10.1007/978-1-4939-9877-7_20.
14. Carding, S. R., Davis, N., & Hoyles, L. (2017). Review article: the human intestinal virome in health and disease. *Alimentary pharmacology & therapeutics*, *46*(9), 800–815. https://doi.org/10.1111/apt.14280 .

15. Castro-López, C., Garcia, H. S., Martinez-Avila, G. C. G., González-Córdova, A. F., Vallejo-Cordoba, B., & Hernández-Mendoza, A. (2021). Genomics-based approaches to identify and predict the health-promoting and safety activities of promising probiotic strains–A probiogenomics review. *Trends in Food Science & Technology*, *108*, 148-163. https://doi.org/10.1016/j.tifs.2020.12.017.
16. Ceapa, C., Davids, M., Ritari, J., Lambert, J., Wels, M., Douillard, F. P., Smokvina, T., de Vos, W. M., Knol, J., & Kleerebezem, M. (2016). The Variable Regions of *Lactobacillus rhamnosus* Genomes Reveal the Dynamic Evolution of Metabolic and Host-Adaptation Repertoires. *Genome biology and evolution*, *8*(6), 1889–1905. https://doi.org/10.1093/gbe/evw123.
17. Chen, C., Li, M., Yu, L., Tian, F., Zhao, J., Chen, W., & Zhai, Q. (2024). Comparative genomics of *Lactiplantibacillus plantarum* reveals the role of the two-component system in response to bile salts stress. *Food Bioscience*, *61*, 104803. https://doi.org/10.1016/j.fbio.2024.104803.
18. Corzo, G., & Gilliland, S. E. (1999). Bile salt hydrolase activity of three strains of *Lactobacillus acidophilus*. *Journal of dairy science*, *82*(3), 472–480. https://doi.org/10.3168/jds.S0022-0302(99)75256-2.
19. Couvin, D., Bernheim, A., Toffano-Nioche, C., Touchon, M., Michalik, J., Néron, B., Rocha, E. P. C., Vergnaud, G., Gautheret, D., & Pourcel, C. (2018). CRISPRCasFinder, an update of CRISRFinder, includes a portable version, enhanced performance and integrates search for Cas proteins. *Nucleic acids research*, *46*(W1), W246–W251. https://doi.org/10.1093/nar/gky425.
20. Daly, J. W., Keely, S. J., & Gahan, C. G. M. (2021). Functional and Phylogenetic Diversity of BSH and PVA Enzymes. *Microorganisms*, *9*(4), 732. https://doi.org/10.3390/microorganisms9040732.
21. da Silva, T. F., Glória, R. A., Americo, M. F., Freitas, A. D. S., de Jesus, L. C. L., Barroso, F. A. L., Laguna, J. G., Coelho-Rocha, N. D., Tavares, L. M., le Loir, Y., Jan, G., Guédon, É., & Azevedo, V. A. C. (2024). Unlocking the Potential of Probiotics: A Comprehensive Review on Research, Production, and Regulation of Probiotics. *Probiotics and*

antimicrobial proteins, *16*(5), 1687–1723. https://doi.org/10.1007/s12602-024-10247-x.

22. da Silva Barreira, D., Lapaquette, P., Novion Ducassou, J., Couté, Y., Guzzo, J., & Rieu, A. (2022). Spontaneous Prophage Induction Contributes to the Production of Membrane Vesicles by the Gram-Positive Bacterium *Lacticaseibacillus casei* BL23. *mBio*, *13*(5), e0237522. https://doi.org/10.1128/mbio.02375-22.
23. Dereeper, A., Summo, M., & Meyer, D. F. (2022). PanExplorer: a web-based tool for exploratory analysis and visualization of bacterial pan-genomes. *Bioinformatics (Oxford, England)*, *38*(18), 4412–4414. https://doi.org/10.1093/bioinformatics/btac504.
24. Desper, R., & Gascuel, O. (2004). Theoretical foundation of the balanced minimum evolution method of phylogenetic inference and its relationship to weighted least-squares tree fitting. *Molecular biology and evolution*, *21*(3), 587–598. https://doi.org/10.1093/molbev/msh049 .
25. Dong, Z., & Lee, B. H. (2018). Bile salt hydrolases: Structure and function, substrate preference, and inhibitor development. *Protein science : a publication of the Protein Society*, *27*(10), 1742–1754. https://doi.org/10.1002/pro.3484.
26. Durmaz, E., Miller, M. J., Azcarate-Peril, M. A., Toon, S. P., & Klaenhammer, T. R. (2008). Genome sequence and characteristics of Lrm1, a prophage from industrial *Lactobacillus rhamnosus* strain M1. *Applied and environmental microbiology*, *74*(15), 4601–4609. https://doi.org/10.1128/AEM.00010-08.
27. Dutra-Silva, L., Matteoli, F. P., & Arisi, A. C. M. (2023). Distribution of Genes Related to Probiotic Effects Across *Lacticaseibacillus rhamnosus* Revealed by Population Structure. *Probiotics and antimicrobial proteins*, *15*(3), 548–557. https://doi.org/10.1007/s12602-021-09868-3.
28. Edgar R. C. (2004). MUSCLE: multiple sequence alignment with high accuracy and high throughput. *Nucleic acids research*, *32*(5), 1792–1797. https://doi.org/10.1093/nar/gkh340.
29. Fang, Y., Chen, H. Q., Zhang, X., Zhang, H., Xia, J., Ding, K., & Fang, Z. Y. (2019). Probiotic administration of *Lactobacillus rhamnosus* GR-1 attenuates atherosclerotic plaque formation in ApoE-/- mice fed with a high-fat diet. *European review for medical and pharmacological*

sciences, *23*(8), 3533–3541. https://doi.org/10.26355/eurrev_201904_17722.

30. Foley, M. H., O'Flaherty, S., Allen, G., Rivera, A. J., Stewart, A. K., Barrangou, R., & Theriot, C. M. (2021). *Lactobacillus* bile salt hydrolase substrate specificity governs bacterial fitness and host colonization. *Proceedings of the National Academy of Sciences of the United States of America*, *118*(6), e2017709118. https://doi.org/10.1073/pnas.2017709118.
31. Foley, M. H., O'Flaherty, S., Barrangou, R., & Theriot, C. M. (2019). Bile salt hydrolases: Gatekeepers of bile acid metabolism and host-microbiome crosstalk in the gastrointestinal tract. *PLoS pathogens*, *15*(3), e1007581. https://doi.org/10.1371/journal.ppat.1007581.
32. Foley, M. H., Walker, M. E., Stewart, A. K., O'Flaherty, S., Gentry, E. C., Patel, S., Beaty, V. V., Allen, G., Pan, M., Simpson, J. B., Perkins, C., Vanhoy, M. E., Dougherty, M. K., McGill, S. K., Gulati, A. S., Dorrestein, P. C., Baker, E. S., Redinbo, M. R., Barrangou, R., & Theriot, C. M. (2023). Bile salt hydrolases shape the bile acid landscape and restrict *Clostridioides difficile* growth in the murine gut. *Nature microbiology*, *8*(4), 611–628. https://doi.org/10.1038/s41564-023-01337-7.
33. EFSA Panel on Additives and Products or Substances used in Animal Feed (FEEDAP); Rychen, G.; Aquilina, G.; Azimonti, G.; Bampidis, V.; de Lourdes Bastos, M.; Bories, G.; Chesson, A.; Cocconcelli, P.S.; Flachowsky, G.; et al. (2018). Guidance on the characterization of microorganisms used as feed additives or as production organisms. *EFSA J.* **2018**, *16*, e05206.
34. European Food Safety Authority (EFSA) (2021). EFSA statement on the requirements for whole genome sequence analysis of microorganisms intentionally used in the food chain. *EFSA journal. European Food Safety Authority*, *19*(7), e06506. https://doi.org/10.2903/j.efsa.2021.6506.
35. Grant, J. R., Enns, E., Marinier, E., Mandal, A., Herman, E. K., Chen, C. Y., Graham, M., Van Domselaar, G., & Stothard, P. (2023). Proksee: in-depth characterization and visualization of bacterial genomes. *Nucleic*

acids research, *51*(W1), W484–W492. https://doi.org/10.1093/nar/gkad32.

36. Grishin N. V. (1995). Estimation of the number of amino acid substitutions per site when the substitution rate varies among sites. *Journal of molecular evolution*, *41*(5), 675–679. https://doi.org/10.1007/BF00175826.
37. Happel, A. U., Kullin, B. R., Gamieldien, H., Jaspan, H. B., Varsani, A., Martin, D., Passmore, J. S., & Froissart, R. (2022). *In Silico* Characterisation of Putative Prophages in *Lactobacillaceae* Used in Probiotics for Vaginal Health. *Microorganisms*, *10*(2), 214. https://doi.org/10.3390/microorganisms10020214.
38. Hernández-Gómez, J. G., López-Bonilla, A., Trejo-Tapia, G., Ávila-Reyes, S. V., Jiménez-Aparicio, A. R., & Hernández-Sánchez, H. (2021). *In Vitro* Bile Salt Hydrolase (BSH) Activity Screening of Different Probiotic Microorganisms. *Foods (Basel, Switzerland)*, *10*(3), 674. https://doi.org/10.3390/foods10030674.
39. International Organization of Standardization/International Dairy Federation. *(ISO 10932/IDF 223) Milk and Milk Products. Determination of the Minimal Inhibitory Concentration (MIC) of Antibiotics Applicable to Bifidobacteria and Non-Enterococcal Lactic Acid Bacteria (LAB)*, 1st ed.; ISO and IDF: Geneva, Switzerland, 2010.
40. Jayashree, S., Pooja, S., Pushpanathan, M., Rajendhran, J., & Gunasekaran, P. (2014). Identification and characterization of bile salt hydrolase genes from the genome of *Lactobacillus fermentum* MTCC 8711. *Applied biochemistry and biotechnology*, *174*(2), 855–866. https://doi.org/10.1007/s12010-014-1118-5.
41. Joyce, S. A., Shanahan, F., Hill, C., & Gahan, C. G. (2014). Bacterial bile salt hydrolase in host metabolism: Potential for influencing gastrointestinal microbe-host crosstalk. *Gut microbes*, *5*(5), 669–674. https://doi.org/10.4161/19490976.2014.969986.
42. Kahm, M., Hasenbrink, G., Lichtenberg-Fraté, H., Ludwig, J., & Kschischo, M. (2010). grofit: fitting biological growth curves with R. *Journal of statistical software*, *33*, 1-21. https://doi.org/10.18637/jss.v033.i07.

43. Kanehisa, M., Sato, Y., & Morishima, K. (2016). BlastKOALA and GhostKOALA: KEGG Tools for Functional Characterization of Genome and Metagenome Sequences. *Journal of molecular biology*, *428*(4), 726–731. https://doi.org/10.1016/j.jmb.2015.11.006.
44. Karlov, D. S., Long, S. L., Zeng, X., Xu, F., Lal, K., Cao, L., Hayoun, K., Lin, J., Joyce, S. A., & Tikhonova, I. G. (2023). Characterization of the mechanism of bile salt hydrolase substrate specificity by experimental and computational analyses. *Structure (London, England : 1993)*, *31*(5), 629–638.e5. https://doi.org/10.1016/j.str.2023.02.014.
45. Kaya, Y., Kök, M. Ş., & Öztürk, M. (2017). Molecular cloning, expression and characterization of bile salt hydrolase from *Lactobacillus rhamnosus* E9 strain. *Food Biotechnology*, *31*(2), 128-140. https://doi.org/10.1080/08905436.2017.1303778.
46. Kim, B., Park, K. Y., Ji, Y., Park, S., Holzapfel, W., & Hyun, C. K. (2016). Protective effects of *Lactobacillus rhamnosus* GG against dyslipidemia in high-fat diet-induced obese mice. *Biochemical and biophysical research communications*, *473*(2), 530–536. https://doi.org/10.1016/j.bbrc.2016.03.107.
47. Kimura M. (1980). A simple method for estimating evolutionary rates of base substitutions through comparative studies of nucleotide sequences. *Journal of molecular evolution*, *16*(2), 111–120. https://doi.org/10.1007/BF01731581.
48. Kusada, H., Arita, M., Tohno, M., & Tamaki, H. (2022). Bile Salt Hydrolase Degrades β-Lactam Antibiotics and Confers Antibiotic Resistance on *Lactobacillus paragasseri*. *Frontiers in microbiology*, *13*, 858263. https://doi.org/10.3389/fmicb.2022.858263.
49. Lambert, J. M., Bongers, R. S., de Vos, W. M., & Kleerebezem, M. (2008). Functional analysis of four bile salt hydrolase and penicillin acylase family members in *Lactobacillus plantarum* WCFS1. *Applied and environmental microbiology*, *74*(15), 4719–4726. https://doi.org/10.1128/AEM.00137-08.
50. Lee, M. H., Nuccio, S. P., Mohanty, I., Hagey, L. R., Dorrestein, P. C., Chu, H., & Raffatellu, M. (2024). How bile acids and the microbiota interact to shape host immunity. *Nature reviews. Immunology*, *24*(11), 798–809. https://doi.org/10.1038/s41577-024-01057-x.

51. Letunic, I., & Bork, P. (2019). Interactive Tree Of Life (iTOL) v4: recent updates and new developments. *Nucleic acids research*, *47*(W1), W256–W259. https://doi.org/10.1093/nar/gkz239.
52. Makarova, K. S., Wolf, Y. I., & Koonin, E. V. (2018). Classification and Nomenclature of CRISPR-Cas Systems: Where from Here? *The CRISPR journal*, *1*(5), 325–336. https://doi.org/10.1089/crispr.2018.0033 .
53. Malberg Tetzschner, A. M., Johnson, J. R., Johnston, B. D., Lund, O., & Scheutz, F. (2020). *In Silico* Genotyping of Escherichia coli Isolates for Extraintestinal Virulence Genes by Use of Whole-Genome Sequencing Data. *Journal of clinical microbiology*, *58*(10), e01269-20. https://doi.org/10.1128/JCM.01269-20.
54. McAuliffe, O., Cano, R. J., & Klaenhammer, T. R. (2005). Genetic analysis of two bile salt hydrolase activities in *Lactobacillus acidophilus* NCFM. *Applied and environmental microbiology*, *71*(8), 4925–4929. https://doi.org/10.1128/AEM.71.8.4925-4929.2005.
55. Mohamed, H. M., Barzideh, Z., Siddiqi, M., & LaPointe, G. (2023). Taxonomy, Sequence Variance and Functional Profiling of the Microbial Community of Long-Ripened Cheddar Cheese Using Shotgun Metagenomics. *Microorganisms*, *11*(8), 2052. https://doi.org/10.3390/microorganisms11082052.
56. Mohanty, I., Allaband, C., Mannochio-Russo, H., El Abiead, Y., Hagey, L. R., Knight, R., & Dorrestein, P. C. (2024). The changing metabolic landscape of bile acids - keys to metabolism and immune regulation. *Nature reviews. Gastroenterology & hepatology*, *21*(7), 493–516. https://doi.org/10.1038/s41575-024-00914-3.
57. Moser, S. A., & Savage, D. C. (2001). Bile salt hydrolase activity and resistance to toxicity of conjugated bile salts are unrelated properties in lactobacilli. *Applied and environmental microbiology*, *67*(8), 3476–3480. https://doi.org/10.1128/AEM.67.8.3476-3480.2001.
58. Nanda, A. M., Thormann, K., & Frunzke, J. (2015). Impact of spontaneous prophage induction on the fitness of bacterial populations and host-microbe interactions. *Journal of bacteriology*, *197*(3), 410–419. https://doi.org/10.1128/JB.02230-14.
59. O'Flaherty, S., Briner Crawley, A., Theriot, C. M., & Barrangou, R. (2018). The *Lactobacillus* Bile Salt Hydrolase Repertoire Reveals

Niche-Specific Adaptation. *mSphere*, *3*(3), e00140-18. https://doi.org/10.1128/mSphere.00140-18.

60. O'Leary, N. A., Wright, M. W., Brister, J. R., Ciufo, S., Haddad, D., McVeigh, R., Rajput, B., Robbertse, B., Smith-White, B., Ako-Adjei, D., Astashyn, A., Badretdin, A., Bao, Y., Blinkova, O., Brover, V., Chetvernin, V., Choi, J., Cox, E., Ermolaeva, O., Farrell, C. M., … Pruitt, K. D. (2016). Reference sequence (RefSeq) database at NCBI: current status, taxonomic expansion, and functional annotation. *Nucleic acids research*, *44*(D1), D733–D745. https://doi.org/10.1093/nar/gkv1189.
61. Panahi, B., Dehganzad, B., & Nami, Y. (2023). CRISPR-Cas systems feature and targeting phages diversity in *Lacticaseibacillus rhamnosus* strains. *Frontiers in microbiology*, *14*, 1281307. https://doi.org/10.3389/fmicb.2023.1281307.
62. Papadopoulos, J. S., & Agarwala, R. (2007). COBALT: constraint-based alignment tool for multiple protein sequences. *Bioinformatics (Oxford, England)*, *23*(9), 1073–1079. https://doi.org/10.1093/bioinformatics/btm076.
63. Park, S., Kang, J., Choi, S., Park, H., Hwang, E., Kang, Y. G., Kim, A. R., Holzapfel, W., & Ji, Y. (2018). Cholesterol-lowering effect of *Lactobacillus rhamnosus* BFE5264 and its influence on the gut microbiome and propionate level in a murine model. *PloS one*, *13*(8), e0203150. https://doi.org/10.1371/journal.pone.0203150.
64. Pei, Z., Sadiq, F. A., Han, X., Zhao, J., Zhang, H., Ross, R. P., Lu, W., & Chen, W. (2021). Comprehensive Scanning of Prophages in *Lactobacillus*: Distribution, Diversity, Antibiotic Resistance Genes, and Linkages with CRISPR-Cas Systems. *mSystems*, *6*(3), e0121120. https://doi.org/10.1128/mSystems.01211-20.
65. Pfaffl, M. W., Horgan, G. W., & Dempfle, L. (2002). Relative expression software tool (REST) for group-wise comparison and statistical analysis of relative expression results in real-time PCR. *Nucleic acids research*, *30*(9), e36. https://doi.org/10.1093/nar/30.9.e36.
66. Pfeiler, E. A., Azcarate-Peril, M. A., & Klaenhammer, T. R. (2007). Characterization of a novel bile-inducible operon encoding a two-component regulatory system in Lactobacillus acidophilus. *Journal of*

bacteriology, *189*(13), 4624–4634. https://doi.org/10.1128/JB.00337-07.

67. Prete, R., Long, S. L., Gallardo, A. L., Gahan, C. G., Corsetti, A., & Joyce, S. A. (2020). Beneficial bile acid metabolism from Lactobacillus plantarum of food origin. *Scientific reports*, *10*(1), 1165. https://doi.org/10.1038/s41598-020-58069-5.
68. Ridlon, J. M., & Bajaj, J. S. (2015). The human gut sterolbiome: bile acid-microbiome endocrine aspects and therapeutics. *Acta pharmaceutica Sinica. B*, *5*(2), 99–105. https://doi.org/10.1016/j.apsb.2015.01.006.
69. Ridlon, J. M., & Gaskins, H. R. (2024). Another renaissance for bile acid gastrointestinal microbiology. *Nature reviews. Gastroenterology & hepatology*, *21*(5), 348–364. https://doi.org/10.1038/s41575-024-00896-2.
70. Rimal, B., Collins, S. L., Tanes, C. E., Rocha, E. R., Granda, M. A., Solanki, S., Hoque, N. J., Gentry, E. C., Koo, I., Reilly, E. R., Hao, F., Paudel, D., Singh, V., Yan, T., Kim, M. S., Bittinger, K., Zackular, J. P., Krausz, K. W., Desai, D., Amin, S., … Patterson, A. D. (2024). Bile salt hydrolase catalyses formation of amine-conjugated bile acids. *Nature*, *626*(8000), 859–863. https://doi.org/10.1038/s41586-023-06990-w.
71. Rossi, F., Amadoro, C., Pallotta, M. L., & Colavita, G. (2022). Variability of Genetic Characters Associated with Probiotic Functions in *Lacticaseibacillus* Species. *Microorganisms*, *10*(5), 1023. https://doi.org/10.3390/microorganisms10051023.
72. Saitou, N., & Nei, M. (1987). The neighbor-joining method: a new method for reconstructing phylogenetic trees. *Molecular biology and evolution*, *4*(4), 406–425. https://doi.org/10.1093/oxfordjournals.molbev.a040454.
73. Sánchez, B., Champomier-Vergès, M. C., Anglade, P., Baraige, F., de Los Reyes-Gavilán, C. G., Margolles, A., & Zagorec, M. (2005). Proteomic analysis of global changes in protein expression during bile salt exposure of *Bifidobacterium longum* NCIMB 8809. *Journal of bacteriology*, *187*(16), 5799–5808. https://doi.org/10.1128/JB.187.16.5799-5808.2005.

74. Schwengers, O., Jelonek, L., Dieckmann, M. A., Beyvers, S., Blom, J., & Goesmann, A. (2021). Bakta: rapid and standardized annotation of bacterial genomes via alignment-free sequence identification. *Microbial genomics*, *7*(11), 000685. https://doi.org/10.1099/mgen.0.000685 .
75. Seppey, M., Manni, M., & Zdobnov, E. M. (2019). BUSCO: Assessing Genome Assembly and Annotation Completeness. *Methods in molecular biology (Clifton, N.J.)*, *1962*, 227–245. https://doi.org/10.1007/978-1-4939-9173-0_14.
76. Solieri, L., Sola, L., Vaccalluzzo, A., Randazzo, C. L., Martini, S., & Tagliazucchi, D. (2022). Characterization of Cell-Envelope Proteinases from Two *Lacticaseibacillus casei* Strains Isolated from Parmigiano Reggiano Cheese. *Biology*, *11*(1), 139. https://doi.org/10.3390/biology11010139.
77. Song, Z., Feng, S., Zhou, X., Song, Z., Li, J., & Li, P. (2023). Taxonomic identification of bile salt hydrolase-encoding lactobacilli: Modulation of the enterohepatic bile acid profile. *iMeta*, *2*(3), e128. https://doi.org/10.1002/imt2.128.
78. Stackebrandt, E. (2006). Taxonomic parameters revisited: tarnished gold standards. *Microbial Today*, *33*, 152. https://doi.org/10.1371/journal.pone.0172164.
79. Starikova, E. V., Tikhonova, P. O., Prianichnikov, N. A., Rands, C. M., Zdobnov, E. M., Ilina, E. N., & Govorun, V. M. (2020). Phigaro: high-throughput prophage sequence annotation. *Bioinformatics (Oxford, England)*, *36*(12), 3882–3884. https://doi.org/10.1093/bioinformatics/btaa250.
80. Tamura, K., Stecher, G., & Kumar, S. (2021). MEGA11: Molecular Evolutionary Genetics Analysis Version 11. *Molecular biology and evolution*, *38*(7), 3022–3027. https://doi.org/10.1093/molbev/msab120.
81. Tuohimaa, A., Riipinen, K. A., Brandt, K., & Alatossava, T. (2006). The genome of the virulent phage Lc-Nu of probiotic *Lactobacillus rhamnosus*, and comparative genomics with *Lactobacillus casei* phages. *Archives of virology*, *151*(5), 947–965. https://doi.org/10.1007/s00705-005-0672-0.
82. Tynkkynen, S., Singh, K. V., & Varmanen, P. (1998). Vancomycin resistance factor of *Lactobacillus rhamnosus* GG in relation to

enterococcal vancomycin resistance (van) genes. *International journal of food microbiology*, *41*(3), 195–204. https://doi.org/10.1016/s0168-1605(98)00051-8.

83. Ventura, M., O'Flaherty, S., Claesson, M. J., Turroni, F., Klaenhammer, T. R., van Sinderen, D., & O'Toole, P. W. (2009). Genome-scale analyses of health-promoting bacteria: probiogenomics. *Nature reviews. Microbiology*, *7*(1), 61–71. https://doi.org/10.1038/nrmicro2047.
84. Wang, X., Kim, Y., Ma, Q., Hong, S. H., Pokusaeva, K., Sturino, J. M., & Wood, T. K. (2010). Cryptic prophages help bacteria cope with adverse environments. *Nature communications*, *1*, 147. https://doi.org/10.1038/ncomms1146.
85. Waterhouse, A. M., Procter, J. B., Martin, D. M., Clamp, M., & Barton, G. J. (2009). Jalview Version 2--a multiple sequence alignment editor and analysis workbench. *Bioinformatics (Oxford, England)*, *25*(9), 1189–1191. https://doi.org/10.1093/bioinformatics/btp033.
86. Wick, R. R., Judd, L. M., Gorrie, C. L., & Holt, K. E. (2017). Unicycler: Resolving bacterial genome assemblies from short and long sequencing reads. *PLoS computational biology*, *13*(6), e1005595. https://doi.org/10.1371/journal.pcbi.1005595.
87. Wonglapsuwan, M., Pahumunto, N., Teanpaisan, R., & Surachat, K. (2024). Unlocking the genetic potential of *Lacticaseibacillus rhamnosus* strains: Medical applications of a promising probiotic for human and animal health. *Heliyon*, *10*(8), e29499. https://doi.org/10.1016/j.heliyon.2024.e29499.
88. Yao, L., Seaton, S. C., Ndousse-Fetter, S., Adhikari, A. A., DiBenedetto, N., Mina, A. I., Banks, A. S., Bry, L., & Devlin, A. S. (2018). A selective gut bacterial bile salt hydrolase alters host metabolism. *eLife*, *7*, e37182. https://doi.org/10.7554/eLife.37182.
89. Zafar, H., Ain, N. U., Alshammari, A., Alghamdi, S., Raja, H., Ali, A., Siddique, A., Tahir, S. D., Akbar, S., Arif, M., Alharbi, M., & Rahman, A. (2022). *Lacticaseibacillus rhamnosus* FM9 and *Limosilactobacillus fermentum* Y57 Are as Effective as Statins at Improving Blood Lipid Profile in High Cholesterol, High-Fat Diet Model in Male Wistar Rats. *Nutrients*, *14*(8), 1654. https://doi.org/10.3390/nu14081654.

90. Zhang, W. Y., Wu, R. N., Sun, Z. H., Sun, T. S., Meng, H., & Zhang, H. P. (2009). Molecular cloning and characterization of bile salt hydrolase in Lactobacillus casei Zhang. *Annals of microbiology*, *59*, 721-726. https://doi.org/10.1007/BF03179214.
91. Zhang, Q., & Ye, Y. (2017). Not all predicted CRISPR-Cas systems are equal: isolated *cas* genes and classes of CRISPR like elements. *BMC bioinformatics*, *18*(1), 92. https://doi.org/10.1186/s12859-017-1512-4

Chapter 3

3 Bile salt hydrolase activity in the food-derived strain *Levilactobacillus brevis* M3R3: genomic and functional characterization

Gianluigi Agolino[1,†], Marianna Cristofolini[2,†], Maria Anna Ronsivalle[1], Alice Cattivelli[2], Davide Tagliazucchi[2], Cinzia Caggia[1,3], Lisa Solieri[2,*] and Cinzia L. Randazzo[1,3]

[1]Department of Agriculture, Food and Environment (Di3A), University of Catania, Via Santa Sofia 100, 95123 Catania, Italy
[2]Department of Life Sciences, University of Modena and Reggio Emilia, Via Amendola, 2-Pad. Besta, 42100 Reggio Emilia, Italy
[3]Probioetna SRL, Spin off of University of Catania, Via Santa Sofia 100, 95123 Catania, Italy

*Corresponding author: lisa.solieri@unimore.it (L. Solieri)
†These authors contributed equally to this work

Published in *Probiotic and Antimicrobial Proteins, 2025, 1-18*
DOI: https://doi.org/10.1007/s12602-025-10810-0

Graphical abstract

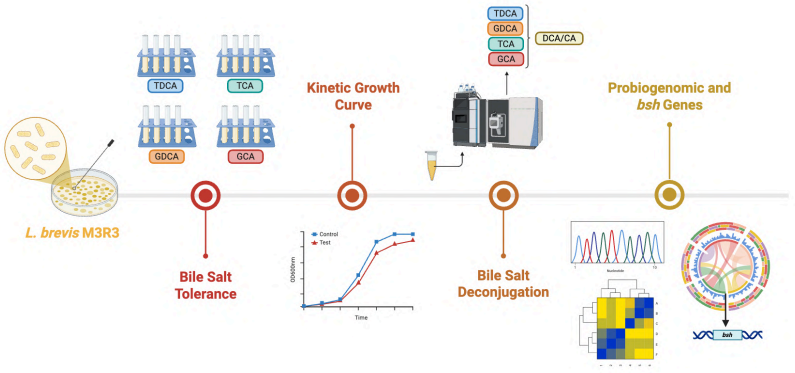

Abstract

In the present study, *Levilactobacillus brevis* M3R3, isolated from traditional Sicilian sourdough, was evaluated for bile salt hydrolase (BSH) activity through kinetic growth assays and bile salts (BSs) deconjugation analysis by UHPLC/HR-MS. Genome sequencing and in silico analyses were performed to assess its safety and probiotic potential. Results showed that strain M3R3 tolerated different concentrations of individual conjugated BSs, with dose-dependent growth inhibition. Exposure to 1.0% glycocholic and glycodeoxycholic acids reduced M3R3 growth, indicating an adaptive stress response. When exposed to a mixed BS solution mimicking intestinal condition, the strain maintained growth despite an extended lag phase and a reduced final biomass, likely due to toxic BSs accumulation. UHPLC/HR-MS confirmed complete deconjugation of glyco-conjugated BSs and partial deconjugation of tauro-conjugated

BSs. Whole-genome sequencing (2.30 Mbp, 2375 CDSs) revealed absence of antimicrobial resistance or virulence genes and identified two *bsh* genes (*bsh_2A* and *bsh_3A*), both expressed under control and BS-exposed conditions. Phylogenetic analysis of *L. brevis* BSH proteins identified three clusters (I, II, and III), with *bsh_2A* and *bsh_3A* from M3R3 grouped in clusters II and III, respectively. Overall, genomic and functional characterizations support that *L. brevis* M3R3 is a safe, BSH-active strain, with potential applications as a functional ingredient in health promoting formulations.

Keywords: bile salt hydrolase, whole genome, glycol-conjugated BSs, *bsh* genes.

3.1 Introduction

Lactobacilli strains of food origin are widely recognized for their capacity to support gastrointestinal health by modulating host functions and contributing to the maintenance of intestinal microbiota homeostasis. To exert these beneficial effects, they must withstand the harsh conditions of the gastrointestinal tract, including gastric acidity and bile salts (Demmpsey & Corr, 2022).

Bile salts (BSs) are endogenous signaling molecules synthesized from cholesterol by hepatocytes. In the liver, cholesterol undergoes a multistep metabolic pathway to form primary bile acids, which are subsequently conjugated with glycine or taurine to increase their solubility (Hundt et al., 2025). Upon secretion into bile, these conjugated acids are associated with cations such as Na^+ and K^+, forming BSs (Hoffmann & Hagey, 2014). Primary BSs represent the initial product of cholesterol catabolism. Their conjugation with glycine and taurine occurs through the formation of an amide bond between the bile acid's carboxyl group and the amino group of the respective amino acid, a modification essential for efficient lipid emulsification and other physiological functions (Hoffmann & Hagey, 2014). Once released into the small intestine, part of primary BSs can be deconjugated by resident bacterial communities and further converted into secondary BSs, a process that also influences the gut microbiota composition.

Bile Salt Hydrolase (BSH) (choloylglycine hydrolase; EC 3.5.1.24) is the microbial enzyme which plays a crucial role in BSs metabolism by cleaving the amide bond of conjugated BSs, thereby releasing unconjugated bile acids with free taurine or glycine (Kang et al., 2025). BSH activity is widely distributed among gastrointestinal

microbes, including various *Lactobacillaceae* species (Agolino et al., 2024; O'Flaherty et al., 2018; Ren et al., 2011; Song et al., 2019), where the presence of multiple *bsh* orthologs reflects strain-specific adaptations into the intestinal environment (Kriaa et al., 2019; Liang & Lv, 2018; O'Flaherty et al., 2018; Ren et al., 2011). BSH-positive bacteria provide an important contribution to host bile detoxification (Agolino et al., 2024). The deconjugation ability enhances bacterial survival and colonization of the gastrointestinal tract, modulates lipid metabolism, and shapes the bile acid pool, ultimately influencing host-microbiome signaling (Agolino et al., 2024; Bustos et al., 2018; Kriaa et al., 2019). Among its metabolic benefits, BSH activity has been implicated in the regulation of host cholesterol levels, contributing to its potential cholesterol-lowering effect (Choi et al., 2015; Jones et al., 2013; Kriaa et al., 2019). Moreover, BSH is associated with other beneficial functions including the regulation of energy balance and glucose metabolism (Taoka et al., 2016).

Considering these physiological roles, increasing attention has been directed toward isolating novel BSH-active strains. Fermented foods are rich sources of probiotic candidates, including BSH-active lactobacilli. Although BSH activity is predominantly associated with gastrointestinal isolates, non-intestinal lactobacilli from fermented foods also show deconjugation ability and thus potential probiotic value (Marco et al., 2018; Ru et al., 2019; Topisirovic et al., 2006). Among these, *Levilactobacillus brevis* has attracted attention due to its functional and probiotic properties (Alizadeh Behbahani et al., 2024; Sethi et al., 2025; Shangpliang & Tamang, 2024; Somashekaraiah et al., 2021; Sreepathi et al., 2023; Wang et al., 2025). It has been granted Qualified Presumption of Safety (QPS) status,

underscoring its safety for food applications (EFSA, 2024). Technologically, *L. brevis* contributes to bioactive compound production, enhancement of aroma and flavor, and improved fermentation outcomes (Du et al., 2022; Gänzle & Zheng, 2019; Molina et al., 2025). Genomic analyses indicate that *L. brevis* carries multiple *bsh* gene copies of different subtypes (Liang & Lv, 2018), consistent with observed bile tolerance and cholesterol-lowering activity *in vitro* (Wang et al., 2025; Watanabe et al., 2013; Munir et al., 2022).

The present study aimed to investigate a *L. brevis* strain isolated from traditional Sicilian sourdough, with the objective of proposing it as a novel BSs-modulating probiotic. To elucidate the mechanisms underlying the BSH activity, phenotypic assays were employed to verify BSs tolerance and deconjugation ability. A combination of genomic and phylogenetic analyses was also performed to characterize the presence and distribution of BSH-related genes inside the *L. brevis* M3R3 strain.

3.2 Material and Methods

3.2.1 Bacterial strain and culture conditions

Levilactibacillus brevis M3R3, previously isolated from sourdough, is part of the microbial culture collection of ProBioEtna srl, a spin-off of the University of Catania, Italy. The strain was routinely propagated anaerobically in de Man, Rogosa and Sharpe (MRS) medium (Oxoid, Basingstoke, Hampshire, UK) at 37°C for 48h in a 2.5 L anaerobic jar (Cat. No. AG0025A; Thermo Fisher Scientific, Waltham, MA, USA). For long-term preservation, the

strain was cryopreserved at −80°C using the same cultivation medium supplemented with 25% (*v/v*) glycerol.

3.2.2 Bile salt tolerance assay

Bile salt tolerance of *L. brevis* strain M3R3 was assessed under static conditions in MRS broth supplemented separately with taurodeoxycholic acid (TDCA; Cat No. 580221), taurocholic acid (TCA; Cat. No. 580217), glycodeoxycholic acid (GDCA; Cat. No. 361311), and glycocholic acid (GCA; Cat. No. 360512) sodium salts at the final concentrations of 0.1% 0.25%, 0.5%, and 1.0% (*w/v*), respectively. All BSs were purchased from Sigma Aldrich (St. Louis, MO, United States). MRS medium without BSs supplementation served as the control. Specifically, exponentially growing cells of strain M3R3 were inoculated into 5 mL of each modified MRS medium at the final density of 1.0×10^5 CFU/mL and incubated anaerobically at 37°C for 24 h. Bacterial counts were determined by plating serial ten-fold dilutions of each bacterial culture onto MRS agar. After the incubation of plates at 37°C for 48 h under anaerobic conditions, colonies were enumerated from plates containing 20-200 colonies. The results were expressed as Log_{10} CFU/mL in the presence of each BS relative to the control.

3.2.3 Growth curve assays

Growth kinetics were assessed under static conditions according to Agolino and co-worker (2025). Specifically, *L. brevis* M3R3 was inoculated in triplicate into MRS broth supplemented with 1.0% (*w/v*) of each BS (TDCA, TCA, GDCA, and GCA) separately or a BSs mixture (Oxoid, Basingstoke, Hampshire, UK) at the final

density of 1.0×10^5 CFU/mL. MRS medium without supplementation was used as the control. Microbial growth was monitored by measuring optical density at 600 nm (OD_{600nm}) in three technical replicates recorded at least three times per day.

Kinetic parameters were determined by fitting the experimental data to either parametric or non-parametric smooth spline models provided by the Grofit package (version 1.1.1-1) in R (Kahm et al., 2010). The best fit model was selected based on the Akaike Information Criterion (AIC). For each curve, the following parameters were derived: maximum growth rate (μ, expressed as h^{-1}), lag phase duration (λ, indicated as h), and maximum cell density reached at stationary phase (A, OD_{600nm}). During the late stationary phase of each growth curve assay, cultures were centrifuged at 8000 x *g* for 10 min under refrigerated conditions to obtain and cell-free supernatants for subsequent UHPLC/HR-MS analysis. In the case of growth assays in presence of BSs mixture, cells pellets were collected for RNA extraction. All the samples were stored at -80 °C until further use.

3.2.4 UHPLC/HR-MS analysis

Ultra-High-Performance Liquid Chromatography High-Resolution Mass Spectrometry (UHPLC/HR-MS) analysis was performed, according to the method described by Karlov and co-worker [33], with slight modifications. Chromatographic separation was performed in UHPLC Ultimate 3000 system (Thermo Fisher Scientific, San Jose, CA, USA), while compound identification and semi-quantitative analysis were carried out with a Q Exactive Hybrid Quadrupole-Orbitrap Mass Spectrometer (Thermo Fisher Scientific, San Jose, CA, USA). Prior to analysis, samples were appropriately

diluted, and 10 µL were injected into the UHPLC system loaded using a a C18 reversed-phase column Acquity UPLC HSS C18, 2.1 × 100 mm, 1.8 µm particle size (Waters, Milan, Italy). The mobile phases consisted of water with 0.1% formic acid (solvent A) and acetonitrile with 0.1% formic acid (solvent B). The gradient elution started at 58% B, increased linearly to 75% over 10 minutes, followed by a rapid increase to 98% B within 1 minute. This condition was maintained for 6 min before re-equilibrating to the initial conditions. The flow rate was maintained at 0.3 ml/min and the column temperature was set at 45 °C. Mass spectrometry analysis was carried out under negative electrospray ionization (ESI) mode using the following parameters: capillary voltage 2.7 kV; capillary temperature, 320 °C; sheath gas flow rate, 40 (arbitrary units); and auxiliary gas flow rate, 30 (arbitrary units). Full MS scans were acquired at a resolution of 70,000 with an AGC target of 3×10^6, a maximum injection time (IT) of 247 ms, and a scan range of 100–1500 m/z. MS/MS scans were performed at a resolution of 16,500, with an AGC target of 5×10^5, a maximum IT of 120 ms, and an isolation window of 1 m/z.

Identification of the different BSs was carried out by comparing the retention time, the m/z value and the fragmentation pattern with authentic standard compounds, as previously reported (Agolino et al., 2025). The relative amount of the residual compound was quantified by integrating the area under the corresponding chromatographic peaks (AUC) and calculated using the equation as follows:

$$\%\ decrease = 100 - \left[\frac{100 \times (AUP\ of\ BAs\ in\ inoculated\ sample)}{AUP\ of\ BAs\ in\ standard\ solution}\right]$$

3.2.5 Genome sequencing

The genomic DNA extraction was carried out as previously reported (Agolino et al., 2025). Library preparation and genome sequencing were outsourced to BMR Genomics (Padua, Italy). Genomic DNA was sequenced using the Illumina MiSeq platform with the V3 reagent kit, generating 2 x 300 bp paired-end reads. Pre-processing step was carried out with Fastq v0.23.2 (Chen, 2023) to remove adapters and filter low quality bases (Q<30) and short reads (length<150). Possible contaminants were assessed by MetaPhlan v4.0.1 (Blanco-Míguez et al., 2023). SPAdes v3.15.5 (Prjibelski et al., 2020) was used to perform *de novo* genome assembly on the cleaned reads. QUAST v5.2.0 (Mikheenko et al., 2018) and BUSCO v5.4.3 (Manni et al., 2021) were used to evaluate genome completeness and assembly quality.

3.2.6 Gene prediction and functional annotation

Gene prediction and annotation were carried out with Prokka v1.14.6 (Seemann, 2014). Graphical representation of the M3R3 genome was generated using the Proksee Server (v1.1.2) based on GenBank-formatted annotation files (Grant et al., 2023). The cluster of orthologous groups (COG) for the protein-coding genes was obtained using Egg-NOG mapper (v2.1.7) tool (Cantalapiedra et al., 2021) from the online Egg-NOG database (v5.0). A complementary functional analysis was performed using the Kyoto Encyclopedia of Genes and Genomes (KEGG) mapper/BLASTKOALA tool (Kaneisha et al., 2016).

3.2.7 Taxonomic identification and comparative genomics

16S rRNA gene sequencing and phylogenetic analysis on was

carried out as previously reported (Martini et al., 2024). The 16S rRNA gene sequence of strain M3R3 was deposited in GenBank under the accession number PV902533. Species identification of strain M3R3 was determined *via* calculation of the Average Nucleotide Identity (ANI) index using the JSpecies web server tool with default parameters (Richter et al. 2016) and calculation of the digital DNA–DNA hybridization (dDDH) values using an online Genome-to-Genome Distance Calculator (GGDC3.0; https://ggdc.dsmz.de/ggdc.php) with formula 2 (Meier-Kolthoff et al., 2022) The species thresholds of 95% and 70% were considered for ANI and dDDH analyses, respectively (Goris et al., 2007). In addition, the Genome BLAST Distance Phylogeny (GBDP) was constructed in the Type Strain Genome Server (TYGS) to infer the taxonomical affiliation at the species level for strain M3R3 (Meier-Kolthoff et al., 2022).

For species-specific phylogeny, a total of 178 *L. brevis* genomes were retrieved from the NCBI database (accessed on 4 January 2024). Four genomes exhibited a completeness lower than 85% and/or a contamination level above 3%, as assessed by CheckM, and were excluded from the analysis, resulting in a final dataset of 174 high-quality genomes (**Table 3.1**). Core genome single nucleotide polymorphisms (SNPs) were identified using Snippy-multi v4.6.0 (https://github.com/tseemann/snippy). Reads and assembled genomes were mapped against the selected *L. brevis* reference genome from strain NCTC13768 (GCA_900475625.1). Recombination regions in the core genome alignment were detected and masked using Gubbins v2.4.1 to reduce phylogenetic bias (Croucher et al., 2015). RAxML program was used to build the phylogenetic tree using the clean core

SNP alignments generated from Gubbins.

A subset of 10 *L. brevis* genomes was included in the subsequent core-genome and pan-genome analyses. In detail, core-genome and pan-genome were computed in the Efficient Database framework for comparative Genome Analyses using BLAST score Ratios (EDGAR v3.2) web tool, which checked for reciprocal best BLAST hits against all other genomes with *L. brevis* strain M3R3 serving as the reference genome (Dieckmann et al., 2021). Since EDGAR uses a bidirectional best BLASTp hits approach for calculating singletons, gene duplication and paralogs are treated as singletons, if unidentical (Dieckmann et al., 2021). All trees generated in this study were visualized using the Interactive Tree Of Life (iTOL v7) (Letunic & Bork, 2019).

Table 3.1 - *Levilactobacillus brevis* reference genome used in this study.

Assembly Accession	Assembly Name	Organism Name	Organism Infraspecific Names Strain	Organism Infraspecific Names Isolate	Assembly Level	Strain	Isolation source	Country	filename
GCA_040194405.1	ASM4019440v1	*Levilactobacillus brevis*	MKMB05		Contig	QD-1	FERMENTED VEGETAGLES	Vietnam	GCA_040194405.1_ASM4019440v1_genomic.fna
GCA_021384515.1	ASM2138451v1	*Levilactobacillus brevis*	TMW 1.313		Contig	7.8.43	FERMENTED VEGETAGLES	USA: Chaska, MN	GCA_021384515.1_ASM2138451v1_genomic.fna
GCA_018991675.1	ASM1899167v1	*Levilactobacillus brevis*	SRCM101174		Contig	3.2.41	FERMENTED VEGETAGLES	USA: Chaska, MN	GCA_018991675.1_ASM1899167v1_genomic.fna
GCA_018257235.1	ASM1825723v1	*Levilactobacillus brevis*	DS1_5		Scaffold	Dm-2019-10	FERMENTED VEGETAGLES	USA: Chaska, MN	GCA_018257235.1_ASM1825723v1_genomic.fna
GCA_018257295.1	ASM1825729v1	*Levilactobacillus brevis*	KL251		Scaffold	Dm-2019-57	FERMENTED VEGETAGLES	USA: Chaska, MN	GCA_018257295.1_ASM1825729v1_genomic.fna

GCA_021384415.1	ASM2138441v1	*Levilactobacillus brevis*	SRCM217016	Contig	3.8.25	FERMENTED VEGETAGLES	USA: Chaska, MN	GCA_021384415.1_ASM2138441v1_genomic.fna
GCA_021384615.1	ASM2138461v1	*Levilactobacillus brevis*	UCCLB521	Contig	30.2.29	FERMENTED VEGETAGLES	USA: Chaska, MN	GCA_021384615.1_ASM2138461v1_genomic.fna
GCA_021384395.1	ASM2138439v1	*Levilactobacillus brevis*	SRCM210362	Contig	7.2.12	FERMENTED VEGETAGLES	USA: Chaska, MN	GCA_021384395.1_ASM2138439v1_genomic.fna
GCA_021384445.1	ASM2138444v1	*Levilactobacillus brevis*	TCI988	Contig	7.2.40	FERMENTED VEGETAGLES	USA: Chaska, MN	GCA_021384445.1_ASM2138444v1_genomic.fna
GCA_021384405.1	ASM2138440v1	*Levilactobacillus brevis*	TOM.290	Contig	7.2.41	FERMENTED VEGETAGLES	USA: Chaska, MN	GCA_021384405.1_ASM2138440v1_genomic.fna
GCA_021384505.1	ASM2138450v1	*Levilactobacillus brevis*	TMW 1.2108	Contig	7.2.49	FERMENTED VEGETAGLES	USA: Chaska, MN	GCA_021384505.1_ASM2138450v1_genomic.fna
GCA_021384555.1	ASM2138455v1	*Levilactobacillus brevis*	TMW 1.2111	Contig	7.8.33	FERMENTED VEGETAGLES	USA: Chaska, MN	GCA_021384555.1_ASM2138455v1_genomic.fna

GCA_021384565.1	ASM2138456v1	*Levilactobacillus brevis*	TOM.66	Contig	7.8.34	FERMENTED VEGETAGLES	USA: Chaska, MN	GCA_021384565.1_ASM2138456v1_genomic.fna
GCA_018991505.1	ASM1899150v1	*Levilactobacillus brevis*	TR055	Contig	14.2.10	FERMENTED VEGETAGLES	USA	GCA_018991505.1_ASM1899150v1_genomic.fna
GCA_018993685.1	ASM1899368v1	*Levilactobacillus brevis*	TUCO-5E	Contig	14.2.24	FERMENTED VEGETAGLES	USA	GCA_018993685.1_ASM1899368v1_genomic.fna
GCA_021384595.1	ASM2138459v1	*Levilactobacillus brevis*	TMW 1.2113	Contig	30.8.38	FERMENTED VEGETAGLES	USA	GCA_021384595.1_ASM2138459v1_genomic.fna
GCA_021384495.1	ASM2138449v1	*Levilactobacillus brevis*	TR052	Contig	7.2.13	FERMENTED VEGETAGLES	USA	GCA_021384495.1_ASM2138449v1_genomic.fna
GCA_018257185.1	ASM1825718v1	*Levilactobacillus brevis*	DRD-136	Scaffold	Dm-2019-67	ANIMALS/HUMAN GUT	USA	GCA_018257185.1_ASM1825718v1_genomic.fna
GCA_018257245.1	ASM1825724v1	*Levilactobacillus brevis*	DRD-139	Scaffold	Dm-2019-70	ANIMALS/HUMAN GUT	USA	GCA_018257245.1_ASM1825724v1_genomic.fna
GCA_018257275.1	ASM1825727v1	*Levilactobacillus brevis*	Dm-2019-57	Contig	Dm-2019-31	FERMENTED VEGETAGLES	USA	GCA_018257275.1_ASM1825727v1_genomic.fna

GCA_000814725.1	ASM81472v1	*Levilactobacillus brevis*	CIRM-BIA 2232	Contig	DmCS_003	UNKNOWN	USA	GCA_000814725.1_ASM81472v1_genomic.fna
GCA_003053125.1	ASM305312v1	*Levilactobacillus brevis*	QD-1	Contig	DS1_5	DAIRY PRODUCT	USA	GCA_003053125.1_ASM305312v1_genomic.fna
GCA_000807975.1	ASM80797v1	*Levilactobacillus brevis* BSO 464	BD-LB	Chromosome	BSO 464	ALCOLIC FERMENTATION	UK	GCA_000807975.1_ASM80797v1_genomic.fna
GCA_025194285.1	ASM2519428v1	*Levilactobacillus brevis*	DRD-12	Contig	CIRM-BIA 2232	ALCOLIC FERMENTATION	UK	GCA_025194285.1_ASM2519428v1_genomic.fna
GCA_001923045.1	ASM192304v1	*Levilactobacillus brevis*	SRCM 103306	Scaffold	BSO 310	ALCOLIC FERMENTATION	UK	GCA_001923045.1_ASM192304v1_genomic.fna
GCA_025194515.1	ASM2519451v1	*Levilactobacillus brevis*	NCTC13768	Contig	CIRM-BIA 899	ALCOLIC FERMENTATION	UK	GCA_025194515.1_ASM2519451v1_genomic.fna
GCA_028411555.1	ASM2841155v1	*Levilactobacillus brevis*		Complete Genome	Atlas17	DAIRY PRODUCT	Turkey	GCA_028411555.1_ASM2841155v1_genomic.fna

GCA_020532035.1	ASM2053203v1	*Levilactobacillus brevis*	KMB_615	Contig	ASK-1	FERMENTED VEGETAGLES	Thailand : Bangkok	GCA_020532035.1_ASM2053203v1_genomic.fna
GCA_040556855.1	ASM4055685v1	*Levilactobacillus brevis*	Atlas17	Chromosome	TCI988	FERMENTED VEGETAGLES	Taiwan	GCA_040556855.1_ASM4055685v1_genomic.fna
GCA_027591835.1	ASM2759183v1	*Levilactobacillus brevis*	LAB 6	Contig	LSF9-1	FERMENTED VEGETAGLES	Tailandia	GCA_027591835.1_ASM2759183v1_genomic.fna
GCA_025186345.1	ASM2518634v1	*Levilactobacillus brevis*	LZB2	Contig	994	DAIRY PRODUCT	Swiss	GCA_025186345.1_ASM2518634v1_genomic.fna
GCA_000474675.1	Lactobacillus brevis EW genome Assembly	*Levilactobacillus brevis EW*		Contig	EW	ANIMALS/HUMAN GUT	South Korea	GCA_000474675.1_Lactobacillus_brevis_EW_genome_Assembly_genomic.fna
GCA_041870135.1	ASM4187013v1	*Levilactobacillus brevis*	ATCC 14869	Chromosome	CHEE98	DAIRY PRODUCT	South Korea	GCA_041870135.1_ASM4187013v1_genomic.fna
GCA_001676805.1	ASM167680v1	*Levilactobacillus brevis*	3.2.41	Complete Genome	NPS-QW-145	FERMENTED VEGETAGLES	South Korea	GCA_001676805.1_ASM167680v1_genomic.fna
GCA_026626025.1	ASM2662602v1	*Levilactobacillus brevis*	7.8.34	Complete Genome	SMB091	FERMENTED VEGETAGLES	South Korea	GCA_026626025.1_ASM2662602v1_genomic.fna

GCA_002318935.1	ASM231893v1	*Levilactobacillus brevis*	BSO 310	Contig	D7	FERMENTED VEGETAGLES	South Korea	GCA_002318935.1_ASM231893v1_genomic.fna
GCA_003813165.1	ASM381316v1	*Levilactobacillus brevis*	47f	Complete Genome	LMT1-73	FERMENTED VEGETAGLES	South Korea	GCA_003813165.1_ASM381316v1_genomic.fna
GCA_900452615.1	49888_E01	*Levilactobacillus brevis*	BSO 464	Contig	NCTC 13386	FERMENTED VEGETAGLES	South Korea	GCA_900452615.1_49888_E01_genomic.fna
GCA_041200015.1	ASM4120001v1	*Levilactobacillus brevis*	7.2.12	Complete Genome	NS2301G3	FERMENTED VEGETAGLES	South Korea	GCA_041200015.1_ASM4120001v1_genomic.fna
GCA_025447255.1	ASM2544725v1	*Levilactobacillus brevis*	3M004	Complete Genome	SRCM210362	FERMENTED VEGETAGLES	South Korea	GCA_025447255.1_ASM2544725v1_genomic.fna
GCA_014905055.1	ASM1490505v1	*Levilactobacillus brevis*	A189	Complete Genome	NSMJ23	ALCOLIC FERMENTATION	South Korea	GCA_014905055.1_ASM1490505v1_genomic.fna
GCA_018798865.1	ASM1879886v1	*Levilactobacillus brevis*	AM92-01-1A	Complete Genome	SPC-SNU70-2	ALCOLIC FERMENTATION	South Korea	GCA_018798865.1_ASM1879886v1_genomic.fna
GCA_002138395.1	ASM213839v1	*Levilactobacillus brevis*	AM88-10A	Complete Genome	100D8	FERMENTED VEGETAGLES	South Korea	GCA_002138395.1_ASM213839v1_genomic.fna

GCA_004055405.1	ASM405540v1	*Levilactobacillus brevis*	CIRM-BIA 1442	Contig	SRCM 103306	FERMENTED VEGETAGLES	South Korea	GCA_004055405.1_ASM405540v1_genomic.fna
GCA_002174235.1	ASM217423v1	*Levilactobacillus brevis*	7.2.41	Complete Genome	SRCM101106	FERMENTED VEGETAGLES	South Korea	GCA_002174235.1_ASM217423v1_genomic.fna
GCA_002173555.1	ASM217355v1	*Levilactobacillus brevis*	7.8.33	Complete Genome	SRCM101174	FERMENTED VEGETAGLES	South Korea	GCA_002173555.1_ASM217355v1_genomic.fna
GCA_040425635.1	ASM4042563v1	*Levilactobacillus brevis*	Lbr-35	Scaffold	KL251	FERMENTED VEGETAGLES	South Korea	GCA_040425635.1_ASM4042563v1_genomic.fna
GCA_030378305.1	ASM3037830v1	*Levilactobacillus brevis*	CHEE98	Contig	SRCM217016	FERMENTED VEGETAGLES	South Korea	GCA_030378305.1_ASM3037830v1_genomic.fna
GCA_003345725.1	ASM334572v1	*Levilactobacillus brevis*	MB2	Contig	WIKIM12	FERMENTED VEGETAGLES	South Korea	GCA_003345725.1_ASM334572v1_genomic.fna
GCA_000784455.1	ASM78445v1	*Levilactobacillus brevis*	MB13	Contig	WK12	FERMENTED VEGETAGLES	South Korea	GCA_000784455.1_ASM78445v1_genomic.fna

GCA_024800685.1	ASM2480068v1	*Levilactobacillus brevis*	AF92-02GAA		Complete Genome	PL102	FERMENTED VEGETAGLES	South Korea	GCA_024800685.1_ASM2480068v1_genomic.fna
GCA_021383565.1	ASM2138356v1	*Levilactobacillus brevis*			Complete Genome	M10	UNKNOWN	South Korea	GCA_021383565.1_ASM2138356v1_genomic.fna
GCA_925285815.1	IM1293	*Levilactobacillus brevis*	P45	IM1293	Contig	IM1293	DAIRY PRODUCT	Slovenia	GCA_925285815.1_IM1293_genomic.fna
GCA_925285845.1	IM1297	*Levilactobacillus brevis*	CIRM-BIA 2230	IM1297	Contig	IM1297	DAIRY PRODUCT	Slovenia	GCA_925285845.1_IM1297_genomic.fna
GCA_925281805.1	IM1457	*Levilactobacillus brevis*	CIRM-BIA 2226	IM1457	Contig	IM1457	FERMENTED VEGETAGLES	Slovenia	GCA_925281805.1_IM1457_genomic.fna
GCA_900116945.1	ASM900116944v1	*Levilactobacillus brevis*	YSJ3	G430	Contig	G430	ALCOLIC FERMENTATION	Slovenia	GCA_900116945.1_ASM900011694v1_genomic.fna
GCA_925279105.1	IM1470	*Levilactobacillus brevis*	F4101	IM1470	Contig	IM1470	FERMENTED VEGETAGLES	slovakia	GCA_925279105.1_IM1470_genomic.fna
GCA_039566335.1	ASM3956633v1	*Levilactobacillus brevis*	SF15B		Contig	A189	DAIRY PRODUCT	slovakia	GCA_039566335.1_ASM3956633v1_genomic.fna
GCA_003346095.1	ASM334609v1	*Levilactobacillus brevis*	SF9B		Contig	KMB_615	DAIRY PRODUCT	slovakia	GCA_003346095.1_ASM334609v1_genomic.fna

GCA_003346245.1	ASM334624v1	*Levilactobacillus brevis*	PL102		Contig	KMB_620	DAIRY PRODUCT	slovakia	GCA_003346245.1_ASM334624v1_genomic.fna
GCA_039566365.1	ASM3956636v1	*Levilactobacillus brevis*	SMB091		Contig	P45	DAIRY PRODUCT	slovakia	GCA_039566365.1_ASM3956636v1_genomic.fna
GCA_006228205.1	ASM622820v1	*Levilactobacillus brevis*	14.2.10		Complete Genome	UCCLBBS124	ALCOLIC FERMENTATION	Singapore	GCA_006228205.1_ASM622820v1_genomic.fna
GCA_000875905.1	ASM87590v1	*Levilactobacillus brevis*	PYN10-6-2		Scaffold	15f	ANIMALS/HUMAN GUT	Russia	GCA_000875905.1_ASM87590v1_genomic.fna
GCA_001010995.2	ASM101099v2	*Levilactobacillus brevis*	7.8.43		Complete Genome	47f	ANIMALS/HUMAN GUT	Russia	GCA_001010995.2_ASM101099v2_genomic.fna
GCA_902386565.1	UHGG_MGYG-HGUT-02380	*Levilactobacillus brevis*	NSMJ23	MGYG-HGUT-02380	Contig	MGYG-HGUT-02380	ANIMALS/HUMAN GUT	Russia	GCA_902386565.1_UHGG_MGYG-HGUT-02380_genomic.fna
GCA_030361165.1	ASM3036116v1	*Levilactobacillus brevis*	LBH1073		Contig	TOM.290	DAIRY PRODUCT	Russia	GCA_030361165.1_ASM3036116v1_genomic.fna
GCA_030361325.1	ASM3036132v1	*Levilactobacillus brevis*	Lb1595		Contig	TOM.66	DAIRY PRODUCT	Russia	GCA_030361325.1_ASM3036132v1_genomic.fna

GCA_025194465.1	ASM2519446v1	*Levilactobacillus brevis*	ZG1	Contig	CIRM-BIA 2227	FERMENTED VEGETAGLES	Poland	GCA_025194465.1_ASM2519446v1_genomic.fna
GCA_025194405.1	ASM2519440v1	*Levilactobacillus brevis*	WK12	Contig	CIRM-BIA 2230	FERMENTED VEGETAGLES	Poland	GCA_025194405.1_ASM2519440v1_genomic.fna
GCA_025194385.1	ASM2519438v1	*Levilactobacillus brevis*	SPC-SNU 70-2	Contig	CIRM-BIA 2231	FERMENTED VEGETAGLES	Poland	GCA_025194385.1_ASM2519438v1_genomic.fna
GCA_025194485.1	ASM2519448v1	*Levilactobacillus brevis*	MYSN105	Contig	CIRM-BIA 907	FERMENTED VEGETAGLES	Poland	GCA_025194485.1_ASM2519448v1_genomic.fna
GCA_006228285.1	ASM622828v1	*Levilactobacillus brevis*	14.2.24	Complete Genome	UCCL BBS449	ALCOLIC FERMENTATION	Netherlands	GCA_006228285.1_ASM622828v1_genomic.fna
GCA_006228265.1	ASM622826v1	*Levilactobacillus brevis*		Complete Genome	UCCL B95	ALCOLIC FERMENTATION	Netherlands	GCA_006228265.1_ASM622826v1_genomic.fna
GCA_006228305.1	ASM622830v1	*Levilactobacillus brevis*	AM92-01b2A	Complete Genome	UCCL B521	ALCOLIC FERMENTATION	Netherlands	GCA_006228305.1_ASM622830v1_genomic.fna

GCA_006228245.1	ASM622824v1	*Levilactobacillus brevis*	AG48	Complete Genome	UCCLB556	ALCOLIC FERMENTATION	Netherlands	GCA_006228245.1_ASM622824v1_genomic.fna
GCA_018588725.1	ASM1858872v1	*Levilactobacillus brevis*	CIRM-BIA 907	Contig	LBH1073	UNKNOWN	Mexico	GCA_018588725.1_ASM1858872v1_genomic.fna
GCA_002017995.1	ASM201799v1	*Levilactobacillus brevis*		Contig	G101	UNKNOWN	South Korea	GCA_002017995.1_ASM201799v1_genomic.fna
GCA_025194505.1	ASM2519450v1	*Levilactobacillus brevis*	M10	Contig	CIRM-BIA 895	FERMENTED VEGETAGLES	Italy	GCA_025194505.1_ASM2519450v1_genomic.fna
GCA_025194545.1	ASM2519454v1	*Levilactobacillus brevis*	TMW 1.6	Contig	CIRM-BIA 2226	FERMENTED VEGETAGLES	Italy	GCA_025194545.1_ASM2519454v1_genomic.fna
GCA_006382065.1	ASM638206v1	*Levilactobacillus brevis*	Dm-2019-31	Contig	TR055	FERMENTED VEGETAGLES	Irland	GCA_006382065.1_ASM638206v1_genomic.fna
GCA_006381875.1	ASM638187v1	*Levilactobacillus brevis*	LSF9-1	Contig	TR169	FERMENTED VEGETAGLES	Irland	GCA_006381875.1_ASM638187v1_genomic.fna
GCA_006381935.1	ASM638193v1	*Levilactobacillus brevis*	D6	Contig	TR052	FERMENTED VEGETAGLES	Irland	GCA_006381935.1_ASM638193v1_genomic.fna

GCA_006228225.1	ASM622822v1	*Levilactobacillus brevis*	7.2.40	Complete Genome	SA-C12	FERMENTED VEGETAGLES	Irland	GCA_006228225.1_ASM622822v1_genomic.fna
GCA_001722065.1	ASM172206v1	*Levilactobacillus brevis*	CD0817	Contig	DPC 6108	ANIMALS/HUMAN GUT	Irland	GCA_001722065.1_ASM172206v1_genomic.fna
GCA_018784425.1	ASM1878442v1	*Levilactobacillus brevis*	SRCM101106	Scaffold	MCC 633	ANIMALS/HUMAN GUT	Irland	GCA_018784425.1_ASM1878442v1_genomic.fna
GCA_020509325.1	ASM2050932v1	*Levilactobacillus brevis*	LMT1-73	Contig	LBX14	ANIMALS/HUMAN GUT	India	GCA_020509325.1_ASM2050932v1_genomic.fna
GCA_021728655.1	ASM2172865v1	*Levilactobacillus brevis*	ES01	Contig	ES01	FERMENTED VEGETAGLES	India	GCA_021728655.1_ASM2172865v1_genomic.fna
GCA_040567705.1	ASM4056770v1	*Levilactobacillus brevis*	TMW 1.465	Scaffold	LAB 6	FERMENTED VEGETAGLES	India	GCA_040567705.1_ASM4056770v1_genomic.fna
GCA_019837695.1	ASM1983769v1	*Levilactobacillus brevis*		Scaffold	MYSN105	ALCOLIC FERMENTATION	India	GCA_019837695.1_ASM1983769v1_genomic.fna
GCA_040149435.1	ASM4014943v1	*Levilactobacillus brevis*		Contig	GOS-2	ANIMALS/HUMAN GUT	India	GCA_040149435.1_ASM4014943v1_genomic.fna
GCA_039839865.1	ASM3983986v1	*Levilactobacillus brevis*	NS2301G3	Contig	MKMB04	DAIRY PRODUCT	India	GCA_039839865.1_ASM3983986v1_genomic.fna

GCA_039839695.1	ASM3983969v1	*Levilactobacillus brevis*	NPS-QW-145	Contig	MKMB05	DAIRY PRODUCT	India	GCA_039839695.1_ASM3983969v1_genomic.fna
GCA_023744455.1	ASM2374445v1	*Levilactobacillus brevis*	DRD-195	Scaffold	DRD-136	DAIRY PRODUCT	Greece	GCA_023744455.1_ASM2374445v1_genomic.fna
GCA_023744035.1	ASM2374403v1	*Levilactobacillus brevis*	LB_AVK	Scaffold	DRD-195	DAIRY PRODUCT	Greece	GCA_023744035.1_ASM2374403v1_genomic.fna
GCA_023744425.1	ASM2374442v1	*Levilactobacillus brevis*	DM9218	Scaffold	DRD-198	DAIRY PRODUCT	Greece	GCA_023744425.1_ASM2374442v1_genomic.fna
GCA_023744005.1	ASM2374400v1	*Levilactobacillus brevis*	Dm-2019-70	Scaffold	DRD-201	DAIRY PRODUCT	Greece	GCA_023744005.1_ASM2374400v1_genomic.fna
GCA_023743515.1	ASM2374351v1	*Levilactobacillus brevis*	EW	Scaffold	DRD-51	DAIRY PRODUCT	Greece	GCA_023743515.1_ASM2374351v1_genomic.fna
GCA_023743355.1	ASM2374335v1	*Levilactobacillus brevis*	DRD-60	Scaffold	DRD-52	DAIRY PRODUCT	Greece	GCA_023743355.1_ASM2374335v1_genomic.fna
GCA_023743375.1	ASM2374337v1	*Levilactobacillus brevis*	HQ1-1	Scaffold	DRD-59	DAIRY PRODUCT	Greece	GCA_023743375.1_ASM2374337v1_genomic.fna
GCA_023744095.1	ASM2374409v1	*Levilactobacillus brevis*	DRD-201	Scaffold	DRD-60	DAIRY PRODUCT	Greece	GCA_023744095.1_ASM2374409v1_genomic.fna

GCA_032841235.1	ASM3284123v1	*Levilactobacillus brevis*	MRS-8		Contig	MRS-8	DAIRY PRODUCT	Greece	GCA_032841235.1_ASM3284123v1_genomic.fna
GCA_032841255.1	ASM3284125v1	*Levilactobacillus brevis*	MKMB04		Contig	MRS-9	DAIRY PRODUCT	Greece	GCA_032841255.1_ASM3284125v1_genomic.fna
GCA_023743495.1	ASM2374349v1	*Levilactobacillus brevis*	EF		Scaffold	DRD-12	DAIRY PRODUCT	Greece	GCA_023743495.1_ASM2374349v1_genomic.fna
GCA_023743475.1	ASM2374347v1	*Levilactobacillus brevis*	Dm-2019-67		Scaffold	DRD-35	DAIRY PRODUCT	Greece	GCA_023743475.1_ASM2374347v1_genomic.fna
GCA_023744105.1	ASM2374410v1	*Levilactobacillus brevis*	DRD-59		Scaffold	DRD-139	DAIRY PRODUCT	Greece	GCA_023744105.1_ASM2374410v1_genomic.fna
GCA_002117325.1	ASM211732v1	*Levilactobacillus brevis*	3.8.25		Complete Genome	TMW 1.2113	ALCOLIC FERMENTATION	Germany	GCA_002117325.1_ASM211732v1_genomic.fna
GCA_002117225.1	ASM211722v1	*Levilactobacillus brevis*			Complete Genome	TMW 1.2112	ALCOLIC FERMENTATION	Germany	GCA_002117225.1_ASM211722v1_genomic.fna
GCA_964382315.1	SRR23946438_binner12_Refined_11	*Levilactobacillus brevis*	ZLB004	SRR23946438_binner12_Refined_11	Contig	SRR23946438_binner12_Ref	ANIMALS/HUMAN GUT	Germany	GCA_964382315.1_SRR23946438_binner12_Refined_11_genomic.fna

						ined_ 11			
GCA_0021 17345.1	ASM211734v 1	*Levilactobacillus brevis*	15f		Complete Genome	TMW 1.210 8	ALCOLIC FERMENTATIO N	Germany	GCA_002117345.1_ASM2 11734v1_genomic.fna
GCA_0021 17375.1	ASM211737v 1	*Levilactobacillus brevis*			Complete Genome	TMW 1.211 1	ALCOLIC FERMENTATIO N	Germany	GCA_002117375.1_ASM2 11737v1_genomic.fna
GCA_0207 41515.1	ASM2074151 v1	*Levilactobacillus brevis*		12991	Contig	12991	ANIMALS/HU MAN GUT	Germany	GCA_020741515.1_ASM2 074151v1_genomic.fna
GCA_0251 94325.1	ASM2519432 v1	*Levilactobacillus brevis*	TMW 1.2112		Contig	CIRM -BIA 875	DAIRY PRODUCT	France	GCA_025194325.1_ASM2 519432v1_genomic.fna
GCA_0251 94305.1	ASM2519430 v1	*Levilactobacillus brevis*	LMT1-73		Contig	CIRM -BIA 2225	FERMENTED VEGETAGLES	France	GCA_025194305.1_ASM2 519430v1_genomic.fna
GCA_0250 00005.1	ASM2500000 v1	*Levilactobacillus brevis*	LBAE A15		Contig	CIRM -BIA 1442	DAIRY PRODUCT	France	GCA_025000005.1_ASM2 500000v1_genomic.fna

GCA_001540905.1	ASM154090v1	*Levilactobacillus brevis*	KB290		Contig	Lb1595	DAIRY PRODUCT	France	GCA_001540905.1_ASM154090v1_genomic.fna
GCA_025122425.1	ASM2512242v1	*Levilactobacillus brevis*	LBX14		Contig	LBAEA15	FERMENTED VEGETAGLES	France	GCA_025122425.1_ASM2512242v1_genomic.fna
GCA_964065285.1	Levilactobacillus_brevis_CIRM-BIA2444	*Levilactobacillus brevis*	AM89-08b2TA	*Levilactobacillus brevis* CIRM-BIA2444	Complete Genome	CIRM-BIA2444	FERMENTED VEGETAGLES	France	GCA_964065285.1_Levilactobacillus_brevis_CIRM-BIA2444_genomic.fna
GCA_964065115.1	Levilactobacillus_brevis_CIRM-BIA2515	*Levilactobacillus brevis*	AF10-19C	*Levilactobacillus brevis* CIRM-BIA2515	Complete Genome	CIRM-BIA2515	FERMENTED VEGETAGLES	France	GCA_964065115.1_Levilactobacillus_brevis_CIRM-BIA2515_genomic.fna
GCA_900116995.1	ASM900116999v1	*Levilactobacillus brevis*	UCCLBBS124	HF01	Contig	HF01	ALCOLIC FERMENTATION	Denmark	GCA_900116995.1_ASM900011699v1_genomic.fna
GCA_900117025.1	ASM900117022v1	*Levilactobacillus brevis*	UCCLBBS449	JK09	Contig	JK09	ALCOLIC FERMENTATION	Denmark	GCA_900117025.1_ASM900011702v1_genomic.fna
GCA_900117015.1	ASM900117011v1	*Levilactobacillus brevis*	UCCLB556	JK09--	Contig	JK09--	ALCOLIC FERMENTATION	Denmark	GCA_900117015.1_ASM900011701v1_genomic.fna

GCA_900116975.1	ASM900116977v1	*Levilactobacillus brevis*	UCCLB95	A	Contig	A	ALCOLIC FERMENTATION	Denmark	GCA_900116975.1_ASM900011697v1_genomic.fna
GCA_900117045.1	ASM900117044v1	*Levilactobacillus brevis*	WIKIM12	Q	Contig	Q	ALCOLIC FERMENTATION	Denmark	GCA_900117045.1_ASM900011704v1_genomic.fna
GCA_027108875.1	ASM2710887v1	*Levilactobacillus brevis*	NBRC 3345		Scaffold	MB13	ANIMALS/HUMAN GUT	Croatia	GCA_027108875.1_ASM2710887v1_genomic.fna
GCA_002532245.1	ASM253224v1	*Levilactobacillus brevis*	NBRC 3960		Contig	SF9B	FERMENTED VEGETAGLES	Croatia	GCA_002532245.1_ASM253224v1_genomic.fna
GCA_026930425.1	ASM2693042v1	*Levilactobacillus brevis*	NBRC 12005		Scaffold	MB1	ANIMALS/HUMAN GUT	Croatia	GCA_026930425.1_ASM2693042v1_genomic.fna
GCA_026930445.1	ASM2693044v1	*Levilactobacillus brevis*	NBRC 13110		Scaffold	MB2	ANIMALS/HUMAN GUT	Croatia	GCA_026930445.1_ASM2693044v1_genomic.fna
GCA_026930365.1	ASM2693036v1	*Levilactobacillus brevis*	N38		Scaffold	MB20	ANIMALS/HUMAN GUT	Croatia	GCA_026930365.1_ASM2693036v1_genomic.fna
GCA_002532185.1	ASM253218v1	*Levilactobacillus brevis*	CIRM-BIA 519		Contig	ZG1	DAIRY PRODUCT	Croatia	GCA_002532185.1_ASM253218v1_genomic.fna

GCA_001541605.1	1153	*Levilactobacillus brevis*	MCC633	Contig	D6	DAIRY PRODUCT	Croatia	GCA_001541605.1_1153_genomic.fna
GCA_002532155.1	ASM253215v1	*Levilactobacillus brevis*	TR169	Contig	SF15B	FERMENTED VEGETAGLES	croatia	GCA_002532155.1_ASM253215v1_genomic.fna
GCA_041228385.1	ASM4122838v1	*Levilactobacillus brevis*	30.8.38	Complete Genome	BD-LB	ANIMALS/HUMAN GUT	China	GCA_041228385.1_ASM4122838v1_genomic.fna
GCA_002179515.1	ASM217951v1	*Levilactobacillus brevis*	CIRM-BIA 875	Scaffold	3M004	FERMENTED VEGETAGLES	China	GCA_002179515.1_ASM217951v1_genomic.fna
GCA_026622905.1	ASM2662290v1	*Levilactobacillus brevis*	NCTC13386	Contig	F4101	FERMENTED VEGETAGLES	China	GCA_026622905.1_ASM2662290v1_genomic.fna
GCA_027686645.1	ASM2768664v1	*Levilactobacillus brevis*	DPC 6108	Scaffold	AF10-19C	ANIMALS/HUMAN GUT	China	GCA_027686645.1_ASM2768664v1_genomic.fna
GCA_027664805.1	ASM2766480v1	*Levilactobacillus brevis*	DRD-35	Scaffold	AF92-02GAA	ANIMALS/HUMAN GUT	China	GCA_027664805.1_ASM2766480v1_genomic.fna
GCA_027699065.1	ASM2769906v1	*Levilactobacillus brevis*	DRD-198	Scaffold	AM87-02A	ANIMALS/HUMAN GUT	China	GCA_027699065.1_ASM2769906v1_genomic.fna
GCA_027698985.1	ASM2769898v1	*Levilactobacillus brevis*	DRD-51	Scaffold	AM88-10A	ANIMALS/HUMAN GUT	China	GCA_027698985.1_ASM2769898v1_genomic.fna

GCA_027698855.1	ASM2769885v1	*Levilactobacillus brevis*	DRD-52	Scaffold	AM89-08b2TA	ANIMALS/HUMAN GUT	China	GCA_027698855.1_ASM2769885v1_genomic.fna
GCA_027698465.1	ASM2769846v1	*Levilactobacillus brevis*	DSM 20054	Scaffold	AM92-01-1A	ANIMALS/HUMAN GUT	China	GCA_027698465.1_ASM2769846v1_genomic.fna
GCA_027698385.1	ASM2769838v1	*Levilactobacillus brevis*	D7	Scaffold	AM92-01b2A	ANIMALS/HUMAN GUT	China	GCA_027698385.1_ASM2769838v1_genomic.fna
GCA_027698185.1	ASM2769818v1	*Levilactobacillus brevis*	DmCS_003	Scaffold	AM93-03b2A	ANIMALS/HUMAN GUT	China	GCA_027698185.1_ASM2769818v1_genomic.fna
GCA_027692245.1	ASM2769224v1	*Levilactobacillus brevis*	Dm-2019-10	Scaffold	OF46-2pH5A	ANIMALS/HUMAN GUT	China	GCA_027692245.1_ASM2769224v1_genomic.fna
GCA_003184305.1	ASM318430v1	*Levilactobacillus brevis*	7.2.13	Complete Genome	ZLB004	ANIMALS/HUMAN GUT	China	GCA_003184305.1_ASM318430v1_genomic.fna
GCA_039880275.1	ASM3988027v1	*Levilactobacillus brevis*	2-34	Complete Genome	PYN10-6-2	ANIMALS/HUMAN GUT	China	GCA_039880275.1_ASM3988027v1_genomic.fna

GCA_026639055.1	ASM2663905v1	*Levilactobacillus brevis*	7.2.49	Complete Genome	SC013	FERMENTED VEGETAGLES	China	GCA_026639055.1_ASM2663905v1_genomic.fna
GCA_037201785.1	ASM3720178v1	*Levilactobacillus brevis*	30.2.29	Complete Genome	LMT1-73	FERMENTED VEGETAGLES	China	GCA_037201785.1_ASM3720178v1_genomic.fna
GCA_026410225.1	ASM2641022v1	*Levilactobacillus brevis*	SA-C12	Scaffold	LZB2	ALCOLIC FERMENTATION	China	GCA_026410225.1_ASM2641022v1_genomic.fna
GCA_024330045.1	ASM2433004v1	*Levilactobacillus brevis*	MRS-9	Scaffold	2-34	ALCOLIC FERMENTATION	China	GCA_024330045.1_ASM2433004v1_genomic.fna
GCA_045012225.1	ASM4501222v1	*Levilactobacillus brevis*		Complete Genome	D17	ALCOLIC FERMENTATION	China	GCA_045012225.1_ASM4501222v1_genomic.fna
GCA_043854055.1	ASM4385405v1	*Levilactobacillus brevis*	CRL 2013	Scaffold	YT108	ANIMALS/HUMAN GUT	China	GCA_043854055.1_ASM4385405v1_genomic.fna
GCA_018916925.1	ASM1891692v1	*Levilactobacillus brevis*	G101	Contig	N38	ANIMALS/HUMAN GUT	China	GCA_018916925.1_ASM1891692v1_genomic.fna
GCA_003666485.1	ASM366648v1	*Levilactobacillus brevis*		Chromosome	CD0817	ANIMALS/HUMAN GUT	China	GCA_003666485.1_ASM366648v1_genomic.fna

GCA_015238595.1	ASM1523859v1	*Levilactobacillus brevis*	ATCC 367	Chromosome	HQ1-1	DAIRY PRODUCT	China	GCA_015238595.1_ASM1523859v1_genomic.fna
GCA_003060705.1	ASM306070v1	*Levilactobacillus brevis*	MB1	Scaffold	DM9218	FERMENTED VEGETAGLES	China	GCA_003060705.1_ASM306070v1_genomic.fna
GCA_022350025.1	ASM2235002v1	*Levilactobacillus brevis*	AM87-02A	Complete Genome	YSJ3	FERMENTED VEGETAGLES	China	GCA_022350025.1_ASM2235002v1_genomic.fna
GCA_003289085.1	ASM328908v1	*Levilactobacillus brevis*	KMB_620	Scaffold	TUCO-5E	DAIRY PRODUCT	Chile	GCA_003289085.1_ASM328908v1_genomic.fna
GCA_000469365.1	ASM46936v1	*Levilactobacillus brevis* ATCC 14869 = DSM 20054	BIO5542	Scaffold	ATCC 14869	ANIMALS/HUMAN GUT	Canada	GCA_000469365.1_ASM46936v1_genomic.fna
GCA_001953605.1	ASM195360v1	*Levilactobacillus brevis*	CIRM-BIA 2231	Contig	EF	ANIMALS/HUMAN GUT	Canada	GCA_001953605.1_ASM195360v1_genomic.fna
GCA_002093065.1	ASM209306v1	*Levilactobacillus brevis*	CIRM-BIA 2227	Contig	CRL 2013	FERMENTED VEGETAGLES	Argetina	GCA_002093065.1_ASM209306v1_genomic.fna
GCA_000833395.1	ASM83339v1	*Levilactobacillus brevis*	YT108	Scaffold	TMW 1.465	ALCOLIC FERMENTATION	UNKNOWN	GCA_000833395.1_ASM83339v1_genomic.fna

GCA_000833405.1	ASM83340v1	*Levilactobacillus brevis*			Scaffold	TMW 1.313	ALCOLIC FERMENTATION	UNKNOWN	GCA_000833405.1_ASM83340v1_genomic.fna
GCA_001433855.1	ASM143385v1	*Levilactobacillus brevis* ATCC 14869 = DSM 20054	BDGP6		Scaffold	DSM 20054	ANIMALS/HUMAN GUT	UNKNOWN	GCA_001433855.1_ASM143385v1_genomic.fna
GCA_000833415.1	ASM83341v1	*Levilactobacillus brevis*	CIRM-BIA 895		Scaffold	TMW 1.6	ANIMALS/HUMAN GUT	UNKNOWN	GCA_000833415.1_ASM83341v1_genomic.fna
GCA_025194365.1	ASM2519436v1	*Levilactobacillus brevis*			Scaffold	CIRM-BIA 519	ANIMALS/HUMAN GUT	UNKNOWN	GCA_025194365.1_ASM2519436v1_genomic.fna
GCA_002762175.1	ASM276217v1	*Levilactobacillus brevis*	100D8		Complete Genome	BDGP6	ANIMALS/HUMAN GUT	UNKNOWN	GCA_002762175.1_ASM276217v1_genomic.fna
GCA_963534875.1	DRR247351_bin.2_MetaWRAP_v1.3_MAG	*Levilactobacillus brevis*		DRR247351_bin.2_MetaWRAP_v1.3_MAG	Contig	DRR247351_bin.2_MetaWRAP_v1.3_MAG	ANIMALS/HUMAN GUT	UNKNOWN	GCA_963534875.1_DRR247351_bin.2_MetaWRAP_v1.3_MAG_genomic.fna

GCA_000526755.1	ASM52675v1	*Levilactobacillus brevis* AG48		Contig	AG48	ANIMALS/HUMAN GUT	UNKNOWN	GCA_000526755.1_ASM52675v1_genomic.fna
GCA_009741845.1	ASM974184v1	*Levilactobacillus brevis*	CIRM-BIA 899	Contig	LB_AVK	DAIRY PRODUCT	UNKNOWN	GCA_009741845.1_ASM974184v1_genomic.fna
GCA_013249075.1	ASM1324907v1	*Levilactobacillus brevis*	GOS-2	Contig	BIO5542	FERMENTED VEGETAGLES	UNKNOWN	GCA_013249075.1_ASM1324907v1_genomic.fna
GCA_000014465.1	ASM1446v1	*Levilactobacillus brevis* ATCC 367	ASK-1	Complete Genome	ATCC 367	UNKNOWN	UNKNOWN	GCA_000014465.1_ASM1446v1_genomic.fna
GCA_000359625.1	ASM35962v1	*Levilactobacillus brevis* KB290	AM93-03b2A	Complete Genome	KB290	UNKNOWN	UNKNOWN	GCA_000359625.1_ASM35962v1_genomic.fna
GCA_900475625.1	45709_F01	*Levilactobacillus brevis*	994	Complete Genome	NCTC 13768	UNKNOWN	UNKNOWN	GCA_900475625.1_45709_F01_genomic.fna
GCA_019693335.1	ASM1969333v1	*Levilactobacillus brevis*	CIRM-BIA 2225	Contig	Lbr-35	UNKNOWN	UNKNOWN	GCA_019693335.1_ASM1969333v1_genomic.fna
GCA_006538905.1	ASM653890v1	*Levilactobacillus brevis*	MB20	Contig	NBRC 12005	UNKNOWN	UNKNOWN	GCA_006538905.1_ASM653890v1_genomic.fna

GCA_006539265.1	ASM653926v1	*Levilactobacillus brevis*	OF46-2pH5A	Contig	NBRC 13110	UNKNOWN	UNKNOWN	GCA_006539265.1_ASM653926v1_genomic.fna
GCA_002933755.1	ASM293375v1	*Levilactobacillus brevis*	D17	Contig	NBRC 3345	UNKNOWN	UNKNOWN	GCA_002933755.1_ASM293375v1_genomic.fna
GCA_006538845.1	ASM653884v1	*Levilactobacillus brevis*	SC013	Contig	NBRC 3960	UNKNOWN	UNKNOWN	GCA_006538845.1_ASM653884v1_genomic.fna

3.2.8 In silico safety and functional assessments

In silico safety assessments were conducted in line with recommendations from the European Food Safety Authority (EFSA, 2018). Comprehensive Antibiotic Resistance Database (CARD) Variants v4.0.0 (Alcock et al., 2020), ARMFinder (Feldgarden et al., 2021), and ResFinder v4.3.2 (Bortolaia et al., 2020) were used to identify the antibiotic resistance genes (ARGs). BLASTN v2.8.1 + was used to detect virulence factors (VFs) by searching against the setB database from the Virulence Factor Database (VFDB) (Liu et al., 2022) and VirulenceFinder v2.0.3 (Scheutz et al., 2024). BLASTP v2.8.1 + search was performed against the Pathogen Host Interaction v4.14 database to identify the probable pathogenic genes (PGs) in the M3R3 genome (Liu et al., 2022). The probiotic potential risk score (PPRS) was computed as defined by Bai et al. (2023) to evaluate the risks associated with M3R3 probiotic candidate. The score was classified as low-risk (≤4), medium-risk (4–6), and high-risk (≥6). All these analyses were implemented in ProbioMinServer (Liu et al., 2023).

Prophage regions and virulence-associated genes were predicted using Phigaro v2.3.0 (Starikova et al., 2020), whereas putative plasmids were identified using the PlasmidFinder database v2.1 (https://cge.food.dtu.dk/services/PlasmidFinder/, accessed 1 December 2024), applying thresholds of ≥ 95% identity and ≥ 60% coverage (Carattoli & Hasman, 2020). CRISPR arrays and associated Cas proteins were annotated with CRISPRCasFinder v2.2 (Couvin et al., 2018).

Mobile genetic elements were screened *via* BLASTX against the mobileOG-db v1.1.3 (Brown et al., 2022), applying cutoff of >90% identity and >90% coverage. Biosynthetic gene clusters were identified using antiSMASH 6.0 with default parameters (Blin et al., 2021).

3.2.9 *In silico search for bsh gene candidates*

Putative *bsh* genes in the genome of strain M3R3 were identified using the BLASTp algorithm with *bsh1* of *Lactiplantibacillus plantarum* WCFS1 as the query (CCC80500). Seventy-eight protein sequences of *L. brevis* annotated as linear amide C-N hydrolase (PFAM: PF02275) were retrieved from NCBI RefSeq proteins database applying both sequence and domain cutoffs above 20.4 (last accessed March 2025). The sequences were collected into a local database, and two truncated proteins were manually removed, resulting in a dataset of 76 high-quality sequences. In addition, seven penicillin V acylases (PVA) proteins were included as reference sequences, comprising three from *L. plantarum* (Q88SP0, Q890F5, and Q88UC9), three from *L. brevis* (Q03PK6, Q03NN7, and Q03P51), and one from *Latilactobacillus sakei* (Q38Z70), as reported by O'Flaherty et al. (2018).

All proteins sequences were aligned using the COBALT multiple sequence alignment tool (Papadopoulos & Agarwala, 2007). Phylogenetic reconstruction was carried out with the NCBI Tree Viewer, using the Fast Minimum Evolution algorithm with the Grishin model for evolutionary distances calculation. The phylogenetic tree was visualized as described above.

3.2.10 *RT-PCR assay*

RNA isolation was carried out from M3R3 cells grown in the presence of BSs mixture and under control condition (MRS medium), as previously reported by Solieri et al. (2022). Residual genomic DNA was eliminated by incubating 2 µg of total RNA with dsDNase (Cat. No. EN0771; Thermo Fisher Scientific, Waltham, MA, USA) at 37 °C for 2 minutes in a pre-warmed thermocycler set with the lid temperature at 37 °C. Samples were then placed on ice, briefly centrifuged, and 12.5 µL of the treated RNA was used for first-strand cDNA synthesis carried out using the RevertAid Reverse Transcriptase (Cat. No. EP0441) in presence of random hexamers (Cat. No. SO142) and oligo $(dT)_{18}$ primers (Cat. No. SO131), according to the manufacturer's recommendations. All reagents for RT were from Thermo Scientific (Waltham, MA, USA). *Pva* and *bsh*-targeted RT-PCR amplifications were carried out using the primer pairs listed in supplementary **Table 3.2**.

Table 3.2 - Primer used in this study.

Target gene	PCR assay	Primer	Sequence (5'->3')	Tm	Length (bp)
bsh ClusterI	End-point PCR	Br_bsh_1F1	GGCAGCGCTTACACCATTTA	62	799
		Br_bsh_1R	CAAGTAGCCGGATCACCATATTC	62	
bsh ClusterII	End-point PCR	Br_bsh_2F1	AAATAGCCAAAGATGGGAGTCATA	62	908
		Br_bsh_2R1	GCCGTCCGCGATAACATTT	62	

bsh ClusterIII	End-point PCR	Br_bsh_3F1	TATCACTGGGAAACGGCC TTA	62	839
		Br_bsh_3R1	GGGAAAGCGTGAGGGAA ATG	62	
PVA	End-point PCR	Br_PVA_F1	CTCACGATGTTGTTGCTTG G	63,7	606
		BR_PVA_R1	AGCGAATCCCTTGTAGTT CTT	63	
16S	End-point PCR	27f	CTGGGATCCATTTACTCG AGAGTTTGATCCTGGCTG GCTCAG	63	1500
		1490R	GGTTCCCCTAAGCTTACCT TGTTACGACTTC	58	

3.2.11 Penicillin V MIC determination

Antibiotic susceptibility to Penicillin V (PenV) was assessed using the broth microdilution method (ISO/IDF, 2010). The Minimum Inhibitory Concentration (MIC) was determined according to the break-point values established for obligate heterofermentative lactobacilli (including *L. brevis*) (Urshev et al., 2024), in order to classify the strain as resistant or susceptible to PenV, as recommended by EFSA (2018).

3.2.12 Statistical analysis

All analyses were conducted in triplicate and results are expressed as mean values ± standard deviation (SD). Statistical analysis and graph generation were performed with GraphPad Prism

v10.3.1 (GraphPad Software, La Jolla, CA, USA). For all the analysis a one-way ANOVA, followed by Dunnett's post-hoc, was applied for all analyses, unless otherwise specified. A p-value < 0.05 was considered statistically significant.

3.3 Results and Discussion

Recently, several studies have underscored the pivotal role of BSH in lipid metabolism and in mediating host–microbe interactions (Dong et al., 2025; Jiang et al., 2025; Joyce et al., 2014). Consequently, BSH activity is widely recognized as a key criterion for probiotic selection, and numerous investigations have examined the distribution of *bsh* genes across different species, correlating them with substrate-specific BSH activities (da Silva et al. 2024). In the present study, we employed a combined phenotypic and genomic approach to characterize *L. brevis* M3R3 as promising probiotic candidate. The strain, part of the microbial collection of Probioetna srl, was subjected to a series of probiotic assays, including a plate-based evaluation of BSH ability. Preliminary results revealed that M3R3 exhibited a marked capacity to deconjugate BSs (data not shown), thereby providing a strong rationale for further studies to validate its selection as a BSH-active candidate.

3.3.1 Inhibitory effect of individual bile salts

As previously demonstrated, BSs tolerance was largely attributed to BSH-mediated deconjugation of BSs, which enhances cell viability under gastrointestinal conditions (Agolino et al., 2024; Bustos et al., 2018). To evaluate the impact of different concentrations

of individual conjugated BSs on the growth of *L. brevis* strain M3R3, a stress response assay was performed by supplementing MRS medium with four individual BSs, each tested at four distinct concentrations. These concentrations were selected to reflect the range of physiological BSs concentrations in the small intestine under fed conditions (0.3 to 0.8%, *w/v*). The growth of M3R3 strain under each condition was assessed by plate counts relative to the control (MRS medium without BSs). The M3R3 strain displayed comparable tolerance to all four tested BSs with plate counts ranging from a minimum of 8.73±0.06 to a maximum of 9.37±0.08 Log_{10} CFU/mL (**Table 3.3**). These findings highlight the robust ability of M3R3 strain to grow in presence of various concentrations of conjugated BSs even exceeding the physiological concentration of BSs.

Except for TCA, increasing concentrations of individual BSs generally corresponded to higher growth inhibition, indicating a dose-dependent effect on strain viability. The highest reduction in plate counts was detected in the presence of 1% and 0.5% GCA, followed by 1% GDCA. This finding is consistent with previous studies reporting that glyco-conjugated BSs exert a more pronounced inhibitory effect on lactobacilli growth than their tauro-conjugated counterparts (Agolino et al., 2024; Begley & Gahan 2006).

Table 3.3 - Effects of different concentrations of individual BSs on the growth of *Levilactobacillus brevis* M3R3 strain. Log_{10} CFU/mL values were measured after 24 h of exposition to conjugated BSs relative to the control (MRS without BSs). Data are the mean of at least three replicates. Statistically significant differences compared with the control were determined by one-way ANOVA ($p<0.05$) and are indicated with different letters. Abbreviations: TDCA (taurodeoxycholic acid), TCA (taurocholic acid), GDCA (glycodeoxycholic acid), GCA (glycocholic

acid), and na, not applicable.

Conditions	Concentrations (%)				
	0.0	**0.1**	**0.25**	**0.5**	**1.0**
MRS (CTRL)	9.45 ± 0.02 [a]	na	na	na	na
TDCA	na	9.31 ± 0.02 [a]	9.22 ± 0.30 [a]	9.12 ± 0.12 [a]	9.07 ± 0.10 [b]
TCA	na	9.13 ± 0.02 [b]	9.17 ± 0.12 [a]	9.19 ± 0.15 [a]	9.20 ± 0.22 [a]
GDCA	na	9.27 ± 0.27 [a]	9.27 ± 0.27 [a]	9.21 ± 0.24 [a]	8.98 ± 0.04 [b]
GCA	na	9.37 ± 0.08 [a]	9.30 ± 0.14 [a]	8.87 ± 0.24 [b]	8.73 ± 0.06 [b]

3.3.2 Growth kinetics and deconjugation activity under exposure to individual conjugated bile salts

To further investigate the adaptive response of strain M3R3 to conjugated BSs and to correlate this response with its deconjugation activity, growth curves were determined in the presence of 1.0% of each individual BS. Growth curves (**Figure 3.1**) were fitted using the three parametric models such as Gompertz, logistic and Richards equations implemented in the Grofit package. Based on AIC values, the Gompertz or logistic models generally provided the best fit to the experimental data, whereas the Richards equation consistently failed to describe the observed growth profiles (**Table 3.4**). In one case (1.0% TCA), the parametric models could not be applied, and data were instead fitted using the spline-based model, a non-parametric smoothing approach that uses smoothing splines to approximate the shape of the observed growth data without assuming a predefined mathematical model (**Table 3.4**). The derived kinetic parameters are summarized in **Figure 3.2**.

It is important to note that, under TCA and GCA exposure, the number of sampling points during the lag and exponential phases was

limited. This scarcity of data in the most informative growth intervals reduces the reliability of the corresponding kinetic estimates and should therefore be interpreted with caution. Despite these limitations, exposure to individual conjugate BSs did not significantly affect the maximum growth rate of M3R3 strain under GDCA, GCA and TDCA exposure, whereas TCA condition resulted in a significant reduction compared to the control condition ($p < 0.05$) (**Figure 3.2A**). Similarly, the lag phase duration remained unchanged in the presence of GDCA and GCA but was significantly shortened under TDCA and TCA exposure compared to the control condition ($p < 0.05$), suggesting a possible stimulatory or priming effect, rather than inhibition (**Figure 3.2B**). Maximum growth efficiency (A) remains unaffected by any of the tested BSs (**Figure 3.2C**).

The deconjugation ability of M3R3 strain was evaluated by determining the percentage of residual conjugated BSs in the cell-free supernatant collected at stationary phase, using UHPLC/HR-MS. As shown in **Figure 3.2D**, semi-quantitative AUC analysis revealed a marked difference in deconjugation efficiency between glyco-conjugated and tauro-conjugated BSs. Strain M3R3 efficiently deconjugated GDCA and GCA, leaving residual concentrations of 14.2% and 0.1%, respectively. By contrast, deconjugation of tauro-conjugated BSs was markedly less efficient, with 83.4% TDCA and

76.3% TCA remaining.

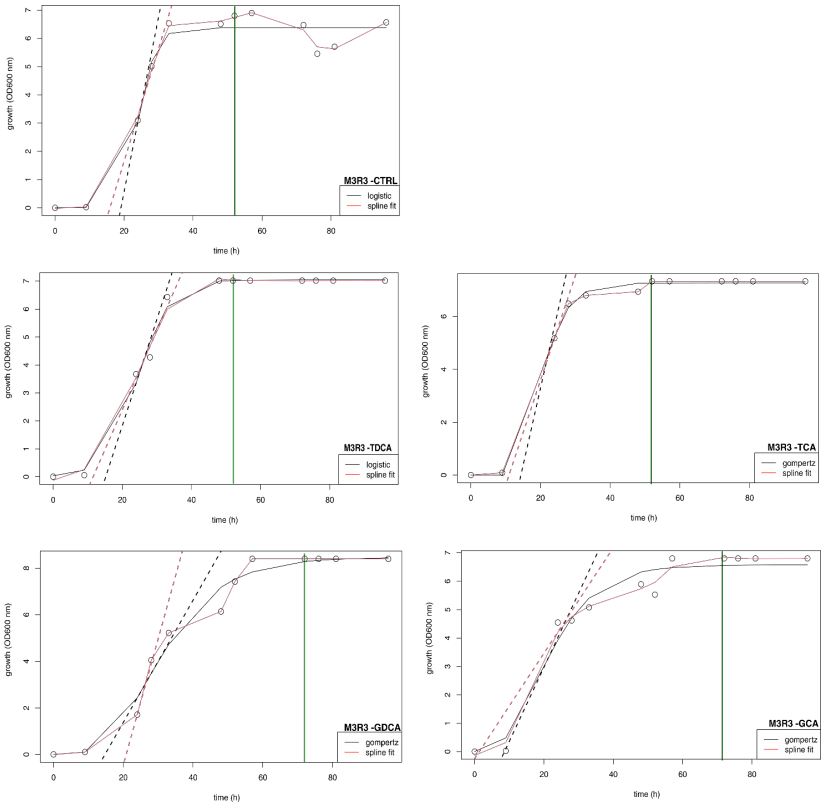

Figure 3.1 - Representative growth kinetics of *Levilactobacillus brevis* strain M3R3 in MRS medium supplemented with 1.0% (w/v) of each individual bile salt (BS), compared with the control condition (MRS only). Optical density at 600 nm (OD_{600}) was recorded over time. Each condition was tested in three independent biological replicates. Growth curves were modeled using the Grofit package in the R environment, applying both parametric (black) and spline-based (red) methods. Black and red dotted lines indicate the intercepts

corresponding to the maximum growth rate (h^{-1}) calculated by the parametric and spline-based approaches, respectively. The vertical green line marks the sampling point used for supernatant collection for UHPLC/HR-MS analysis. Abbreviations: TDCA, taurodeoxycholic acid; TCA, taurocholic acid; GDCA, glycodeoxycholic acid; GCA, glycocholic acid.

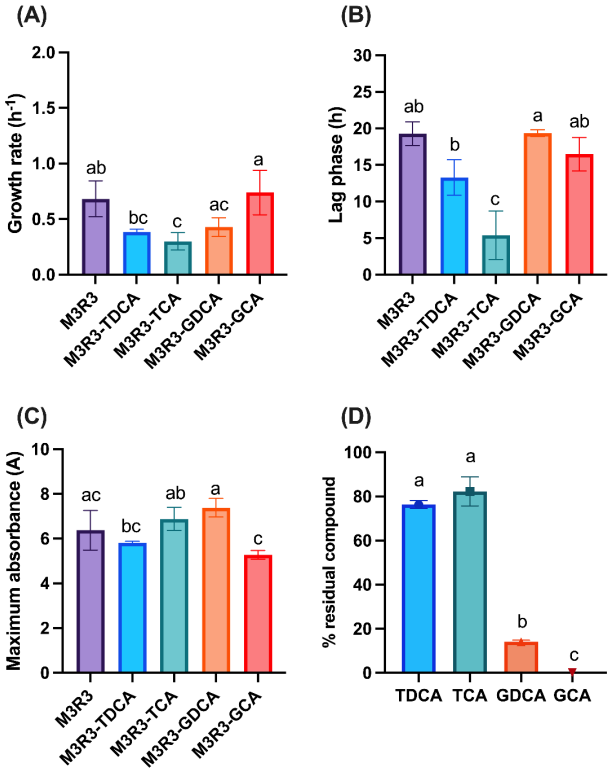

Figure 3.2 - Growth kinetics parameters and bile salts deconjugation ability of *Levilactobacillus brevis* M3R3 in the presence of 1.0 % (w/v) of individual bile salts (TDCA, TCA, GDCA and GCA) compared with the control condition (MRS

medium). Kinetics parameters, such as (A) maximum growth rate (μ, h^{-1}), (B) lag phase (λ, h), and (C) maximum cell density (A, OD_{600nm}), were estimated using Grofit package. (D) Deconjugation ability expressed as the percentage of residual conjugated bile salt (TDCA, TCA, GDCA, or GCA) quantified in cell-free supernatants collected during the late stationary phase. Significant differences were calculated with one-way ANOVA and indicated with different letters. Graphs are visualized with GraphPad Prism v10.3.1 software (San Diego, CA, USA). Abbreviations: TDCA, taurodeoxycholic acid; TCA, taurocholic acid; GDCA, glycodeoxycholic acid; and GCA, glycocholic acid.

Table 3.4 – Summary of the best models used to fit growth curves of *Levilactobacillus brevis* M3R3 strain. Best-fit models were choosen using AIC (implementing in Grofit)

		Growth parameters			
Condition	**Replicates**	**Best-fitting model**	**Growth rate (h-1)**	**Lag phase (h)**	**Maximum cell density (A)**
MRS	R1	Logistic	0,47803199	17,39302124	7,87320875
	R2	Gompertz	0,80376641	20,00653025	6,441517553
	R3	Logistic	0,49827127	17,40567748	5,46074947
MRS-TDCA 1%	R1	Logistic	0,411143211	16,09833351	5,86027886
	R2	Gompertz	0,37169556	11,5176879	5,827845323
	R3	Gompertz	0,36788345	12,26605675	5,728381729
MRS-TCA 1%	R1	Spline	0,30319229	6,367493668	7,296320552
	R2	Spline	0,21962339	1,69468462	6,310928653
	R3	Spline	0,37570285	8,109782384	7,04
MRS-GDCA 1%	R1	Gompertz	0,42857668	19,07983375	7,23799462
	R2	Gompertz	0,34201153	19,08385644	7,84550895
	R3	Logistic	0,51220201	19,92297408	7,06262106
MRS-GCA 1%	R1	Logistic	0,97017668	19,12155777	5,11653799
	R2	Gompertz	0,6104924	15,0593605	5,49253407
	R3	Gompertz	0,63731794	15,24211202	5,21298001
MRS-BS 1%	R1	Logistic	0,87399789	24,49094801	2,941018484
	R2	Gompertz	0,69754523	24,11888052	2,653516042

R3	Logistic	0,75585851	25,08218394	2,260561967

3.3.3 *Growth kinetics and deconjugation activity under bile salt mixture exposure*

The survival and deconjugation activity of M3R3 strain were further assessed in the presence of BSs mixture, a condition which more closely mimics the complex *in vivo* bile environment compared to individual BSs exposure (Kahm et al., 2010; Hu et al., 2018). The resulting growth curves (**Figure 3.3**) were modeled to determine the kinetic parameters μ, A, and λ (**Table 3.4**). As shown in **Figure 3.4A**, exposure to the BSs mixture did not significantly affect the maximum growth rate, consistent with the results obtained using individual BSs (**Figure 3.2A**). In contrast, the BSs mixture significantly increased the lag phase duration ($p < 0.01$) (**Figure 3.4B**), supporting a delayed adaptation to the complex bile environment. This effect contrasts with the response observed under exposure to TDCA and TCA alone (**Figure 3.2B**), where the lag phase was shortened. Furthermore, a significant decrease in A value was observed under BSs mixture stress compared to the control ($p < 0.01$), indicating that the biomass production is markedly inhibited under this condition (**Figure 3.4C**). A study conducted by Hu and co-workers (2018) characterized commercial BSs mixture powders and demonstrated the presence of several other BSs beyond TDCA, TCA, GDCA, and GCA, which can impair the growth of strain M3R3 more severely than the individual BSs. Furthermore, it can be speculated that, unlike the *in vivo* gut environment, the experimental system used here is closed and lacks efflux mechanisms, leading to the accumulation of deconjugated BSs. Such accumulation may reduce cell viability and contribute to the

delayed adaptation observed in strain M3R3, thereby potentially overestimating its sensitivity to BS mixture. Consistently, a recent study revealed that, contrary to the earlier assumptions, certain deconjugated BSs can exert more toxic effects on bacterial cells than their conjugated counterparts (Foley et al., 2021).

The semi-quantitative analysis of residual conjugate BSs revealed a marked variability in BSH activity of M3R3 strain related to the substrate. Notably, GCDCA and GDCA were completely deconjugated, while GCA exhibited a residual compound of 2.5%. Among tauro-conjugated BSs, TDCA displayed the lowest residual percentage (**Figure 3.4D**). By contrast, M3R3 strain displayed the lowest efficiency in deconjugating TCDCA and TCA, which persisted in their conjugated forms, showing a residual percentage of 46.6% and 60.7% respectively (**Figure 3.4D**).

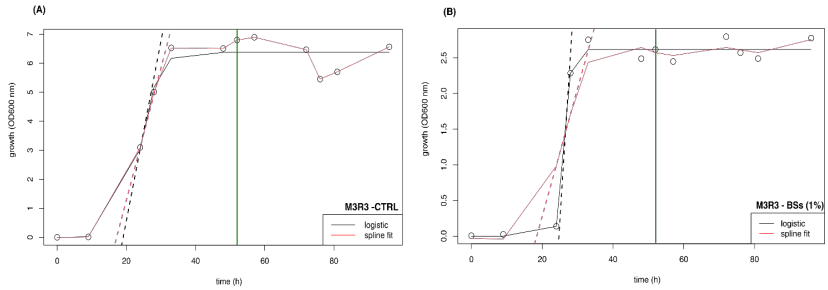

Figure 3.3 - Representative growth curves of *Levilactobacillus brevis* strain M3R3 in presence of 1.0 % (*w/v*) bile salts (BSs) mixture (B) compared with the control condition (A; MRS medium). Optical density at 600 nm (OD_{600}) was recorded over time. Each condition was tested in three independent biological replicates. Growth curves were modeled using the Grofit package in the R environment, applying both parametric (black) and spline-based (red) methods. Black and red dotted lines indicate the intercepts corresponding to the maximum growth rate

(h^{-1}) calculated by the parametric and spline-based approaches, respectively. The vertical green line marks the sampling point used for supernatant and cells collection for UHPLC/HR-MS analysis and RNA extraction, respectively.

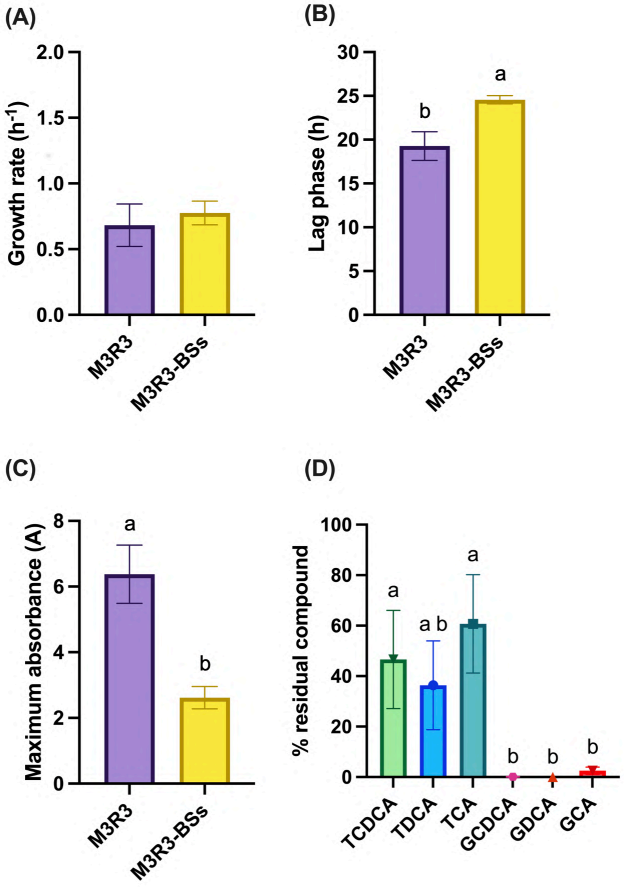

Figure 3.4 - Growth kinetics parameters and bile salts deconjugation ability of *Levilactobacillus brevis* M3R3 in the presence of 1.0 % (w/v) of bile salts (BSs) mixture compared with the control condition (MRS medium). Kinetics parameters, such as (A) maximum growth rate (μ, h^{-1}), (B) lag phase (λ, h), and (C) maximum cell density (A, OD_{600nm}), were estimated using Grofit package. Significant differences in growth kinetics parameters were calculated between control and stress conditions with a two-tailed *t*-test and indicated with different letters, $p \leq 0.01$. (d) Deconjugation ability expressed as the percentage of residual conjugated bile salt (TDCA, TCA, GDCA, or GCA) quantified in cell-free supernatants collected during the late stationary phase. Significant differences among residual compound percentages were calculated with one-way ANOVA and indicated with different letters. Graphs are visualized with GraphPad Prism v10.3.1 software (San Diego, CA, USA). Abbreviations: TCDCA, taurochenodeoxycholic acid TDCA, taurodeoxycholic acid; TCA, taurocholic acid; GCDCA, glycochenodeoxycholic acid; GDCA, glycodeoxycholic acid; and GCA, glycocholic acid.

Collectively, the BSs deconjugation assays in presence of both individual BSs and BSs mixture supported that the M3R3 strain exhibits a higher deconjugation capacity toward glyco-conjugated BSs compared to tauro-conjugated forms, suggesting the presence of BSH activity under the tested conditions. Notably, BSH-positive lactobacilli strains have been reported to have a preferential deconjugation activity towards glyco-conjugated BSs, which are more cytotoxic than tauro-conjugated counterparts (Agolino et al., 2024; Begley et al., 2006). Glycine preference could reflect the increased abundance of glycine-conjugated BSs among vertebrates, whereas taurine specificity is restricted to only a few related BSHs (Foley et al., 2021). This trend was consistently observed in all experimental conditions, with the most pronounced deconjugation observed in M3R3 exposed to the BSs mixture, reflecting a scenario that more

closely resembles physiological conditions.

3.3.4 General genomic features and taxonomic evaluation

To investigate the genetic determinants underlying the BSH-positive phenotype of *L. brevis* strain M3R3 and to evaluate its probiotic potential, whole-genome sequencing was performed. Reads assembly resulted in 72 contigs, corresponding to a total genome length of 2,406,595 bp (**Figure 3.5**). The GC content was 45.93% and the orientation of positive and negative strands was clearly defined.

Genome annotation predicted a total of 2442 genes in the M3R3 genome assembly, including 2373 CDS, 66 tRNA, 6 rRNA, and 1 tmRNA (**Table 3.5**). The functional annotation by BLASTKOALA assigned approximately 50.08% of these CDS (1207 genes) into 23 different functional KEGG categories. The most represented categories were the followings: protein families: genetic information processing (190, 15.73%), genetic information processing (156, 12.91%), protein families: signaling and cellular processes (142, 11.75%), and carbohydrate metabolism (125, 10.35%) (**Figure 3.6**). 50.02% of CDS were assigned to an unknown function. A plasmid replicon sequence, rep28(pCIS4), was identified in the M3R3 genome with 99.78% identity and 100% query coverage, indicating the presence of a plasmid homologous to the *Lactococcus lactis* subsp. *cremoris* UC509.9 plasmid pCIS4 (NCBI accession: CP003162.1). A similar plasmid was found in the probiotic candidate *L. brevis* strain H3 isolated from a traditional fermented beverage in India (Sethi et al., 2025). Two CRISPR arrays and one ORF encoding a Cas4-type II protein were detected in the genome of strain M3R3. However, no CRISPR arrays were found in proximity to this ORF (**Table 3.6**).

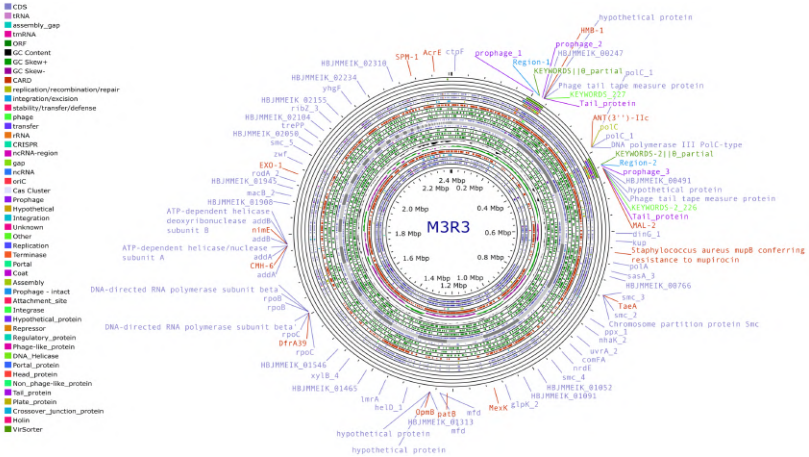

Figure 3.5 - Circular graphical representations of the *Levilactobacillus brevis* M3R3 strain contigs obtained using Proksee (https://proksee.ca; last accessed 13 February 2025). Starting from the outermost ring: Ring 1: PHASTEST, Ring 2: Phigaro, Ring 3: CRISPRCasFinder Annotation (+), Ring 4: Bakta Annotation (+), Ring 5: Prokka Annotation (+), Ring 6: mobileOG-db Annotation (+), Ring 7: CARD RGI Results (+), Rings 8 to 10: ORFs (+3,+2,+1), Ring 11: Features (+), Backbone (Contigs), Ring 13: Features (-), Rings 14 to 16: ORFs (-1,-2,-3), Ring 17: GC Content, Ring 18: GC Skew, Ring 19: CARD RGI Results (-), Ring 20: mobileOG-db Annotation (-), Ring 21: Prokka Annotation (-), Ring 22: Bakta Annotation (-), Ring 23: CRISPRCasFinder Annotation (-).

Table 3.5 - Assembly and annotation of *Levilactobacillus brevis* M3R3 genome.

Assembly statics	Features	Annotation statics	Features
Contigs	72	CDS	2373
Contigs (>= 1000 bp)	65	tRNA	66
Contigs (>= 5000 bp)	41	tmRNA	1
Contigs (>= 10000 bp)	34	rRNA	6

Contigs (>= 25000 bp)	24	ncRNA	6
Contigs (>= 50000 bp)	14	ncRNA Region	22
Largest contig	239718	sORF	0
Total length	2406595	gap	2
GC (%)	45.93	oriC	2
N50	124627	oriV	0
N90	24367	oriT	0
auN	118405.8		
L50	7		
L90	25		
Properly paired (%)	99.3		
Avg. coverage depth	117		
Coverage >= 1x (%)	99.99		

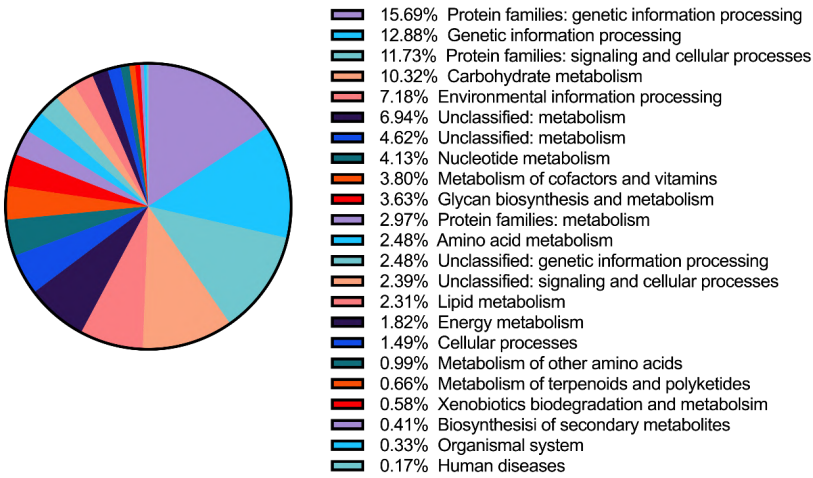

Figure 3.6 - Distribution of KEGG orthology (KO) categories of identified protein-coding genes in the *Levilactobacillus brevis* M3R3 genome.

Table 3.6 - Overview of *cas* gene clusters and CRISPR regions in *Levilactobacillus brevis* M3R3 genome.

Element ID (Cas)	Cas-type/subtype	System	Contig	Begin	End	Strand	Other_information		
1	cas4_TypeI-II	CAS-TypeII	16	21767	24133	-	ID=1_20;partial=00;start_type=ATG;rbs_motif=AGGAG/GGAGG;rbs_spacer=11-12bp;gc_cont=0.480;conf=99.99;score=209.91;cscore=195.90;sscore=14.01;rscore=7.50;uscore=3.18;tscore=3.99;		
Element ID (CRISPR)	**Contig**	**Begin**	**End**	**CRSIPR lenght**	**Potential**	**Consensus**	**Repeat lenght**	**Number of spacers**	**Evidence level**
1	4	141388	141720	332	+	GTATTCCCCACACGTGTGGGGGTGATCC	28	5	4
2	15	28089	28360	271	-	GGATCACCCCCACACCTGTGGGGAATAC	28	4	4

Phylogenetic analysis based on 16S rRNA gene sequences and genome-based taxonomic analysis using the TYGS web server revealed that *L. brevis* strains M3R3 clustered with *L. brevis* reference strains and was clearly distinguished from closely related species (**Figure 3.7**). Accordingly, the average nucleotide identity (ANI) and dDDH values between strain M3R3 and *L. brevis* DSM 20054^{T} were 97.73% and of 79.4%, respectively, both exceeding the accepted thresholds for species delineation (**Table 3.7 and 3.8**). The results confirm that strain M3R3 indeed belongs to the species *L. brevis*.

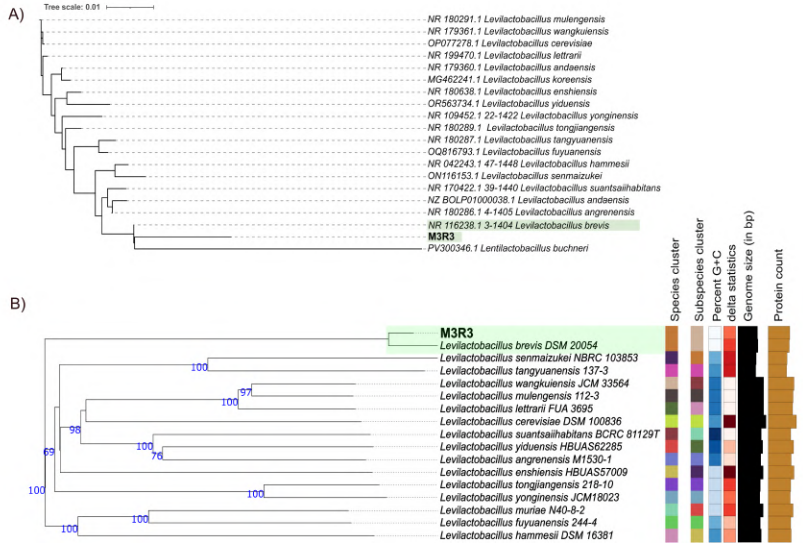

Figure 3.7 - Phylogenetic analyses inferring the taxonomical position of *L. brevis* M3R3. (A) 16S rRNA gene-based phylogeny constructed using Neighbor-Joining (NJ) algorithm. (B) Phylogenomic tree constructed using GBDP distances derived from the genomes of TYGS type strains most closely related to L. brevis M3R3

Table 3.7 – Matrix of ANIm values.

	Levilactobacillus brevis ATCC 14869 = DSM 20054 ATCC 14869 [T]	*Levilactobacillus angrenensis* M1530-1 [T]	*Levilactobacillus angrenensis* CCM 8893 [T]	*Levilactobacillus hammesii* DSM 16381 [T]	*Levilactobacillus yonginensis* JCM 18023 [T]	*Lentilactobacillus buchneri* ATCC 4005 [T]	*Levilactobacillus andaensis* 866-3 [T]	*Levilactobacillus koreensis* 26-25	*Levilactobacillus lettrarii* FUA3695	*Levilactobacillus wangkuiensis* 6-5(1) [T]	*Levilactobacillus suantsaithabitans* BCRC 81129 [T]	*Levilactobacillus yiduensis* HBUAS62285 [T]	*Levilactobacillus enshiensis* HBUAS57009 [T]	*Levilactobacillus tangyuanensis* CCM 8907 [T]	*Levilactobacillus fuyuanensis* 244-4 [T]	*Levilactobacillus tongjiangensis* 218-10 [T]	*Levilactobacillus cerevisiae* DSM 100836 [T]	*Levilactobacillus mulengensis* 112-3 [T]	*Levilactobacillus senmaizukei* DSM 21775 = NBRC 103853 DSM 21775 [T]	M3R3
Levilactobacillus brevis ATCC 14869 = DSM 20054 ATCC 14869 [T]	*	84,58	84,47	84,5	84,66	86,19	84,48	84,49	84,24	84,24	84,63	84,33	84,56	85,47	84,46	84,43	84,14	84,14	85,02	97,73
Levilactobacillus angrenensis M1530-1 [T]	84,58	*	99,99	85,26	85,74	87,24	85,75	85,17	85,81	85,86	88,44	88,53	85,87	85,53	85,56	85,59	85,48	85,82	85,59	85,28
Levilactobacillus	84,47	99,99	*	85,2	85,7	87,57	85,71	85,12	85,79	85,8	88,42	88,5	85,83	85,43	85,49	85,53	85,41	85,79	85,5	85,18

angrenensis CCM 8893 [T]																				
Levilactobacillus hammesii DSM 16381 [T]	84,5	85,28	85,21	*	84,92	86,58	85,17	84,62	85,12	85,12	85,11	85,18	85,84	84,82	85,96	85,05	85,24	85,29	84,72	85
Levilactobacillus yonginensis JCM 18023 [T]	84,67	85,74	85,69	84,92	*	88,01	85,73	85,01	85,6	85,51	85,34	85,35	85,4	85,29	85,62	92,8	85,77	85,52	85,31	85,49
Lentilactobacillus buchneri ATCC 4005 [T]	86,19	87,24	87,57	86,75	88,03	*	86,83	86,65	89,11	87,63	87,78	89,72	87,27	86,43	87,13	89,16	90,16	88,45	86,9	90,96
Levilactobacillus andaensis 866-3 [T]	84,46	85,75	85,71	85,16	85,72	86,83	*	90,28	86,08	85,57	85,56	85,47	88,3	85,48	86,43	86,05	85,75	85,77	85,49	85,51
Levilactobacillus koreensis 26-25	84,47	85,17	85,12	84,61	85,02	86,65	90,27	*	85,68	85,22	85,11	85,02	87,75	84,82	84,81	84,94	85,21	85,34	84,72	84,42
Levilactobacillus lettrarii FUA3695	84,25	85,82	85,8	85,12	85,56	89,37	86,06	85,69	*	93,53	85,57	85,79	85,67	85,2	85,65	85,74	86,07	92,8	85,19	85,02
Levilactobacillus wangkuiensis 6-5(1) [T]	84,23	85,86	85,8	85,12	85,46	87,64	85,58	85,23	93,51	*	85,65	85,94	85,56	85,18	85,57	85,99	86,08	94	85,41	85,25

Levilactobacillus suantsaiihabitans BCRC 81129 [T]	84,59	88,44	88,42	85,11	85,33	87,78	85,56	85,11	85,55	85,65	*	87,82	85,56	85,03	85,13	85,29	85,31	85,66	85,35	84,99
Levilactobacillus yiduensis HBUAS62285 [T]	84,32	88,53	88,51	85,18	85,35	89,72	85,47	85,04	85,79	85,93	87,82	*	85,54	85,08	85,03	85,38	85,44	85,95	85,54	84,94
Levilactobacillus enshiensis HBUAS57009 [T]	84,53	85,87	85,83	85,84	85,41	87,27	88,3	87,74	85,66	85,54	85,56	85,53	*	85,3	85,29	85,53	85,72	85,84	85,03	85,12
Levilactobacillus tangyuanensis CCM 8907 [T]	85,47	85,54	85,44	84,82	85,29	86,42	85,49	84,82	85,18	85,17	85,03	85,09	85,3	*	85,34	85,48	85,31	85,12	87,58	86,37
Levilactobacillus fuyuanensis 244-4 [T]	84,46	85,54	85,48	85,96	85,58	87,18	86,46	84,81	85,49	85,56	85,12	85,03	85,3	85,33	*	86,5	85,72	85,67	85,58	86,27
Levilactobacillus tongjiangensis 218-10 [T]	84,43	85,6	85,52	85,05	92,8	89,16	86,03	84,93	85,76	86	85,29	85,38	85,51	85,48	86,45	*	85,5	86,41	85,63	86,07
Levilactobacillus cerevisiae DSM 100836	84,04	85,48	85,41	85,24	85,77	90,15	85,76	85,22	86,09	86,08	85,31	85,42	85,72	85,32	85,71	85,5	*	86,1	85,6	85,18

[T]																			
Levilactobacillus mulengensis 112-3 [T]	84,14	85,82	85,79	85,29	85,51	88,44	85,76	85,34	92,79	93,99	85,66	85,96	85,85	85,12	85,66	86,38	86,11	*	85,65	85,46
Levilactobacillus senmaizukei DSM 21775 = NBRC 103853 DSM 21775 [T]	85,01	85,59	85,5	84,72	85,3	86,9	85,49	84,69	85,19	85,41	85,35	85,54	85,03	87,57	85,57	85,61	85,59	85,65	*	85,9
M3R3	97,73	85,28	85,17	85	85,5	90,99	85,54	84,44	85,02	85,25	85,05	84,96	85,14	86,39	86,27	86,07	85,29	85,47	85,92	*

Table 3.8 - Digital DNA-DNA Hybridization (dDDH) values of strain M3R3 compared with other species, as calculated with Formula 2 (identities / HSP length).

Query genome	Subject strain	Reference genome	DDH	Model C.I.	Distance	Prob. DDH >= 70%	G+C difference
M3R3	*Levilactobacillus angrenensis* CCM 8893	GCA_042659575.1	21,7	[19.4 - 24.1%]	0,2024	0	4,61
M3R3	*Levilactobacillus andaensis* 866-3	GCA_016861695.1	21,9	[19.6 - 24.3%]	0,2002	0	3,23
M3R3	*Levilactobacillus koreensis* 26-25	GCA_001050435.1	21,2	[18.9 - 23.6%]	0,2072	0	3,3
M3R3	*Levilactobacillus lettrarii*	GCF_044053895	22,2	[19.9 - 24.6%]	0,1977	0	4,38
M3R3	*Levilactobacillus wangkuiensis*	GCF_016861605	21,9	[19.6 - 24.3%]	0,2005	0	4,42
M3R3	*Levilactobacillus yiduensis*	GCA_024718525	21,6	[19.4 - 24.1%]	0,2027	0	4,6
M3R3	*Levilactobacillus enshiensis*	GCA_007115095	21,4	[19.2 - 23.9%]	0,2047	0	1,95
M3R3	*Levilactobacillus tangyuanensis*	GCA_003946545	19,7	[17.5 - 22.1%]	0,2228	0	3,87
M3R3	*Levilactobacillus fuyuanensis*	GCA_003946395	22,3	[20 - 24.7%]	0,1969	0	2,92
M3R3	*Levilactobacillus tongjiangensis*	GCA_003946345	21,7	[19.5 - 24.2%]	0,202	0	1,8
M3R3	*Levilactobacillus cerevisiae*	GCA_003946245	22,2	[19.9 - 24.6%]	0,1975	0	3,63
M3R3	*Levilactobacillus mulengensis*	GCA_003946045	22,4	[20.1 - 24.8%]	0,1958	0	4,4

M3R3	*Levilactobacillus senmaizukei*	GCA_001592085	19,2	[17 - 21.6%]	0,2289	0	2,74
M3R3	*Levilactobacillus angrenensis* M1530-1	GCA_003946085.1	21,7	[19.5 - 24.2%]	0,2019	0	4,56
M3R3	*Levilactobacillus hammesii* DSM 16381	GCA_001434395.1	21,4	[19.1 - 23.8%]	0,2052	0	3,46
M3R3	*Levilactobacillus yonginensis* JCM 18023	GCA_003946265.1	21	[18.8 - 23.5%]	0,2088	0	1,92
M3R3	*Lentilactobacillus buchneri* ATCC 4005	GCA_018314255.1	29,3	[26.9 - 31.8%]	0,1461	0,08	1,5
M3R3	*Levilactobacillus brevis* DSM20054T	GCA_001433855.1	79,4	[76.4 - 82%]	0,0241	90,09	0,04
M3R3	*Levilactobacillus suantsaiihabitans*	GCF_004745505	21,3	[19.1 - 23.8%]	0,2057	0	5,87

3.3.5 Comparative genomics

The genome of strain M3R3 was compared with 174 publicly available *L. brevis* genomes deposited in the NCBI database. These genomes were categorized according to four major isolation sources: alcohol fermentation (25 strains, 14.4%), animal/human gut (38 strains, 21.8%), dairy products (35 strains, 20.1%), and fermented vegetables (64 strains, 36.8%). The remaining 6.9% were unknown. The resulting phylogenetic tree revealed the presence of three distinct *L. brevis* lineages, designated as cluster A, B, and C (**Figure 3.8**). Although the clustering of strains did not perfectly correlate with their isolation sources, strains from alcoholic fermentation and from animal/human gut were mainly associated with cluster A. In contrast, the majority of strains isolated from dairy products (85.7%) and fermented vegetables (56.9%) were grouped in cluster B, which included also strain M3R3, whereas cluster C comprised a small number of strains with diverse origins. These findings supported a high degree of genomic diversity and potential functional adaptation within the species and are consistent with previous studies describing *L. brevis* as a genetically diverse species possessing a remarkably large pan-genome (Feyereisen et al., 2019; Fraunhofer et al., 2019).

A comparative genome analysis was carried out on a subset of 10 strains representative of the three distinct clusters previously described. The pan-genome comprised 4,288 COGs, with 36.3% classified as core genes and 32.9% as strain-specific genes. Non-essential genes, defined as those absent in at least one strain, accounted for 30.8% (**Figure 3.9A** and **Figure 3.9B**). Together with the strain-

specific genes, these constituted the accessory genome. These findings are consistent with the high plasticity of the *L. brevis* genome, which tends to adapt its features depending on the environment (Feyereisen et al., 2019; Fraunhofer et al., 2019). This is also reflected in the relatively low percentage of core genes shared among the ten *L. brevis* strains, which falls below 50%.

The distribution of strain-specific clusters revealed that strain M3R3 differed from other *L. brevis* strains in the number of singleton genes. Specifically, 63 genes were uniquely found in the M3R3 genome. Among all strains, *L. brevis* TMW 1.2113 had the highest number of unique genes (114), whereas the NTC13768 genome had the fewest, with only 1 singleton (**Figure 3.9C**). Based on KEGG Orthology (KO) annotation, the singletons of strain M3R3 were predominantly classified as hypothetical proteins (93.65%), with only four genes assigned to functional categories, including genetic information processing, signaling and cellular processes, carbohydrate metabolism, and genetic information processing (**Figure 3.9C**).

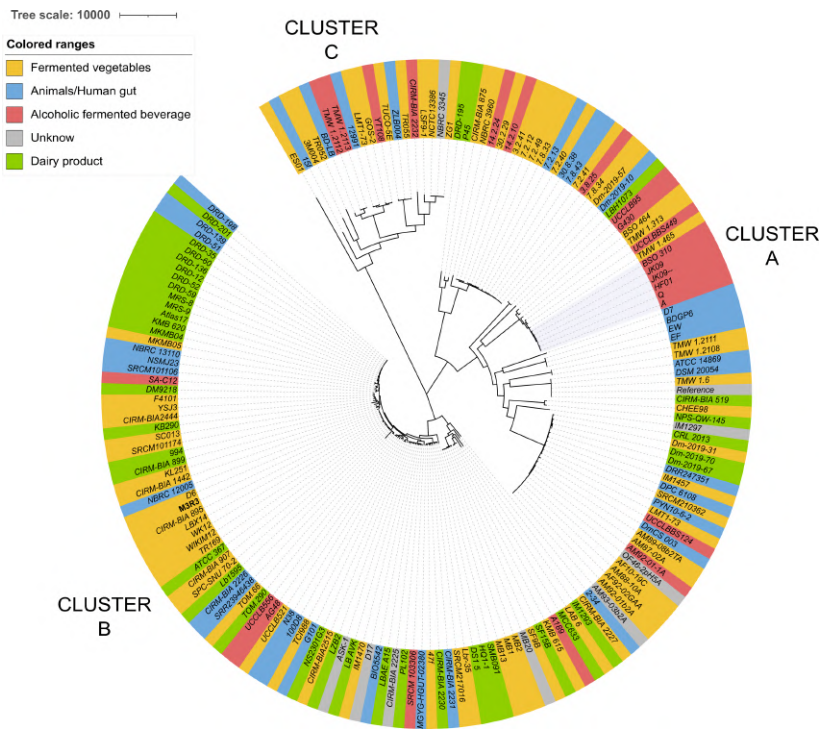

Figure 3.8 - Maximum-likelihood phylogenetic tree of 175 *Levilactobacillus brevis* strains built on core SNP alignments (3059 SNP found with snippy multi v4.6.0). Branch colors indicate isolation sources: yellow, fermented vegetables; light blue, animal and human gut; red, alcoholic fermented beverages; green, dairy products; grey, unknown, respectively. Clusters A, B, and C are indicated. The tree was visualized using iTOL v7 (Letunic & Bork, 2019).

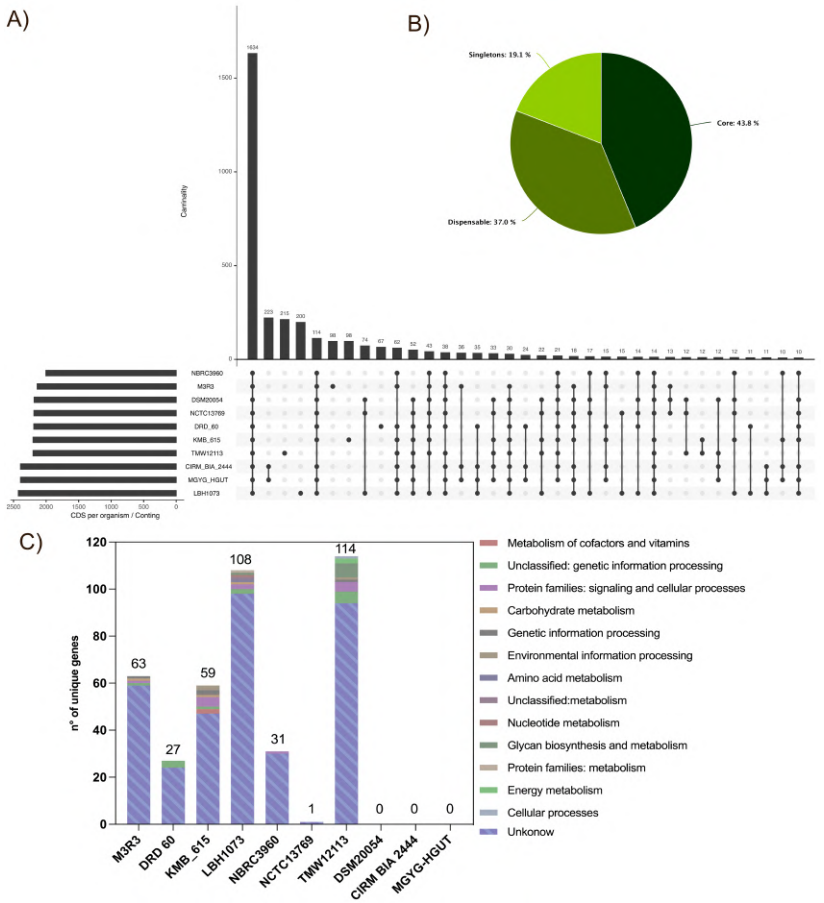

Figure 3.9 - Comparative genomic analysis of *Levilactobacillus brevis* M3R3 and nine conspecific strains. (A) Upset plot showing shared orthogroups of *L. brevis* strains (n=10). (B) Percentage distribution of core, dispensable, singleton genes. (C) KEGG Orthology (KO) annotation of singletons across the ten *L. brevis* genomes.

3.3.6 Biosafety Assessment and genome stability evaluation

CARD and ARMFinder analyses did not reveal any ARGs, indicating that strain M3R3 can be considered safe in relation to the potential dissemination of antibiotic resistances. In contrast, ResFinder analysis identified the *ClpL* gene as a potential antimicrobial resistance gene (**Table 3.9**). However, in *Lactobacillaceae* family, this gene encodes an ATP-dependent Clp protease with chaperone activity which is involved in degrading misfolded or damaged intracellular proteins (Frees et al., 2007). Clp is inducible under acidic shock (Wall et al., 2007) and contributes to the fast response of lactobacilli to harsh gastro-intestinal conditions, especially to acid and bile stresses (Frees et al., 2007).

Search for pathogenic genes did not find any candidates, except for the *WalR* gene, which a member of one of the two-component systems involved in sensing and reacting to environmental changes (**Table 3.9**). The *walR* regulates cell wall metabolism, ensuring structural integrity and adaptability in harsh environments such as the gastrointestinal tract (Duru et al., 2021). The M3R3 genome displayed the *WalK* gene upstream to *WalR*, suggesting that the two-component system is complete. The same two-components system was found in a *L. brevis* GABA-producing probiotic candidate (Matta et al., 2025). According to its safe status, the associated PPRS, calculated by ProbioMin was 1.00 for strain M3R3 (low risk) (**Table 3.9**).

Three prophage regions were identified in the M3R3 genome, one belonging to *Siphoviridae* and the other two belonging to *Myoviridae* family (**Table 3.10**). *Siphoviridae* and *Myoviridae* are prophages frequently detected in *L. brevis* genomes (Feyereisen et al., 2019). Furthermore, the genome of strain M3R3 accounted for 140

mobile elements, most of them were associated with integration/excision (47) and replication/recombination/repair (44) (**Figure 3.10**).

Table 3.9 - Biosafety evaluations implemented in ProbioMinServer.

ResFinder

Resistance gene	Identity	Coverage	Phenotype	Accession no.
ClpL	98.35	00.00	Disinfectant resistance	CP023753

AMRFinder

Gene symbol	Sequence name	Method	Identity	Coverage	Accession no.
No hit found					

VFDB

Gene ID	Gene name	Identity	Coverage	e-value	VF name	F category	Accession no.
No hit found							

Vfinder

Database	Virulence factor	Identity	Coverage	Protein function	Accession no.
No hit found					

PG

Protein ID	Gene name	Identity	Coverage	e-value	Function	Gene ID
S4E4Q5	WalR	80.77	99.15	1.49e-139	Transcriptional regulatory protein	EPH95667

ARGs (CARD)	VFs (VFDB)	PGs (PHI-base)	PPRS
0	0	1	1.00

Table 3.10 - Putative prophage regions predicted in *Levilactobacillus brevis* M3R3 using Phigaro.

Conting	Begin	End	Transposable	Taxonomy	pVOGs
C00000001	190907	205892	False	*Siphoviridae*	VOG10391, VOG0275, VOG0801, VOG0774, VOG8483, VOG0862, VOG8520, VOG1656, VOG4552, VOG3015, VOG0650, VOG6495, VOG0685, VOG0322, VOG0226, VOG4799, VOG0025

C00000001	208328	238846	False	*Myoviridae*	VOG1298, VOG4010, VOG0198, VOG5446, VOG0796, VOG0275, VOG4544, VOG0720, VOG4564, VOG4555, VOG3434, VOG1887, VOG4710, VOG1353, VOG1881, VOG1883, VOG1352, VOG4699, VOG5706, VOG4910, VOG1956, VOG1433, VOG1348, VOG0573, VOG4691, VOG4845, VOG1857, VOG3298
C00000002	182447	217534	False	PV902533	VOG1309, VOG0186, VOG7236, VOG4693, VOG6005, VOG0044, VOG4010, VOG0198, VOG0796, VOG10227, VOG1912, VOG4564, VOG4865, VOG1915, VOG2779, VOG1942, VOG4778, VOG1353, VOG1881, VOG1883, VOG1352, VOG4699, VOG6131, VOG5068, VOG6163, VOG1956, VOG1433, VOG1348, VOG0573, VOG4550, VOG4691, VOG4845, VOG4894, VOG0565, VOG3298

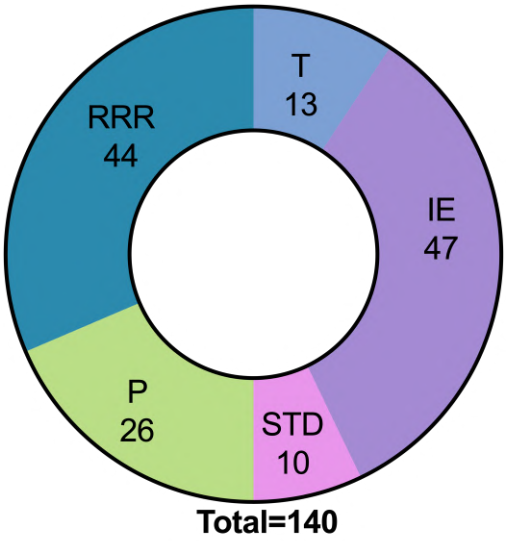

Figure 3.10 - Distribution of mobile genetic elements in *Levilactobacillus brevis* M3R3 genome. Major categories considered were IE, integration/excision; RRR, replication/recombination/repair; P, phage; STD, stability/transfer/defense; and T, transfer.

3.3.7 Search for probiotic-related functional traits

AntiSMASH analysis revealed that the genome of strain M3R3 contained four BGCs encoding lanthipeptide class IV, Type III polyketide synthase (T3PKS), a ribosomally synthesized, post-translationally modified peptide (RiPP-like compound), and terpen precursors (**Figure 3.11**). Three of them matched with experimentally validated BGCs present in MIBiG 2.0 repository (**Table 3.11**). All the BGCs were predicted to encode antimicrobials or enzymes involved in the synthesis of antimicrobials. In detail, class IV lanthipeptides are characterized by multiple lanthionine rings and exert strong

antimicrobial activity against several Gram-positive bacteria, including *Streptococcus* spp., *Clostridium difficile*, and *Bacillus* spp. (Han, 2024; Travin et al., 2020). RiPPs encompass a broad category of natural products derived from ribosomal synthesis followed by enzymatic modifications. The detection of RiPP-like regions suggests the presence of additional pathways for producing bioactive peptides that could function as antimicrobials or signaling molecules (**Figure 3.11**). Type III polyketide synthases (T3PKS) are involved in the biosynthesis of polyketides, which are secondary metabolites with diverse biological activities, including antimicrobial, antifungal, and anticancer properties (Dicks & Vermeulen, 2022). Lactobacilli-derived terpenes have been recently demonstrated to inhibit efflux pumps in drug-resistant pathogens (Nair et al., 2025).

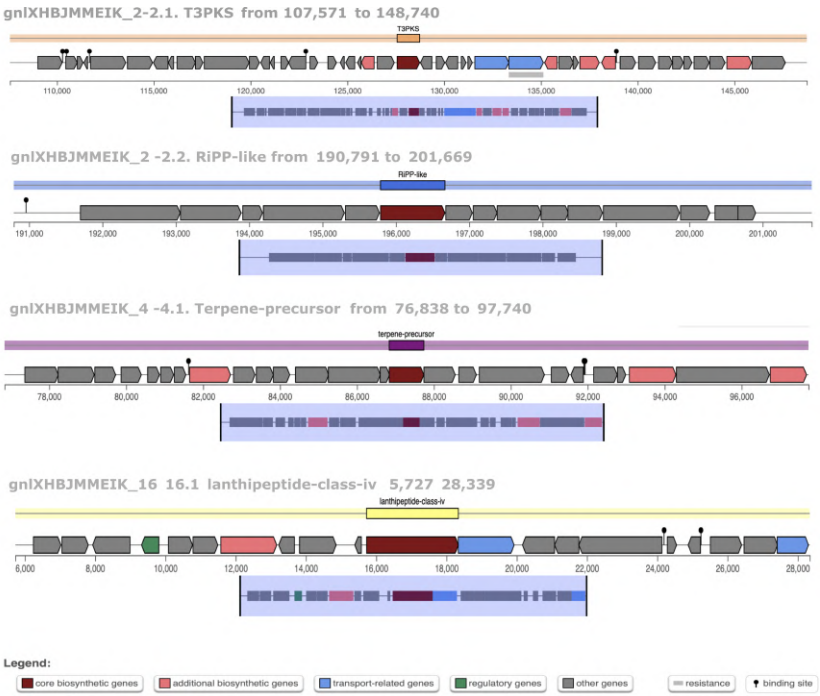

Figure 3.11 - Biosynthetic gene clusters (BGCs) in the genome of *Levilactobacillus brevis* M3R3 predicted by antiSMASH. Candidate clusters were stringently filtered and grouped into families. Arrows are color-coded according to the enzyme family of the predicted product, with gene annotations shown below each arrow. One candidate cluster overlapped with or showed similarity to ribosomally synthesized and post-translationally modified peptide (RiPP) BGCs. Representative clusters included a type III polyketide synthase (T3PKS) region, a terpene precursor region, and a class IV lanthipeptide cluster.

Table 3.11 - Prediction of metabolite biosynthetic gene clusters (BGCs) carried out in *Levilactobacillus brevis* M3R3 with antiSMASH.

Tools	Contig	Region	Type	from	to	Reference	Similarity score	Type	Compound(s)	Organism
antiSMAH	gnlXHBJMMEIK_2	2,1	T3PKS	107.571	148.740	BGC0000558.5	0,42	ribosomal	sublancin 168	*Bacillus subtilis* subsp. *subtilis* str. 168
						BGC0002306.2	0,42	ribosomal	freyrasin	*Paenibacillus polymyxa* ATCC 842
antiSMAH	gnlXHBJMMEIK_2	2,2	RiPP-like	190.791	201.669	No matches found.				
antiSMAH	gnlXHBJMMEIK_4	4,1	terpene-precursor	76.838	97.740	BGC0002397.2	0,47	terpene	astallatene	*Arabidopsis thaliana*
						BGC0002400.2	0,44	terpene	boleracene	*Brassica oleracea var. oleracea*
antiSMAH	gnlXHBJMMEIK_16	16,1	lanthipeptide-class-iv	5.727	28.339	BGC0000501.3	0,48	ribosomal	catenulipeptin	*Catenulispora acidiphila* DSM 44928
						BGC0002698.2	0,44	ribosomal	phaeornamide	*Pseudophaeobacter arcticus* DSM 23566

3.3.8 Identification of bsh gene candidates and RT-PCR assay

To identify putative *bsh* genes responsible for the previously observed BSs-deconjugation activity, the genome sequence of strain M3R3 was screened for linear amide C-N hydrolase proteins that encompass choloylglycine hydrolase (conjugated bile acid hydrolase, CBAH, EC:3.5.1.24), penicillin acylase (EC:3.5.1.11) and acid ceramidase (EC:3.5.1.23). The analysis identified 3 putative candidates, classified as *bsh_1A* (984 nt; 327 amino acids), *bsh_2A*, (978 nt; 325 amino acids), and *bsh_3A* (957 bp; 318 amino acids). BLASTp search against RefSeq NCBI protein database revealed that the deduced amino acid protein of *bsh_1A* was 100% identical to the choloylglycine hydrolase family protein WP_011668641.1, which displayed the Ntn_PVA domain (cd00542), described as Penicillin V acylase (PVA) (*E*-value: 5.13e-138). The amino acid sequences of *bsh_2A* and *bsh_3A* genes were 100% identical to the linear amide C-N hydrolases WP_011668417.1 and WP_011668908.1, respectively. These proteins possessed the conserve nnt_hydrolase domain (cI00467), which is present in the diverse superfamily of NtN hydrolases (*E*-value: 4.26e-71).

BSH and PVA are evolutionary related enzymes with high similarity in terms of the amino acid residues involved in their active site (Daly et al., 2021; O'Flaherty et al., 2018). This similarity makes it challenging to distinguish between the two proteins. The role of BSH in deconjugation of BSs is well established, whereas PVA appears to be involved in the degradation of penicillin-class antibiotics (Kusada et al., 2022). To further investigate whether the candidate

genes found in M3R3 genome were truly *bsh* genes, the putative BSH proteins of M3R3 were aligned against 76 *L. brevis* RefSeq proteins annotated as amide C-N hydrolases in the NCBI database using the COBALT alignment tool. Seven representative PVA proteins and one representative BSH protein from *L. plantarum* WCFS1 (*bsh1*) were also included as controls. Based on the topology of the tree, the amide C-N hydrolases of *L. brevis* grouped into three distinct clusters, classified as I, II, and III (**Figure 3.12**). Cluster I included 16 Protein IDs with an average length of 335.2 aa ± 29.4; cluster II included 29 Protein IDs (average length 325 ± 1.4 aa); and cluster III consisted of 31 Protein IDs with an average length of 316.8 ± 6.8 aa. These results were consistent with previous studies with demonstrated that putative *L. brevis bsh* genes clustered into three distinct phylotypes (Liand &Lv, 2018). Notable, the majority of PVAs placed outside the clusters at the intersection between cluster I and cluster II. The putative BSH proteins identified in M3R3 genome were distributed differently across the clusters: bsh_2A and bsh_3A are located into the cluster II and III, respectively, whereas bsh_1A clustered away from other *bsh* genes and was closely related to PVAs (**Figure 3.12**). Based on these findings, we concluded that the genome of *L. brevis* M3R3 possesses two *bsh* genes, namely *bsh_2A* and *bsh_3A*, and one putative PVA-encoding gene (previously referred to as *bsh_1A*, now re-called *pva*). Remarkably, no genes encoding BSH proteins from cluster I were found in the M3R3 genome.

To evaluate whether strain M3R3 modulates the expression of these genes in response to BSs mixture, we performed a RT-PCR assay targeting *pva*, *bsh_2A* and *bsh_3A*. As shown in (**Figure 3.13**), strain M3R3 actively transcribed all three target genes under both BSs

stress and control conditions at stationary phase. These findings suggest that the genes are actively transcribed at the stage where the BSH activity has been evaluated and that the genes may be constitutively expressed or, alternatively, that their transcriptional regulation occurs at growth phases other than the stationary phase examined in this study. This result is also consistent with previous works indicating that exposure to bile does not necessarily induce *bsh* gene expression in BSH-active lactobacilli strains (Foley et al., 2021; Pfeiler et al., 2007). Nevertheless, expanding the sampling strategy to earlier growth phases, particularly the early and the mid-exponential stages, would provide a more comprehensive understanding of *bsh* genes regulation in response to BSs-induced stress in strain M3R3. Furthermore, N-terminal autocatalysis and oligomeric assembly in homotetramers are critical post-translational modifications to ensure active BSH enzyme (Dong & Lee, 2018). Therefore, analysis of protein patterns will be also necessary to definitively link one or more of these three genes to the observed BSH activity in M3R3.

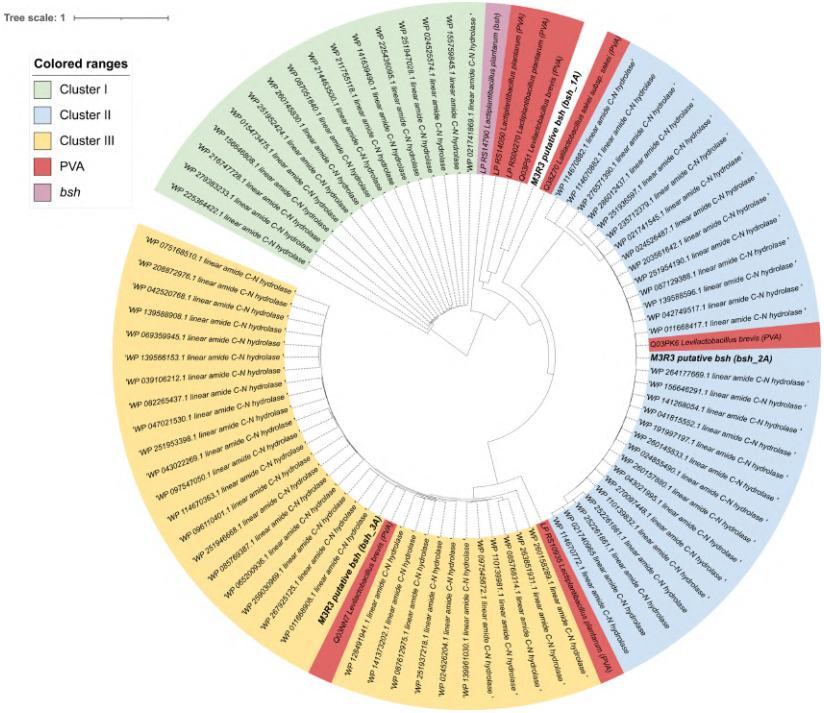

Figure 3.12 - Fast minimum evolution tree of 79 putative linear amide C-N hydrolase proteins from *Levilacactobacillus brevis*. Seventy-six linear amide C-N hydrolase proteins of *L. brevis* were retrieved from, whereas three linear amide C-N hydrolase proteins (in bold) were found in *L. brevis* M3R3 genome. Seven PVA (red) and one BSH (purple) proteins were used as control. Sequences were aligned using the COBALT tool with default parameters, while Grishin model was used to infer evolutionary distances. Labels represent protein ID. Clusters I, II, and III are depicted in green, blue, and yellow, respectively. The image was created using the interactive tree of life (iTOL) (Letunic & Bork, 2019).

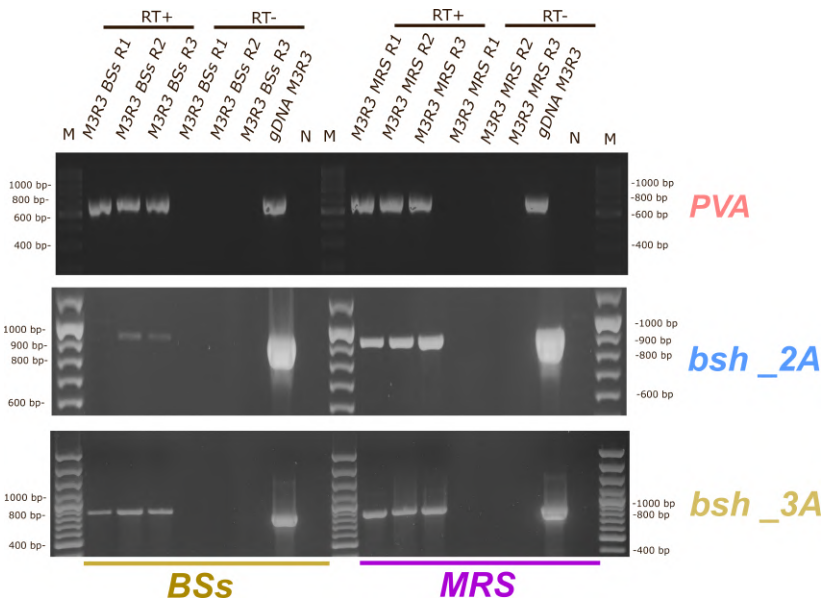

Figure 3.13 - RT-PCR assay targeting the *pva*, *bsh_2A*, and *bsh_3A* genes in *Levilactobacillus brevis* M3R3 strain cells grown on MRS medium supplemented with 1% (*w/v*) BSs mixtures. MRS medium without any supplementation was used as control. The figure depicts amplified cDNAs, gDNA amplification was used as a positive PCR control. Abbreviations—M: molecular weight marker; N: negative control.

3.3.9 Antibiotic susceptibility

Recently, PVA enzymes have been widely used in pharmaceutics to produce the 6-aminopenicillanic acid (6-APA), a key intermediate in the synthesis of semi-synthetic antibiotics (Pan et al., 2022). Therefore, the presence of PVA in M3R3 could be considered a relevant genetic trait for future biotechnological applications. Although, PVA may also hydrolyze PenV, conferring resistance to

this antibiotic (Kusada et al., 2022). To exclude that this gene can contribute to PenV antibiotic resistance, strain M3R3 was subjected to antibiotic susceptibility test against PenV. Strain M3R3 showed a MIC < 0.25 µg/mL. According to the EFSA breakpoints for obligately heterofermentative lactobacilli, this value indicates that the strain is sensible to PenV.

3.4 Conclusion

BSH-active probiotics are increasingly recognized as valuable tools to modulate BSH activity in the human gut and promote host health. Studies in animal models showed that increasing BSH activity in the gut ecosystem can result to lower body weight gain, lower adiposity and reduction of both circulating Low Density Lipoprotein (LDL) cholesterol and triglycerides (Dong et al., 2025). A recent study reported that non-obese liver fibrotic individuals displayed a significantly lower copy number of BSH encoding genes in their gut microbiome (Lee et al., 2020). In the present study, the probiotic candidate M3R3 strain, ascribed to the *L. brevis* species, demonstrated a robust tolerance to BSs, with a stronger adaptive response when exposed to a BSs mixture and to the individual BSs. Remarkably, the strain M3R3showed a consistent capacity to deconjugate BSs, with a marked preference for glyco-conjugated forms, which are known to exert higher cytotoxicity. Whole-genome analysis and comparative genomics identified two *bsh* genes, *bsh2*_A and *bsh3_A*, which are actively transcribed under BSs stress and are likely responsible for the observed deconjugation activity of *L. brevis* M3R3. Although a *pva* gene was also detected, it did not confer resistance to PenV. The absence of ARGs and virulence determinants further support the safe

profile for probiotic use of *L. brevis* strain M3R3. Additionally, the presence of BGCs with antimicrobial activity further emphasizes the potential of M3R3 as a multifunctional probiotic candidate.

Collectively, these findings underscore the relevance of *L. brevis* M3R3 as BSH-active, bile tolerant and genomically safe strain, with potential applications as probiotic supplement aimed at supporting lipid homeostasis and gut health. This study also reinforces the emerging role of non-intestinal lactobacilli in targeted modulation of the bile acid pool and cholesterol homeostasis.

This work was conducted in collaboration with the University of Modena and Reggio Emilia, under the supervision of Professors Lisa Solieri and Davide Tagliazucchi, with the contribution of Dr. Marianna Cristofolini and Alice Cattivelli, during a research and training period within the doctoral project at the Department of Life Sciences.

Author contributions

G.A: Data curation, Methodology, Writing—original draft preparation, Writing—review and editing. M.C.: Data curation, Software, Writing—original draft preparation, Writing—review and editing. M.A.R.: Data curation. A.C.: Data curation, Writing—review and editing. D.T.: Data curation, Methodology, Investigation, Writing—review and editing. C.C: Investigation, Supervision, Writing—review and editing. L.S.: Data curation, Funding, Investigation, Supervision, Writing—review and editing. C.L.R.: Data curation, Investigation, Supervision, Writing—review and editing.

Funding

The project was founded by FAR2024 (University of Modena and Reggio Emilia) and by the NRRP, Mission 4 Component 2 Investment 1.4 – Call for tender No. 3138 of 16 December 2021, rectified by Decree n. 3175 of 18 December 2021 of the Italian Ministry of University and Research funded by the European Union – NextGenerationEU. Project Code CN_00000033, Concession Decree No. 1034 of 17 June 2022 adopted by the Italian Ministry of University and Research, CUP E93C22001090001, "National Biodiversity 648 Future Center – NBFC''.

Data availability

Sequence data that support the findings of this study have been deposited in the GenBank database with the accession codes PV902533 and 651 PRJNA1293146.

Conflict of interest

The authors Cinzia Caggia and Cinzia Randazzo are founders of ProBioEtna, a Spin off of the University of Catania. They have two affiliations, but the employer is the University of Catania. The remaining authors declare that the research was conducted in the absence of any

commercial or financial relationship that could be construed as a potential conflict of interest.

References

1. Agolino, G., Cristofolini, M., Vaccalluzzo, A., Tagliazucchi, D., Cattivelli, A., Pino, A., Caggia, C., Solieri, L., & Randazzo, C. L. (2025). Genome Mining and Characterization of Two Novel *Lacticaseibacillus rhamnosus* Probiotic Candidates with Bile Salt Hydrolase Activity. *Biomolecules*, *15*(1), 86. https://doi.org/10.3390/biom15010086.
2. Agolino, G., Pino, A., Vaccalluzzo, A., Cristofolini, M., Solieri, L., Caggia, C., & Randazzo, C. L. (2024). Bile salt hydrolase: The complexity behind its mechanism in relation to lowering-cholesterol lactobacilli probiotics. *Journal of Functional Foods*, *120*, 106357. https://doi.org/10.1016/j.jff.2024.106357.
3. Alcock, B. P., Huynh, W., Chalil, R., Smith, K. W., Raphenya, A. R., Wlodarski, M. A., Edalatmand, A., Petkau, A., Syed, S. A., Tsang, K. K., Baker, S. J. C., Dave, M., McCarthy, M. C., Mukiri, K. M., Nasir, J. A., Golbon, B., Imtiaz, H., Jiang, X., Kaur, K., Kwong, M., Liang, X., Niu, K. C., Shan, P., Yang, J. Y. J., Gray, K. L., Hoad, G. R., Jia, B., Bhando, T., Carfrae, L. A., Farha, M. A., French, S., Gordevich, R., Rachwalski, K., Tu, M. M., Bordeleau, E., Dooley, D., Griffiths, E., Zubyk, H. L., Brown, E. D., Maguire, F., Beiko, R. G., Hsiao, W. W. L., Brinkman, F. S. L., Van Domselaar, G., & McArthur, A. G. (2023). CARD 2023: expanded curation, support for machine learning, and resistome prediction at the Comprehensive Antibiotic Resistance Database. *Nucleic acids research*, *51*(D1), D690–D699. https://doi.org/10.1093/nar/gkac920.
4. Alizadeh Behbahani, B. A., Jooyandeh, H., Hojjati, M., & Sheikhjan, M. G. (2024). Evaluation of probiotic, safety, and anti-pathogenic properties of *Levilactobacillus brevis* HL6, and its potential application as bio-preservatives in peach juice. *Lwt*, *191*, 115601. https://doi.org/10.1016/j.lwt.2024.116391.

5. Bai, Z., Zhang, N., Jin, Y., Chen, L., Mao, Y., Sun, L., Fang, F., Liu, Y., Han, M., & Li, G. (2023). Comprehensive analysis of 84 *Faecalibacterium prausnitzii* strains uncovers their genetic diversity, functional characteristics, and potential risks. *Frontiers in cellular and infection microbiology*, *12*, 919701. https://doi.org/10.3389/fcimb.2022.919701.
6. Begley, M., Hill, C., & Gahan, C. G. (2006). Bile salt hydrolase activity in probiotics. *Applied and environmental microbiology*, *72*(3), 1729–1738. https://doi.org/10.1128/AEM.72.3.1729-1738.2006.
7. Blanco-Míguez, A., Beghini, F., Cumbo, F., McIver, L. J., Thompson, K. N., Zolfo, M., Manghi, P., Dubois, L., Huang, K. D., Thomas, A. M., Nickols, W. A., Piccinno, G., Piperni, E., Punčochář, M., Valles-Colomer, M., Tett, A., Giordano, F., Davies, R., Wolf, J., Berry, S. E., … Segata, N. (2023). Extending and improving metagenomic taxonomic profiling with uncharacterized species using MetaPhlAn 4. *Nature biotechnology*, *41*(11), 1633–1644. https://doi.org/10.1038/s41587-023-01688-w.
8. Bortolaia, V., Kaas, R. S., Ruppe, E., Roberts, M. C., Schwarz, S., Cattoir, V., Philippon, A., Allesoe, R. L., Rebelo, A. R., Florensa, A. F., Fagelhauer, L., Chakraborty, T., Neumann, B., Werner, G., Bender, J. K., Stingl, K., Nguyen, M., Coppens, J., Xavier, B. B., Malhotra-Kumar, S., West, H., Pinholt, M., Anjum, M., F., Dugget, N. A., Kempf, I., Nykäsenoja, S., Olkkola, S., Wieczorek, K., Amaro, A., Clemente, L., Mossong, J., Losch, S., Ragimbeau, C., Lund, O., & Aarestrup, F. M. (2020). ResFinder 4.0 for predictions of phenotypes from genotypes. *The Journal of antimicrobial chemotherapy*, *75*(12), 3491–3500. https://doi.org/10.1093/jac/dkaa345.
9. Bustos, A. Y., Font de Valdez, G., Fadda, S., & Taranto, M. P. (2018). New insights into bacterial bile resistance mechanisms: the role of bile salt hydrolase and its impact on human health. *Food research international (Ottawa, Ont.)*, *112*, 250–262. https://doi.org/10.1016/j.foodres.2018.06.035.
10. Brown, C. L., Mullet, J., Hindi, F., Stoll, J. E., Gupta, S., Choi, M., Keenum, I., Vikesland, P., Pruden, A., & Zhang, L. (2022). mobileOG-db: a Manually Curated Database of Protein Families Mediating the Life

Cycle of Bacterial Mobile Genetic Elements. *Applied and environmental microbiology*, *88*(18), e0099122. https://doi.org/10.1128/aem.00991-22.

11. Cantalapiedra, C. P., Hernández-Plaza, A., Letunic, I., Bork, P., & Huerta-Cepas, J. (2021). eggNOG-mapper v2: Functional Annotation, Orthology Assignments, and Domain Prediction at the Metagenomic Scale. *Molecular biology and evolution*, *38*(12), 5825–5829. https://doi.org/10.1093/molbev/msab293.
12. Carattoli, A., & Hasman, H. (2020). PlasmidFinder and In Silico pMLST: Identification and Typing of Plasmid Replicons in Whole-Genome Sequencing (WGS). *Methods in molecular biology (Clifton, N.J.)*, *2075*, 285–294. https://doi.org/10.1007/978-1-4939-9877-7_20.
13. Chen S. (2023). Ultrafast one-pass FASTQ data preprocessing, quality control, and deduplication using fastp. *iMeta*, *2*(2), e107. https://doi.org/10.1002/imt2.107.
14. Choi, S. B., Lew, L. C., Yeo, S. K., Nair Parvathy, S., & Liong, M. T. (2015). Probiotics and the BSH-related cholesterol lowering mechanism: a Jekyll and Hyde scenario. *Critical reviews in biotechnology*, *35*(3), 392–401. https://doi.org/10.3109/07388551.2014.889077.
15. Couvin, D., Bernheim, A., Toffano-Nioche, C., Touchon, M., Michalik, J., Néron, B., Rocha, E. P. C., Vergnaud, G., Gautheret, D., & Pourcel, C. (2018). CRISPRCasFinder, an update of CRISRFinder, includes a portable version, enhanced performance and integrates search for Cas proteins. *Nucleic acids research*, *46*(W1), W246–W251. https://doi.org/10.1093/nar/gky425
16. Croucher, N. J., Page, A. J., Connor, T. R., Delaney, A. J., Keane, J. A., Bentley, S. D., Parkhill, J., & Harris, S. R. (2015). Rapid phylogenetic analysis of large samples of recombinant bacterial whole genome sequences using Gubbins. *Nucleic acids research*, *43*(3), e15. https://doi.org/10.1093/nar/gku1196.
17. Daly, J. W., Keely, S. J., & Gahan, C. G. M. (2021). Functional and Phylogenetic Diversity of BSH and PVA Enzymes. *Microorganisms*, *9*(4), 732. https://doi.org/10.3390/microorganisms9040732.
18. da Silva, T. F., Glória, R. A., Americo, M. F., Freitas, A. D. S., de Jesus, L. C. L., Barroso, F. A. L., Laguna, J. G., Coelho-Rocha, N. D., Tavares, L. M., le Loir, Y., Jan, G., Guédon, É., & Azevedo, V. A. C. (2024).

Unlocking the Potential of Probiotics: A Comprehensive Review on Research, Production, and Regulation of Probiotics. *Probiotics and antimicrobial proteins*, *16*(5), 1687–1723. https://doi.org/10.1007/s12602-024-10247-x.

19. Dempsey, E., & Corr, S. C. (2022). Lactobacillus spp. for Gastrointestinal Health: Current and Future Perspectives. *Frontiers in immunology*, *13*, 840245. https://doi.org/10.3389/fimmu.2022.840245.
20. Dicks, L. M. T., & Vermeulen, W. (2022). Do Bacteria Provide an Alternative to Cancer Treatment and What Role Does Lactic Acid Bacteria Play?. *Microorganisms*, *10*(9), 1733. https://doi.org/10.3390/microorganisms10091733.
21. Dieckmann, M. A., Beyvers, S., Nkouamedjo-Fankep, R. C., Hanel, P. H. G., Jelonek, L., Blom, J., & Goesmann, A. (2021). EDGAR3.0: comparative genomics and phylogenomics on a scalable infrastructure. *Nucleic acids research*, *49*(W1), W185–W192. https://doi.org/10.1093/nar/gkab341.
22. Dong, Z., & Lee, B. H. (2018). Bile salt hydrolases: Structure and function, substrate preference, and inhibitor development. *Protein science : a publication of the Protein Society*, *27*(10), 1742–1754. https://doi.org/10.1002/pro.3484.
23. Dong, Z., Yang, S., Tang, C., Li, D., Kan, Y., & Yao, L. (2025). New insights into microbial bile salt hydrolases: from physiological roles to potential applications. *Frontiers in microbiology*, *16*, 1513541. https://doi.org/10.3389/fmicb.2025.1513541.
24. Du, R., Yu, L., Yu, N., Ping, W., Song, G., & Ge, J. (2022). Characterization of exopolysaccharide produced by Levilactobacillus brevis HDE-9 and evaluation of its potential use in dairy products. *International journal of biological macromolecules*, *217*, 303–311. https://doi.org/10.1016/j.ijbiomac.2022.07.057.
25. Duru, I. C., Ylinen, A., Belanov, S., Pulido, A. A., Paulin, L., & Auvinen, P. (2021). Transcriptomic time-series analysis of cold- and heat-shock response in psychrotrophic lactic acid bacteria. *BMC genomics*, *22*(1), 28. https://doi.org/10.1186/s12864-020-07338-8.
26. EFSA Panel on Additives and Products or Substances used in Animal Feed (FEEDAP), Bampidis, V., Azimonti, G., Bastos, M. L.,

Christensen, H., Dusemund, B., Fašmon Durjava, M., Kouba, M., López-Alonso, M., López Puente, S., Marcon, F., Mayo, B., Pechová, A., Petkova, M., Ramos, F., Sanz, Y., Villa, R. E., Woutersen, R., Brozzi, R., Galobart, J., Gregoretti, L., López-Gálvez, G., Innocenti, M. L., & Vettori, M. V. (2021). Safety and efficacy of a feed additive consisting of acetic acid for all animal species. *EFSA journal. European Food Safety Authority*, *19*(6), e06615. https://doi.org/10.2903/j.efsa.2021.6615.

27. EFSA Panel on Additives and Products or Substances used in Animal Feed (FEEDAP), Rychen, G., Aquilina, G., Azimonti, G., Bampidis, V., Bastos, M. L., Bories, G., Chesson, A., Cocconcelli, P. S., Flachowsky, G., Gropp, J., Kolar, B., Kouba, M., López-Alonso, M., López Puente, S., Mantovani, A., Mayo, B., Ramos, F., Saarela, M., Villa, R. E., … Galobart, J. (2018). Guidance on the characterisation of microorganisms used as feed additives or as production organisms. *EFSA journal. European Food Safety Authority*, *16*(3), e05206. https://doi.org/10.2903/j.efsa.2018.5206.
28. Feldgarden, M., Brover, V., Gonzalez-Escalona, N., Frye, J. G., Haendiges, J., Haft, D. H., Hoffmann, M., Pettengill, J. B., Prasad, A. B., Tillman, G. E., Tyson, G. H., & Klimke, W. (2021). AMRFinderPlus and the Reference Gene Catalog facilitate examination of the genomic links among antimicrobial resistance, stress response, and virulence. *Scientific reports*, *11*(1), 12728. https://doi.org/10.1038/s41598-021-91456-0.
29. Feyereisen, M., Mahony, J., Kelleher, P., Roberts, R. J., O'Sullivan, T., Geertman, J. A., & van Sinderen, D. (2019). Comparative genome analysis of the *Lactobacillus brevis* species. *BMC genomics*, *20*(1), 416. https://doi.org/10.1186/s12864-019-5783-1.
30. Foley, M. H., O'Flaherty, S., Allen, G., Rivera, A. J., Stewart, A. K., Barrangou, R., & Theriot, C. M. (2021). *Lactobacillus* bile salt hydrolase substrate specificity governs bacterial fitness and host colonization. *Proceedings of the National Academy of Sciences of the United States of America*, *118*(6), e2017709118. https://doi.org/10.1073/pnas.2017709118.
31. Fraunhofer, M. E., Geißler, A. J., Behr, J., & Vogel, R. F. (2019). Comparative Genomics of Lactobacillus brevis Reveals a Significant

Plasmidome Overlap of Brewery and Insect Isolates. *Current microbiology*, *76*(1), 37–47. https://doi.org/10.1007/s00284-018-1581-2.

32. Frees, D., Savijoki, K., Varmanen, P., & Ingmer, H. (2007). Clp ATPases and ClpP proteolytic complexes regulate vital biological processes in low GC, Gram-positive bacteria. *Molecular microbiology*, *63*(5), 1285–1295. https://doi.org/10.1111/j.1365-2958.2007.05598.x85–1295.
33. Gänzle, M. G., & Zheng, J. (2019). Lifestyles of sourdough lactobacilli - Do they matter for microbial ecology and bread quality?. *International journal of food microbiology*, *302*, 15–23. https://doi.org/10.1016/j.ijfoodmicro.2018.08.019.
34. Goris, J., Konstantinidis, K. T., Klappenbach, J. A., Coenye, T., Vandamme, P., & Tiedje, J. M. (2007). DNA-DNA hybridization values and their relationship to whole-genome sequence similarities. *International journal of systematic and evolutionary microbiology*, *57*(Pt 1), 81–91. https://doi.org/10.1099/ijs.0.64483-0.
35. Grant, J. R., Enns, E., Marinier, E., Mandal, A., Herman, E. K., Chen, C. Y., Graham, M., Van Domselaar, G., & Stothard, P. (2023). Proksee: in-depth characterization and visualization of bacterial genomes. *Nucleic acids research*, *51*(W1), W484–W492. https://doi.org/10.1093/nar/gkad326.
36. Han, S. W., & Won, H. S. (2024). Advancements in the Application of Ribosomally Synthesized and Post-Translationally Modified Peptides (RiPPs). *Biomolecules*, *14*(4), 479. https://doi.org/10.3390/biom14040479.
37. Hofmann, A. F., & Hagey, L. R. (2014). Key discoveries in bile acid chemistry and biology and their clinical applications: history of the last eight decades. *Journal of lipid research*, *55*(8), 1553–1595. https://doi.org/10.1194/jlr.R049437.
38. Hu, P. L., Yuan, Y. H., Yue, T. L., & Guo, C. F. (2018). Bile acid patterns in commercially available oxgall powders used for the evaluation of the bile tolerance ability of potential probiotics. *PloS one*, *13*(3), e0192964. https://doi.org/10.1371/journal.pone.0192964.
39. Hundt, M., Basit, H., & John, S. (2022). Physiology, Bile Secretion. In *StatPearls*. StatPearls Publishing.

40. International Organization of Standardization/International Dairy Federation. *(ISO 10932/IDF 223) Milk and Milk Products. Determination of the Minimal Inhibitory Concentration (MIC) of Antibiotics Applicable to Bifidobacteria and Non-Enterococcal Lactic Acid Bacteria (LAB)*, 1st ed.; ISO and IDF: Geneva, Switzerland, 2010.
41. Jiang, J., Zhang, H., Hussain, M., Abdullah, Feng, F., Guan, R., & Zhong, H. (2025). Novel Approaches in Glucose and Lipid Metabolism Disorder Therapy: Targeting the Gut Microbiota-Bile Acid Axis. *Biology*, *14*(7), 802. https://doi.org/10.3390/biology14070802.
42. Jones, M. L., Tomaro-Duchesneau, C., Martoni, C. J., & Prakash, S. (2013). Cholesterol lowering with bile salt hydrolase-active probiotic bacteria, mechanism of action, clinical evidence, and future direction for heart health applications. *Expert opinion on biological therapy*, *13*(5), 631–642. https://doi.org/10.1517/14712598.2013.758706.
43. Joyce, S. A., MacSharry, J., Casey, P. G., Kinsella, M., Murphy, E. F., Shanahan, F., Hill, C., & Gahan, C. G. (2014). Regulation of host weight gain and lipid metabolism by bacterial bile acid modification in the gut. *Proceedings of the National Academy of Sciences of the United States of America*, *111*(20), 7421–7426. https://doi.org/10.1073/pnas.1323599111.
44. Kahm, M., Hasenbrink, G., Lichtenberg-Fraté, H., Ludwig, J., & Kschischo, M. (2010). grofit: fitting biological growth curves with R. *Journal of statistical software*, *33*, 1-21. https://doi.org/10.18637/jss.v033.i07.
45. Kanehisa, M., Sato, Y., & Morishima, K. (2016). BlastKOALA and GhostKOALA: KEGG Tools for Functional Characterization of Genome and Metagenome Sequences. *Journal of molecular biology*, *428*(4), 726–731. https://doi.org/10.1016/j.jmb.2015.11.006.
46. Kang, M. H., Elnar, A. G., & Kim, G. B. (2025). Review on the Function, Substrate Affinity, and Potential Application of Bile Salt Hydrolase Originated from Probiotic Strains of *Lactobacillus*, *Bifidobacterium*, and *Enterococcus*. *Food science of animal resources*, *45*(2), 353–374. https://doi.org/10.5851/kosfa.2025.e1.
47. Karlov, D. S., Long, S. L., Zeng, X., Xu, F., Lal, K., Cao, L., Hayoun, K., Lin, J., Joyce, S. A., & Tikhonova, I. G. (2023). Characterization of

the mechanism of bile salt hydrolase substrate specificity by experimental and computational analyses. *Structure (London, England : 1993)*, *31*(5), 629–638.e5. https://doi.org/10.1016/j.str.2023.02.014.

48. Kriaa, A., Bourgin, M., Potiron, A., Mkaouar, H., Jablaoui, A., Gérard, P., Maguin, E., & Rhimi, M. (2019). Microbial impact on cholesterol and bile acid metabolism: current status and future prospects. *Journal of lipid research*, *60*(2), 323–332. https://doi.org/10.1194/jlr.R088989.
49. Kusada, H., Arita, M., Tohno, M., & Tamaki, H. (2022). Isolation of a Highly Thermostable Bile Salt Hydrolase With Broad Substrate Specificity From *Lactobacillus paragasseri*. *Frontiers in microbiology*, *13*, 810872. https://doi.org/10.3389/fmicb.2022.810872.
50. Lee, G., You, H. J., Bajaj, J. S., Joo, S. K., Yu, J., Park, S., Kang, H., Park, J. H., Kim, J. H., Lee, D. H., Lee, S., Kim, W., & Ko, G. (2020). Distinct signatures of gut microbiome and metabolites associated with significant fibrosis in non-obese NAFLD. *Nature communications*, *11*(1), 4982. https://doi.org/10.1038/s41467-020-18754-5
51.
52. Letunic, I., & Bork, P. (2019). Interactive Tree Of Life (iTOL) v4: recent updates and new developments. *Nucleic acids research*, *47*(W1), W256–W259. https://doi.org/10.1093/nar/gkz239.
53. Liu, B., Zheng, D., Zhou, S., Chen, L., & Yang, J. (2022). VFDB 2022: a general classification scheme for bacterial virulence factors. *Nucleic acids research*, *50*(D1), D912–D917. https://doi.org/10.1093/nar/gkab1107.
54. Liu, Y. Y., Hsu, C. Y., Yang, Y. C., Huang, C. H., & Chen, C. C. (2023). ProbioMinServer: an integrated platform for assessing the safety and functional properties of potential probiotic strains. *Bioinformatics advances*, *3*(1), vbad153. https://doi.org/10.1093/bioadv/vbad153.
55. Liang, L., Yi, Y., Lv, Y., Qian, J., Lei, X., & Zhang, G. (2018). A Comprehensive Genome Survey Provides Novel Insights into Bile Salt Hydrolase (BSH) in *Lactobacillaceae*. *Molecules (Basel, Switzerland)*, *23*(5), 1157. https://doi.org/10.3390/molecules23051157.

56. Manni, M., Berkeley, M. R., Seppey, M., & Zdobnov, E. M. (2021). BUSCO: Assessing Genomic Data Quality and Beyond. *Current protocols*, *1*(12), e323. https://doi.org/10.1002/cpz1.323.
57. Marco, M. L., Heeney, D., Binda, S., Cifelli, C. J., Cotter, P. D., Foligné, B., Gänzle, M., Kort, R., Pasin, G., Pihlanto, A., Smid, E. J., & Hutkins, R. (2017). Health benefits of fermented foods: microbiota and beyond. *Current opinion in biotechnology*, *44*, 94–102. https://doi.org/10.1016/j.copbio.2016.11.010.
58. Martini, S., Sola, L., Cattivelli, A., Cristofolini, M., Pizzamiglio, V., Tagliazucchi, D., & Solieri, L. (2024). Cultivable microbial diversity, peptide profiles, and bio-functional properties in Parmigiano Reggiano cheese. *Frontiers in microbiology*, *15*, 1342180. https://doi.org/10.3389/fmicb.2024.1342180.
59. Matta, T., Agrawal, K., Datta, P., Kumari, L., Bishnoi, M., Chopra, K., & Kondepudi, K. K. (2025). Safety Assessment of GABA-Producing Levilactobacillus brevis LAB6 MTCC 25662 and Its Anti-inflammatory Effects in Murine Macrophages. *Probiotics and antimicrobial proteins*, 10.1007/s12602-025-10628-w. Advance online publication. https://doi.org/10.1007/s12602-025-10628-w.
60. Meier-Kolthoff, J. P., & Göker, M. (2019). TYGS is an automated high-throughput platform for state-of-the-art genome-based taxonomy. *Nature communications*, *10*(1), 2182. https://doi.org/10.1038/s41467-019-10210-3.
61. Moreno, C. N., Gomez, J. N., Taranto, M. P., Ledesma, A. E., & Bustos, A. Y. (2024). Molecular Insight into the Response of Lactic Acid Bacteria to Bile Acids. *Biotech (Basel (Switzerland))*, *13*(3), 29. https://doi.org/10.3390/biotech13030029
62. Mikheenko, A., Prjibelski, A., Saveliev, V., Antipov, D., & Gurevich, A. (2018). Versatile genome assembly evaluation with QUAST-LG. *Bioinformatics (Oxford, England)*, *34*(13), i142–i150. https://doi.org/10.1093/bioinformatics/bty266.
63. Molina, G. E. S., Ras, G., da Silva, D. F., Duedahl-Olesen, L., Hansen, E. B., & Bang-Berthelsen, C. H. (2025). Metabolic insights of lactic acid bacteria in reducing off-flavors and antinutrients in plant-based

fermented dairy alternatives. *Comprehensive reviews in food science and food safety*, *24*(2), e70134. https://doi.org/10.1111/1541-4337.70134.

64. Munir, A., Javed, G. A., Javed, S., & Arshad, N. (2022). *Levilactobacillus brevis* from carnivores can ameliorate hypercholesterolemia: In vitro and in vivo mechanistic evidence. *Journal of applied microbiology*, *133*(3), 1725–1742. https://doi.org/10.1111/jam.15678.
65. Nair, V. G., Unnikrishnan, V. K., Muralidharan, N., SV, B. N., YBRD, R., Narbhavi, D., & Nagarajan, S. (2025). Human Vaginal Lactobacillus-Derived (-)-Terpinen-4-ol restores antibiotic sensitivity by inhibiting efflux pumps in drug resistant *E. coli* and *K. pneumoniae*. https://doi.org/10.21203/rs.3.rs-5122361/v1.
66. O'Flaherty, S., Briner Crawley, A., Theriot, C. M., & Barrangou, R. (2018). The *Lactobacillus* Bile Salt Hydrolase Repertoire Reveals Niche-Specific Adaptation. *mSphere*, *3*(3), e00140-18. https://doi.org/10.1128/mSphere.00140-18.
67. Pan, X., Xu, L., Li, Y., Wu, S., Wu, Y., & Wei, W. (2022). Strategies to Improve the Biosynthesis of β-Lactam Antibiotics by Penicillin G Acylase: Progress and Prospects. *Frontiers in bioengineering and biotechnology*, *10*, 936487. https://doi.org/10.3389/fbioe.2022.936487.
68. Papadopoulos, J. S., & Agarwala, R. (2007). COBALT: constraint-based alignment tool for multiple protein sequences. *Bioinformatics (Oxford, England)*, *23*(9), 1073–1079. https://doi.org/10.1093/bioinformatics/btm076.
69. Pfeiler, E. A., Azcarate-Peril, M. A., & Klaenhammer, T. R. (2007). Characterization of a novel bile-inducible operon encoding a two-component regulatory system in *Lactobacillus acidophilus*. *Journal of bacteriology*, *189*(13), 4624–4634. https://doi.org/10.1128/JB.00337-07.
70. Prjibelski, A., Antipov, D., Meleshko, D., Lapidus, A., & Korobeynikov, A. (2020). Using SPAdes De Novo Assembler. Current protocols in bioinformatics, *70*(1), e102. https://doi.org/10.1002/cpbi.102.
71. Ren, J., Sun, K., Wu, Z., Yao, J., & Guo, B. (2011). All 4 bile salt hydrolase proteins are responsible for the hydrolysis activity in

Lactobacillus plantarum ST-III. *Journal of food science*, *76*(9), M622–M628. https://doi.org/10.1111/j.1750-3841.2011.02431.x.

72. Richter, M., Rosselló-Móra, R., Oliver Glöckner, F., & Peplies, J. (2016). JSpeciesWS: a web server for prokaryotic species circumscription based on pairwise genome comparison. *Bioinformatics (Oxford, England)*, *32*(6), 929–931. https://doi.org/10.1093/bioinformatics/btv681.
73. Ru, X., Zhang, C. C., Yuan, Y. H., Yue, T. L., & Guo, C. F. (2019). Bile salt hydrolase activity is present in nonintestinal lactic acid bacteria at an intermediate level. *Applied microbiology and biotechnology*, *103*(2), 893–902. https://doi.org/10.1007/s00253-018-9492-5.
74. Scheutz, F., Nielsen, C. H., & von Mentzer, A. (2024). Construction of the ETECFinder database for the characterization of enterotoxigenic *Escherichia coli* (ETEC) and revision of the VirulenceFinder web tool at the CGE website. *Journal of clinical microbiology*, *62*(6), e0057023. https://doi.org/10.1128/jcm.00570-23.
75. Seemann T. (2014). Prokka: rapid prokaryotic genome annotation. *Bioinformatics (Oxford, England)*, *30*(14), 2068–2069. https://doi.org/10.1093/bioinformatics/btu153.
76. Sethi, M., Ok, A., Dash, J., Parida, D., Kar, S., Mishra, S., Minz, A. P., Padhi, A., Das, K. R., Pradhan, B., Prakash, T., & Senapati, S. (2025). Whole Genome Mining and Characterization of a New Probiotic Strain *Levilactobacillus brevis* ILSH3 from Handia: An Ethnic Fermented Beverage of Odisha, India. *Probiotics and antimicrobial proteins*, *17*(3), 1596–1614. https://doi.org/10.1007/s12602-024-10217-3.
77. Shangpliang, H. N. J., & Tamang, J. P. (2024). Genome Analysis of Potential Probiotic Levilactobacillus brevis AcCh91 Isolated from Indian Home-Made Fermented Milk Product (Chhurpi). *Probiotics and antimicrobial proteins*, *16*(5), 1583–1607. https://doi.org/10.1007/s12602-023-10125-y.
78. Solieri, L., Sola, L., Vaccalluzzo, A., Randazzo, C. L., Martini, S., & Tagliazucchi, D. (2022). Characterization of Cell-Envelope Proteinases from Two *Lacticaseibacillus casei* Strains Isolated from Parmigiano Reggiano Cheese. *Biology*, *11*(1), 139. https://doi.org/10.3390/biology11010139.

79. Somashekaraiah, R., Mottawea, W., Gunduraj, A., Joshi, U., Hammami, R., & Sreenivasa, M. Y. (2021). Probiotic and Antifungal Attributes of *Levilactobacillus brevis* MYSN105, Isolated From an Indian Traditional Fermented Food Pozha. *Frontiers in microbiology*, *12*, 696267. https://doi.org/10.3389/fmicb.2021.696267.
80. Song, Z., Cai, Y., Lao, X., Wang, X., Lin, X., Cui, Y., Kalavagunta, P. K., Liao, J., Jin, L., Shang, J., & Li, J. (2019). Taxonomic profiling and populational patterns of bacterial bile salt hydrolase (BSH) genes based on worldwide human gut microbiome. *Microbiome*, *7*(1), 9. https://doi.org/10.1186/s40168-019-0628-3.
81. Sreepathi, N., Kumari, V. B. C., Huligere, S. S., Al-Odayni, A. B., Lasehinde, V., Jayanthi, M. K., & Ramu, R. (2023). Screening for potential novel probiotic *Levilactobacillus brevis* RAMULAB52 with antihyperglycemic property from fermented *Carica papaya* L. *Frontiers in microbiology*, *14*, 1168102. https://doi.org/10.3389/fmicb.2023.1168102.
82. Starikova, E. V., Tikhonova, P. O., Prianichnikov, N. A., Rands, C. M., Zdobnov, E. M., Ilina, E. N., & Govorun, V. M. (2020). Phigaro: high-throughput prophage sequence annotation. *Bioinformatics (Oxford, England)*, *36*(12), 3882–3884. https://doi.org/10.1093/bioinformatics/btaa250.
83. Taoka, H., Yokoyama, Y., Morimoto, K., Kitamura, N., Tanigaki, T., Takashina, Y., Tsubota, K., & Watanabe, M. (2016). Role of bile acids in the regulation of the metabolic pathways. *World journal of diabetes*, *7*(13), 260–270. https://doi.org/10.4239/wjd.v7.i13.260.
84. Topisirovic, L., Kojic, M., Fira, D., Golic, N., Strahinic, I., & Lozo, J. (2006). Potential of lactic acid bacteria isolated from specific natural niches in food production and preservation. *International journal of food microbiology*, *112*(3), 230–235. https://doi.org/10.1016/j.ijfoodmicro.2006.04.009.
85. Travin, D. Y., Bikmetov, D., & Severinov, K. (2020). Translation-Targeting RiPPs and Where to Find Them. *Frontiers in genetics*, *11*, 226. https://doi.org/10.3389/fgene.2020.00226.
86. Urshev, Z., Doynova, D., Prasev, I., Denkova-Kostova, R., Koleva, A., Denkova, Z., Goranov, B., & Kostov, G. (2024). Identification of lactic

acid bacteria strains isolated from Sourdoughs prepared with different flour types. *Applied Sciences*, *14*(5), 2093. https://doi.org/10.3390/app14052093.

87. Wall, T., Båth, K., Britton, R. A., Jonsson, H., Versalovic, J., & Roos, S. (2007). The early response to acid shock in Lactobacillus reuteri involves the ClpL chaperone and a putative cell wall-altering esterase. *Applied and environmental microbiology*, *73*(12), 3924–3935. https://doi.org/10.1128/AEM.01502-06.
88. Wang, Q., Peng, J., Tian, Y., Li, J., Cai, J., & Qin, W. (2024). Evaluation of the Decreased Cholesterol Potential of Levilactobacillus brevis M-10 Isolated from Spontaneously Fermented Sour Porridge in Mice with High-Cholesterol Levels. *Current microbiology*, *82*(1), 24. https://doi.org/10.1007/s00284-024-03974-5.
89. Wang, Q., Zhang, W., Liu, J., Qin, W., & Cai, J. (2025). Exopolysaccharide of Levilactobacillus brevis M-10 Improved Physiological and Biochemical Indicators and Gut Microbiota in DSS-Induced Colitis Mice. *Current microbiology*, *82*(5), 204. https://doi.org/10.1007/s00284-025-04190-5.
90. Watanabe, S., Katsube, T., Hattori, H., Sato, H., Ishijima, T., Nakai, Y., Abe, K., & Sonomoto, K. (2013). Effect of Lactobacillus brevis 119-2 isolated from Tsuda kabu red turnips on cholesterol levels in cholesterol-administered rats. *Journal of bioscience and bioengineering*, *116*(1), 45–51. https://doi.org/10.1016/j.jbiosc.2013.01.009.

Chapter 4

4 Gastrointestinal survivability of a BSH-positive *Lacticaseibacillus rhamnosus* VB4 strain and its effects on bile acid deconjugation in a dynamic *in vitro* gut model

Amanda Vaccalluzzo[1†], **Gianluigi Agolino**[1†], Alessandra Pino[1,2], Marianna Cristofolini[3], Davide Tagliazucchi[3], Alice Cattivelli[3], Cinzia Caggia[1,2], Lisa Solieri[3], and Cinzia Lucia Randazzo[1,2,*]

[1]Department of Agriculture, Food and Environment (Di3A), University of Catania, Via Santa Sofia 100, 95123 Catania, Italy
[2] ProBioEtna srl, Spin Off of the University of Catania, Santa Sofia Street, 100, 95123 Catania, Italy;
[3]Department of Life Science, University of Modena and Reggio Emilia, 42122 Reggio Emilia, Italy;

*Corresponding author: cinzia.randazzo@unict.it (C. L. Randazzo)
†These authors contributed equally to this work

Published in *Nutrients 2025, 17(19), 3179*
DOI: https://doi.org/10.3390/nu17193179

Graphical abstract

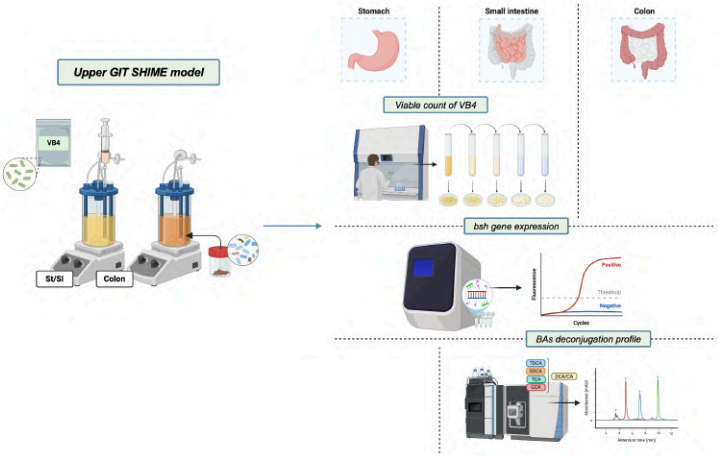

Abstract

Background: Bile salt hydrolase (BSH) is a key probiotic trait, as it facilitates both host metabolism and bacterial survival into the gastrointestinal tract (GIT), through bile acid (BA) deconjugation, keeping intestinal homeostasis. Objectives: The present study aims to investigate the viability of the *Lacticaseibacillus rhamnosus* VB4 strain and its effects on bile acid deconjugation during the gastrointestinal tract (GIT) passage, under a fed condition, using the in vitro SHIME® (Simulator of the Human Intestinal Microbial Ecosystem) model. Methods: Gastric, small intestinal and colonic

fractions were monitored and a fecal slurry from a healthy donor was inoculated into the colonic compartment to establish the intestinal microbiota. Samples were collected at the end of stomach, duodenum, jejunum, ileum phases, and colon after 0, 16 and 24 h. Strain survival was assessed by culturing method, and *bsh* gene expression was revealed by quantitative PCR (qPCR). In addition, UHPLC/HR-MS was performed to reveal the hypothetical changes in BAs profile after strain administration. Results: Good survivability of the VB4 strain in the upper GIT was revealed. Furthermore, VB4-inculated sample showed sustained expression of *bsh* in both the stomach/small intestine and colon fractions at all sampling times. Analysis of the BAs profile shown that the VB4 strain reduced the levels of the main conjugated BAs in the small intestine under fed condition and improved the deconjugation efficiency during colonic transit compared with the control. Conclusions: These findings highlight the survivability of *L. rhamnosus* VB4 strain inside the gut and its potential as biotherapeutic BAs-mediator candidate, demonstrating that transcriptomic and metabolomic approaches coupled to a dynamic in vitro gut model represent a robust tool for selection of a BSH-positive probiotic candidate.

Keywords: bile salt hydrolase, bile acids, dynamic simulator, strain survivability, *bsh* gene expression, metabolomic profile.

4.1 Introduction

Lactobacilli, as natural inhabitant of the gastrointestinal tract (GIT), have attracted considerable attention for their probiotic trait and for the capacity to synthesize the bile salt hydrolase (BSH) (Kumar et al., 2012). BSH is a gut microbial enzyme closely related to bile acids (BAs) metabolism, which catalyzes the first reaction of conjugated BAs hydrolysis, necessary for their biotransformation into deconjugated ones. Gastrointestinal bacteria play a crucial role in the recovery of BAs, acting as molecules with endocrine and paracrine signals, involved in intestinal absorption of dietary and endogenous-derived lipids, as well as glucose metabolism. Primary BAs are synthesized in the liver, and subsequently bond glycine or taurine, thus forming conjugated BAs. After being released into the small intestine, BSH enzyme cleaves the amide bond of glyco- and tauro-conjugated BAs, forming free amino acids and deconjugated BAs, which reaching the colon as secondary BAs through further bioconversion. As suggested, BSH ability is directly implicated in different metabolic pathways, including its role on endogenous cholesterol metabolism (Agolino et al., 2024; Deng et al., 2023; Joyce et al., 2014; Kumar et al., 2012). Since free BAs are less soluble and are reabsorbed less efficiently in the ileum, their fecal excretion increases, which in turn stimulates the liver to convert endogenous cholesterol into new BAs. This compensatory mechanism reduces the pool of circulating cholesterol, thus explaining the role of BSH in endogenous cholesterol metabolism (Joyce et al., 2014). However, the full mechanisms underlying the complex interaction between BAs and cholesterol metabolisms remain poorly known (Agolino et al., 2024). The activity of BSH was further validated by the presence of genes encoding the

BSH enzyme in the genome of intestinal bacteria. This activity could further support the survivability of BSH-positive microorganisms and improve their colonization within the intestine. In this regard, studies on *bsh* mutants showed growth deficiency by in vitro testing, suggesting the involvement of *bsh* genes in bile tolerance (De Boever et al., 2023; Li et al., 2015; O'Flaherty et al., 2018). Taxonomic study on *bsh* gene distribution distinguish different phylotype, highlighting different copy number of the gene across *Lactobacillus* genera, as well as the synthesis of several BSH variant with different functional properties (Kusada et al., 2021; Song et al., 2019; Song et al., 2023). Given the pivotal impact of BSH activity on bacterial survival gut microbiota, *bsh* gene detection in lactobacilli, has been recognized as a functional biomarker for probiotic selection (Kusada et al., 2021).

More recently, research is focused on the use of predictive methods, such as SHIME® system, often integrated with high-throughput technologies, to quantify and characterize cells and molecules involved in the microbial ecosystem. These strategies are applied to detect functional properties arising from the interaction between probiotic supplementation and the gut microbiota. At this regard, in vitro studies conducted using the Simulator of the Human Microbial Ecosystem (SHIME®, ProDigest, Belgium) are considered a viable strategy to better understand the effect of potential probiotic strains and to make them a more suitable product for the formulation of dietary and/or pharmaceutical supplements (Duysburgh et al., 2018). The SHIME® is a GIT model, which mimics the dynamic and physiological processes starting from the stomach until the colonic fractions, in response to a probiotic or prebiotic action (Rudzka et al., 2023; Van de Wiele et al., 2015). Therefore, in this work, the upper GIT SHIME® model, extended to the colonic fraction, was used to

assess the survival and BAs deconjugation capacity of the BSH-positive *Lacticaseibacillus rhamnosus* VB4 strain, previously selected according to Agolino and co-workers (2025). Briefly, the strain demonstrated BSH activity, by in vitro test under simulated gastrointestinal conditions, and the expression putative *bsh* genes, by transcriptional profile analysis. In particular, by combining transcriptomic and metabolomic approaches, we sought to better understand the action of BSH by evaluating a dynamic process of BAs colonization and conjugation, monitoring its passage from the upper part of the GIT to the colonic fraction.

4.2 Material and Methods

4.2.1 BSH-positive L. rhamnosus VB4 strain

The *Lacticaseibacillus rhamnosus* VB4 strain, belonging to the microbial collection of ProBioEtna srl, Spin Off of the University of Catania (Catania, Italy), was selected for its probiotic properties and high ability to deconjugate BAs, in accordance with the results obtained in the previous work conducted by Agolino and co-workers (2025). The VB4 strain was freeze-dried by SACCO Srl (Cadorago, Italy) and, prior to inoculation into SHIME® system, its viability was verified using plate culture method with Lactobacilli MRS agar medium (BD Difco™, Milan, Italy). The freeze-dried strain was directly inoculated into the stomach/small intestine reactors and the starting cell density of the VB4 strain was at 9 $\log_{10}$ CFU/g.

4.2.2 SHIME® Experiment set-up

The dynamic SHIME® model (ProDigest, Ghent, Belgium) was

set up under feeding condition according to the protocols proposed by Marzorati and co-workers (2021) and Jannin and collaborators (2023) to mimic the incubation of stomach, small intestine (St/SI) and colon (C) compartments, using two double-jacketed reactors serially connected, maintained at 37 °C under constant agitation. Both reactors, St/SI and C were maintained under anaerobic conditions, by controlled N_2, in accordance with the requirements of the nitrogen flushing system. The lyophilized strain was inoculated with an initial cell density of 9 $\log_{10}$ CFU/g in the first reactor (St/SI), simulating the digestion of the stomach and small intestine. In detail, under fed condition, a gastric solution (76 mL), containing SHIME® nutritional medium (PDNM001B 20.53 g/L, ProDigest), NaCl (3.63 g/L), KCl (0.65 g/L), 0.4 mL lecithin (13.5 g/L), and 3.6 mL pepsin (40 g/L) at pH 4.6 was added to the vessel and maintained for 120 min with a sigmoidal pH decrease from 4.6 to 2. After incubation in the stomach, a small intestine phase, comprising the duodenum, jejunum, and ileum, was performed. In accordance with published SHIME® protocols (Jannin et al., 2023; Marzorati et al., 2021), BAs were supplemented as Oxgall (Difco, bovine bile extract) in the duodenal phase together with pancreatic juice solution, in order to reproduce the physiological presence of BAs in the small intestine. No bile salts were added in the gastric phase. Specifically, during the duodenal phase, a pancreatic juice composition ($NaHCO_3$ 7.7 g/L, Oxgall 15 g/L, and pancreatin 10 g/L, added with 2.15 mL trypsin 10 g/L and 2.7 mL chymotrypsin 10 g/L) was added. The pH of the small intestine was gradually increased from 2.0 to 6.5 and maintained at this pH over 27 min to simulate the duodenal fraction, followed by jejunal (pH up to 7.5 maintained for 63 min) and ileal (constant pH 7.5

for 90 min) fractions. An increase in pH was achieved by the addition of $NaHCO_3$ (4.8 g/L) at 60, 90, and 120 min, mimicking the dilution of the intestinal contents. The increase and decrease in pH were automatically controlled, by pH-meter probe (ProSense, Oosterhout, The Netherlands), and adjusted by the dosage of HCl (0.5 M) and NaOH (0.5 M). All reagents and chemicals used were of analytical grade and were purchased from Merck (Milan, Italy).

4.2.2.1 Fecal slurry preparation and colonic incubation

An extension of the colonic incubation was further proposed. The digested solution from the stomach/small intestine reactor was transferred to the second reactor, simulating colonic conditions, and maintained for 24 h. A fecal sample from a healthy donor (male, 50y) was chosen for the SHIME® experiment. The collection of data from the use of the human fecal sample was approved by the Ethics Committee of the University of Modena and Reggio Emilia (CEAR) on 20.01.2025, and informed consent for the experimentation was obtained from the subject involved in the study. The fecal slurry was obtained according to the protocol proposed by Marzorati and collaborators (2021) and inoculated into the colonic reactor. In detail, a 1:10 (*w*/*v*) mixture of fecal sample and anaerobic phosphate buffer (K_2HPO_4 8.8 g/L; KH_2PO_4 6.8 g/L; sodium thioglycolate 0.1 g/L; sodium dithionite 0.015 g/L) was homogenized for 10 min (BagMixer 400, Interscience, Louvain-LaNeuve, Belgium), and the mixture was centrifuged (2 min, 500 g) and the large particles were removed. The obtained fecal slurry (20% *v*/*v*) was added to 160 mL fresh colonic anaerobic medium [KH_2PO_4 (6.6 g/L), K_2HPO_4 (20.5 g/L), NaCl (5 g/L), yeast extract (2 g/L), peptone (2 g/L), glucose (1 g/L), starch (2

g/L), mucin (1 g/L), L-cysteine HCl (0.5 g/L), Tween® 80 (2 mL)], 40 mL of anaerobic PBS [K_2HPO_4 (8.8 g/L), KH_2PO_4 (6.4 g/L), NaCl (8.5 g/L) and L-cysteine HCl (0.5 g/L)]. In the colonic compartment, a fixed pH range between 6.5 and 5.8 was implemented, adjusted automatically, maintaining an anaerobic condition at 37 °C and an agitation of 90 rpm. A reactor without the addition of the probiotic strain was used as a control sample, following all of the steps of the digestion, from the stomach to the colon compartments. After few minutes of stabilization, aliquots collected from both reactors were subjected to qPCR analysis for Lactobacilli quantification. All the SHIME®assays were performed in duplicate. In the stomach/small intestine reactor, samples were collected at the end of the incubation phases of the stomach, duodenum, jejunum, and ileum, and subjected to culture-dependent and culture-independent analysis. While in the colonic fraction, lumen samples were collected after 0, 16, and 24 h of colonic incubation. All the analyses were assessed in triplicate. All reagents and chemicals used were of analytical grade and were purchased from Merck (Milan, Italy). A schematic representation of the experimental workflow is shown in **Figure 4.1**.

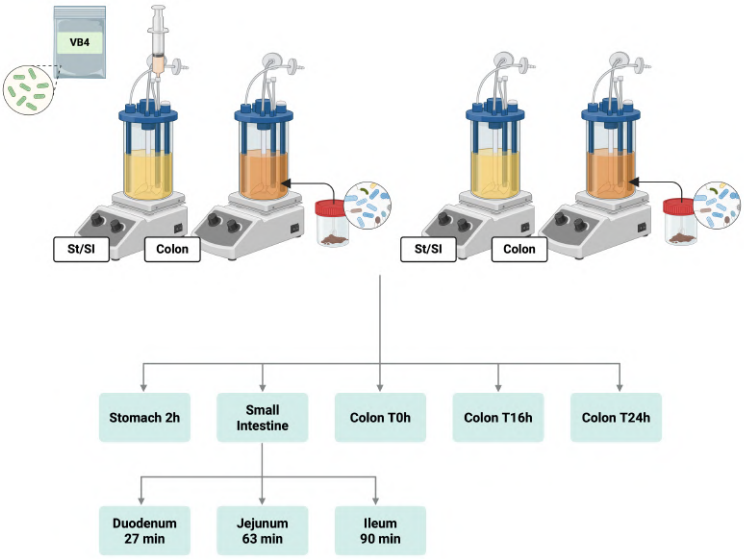

Figure 4.1 - Overview of the SHIME® system setup. The stomach/small intestine (St/SI) reactor connected in series to the colon (C) reactor. The unit was designed for both VB4-inoculated samples (left) and control samples (right). In addition, a workflow is shown describing the incubation steps and times performed and the collection of intestinal and colon fraction samples. St/SI, stomach/small intestine; VB4, *L. rhamnosus* VB4 strain.

4.2.3 Detection of viability by culture-dependent method

The viability of *L. rhamnosus* VB4 strain was evaluated during GIT passage, from the stomach to ileal phase, by plate count. Briefly, the bacterial count was performed by plating serial ten-fold dilutions using the anaerobic PBS, containing 8.8 g/L of K_2HPO_4, 6.4

g/L of KH_2PO_4, 8.5 g/L of NaCl, and 0.5 g/L of L-cysteine HCl, then cultured on Lactobacilli MRS Agar medium (BD Difco™) and incubated under anaerobic conditions at 37 °C for 48 h. Colony counts were performed on plates yielding between 30 and 300 colonies. The plate count assays were performed in triplicate and results were reported as mean values $\log_{10}$ CFU/mL and standard deviation.

4.2.4 Detection gene expression of BSH-positive VB4 strain

4.2.4.1 RNA extraction

All samples collected during the simulation with the SHIME® model were subjected to RNA extraction. Specifically, 2 mL of stomach/intestinal small intestine and lumen samples and 0.3 g of mucosal samples were centrifuged at 20,000× *g* for 10 min, washed twice with anaerobic PBS and subjected to ZymoBIOMICS™ RNA Miniprep Kit (Zymo Research, Orange, CA, USA), with prior mechanical breakage with Precellys Evolution Homogenizer (Bertin Technologies, Montigny-le-Bretonneux, France) at 10,000 rpm for 2 min, repeated three times, interspersed with breaks on ice. The concentration, integrity and quality of RNA templates were checked using the Qubit™ 4 Fluorometer (Thermo Fisher Scientific, San Jose, CA, USA).

4.2.4.2 RT-PCR and RT-qPCR assay

The RNA templates were subjected to reverse transcription PCR (RT-PCR) analysis using the QuantiTect Reverse Transcription Kit (Qiagen, Hilden, Germany), according to the manufacturer's instructions. The complementary DNA (cDNA) obtained was subjected to RT-qPCR with a *L. rhamnosus* species-specific primer

pair, designed in the previous study conducted by Agolino and collaborators [**14**]. In detail, the reaction included 10 µL of QuantiNovaTM SYBR Green PCR Kit (Qiagen), 0.7 µM of each primer Bsh_rha_qF2 (GGAATACGGGTGCATACAA) and Bsh_rha_qR2 (CAGGCCAAACATGCCATAAC), 50 ng of cDNA template and 4.2 µL of Dnase/Rnase-free water (Thermo Fisher Scientific). Cycling conditions comprised a holding phase at 95 °C for 2 min, followed by 40 cycles at 95 °C for 5 s, 60 °C for 10 s, and 60 °C for 30 s. The melting range was set between 60 °C and 95 °C. In addition, according to the protocol proposed by Agolino and co-workers (Agolino et al., 2025), RT-qPCR was also performed for the 16S rRNA housekeeping (*HKG*) gene with *L. rhamnosus*-specific primers 16S_F1 (GTAGGTGGCAAGCGTTATCC), and 16S_Rw1 (GATGCGCTTCCTCGGTTAAG). The reaction mixture and reagent concentrations included 10 µL of QuantiNovaTM SYBR Green PCR Kit (Qiagen), 0.7 µM of each primer. The qPCR cycling parameters include a holding phase at 95 °C for 2 min, followed by 40 cycles at 95 °C for 5 sec and 60 °C for 60 sec. The melting range was set from 60 °C to 95 °C. Specificity and amplification efficiency (E) were performed using a 10× dilution of the microbial gDNA of *L. rhamnosus* VB4 as a reference standard. Slope of the regression curve between the logical values of the cDNA concentrations and the mean values of the cycle threshold (Ct) was used to calculate the primer efficiency using the equation: E= 0.5 (10 (−1/slope)) × 100. A Rotor Gene Q instrument (Qiagen, Milan, Italy) was used to perform the reaction. Each reaction was repeated at least three times.

For both *HSG* and *bsh* genes, standard curves were created by plotting qPCR Ct values against the log inputs genome copy number

obtained from standard genomic DNA. The copy numbers determined for DNA standards were calculated using the formula:

$$number\ of\ copies = \frac{amount\ of\ DNA\ (ng)\ \times\ 6.022 \times 10^{23}}{lenght\ of\ the\ genome\ (bp) \times\ 10^{9} \times 650}$$

where length of genome was established in Agolino et al. (2025); Na is the (6.022×10^{23} molecules/mol is the Avogadro's number), 660 g/mol is the average weight of a single base pair, and 10^{9} is the conversion factor. For *bsh*-based RT-qPCR standard curves enabled an estimation of cDNA copy number as *bsh* gene was in single copy. For 16S-based RT-qPCR, a correction was applied to take into account the number of ribosomal RNA operon copies, as established in Agolino et al. (2025).

4.2.5 Detection of BAs from SHIME samples

The semi-quantitative analysis of individual BAs in samples from the SHIME® model (both in control and VB4-inoculated samples) was carried out as reported in Agolino and collaborators (2025) by using a high-resolution mass spectrometer. In detail, samples collected from small intestine fractions, including duodenum, jejunum, and ileum phases, and colonic fraction collected after 16 and 24 h of incubation were subjected to BAs detection. Chromatographic separation was performed with a UHPLC Ultimate 3000 module (Thermo Fisher Scientific) equipped with a C18 column (Acquity UPLC HSS C18 Reversed phase, 2.1 × 100 mm, 1.8 µm particle size, Waters, Milan, Italy). Mass spectrometry analysis was carried out through a Q Exactive Hybrid Quadrupole-Orbitrap Mass Spectrometer

(Thermo Fisher Scientific). Mobile phases were water with 0.1% formic acid (mobile phase A) and acetonitrile with 0.1% formic acid (mobile phase B) and the flow rate was 0.3 mL/min. An amount of 10 µL of appropriately diluted sample was injected. The chromatographic and mass spectrometry parameters were fully described in Agolino et al. (2025). The analyzed BAs were glycocholic acid (GCA), taurocholic acid (TCA); glycodeoxycholic acid (GDCA) and taurodeoxycholic acid (TDCA). Preliminary analysis demonstrated that taurochenodeoxycholic acid was not present in this specific Oxgall preparation whereas glycochenodeoxycholic acid was only present in minor amounts. Therefore, these two BAs were not further considered for the subsequent analysis. The relative amount of bile acids was determined by integrating the area under the peak (AUP). AUP values were quantified from the extracted ion chromatograms (EIC) calculated for each mass-to-charge ratio of a specific compound (tolerance ± 5 ppm) using the Genesis algorithm function in the Thermo Xcalibur Quantitative Browser.

4.2.6 Statistical analysis

All the analyses were performed in technical triplicate, and data are presented as mean values ± standard deviation (SD). Statistical analyses and graph generation were conducted using GraphPad Prism 10 (GraphPad Software, La Jolla, CA, USA). Given the small sample size ($n = 3$), formal tests of normality and variance homogeneity could not be reliably applied. Parametric methods were therefore used under the assumption of approximate normality, considering the robustness of ANOVA to moderate variance differences in balanced designs. Microbiological counts and gene expression were analyzed using

ANOVA One-way, by using Tukey's post-hoc test. Whereas the BAs profile was assessed using an ANOVA Two-way. Followed by Dunnett's post-hoc. Statistical significance was set at p-value < 0.05.

4.3 Results

4.3.1 L. rhamnosus VB4 strain viability in stomach/small intestine

The *L. rhamnosus* VB4 strain viability in the stomach and small intestine was achieved by plate count and results are displayed in **Figure 4.2**. Overall, no substantial differences were detected between the stomach and the small intestine ($p > 0.05$). In detail, the strain exhibited a slight reduction during the final gastric phase, decreasing from the initial inoculum (9 $\log_{10}$ CFU/mL) to 8.49 ± 0.40 $\log_{10}$CFU/mL ($p < 0.05$), mainly due to the acidic condition and gastric enzymes of the stomach environment. During the small intestine transit, a progressive decrease of the VB4 cell density was observed from duodenum to jejunum, with values of 8.29 ± 0.11 $\log_{10}$CFU/mL ($p < 0.05$) and 7.67 ± 0.19 $\log_{10}$ CFU/mL ($p < 0.05$), respectively. A slight increase in the ileum with a cell density of 8.14 ± 0.23 $\log_{10}$ CFU/mL ($p < 0.05$) was achieved.

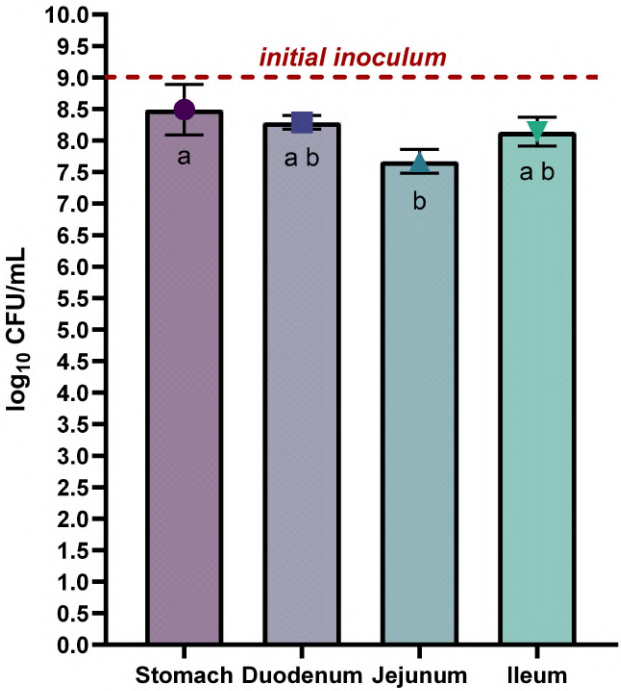

Figure 4.2 - Survival of *Lacticaseibacillus rhamnosus* VB4 in Stomach/Small Intestine compartments. Viable counts were enumerated on agar plate. Data are expressed as average ± SD of the three independent biological replicates. Results are expressed as mean ± SD of $\log_{10}$ CFU/mL. Data were analysed using ANOVA One-way with Tukey's post-hoc test. The horizontal red line indicates the starting cell density of the VB4 strain (9 $\log_{10}$ unit). $^{a–b}$ Different superscript letters indicate significant differences within samples at different GI fractions (at $p < 0.05$).

4.3.2 Bsh gene detection through qPCR analysis

For the evaluation of the transcriptional profile of the *bsh* gene in different gastrointestinal compartments, gene expression quantification in both the upper gastrointestinal tract and colonic fractions was assessed. The raw qPCR results expressed in ng/µL were converted into absolute copy numbers using an equation based on Avogadro's constant, the genome length of the reference strain (*L. rhamnosus* VB4) and the intercept of the standard curve. In addition, the housekeeping (*HKG*) gene was also quantified for a more accurate estimate of gene expression capacity. **Figure 4.3** shows the data obtained from the transcriptional test. Specifically, **Figure 4.3A** shows significant differences in the *bsh* gene expression profile between the stomach, and ileum phases, with values of 3.90 and 3.35 $\log_{10}$ copies qPCR ($p < 0.05$), respectively, and between the jejunum and ileum phases, with a value of 3.83 $\log_{10}$copies qPCR ($p < 0.05$). Conversely, the *HKG* gene was lower in the stomach phase with a value of 5.84 $\log_{10}$ copies qPCR ($p < 0.05$), which was significantly different from the duodenum (7.40 $\log_{10}$ copies qPCR), jejunum (7.44 $\log_{10}$ copies qPCR), and ileum (7.50 $\log_{10}$ qPCR copies), which showed a slight increase towards the end of the small intestine.

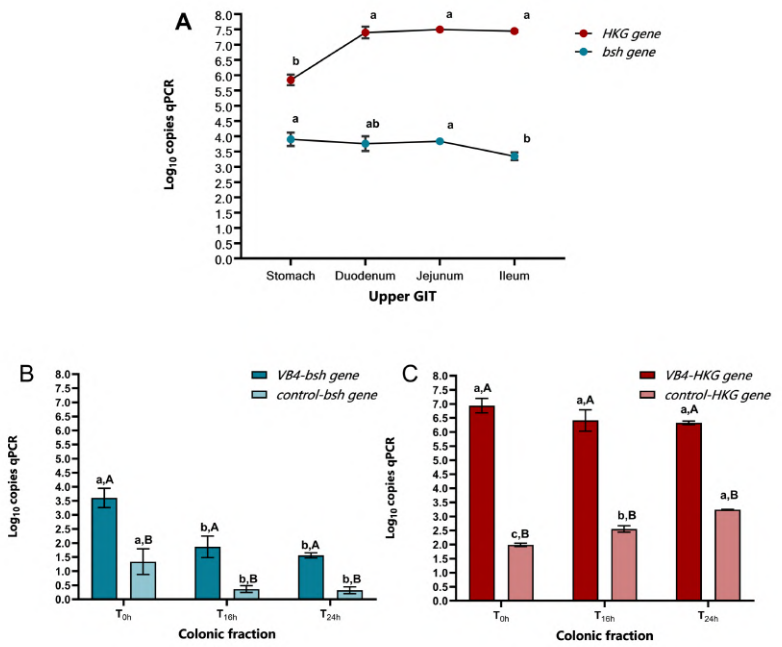

Figure 4.3 - Transcriptional profiles of *bsh* and *HKG* genes in SHIME® samples. (A) Gene expression of *bsh* and *HKG* genes in VB4-inoculated sample, along upper GIT. (B) *bsh* gene expression in colonic fraction, at 0, 16 and 24 sampling times, of VB4-inoculated and control samples. (C) *HKG* gene expression in colonic fraction, at 0, 16 and 24 sampling times, of VB4-inoculated and control samples. Results are expressed as mean ± SD of log_{10} copies qPCR. Data were analysed using ANOVA One-way with Tukey's post-hoc test. $^{a–c}$ The different superscript letters indicate significant differences within the same sample over time at $p < 0.05$. $^{A–B}$ The different superscript letters within the sampling time indicate significant differences between the two treated and control theses at $p < 0.05$. *Bsh*, bile salt hydrolase gene; GIT, gastrointestinal tract; *HKG*, housekeeping gene; qPCR, quantitative PCR; VB4, *L. rhamnosus* VB4 strain.

In **Figure 4.3B**, the transcriptional profile of the *bsh* gene of the VB4-inoculated sample in the colonic fraction showed a slight decrease of expression from T_{0h} to T_{24h}, with significant differences ($p < 0.05$) of T_{16h} (1.87 $\log_{10}$ copies qPCR) and T_{24h} (1.56 $\log_{10}$copies qPCR) compared to T_{0h} (3.61 $\log_{10}$ copies qPCR). A similar trend was shown in the control sample, where T_{0h} with a value of 1.34 $\log_{10}$ copies qPCR ($p < 0.05$) resulted significantly different compared to T_{16h} and T_{24h} with 0.36 and 0.32 $\log_{10}$ copies qPCR, respectively. At the same sampling time, *bsh* gene expression resulted more evident in the VB4-inoculated sample compared to the control one, which exhibited a low *bsh* gene expression due to the presence of commensal *L. rhamnosus* species.

For the *HKG* gene expression (**Figure 4.3C**), no significant differences ($p > 0.05$) were found between the VB4-inoculated sample at the sampling times, with a slight decrease from T_{0h} to T_{24h}, with 6.94 to 6.33 $\log_{10}$ copies qPCR, respectively. Whereas in the control samples a significant difference was observed at all sampling times, with an increase from T_{0h} to T_{24h}, with 1.99 and 3.24 $\log_{10}$ copies qPCR ($p < 0.05$), respectively. At the same sampling time, *HKG* gene expression confirmed the higher transcriptional ability of VB4-inoculated compared to control samples.

4.3.3 Semi-quantitative analysis of BAs in small intestine and colon

In order to test whether the inoculum of *L. rhamnosus* VB4 strain changed the BAs profile, the amount of four conjugated BAs (taurocholic, glycocholic, taurodeoxycholic, and glycodeoxycholic acids), was detected by high-resolution mass spectrometry during

small intestine and colon digestion.

The amount of the conjugated BAs increased from the duodenum to the jejunum in the control vessels (**Figure 4.4** and **Table 4.1**). Differently, a significant decrease was detected among the VB4-inoculated samples ($p < 0.05$), with the exception of the GCA sample, with values of $4.40 \times 10^{11} \pm 3.03 \times 10^{10}$ AUP and $4.25 \times 10^{11} \pm 8.87 \times 10^{8}$ AUP, in duodenum and jejunum, respectively (**Figure 4.4** and **Table 4.1**). The amount of GCA, in control sample, was not affected after passing into the ileum ($4.37 \times 10^{11} \pm 2.73 \times 10^{9}$ AUP), whereas a significant ($p < 0.05$) decrease in the amount of the other conjugated acids was observed, while significant decrease ($p < 0.05$) was showed for the VB4-inoculated sample (Figure 4.4 and Table 4.1).

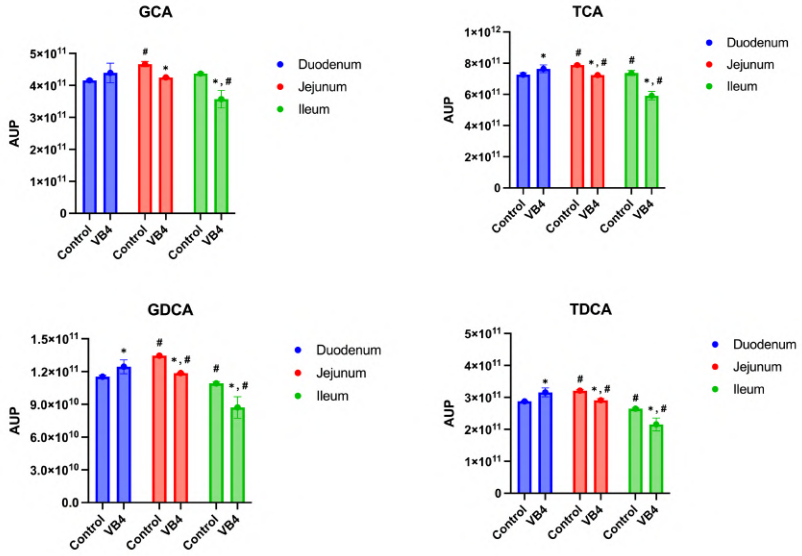

Figure 4.4 - Conjugated BAs in the small intestine. Glycocholic acid (GCA);

Taurocholic acid (TCA); Glycodeoxycholic acid (GDCA); Taurodeoxycholic acid (TDCA). Blue bars indicated duodenum samples, jejunum was identified by red bars, while green bars represent ileum. AUP means area under the peak and is an average of at least three replicates. Significant differences were established by two-way ANOVA using Dunnett's post-hoc test ($p < 0.05$). * The superscript asterisks symbol indicates significant differences between inoculated and control samples at the same time at $p < 0.05$. # The hash symbol indicates significant differences within the same sample over time at $p < 0.05$. VB4, *L. rhamnosus* VB4 strain.

As expected, a decline of 2/3 orders of magnitude from ileum to colonic fraction were observed in both control and VB4-inoculates samples, probably due to the physiological dilution of digested during the transit in the colonic fraction, reaching a value of approximately of 10^9–10^8 and AUP in the colon fraction, after 16 h (T_{16h}) of incubation (**Figure 4.5** and **Table 4.1**). It is interesting to highlight that a more pronounced decrease of BAs was revealed in the VB4-inoculated samples, compared to the control. In the T_{24h}colon sample, no significant differences ($p < 0.05$) between the control and the inoculated conjugated BAs were found. Otherwise, in the VB4-inoculated reactor, the amount of conjugated BAs significantly decreased ($p < 0.05$) in T_{24h} colon samples compared with T_{16h} (**Figure 4.5** and **Table 4.1**).

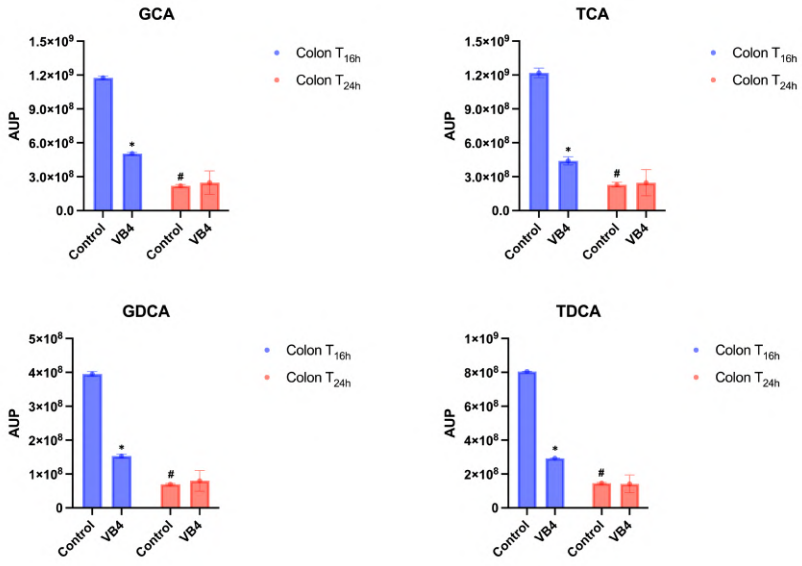

Figure 4.5 - Conjugated BAs in the colon. Glycocholic acid (GCA); Taurocholic acid (TCA); Glycodeoxycholic acid (GDCA); Taurodeoxycholic acid (TDCA). Semi-transparent blue and red bars identified the different sampling time of colon samples, at 16 and 24 h, respectively. Two-way ANOVA using Dunnett's post-hoc test was performed to assess the BAs profile changes after VB4 administration and BAs type. AUP means area under the peak (n = 3). * The superscript asterisks symbol indicates significant differences between inoculated and control samples at the same time at $p < 0.05$. # The hash symbol indicates significant differences within the same sample over time at $p < 0.05$. VB4, *L. rhamnosus* VB4 strain

Table 4.1 - Conjugated bile acids (BAs) detection in control and VB4-inoculated samples, under upper GIT SHIME® system. Glycocholic acid (GDCA), taurocholic acid (TCA), glycodeoxycholic acid (GDCA), and taurodeoxycholic acid (TDCA) in dudenum, jejunum, ileum, and colon (T_{16h} and T_{24h}). reported values are expressed as AUP ± SD.

Reactors	GCA		TCA		GDCA		TDCA	
	Control	VB4	Control	VB4	Control	VB4	Control	VB4
Duodenum	$4.16\times10^{11}\pm2.61\times10^{9}$	$4.40\times10^{11}\pm3.03\times10^{10}$	$7.26\times10^{11}\pm1.20\times10^{10}$	$7.64\times10^{11}\pm2.51\times10^{10}$	$1.15\times10^{11}\pm1.49\times10^{9}$	$1.24\times10^{11}\pm6.31\times10^{9}$	$2.88\times10^{11}\pm1.27\times10^{9}$	$3.16\times10^{11}\pm1.37\times10^{10}$
Jejunum	$4.67\times10^{11}\pm8.38\times10^{9}$	$4.25\times10^{11}\pm8.87\times10^{8}$	$7.88\times10^{11}\pm7.17\times10^{9}$	$7.23\times10^{11}\pm2.42\times10^{8}$	$1.35\times10^{11}\pm0.00$	$1.19\times10^{11}\pm3.22\times10^{8}$	$3.21\times10^{11}\pm4.11\times10^{9}$	$2.91\times10^{11}\pm5.16\times10^{9}$
Ileum	$4.37\times10^{11}\pm2.73\times10^{9}$	$3.57\times10^{11}\pm2.74\times10^{10}$	$7.37\times10^{11}\pm1.64\times10^{10}$	$5.91\times10^{11}\pm2.72\times10^{10}$	$1.09\times10^{11}\pm1.70\times10^{9}$	$8.72\times10^{10}\pm9.84\times10^{9}$	$2.65\times10^{11}\pm3.94\times10^{9}$	$2.16\times10^{11}\pm2.02\times10^{10}$
Colon T_{16h}	$1.18\times10^{9}\pm1.60\times10^{7}$	$5.06\times10^{8}\pm1.06\times10^{7}$	$1.22\times10^{9}\pm4.24\times10^{7}$	$4.40\times10^{8}\pm3.60\times10^{7}$	$3.95\times10^{8}\pm7.25\times10^{6}$	$1.53\times10^{8}\pm5.87\times10^{6}$	$8.04\times10^{8}\pm1.77\times10^{6}$	$2.93\times10^{8}\pm7.07\times10^{5}$
Colon T_{24h}	$2.20\times10^{8}\pm1.21\times10^{7}$	$2.48\times10^{8}\pm1.04\times10^{8}$	$2.29\times10^{8}\pm2.13\times10^{7}$	$2.47\times10^{8}\pm1.16\times10^{8}$	$7.00\times10^{7}\pm2.55\times10^{6}$	$8.00\times10^{7}\pm3.06\times10^{7}$	$1.46\times10^{8}\pm3.85\times10^{6}$	$1.42\times10^{8}\pm5.23\times10^{7}$

4.4 Discussion

Bile salt hydrolase (BSH) activity is a key probiotic function, particularly in *Lactobacillus* species, as it promotes gastrointestinal survival, modulates bile acid metabolism, and contributes to cholesterol reduction and cardiovascular health (Foley et al., 2021; Yang et al., 2019). In the present study, BSH activity of the *L. rhamnosus* VB4 strain was assessed using the upper GIT SHIME® model, under fed condition, providing a more realistic physiological state in which BSH activity can be optimally expressed as a probiotic feature. Furthermore, to elucidate the behavior of the VB4 administration under the influence of the gut microbial community, which represents a natural reservoir of BSH-positive bacteria in healthy individuals (Bourgin et al., 2021), the experiment was extended to the colonic fraction.

The strain survivability through the GIT passage was revealed by culture-dependent analysis and *bsh* gene expression profile was detected by qPCR. Across the simulated GI transit, the VB4 strain exhibited high resilience, with a modest loss of around 1 log unit, from the stomach to the ileum-end in fed condition. A similar upper GIT SHIME® experiment was conducted by Govaert and collaborators (2024), in which a freeze-dried probiotic formulation, inoculated at 9.7 $\log_{10}$ CFU/g under fasted (probiotic administration before a meal) condition, preserved high viability from the stomach to the ileal phases, showing around 2 log reduction in cell density at the final stage. According to that, previous studies have highlighted that exposure to gastric juice can drastically reduce probiotic survival.

These findings figure out the ability of the probiotic strain to adapt to gastric pH and enzymes, as well as to bile salts and pancreatic enzymes, which represent an additional critical factor to be overcome.

According to transcriptional data, *bsh* gene expression showed significant variations in several compartments of the gastrointestinal tract. In particular, when inoculated, *L. rhamnosus* VB4 showed higher gene expression levels in the stomach and a gradual decline towards the duodenal, jejunal, and ileal phases.

Conversely, as observed in literature (Duary et al., 2012), that *bsh* gene expression is inducible in conditions of bile richness, in this study it is clear to see that its expression is already present and detectable in the gastric compartment and then attenuates with the decrease in bile salt concentrations along the small intestine. These data suggest that, applying the upper GIT SHIME® system, in VB4 *bsh* transcription is detectable already in the gastric compartment (where no bile salts are present), consistent with a basal or 'constitutive-like' expression specific to this strain. In addition, *bsh* gene was further detected in the colon compartment up to 24 h of incubation. Despite the *bsh* expression being associated with the species *L. rhamnosus* as part of the commensal microbiota, VB4-inoculated samples displayed sustained *bsh* expression compared to the control sample, suggesting an overtime contribution of the VB4 strain in enhancing the deconjugation of BAs compared to the control.

Scientific evidence has revealed a close relationship between BAs deconjugation ability and *bsh* gene expression (Huang et al. 2025, Song et al., 2019). According to that, in this study the impact of the BAs profile after VB4 administration by detecting the main human glyco- and tauro-conjugated acids was demonstrated. Nevertheless, in

human bile, conjugated bile acids are predominantly glycine- and taurine-conjugated forms, approximately with a ratio of 3:1, respectively. Total bile salt concentrations in human typically range from 20 to 40 mM (Hofmann et al., 2008). Conversely, pancreatic juice for SHIME® system included Oxgall (Difco), in which the taurine-conjugated fraction is proportionally higher than in human bile and the overall composition is less representative of the exact spectrum of human BAs (Hu et al., 2018). Although Oxgall (bovine bile) is widely used in vitro to simulate the gastrointestinal environment of bile acids, these compositional differences must be taken into account for the comparison with human physiology.

In physiological conditions, BAs deconjugation starts in the small intestine with maximal activity occurring in the ileum and in the proximal colon (Deyaert et al., 2023; Gadaleta et al., 2022). On this basis, our study showed a progressive decrease in each detected conjugated BAs from the duodenum to the jejunum phases after VB4 administration, followed by a substantial decrease after the ileal phase. These results could confirm the highest deconjugation potential at the end of the small intestine. After 16 h of incubation (T_{16h}), the colonic fraction with VB4 administration showed significantly lower levels of conjugated bile acids compared to the control. This reduction reflects both the prolonged effect of VB4-mediated deconjugation in the small intestine and the physiological dilution of digested intestinal contents in the colon, which was also revealed in the control reactor. However, at T_{24h}, although the further reduction, VB4 did not alter BAs profile in the colonic fraction, except for a slight increase in GDCA (compared to the control). These finding suggests that, at this stage, VB4 is starting to lose its BSH potential, mainly expressed in the

proximal colon stages, as described by Ridlon and co-worker (2006) in their review article, which described the BAs metabolism.

4.5 Conclusions

This study provides novel insight into the dynamic interplay between the BSH-positve *L. rhamnosus* VB4 strain and BAs metabolism during the GIT. The obtained results demonstrate that VB4 exhibits robust gastrointestinal survivability and maintains transcriptional activity of the *bsh* gene, indicating its resilience during the harsh conditions of the digestive process. The modulation of the BAs profile, characterized by a marked reduction of conjugated BAs in the ileal phase, supports the strain's active deconjugation potential. These findings contribute to the growing body of evidence to support the use of BSH-positive probiotics shaping host BAs pools. Combining untargeted metabolomics with dynamic gut models offers a valuable approach to study the probiotic influence on BAs biotransformation, posing a new possibility for developing a personalized probiotic treatment in restoring gut microbiota and BAs dysregulation. These approaches will enable future studies to be conducted focusing on the effect of a daily administration of BSH-positive strains on the gut microbiota, using hypercholesterolemic subjects, in order to clarify the positive and negative effects of BSH probiotic activity on host physiology.

This work was conducted in collaboration with the University of Modena and Reggio Emilia, under the supervision of Professors Lisa Solieri and Davide Tagliazucchi, with the contribution of Dr. Marianna Cristofolini and Alice Cattivelli, during a research and training period within the doctoral project at the Department of Life Sciences.

Author contributions

Writing—original draft preparation, A.V, G.A., and A.C.; writing—review and editing, A.P., D.T., L.S., C.C. and C.L.R.; data curation, A.V., G.A., A.P., M.C., and A.C.; formal analysis, A.V, G.A., M.C., D.T., and A.C..; investigation, A.P., D.T., C.C., L.S. and C.L.R.; methodology, A.P., D.T., L.S. and C.L.R.; conceptualization, L.S., C.C., and C.L.R.; visualization, A.V, A.P, D.T., A.C., and C.L.R; and funding acquisition, A.P., L.S. and C.L.R. All authors have read and agreed to the published version of the manuscript.

Funding

The project was partially supported by FAR2024 (University of Modena and Reggio Emilia) and by the NRRP, Mission 4 Component 2 Investment 1.4—Call for tender No. 3138 of 16 December 2021, rectified by Decree n. 3175 of 18 December 2021 of the Italian Ministry of University and Research funded by the European Union—NextGenerationEU. Project Code CN_00000033, Concession Decree No. 1034 of 17 June 2022 adopted by the Italian Ministry of University and Research, CUP E93C22001090001, "National Biodiversity Future Center—NBFC".

Institutional review board statement

Fecal samples of the donor were collected according to the ethical approval issued by the Ethics Committee of the University of Modena and Reggio Emilia (CEAR) on 20/01/2025 related to the project "LEVANTE—Analisi probiogenomica e caratterizzazione funzionale di nuovi candidate lattobacillari probiotici con attività idrolasica degli acidi biliari (BSH)" (num. Prot. 332033).

Acknowledgment

The authors acknowledge the project PIAno di inCEntivi per la

RIcerca di Ateneo 2020/2022—Linea di Intervento 3 "Starting Grant". Project Title "Selezione di probiotici con attività idrolasica dei sali biliari (BSH) per la salute umana", ProBSH.

Conflict of interest

The authors Alessandra Pino, Cinzia Caggia and Cinzia Lucia Randazzo are founder of ProBioEtna a spinoff of the University of Catania. They have two affiliations but the employer is the University of Catania. The remaining authors declare that the research was conducted in the absence of any commercial or financial relationships that could be construed as a potential conflict of interest.

References

1. Agolino, G., Cristofolini, M., Vaccalluzzo, A., Tagliazucchi, D., Cattivelli, A., Pino, A., Caggia, C., Solieri, L., & Randazzo, C. L. (2025). Genome Mining and Characterization of Two Novel *Lacticaseibacillus rhamnosus* Probiotic Candidates with Bile Salt Hydrolase Activity. *Biomolecules*, *15*(1), 86. https://doi.org/10.3390/biom15010086.
2. Agolino, G., Pino, A., Vaccalluzzo, A., Cristofolini, M., Solieri, L., Caggia, C., & Randazzo, C. L. (2024). Bile salt hydrolase: The complexity behind its mechanism in relation to lowering-cholesterol lactobacilli probiotics. *Journal of Functional Foods*, *120*, 106357. https://doi.org/10.1016/j.jff.2024.106357.
3. Bourgin, M., Kriaa, A., Mkaouar, H., Mariaule, V., Jablaoui, A., Maguin, E., & Rhimi, M. (2021). Bile Salt Hydrolases: At the Crossroads of Microbiota and Human Health. *Microorganisms*, *9*(6), 1122. https://doi.org/10.3390/microorganisms9061122.
4. De Boever, P., Wouters, R., Verschaeve, L., Berckmans, P., Schoeters, G., & Verstraete, W. (2000). Protective effect of the bile salt hydrolase-active Lactobacillus reuteri against bile salt cytotoxicity. *Applied*

microbiology and biotechnology, *53*(6), 709–714. https://doi.org/10.1007/s002530000330.

5. Deng, C., Pan, J., Zhu, H., & Chen, Z. Y. (2023). Effect of Gut Microbiota on Blood Cholesterol: A Review on Mechanisms. *Foods (Basel, Switzerland)*, *12*(23), 4308. https://doi.org/10.3390/foods12234308.
6. Deyaert, S., Moens, F., Pirovano, W., van den Bogert, B., Klaassens, E. S., Marzorati, M., Van de Wiele, T., Kleerebezem, M., & Van den Abbeele, P. (2023). Development of a reproducible small intestinal microbiota model and its integration into the SHIME®-system, a dynamic *in vitro* gut model. *Frontiers in microbiology*, *13*, 1054061. https://doi.org/10.3389/fmicb.2022.1054061.
7. Duary, R. K., Batish, V. K., & Grover, S. (2012). Relative gene expression of bile salt hydrolase and surface proteins in two putative indigenous Lactobacillus plantarum strains under in vitro gut conditions. *Molecular biology reports*, *39*(3), 2541–2552. https://doi.org/10.1007/s11033-011-1006-9.
8. Duysburgh, C.; Van den Abbeele, P.; Marzorati, M. SHIME®: An Advanced In Vitro Technology Platform for Studying the Mode-of-Action of Probiotics in the Gastrointestinal Tract. *Nutrafoods*, *30*, 121–136. https://www.nutrafoods.eu/index.php/nutra/article/view/42 (accessed on 4 October 2025)
9. Foley, M. H., O'Flaherty, S., Allen, G., Rivera, A. J., Stewart, A. K., Barrangou, R., & Theriot, C. M. (2021). *Lactobacillus* bile salt hydrolase substrate specificity governs bacterial fitness and host colonization. *Proceedings of the National Academy of Sciences of the United States of America*, *118*(6), e2017709118. https://doi.org/10.1073/pnas.2017709118.
10. Gadaleta, R. M., Cariello, M., Crudele, L., & Moschetta, A. (2022). Bile Salt Hydrolase-Competent Probiotics in the Management of IBD: Unlocking the "Bile Acid Code". *Nutrients*, *14*(15), 3212. https://doi.org/10.3390/nu14153212.
11. Govaert, M., Rotsaert, C., Vannieuwenhuyse, C., Duysburgh, C., Medlin, S., Marzorati, M., & Jarrett, H. (2024). Survival of Probiotic Bacterial Cells in the Upper Gastrointestinal Tract and the Effect of the

Surviving Population on the Colonic Microbial Community Activity and Composition. *Nutrients*, *16*(16), 2791. https://doi.org/10.3390/nu16162791.

12. Huang, Y., Xu, W., Dong, W., Chen, G., Sun, Y., & Zeng, X. (2025). Anti-diabetic effect of dicaffeoylquinic acids is associated with the modulation of gut microbiota and bile acid metabolism. *Journal of advanced research*, *72*, 17–35. https://doi.org/10.1016/j.jare.2024.06.027.
13. Hofmann, A. F., & Hagey, L. R. (2008). Bile acids: chemistry, pathochemistry, biology, pathobiology, and therapeutics. *Cellular and molecular life sciences : CMLS*, *65*(16), 2461–2483. https://doi.org/10.1007/s00018-008-7568-6.
14. Hu, P. L., Yuan, Y. H., Yue, T. L., & Guo, C. F. (2018). Bile acid patterns in commercially available oxgall powders used for the evaluation of the bile tolerance ability of potential probiotics. *PloS one*, *13*(3), e0192964. https://doi.org/10.1371/journal.pone.0192964.
15. Jannin, V., Duysburgh, C., Gonzalez, V., Govaert, M., Agisson, M., Marzorati, M., & Madit, N. (2023). In vitro evaluation of the gastrointestinal delivery of acid-sensitive pancrelipase in a next generation enteric capsule using an exocrine pancreatic insufficiency disease model. *International journal of pharmaceutics*, *630*, 122441. https://doi.org/10.1016/j.ijpharm.2022.122441.
16. Joyce, S. A., MacSharry, J., Casey, P. G., Kinsella, M., Murphy, E. F., Shanahan, F., Hill, C., & Gahan, C. G. (2014). Regulation of host weight gain and lipid metabolism by bacterial bile acid modification in the gut. *Proceedings of the National Academy of Sciences of the United States of America*, *111*(20), 7421–7426. https://doi.org/10.1073/pnas.1323599111.
17. Kumar, M., Nagpal, R., Kumar, R., Hemalatha, R., Verma, V., Kumar, A., Chakraborty, C., Singh, B., Marotta, F., Jain, S., & Yadav, H. (2012). Cholesterol-lowering probiotics as potential biotherapeutics for metabolic diseases. *Experimental diabetes research*, *2012*, 902917. https://doi.org/10.1155/2012/902917.
18. Kusada, H., Morinaga, K., & Tamaki, H. (2021). Identification of Bile Salt Hydrolase and Bile Salt Resistance in a Probiotic

Bacterium *Lactobacillus gasseri* JCM1131^{T}. *Microorganisms*, *9*(5), 1011. https://doi.org/10.3390/microorganisms9051011.

19. Li, T., & Chiang, J. Y. (2015). Bile acids as metabolic regulators. *Current opinion in gastroenterology*, *31*(2), 159–165. https://doi.org/10.1097/MOG.0000000000000156.
20. Marzorati, M., Calatayud, M., Rotsaert, C., Van Mele, M., Duysburgh, C., Durkee, S., White, T., Fowler, K., Jannin, V., & Bellamine, A. (2021). Comparison of protection and release behavior of different capsule polymer combinations based on L. acidophilus survivability and function and caffeine release. *International journal of pharmaceutics*, *607*, 120977. https://doi.org/10.1016/j.ijpharm.2021.120977.
21. O'Flaherty, S., Briner Crawley, A., Theriot, C. M., & Barrangou, R. (2018). The *Lactobacillus*Bile Salt Hydrolase Repertoire Reveals Niche-Specific Adaptation. *mSphere*, *3*(3), e00140-18. https://doi.org/10.1128/mSphere.00140-18.
22. Ridlon JM, Kang DJ, Hylemon PB. Bile salt biotransformations by human intestinal bacteria. *J Lipid Res*. 2006;47(2):241-259. https://doi.org/10.1194/jlr.R500013-JLR200.
23. Rudzka, A., Patloka, O. N. D. Ř. E. J., Plecha, M., Królikowski, T., Oczkowski, M., Zborowski, M., ... & Zielinska, D. (2023). Changes in the microbiome of a human and in the simulator of human intestinal microbial ecosystem (SHIME®) in response to a diet and probiotic supplementation. *Żywność Nauka Technologia Jakość*, *30*. http://dx.doi.org/10.15193/zntj/2023/134/437.
24. Song, Z., Cai, Y., Lao, X., Wang, X., Lin, X., Cui, Y., Kalavagunta, P. K., Liao, J., Jin, L., Shang, J., & Li, J. (2019). Taxonomic profiling and populational patterns of bacterial bile salt hydrolase (BSH) genes based on worldwide human gut microbiome. *Microbiome*, *7*(1), 9. https://doi.org/10.1186/s40168-019-0628-3.
25. Song, Z., Feng, S., Zhou, X., Song, Z., Li, J., & Li, P. (2023). Taxonomic identification of bile salt hydrolase-encoding lactobacilli: Modulation of

the enterohepatic bile acid profile. *iMeta*, *2*(3), e128. https://doi.org/10.1002/imt2.128.

26. Van de Wiele, T., Van den Abbeele, P., Ossieur, W., Possemiers, S., & Marzorati, M. (2015). The Simulator of the Human Intestinal Microbial Ecosystem (SHIME®). In K. Verhoeckx (Eds.) et. al., *The Impact of Food Bioactives on Health: in vitro and ex vivo models*. (pp. 305–317). Springer. https://doi.org/10.1007/978-3-319-16104-4_27.
27. Yang, Y., Liu, Y., Zhou, S., Huang, L., Chen, Y., & Huan, H. (2019). Bile salt hydrolase can improve Lactobacillus plantarum survival in gastrointestinal tract by enhancing their adhesion ability. *FEMS microbiology letters*, *366*(8), fnz100. https://doi.org/10.1093/femsle/fnz100.

Chapter 5

5 Probiotic strains with Bile Salt Hydrolase activity reduce micellar cholesterol uptake in Caco-2 cells

Gianluigi Agolino[1], Kaisa Hiippala[2], Reetta Satokari[2], Cinzia L. Randazzo[1]

[1]Department of Agriculture, Food and Environment (Di3A), University of Catania, Via Santa Sofia 100, 95123 Catania, Italy
[2]Human Microbiome Research Program, Faculty of Medicine, University of Helsinki, Helsinki, Finland

Manuscript preparation

Graphical abstract

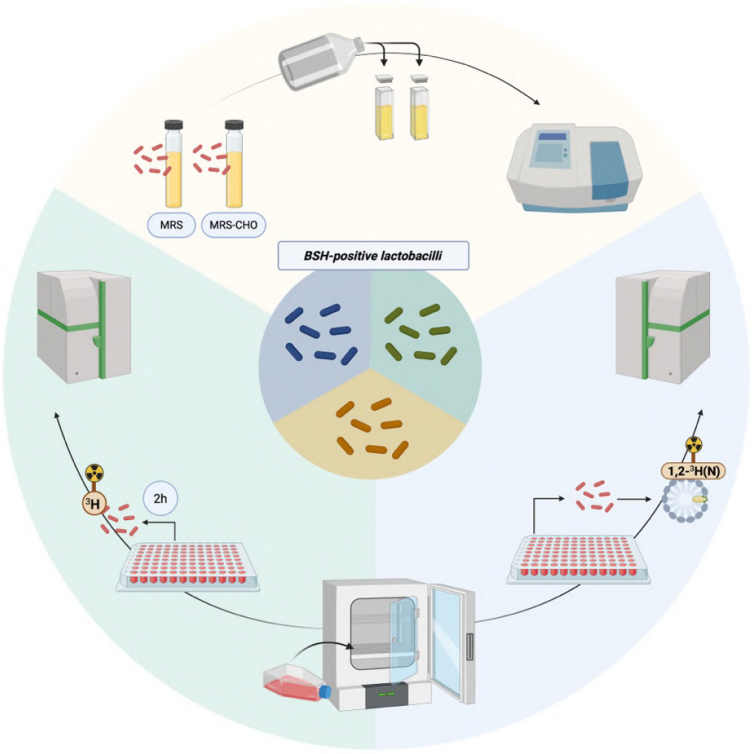

Abstract

Cardiovascular diseases (CVDs) remain the leading cause of global mortality, with hypercholesterolemia representing a critical risk factor in their onset and progression. Probiotics have emerged as

promising non-pharmacological strategies for cholesterol management, largely attributed to bile salt hydrolase (BSH) activity and their capacity to modulate host-microbiota interactions. In this study, three BSH-positive lactic acid bacteria (LAB) strains, *Lacticaseibacillus rhamnosus* VB1, *Lacticaseibacillus rhamnosus* VB4, and *Levilactobacillus brevis* M3R3, were investigated for their cholesterol-lowering potential using *in vitro* models. Cholesterol assimilation assays in MRS-CHO medium revealed variable assimilation efficiencies among strains, with VB1 displaying the highest activity. Adhesion tests to Caco-2 intestinal epithelial cells demonstrated strain-dependent adherence, with VB1 showing superior adhesive capacity. Furthermore, pre-incubation of Caco-2 cells with the tested strains significantly reduced micellar cholesterol uptake, suggesting an active role of bacterial adhesion and BSH activity in cholesterol modulation. These findings are consistent with previous reports, highlighting the role of probiotic adhesion and bile acid deconjugation in regulating lipid metabolism. Collectively, the results indicate that VB1, VB4, and M3R3 exhibit cholesterol-lowering properties, with VB1 emerging as the most efficient strain, a finding consistent with its strong BSH-related activity.

Keywords: cholesterol metabolism, cholesterol uptake, intestinal adhesion, bile salt hydrolase, probiotic

5.1 Introduction

In recent years, metabolic diseases have been increasingly recognized as major contributors to the development of cardiovascular diseases (CVD), which remains the leading cause of worldwide death according to the World Health Organization (WHO, 2015). Hypercholesterolemia, represent a critical factor in the progression of CVD, playing a pivotal role in metabolic dysfunction (Jiang et al., 2020); however, its effective management can markedly reduce the risk of CVD-related morbidity and mortality (Sivamaruthi et al. 2021). Currently, is emphasized the role of lifestyle modification and the use of non-pharmacological approaches as a first strategy in the management of hypercholesterolemia, considered sufficient to achieve therapeutic outcomes (Mannarino et al., 2014). In this context, a growing body of evidence has highlighted the beneficial effects of specific probiotic strains in prevention and treatment of metabolic disease (Cani & Van Hul, 2015), to avoid the use of drug therapies, particularly in mild hypercholesterolemic subjects (Mannarino et al., 2014). The use of probiotics has been extensively recognized for decades, due to their capacity to positively influence the gut microbiota and support overall host health. Emerging evidence suggested that probiotic strains may contribute to regulate the physiological serum cholesterol levels (Sharma et al., 2016). Probiotics exert cholesterol-lowering effects through various mechanisms, by influencing the gut microbial composition and function, although the underlying mechanisms are not fully elucidated (Le et al., 2019). Among these, probiotic may contribute to cholesterol reduction through the production of short-chain fatty acids (SCFAs), which can lower cholesterol levels by inhibiting 3-hydroxy-3-methyl-

glutaryl-coenzyme A (HMG-CoA) reductase and modulating lipid metabolism by activating peroxisome proliferation-activated receptors (PPARs), which reduce fat storage (Ishimwe et al., 2015). Additionally, probiotic strains can incorporate cholesterol molecules into their cell membrane, limiting its absorption in the host. The cholesterol-lowering effect was also linked to the cooperative relationship between the intestinal wall and the resident microbiota. The first mechanisms consist in the transformation of cholesterol by the cholesterol dehydrogenase/isomerase enzyme into coprostanol, a molecule more easily absorbed by the intestinal epithelium, and directly excreted by feces (Juste & Gérard, 2021). Lastly, some potential probiotic strains can inhibit cholesterol absorption by reducing its solubility through bile acid deconjugation mediated by bile salt hydrolase (BSH) enzyme, which promote fecal excretion of free bile acids (Agolino et al., 2024; Kim et al., 2004; Le et al., 2019).

The BSH activity is acknowledge by the European Food and Safety Authority (EFSA, 2023) as a probiotic trait, and it's supported by numerous *in vitro* and *in vivo* studies, demonstrating its role in the treatment of the hypercholesterolemia (Horackova et al., 2020; Liu et al., 2021; Palaniyandi et al., 2020; Zafar et al., 2022). At this regard, lactobacilli strains, abundantly recognized for their support in prevention and therapeutic interventions (Khare & Gaur, 2020), were extensively used for their ability to modulate the gut microbiota in maintaining the cholesterol homeostasis, mainly attributed to the BSH activity (Agolino et al., 2024; Begley et al., 2006). Although the BSH activity is commonly linked to gut-associated bacteria, several non-intestinal *Lactobacillus* strains have shown significant BSH potential, highlighting these as an alternative valuable source of probiotic with

bile acids deconjugation capacity (Fontana et al., 2013; Ru et al., 2019). In the present study, two human-derived *Lacticaseibacillus rhamnosus* strains (VB4 and VB1), along with a *Levilactobacillus brevis* strain (M3R3) isolated from sourdough, were investigated for their involvement in cholesterol-lowering activity. For this purpose, *in vitro* tests were conducted in order to understand the potential cholesterol-lowering mechanisms associated to BSH-positive strains, by using Caco-2 cell lines, in order to assess the strains' ability to adhere at the intestinal epithelia barrier and reduce the cholesterol uptake into Caco-2 cells during lipid micelles exposure. These tests may provide preliminary insight into the potential impact of the selected strains on cholesterol metabolism and their interaction with the intestinal conditions.

5.2 Material and Methods

5.2.1 Bacterial strains and culture conditions

The three BSH-positive *Lacticaseibacillus rhamnosus* VB1, *Lacticaseibacillus rhamnosus* VB4, and *Levilactobacillus brevis* M3R3 strains, belonging to the microbial collection of ProBioEtna srl, Spin Off of the University of Catania (Italy), were previously characterized for their BSH activity at both phenotypic and genomic level. These strains were selected for its probiogenomic profile and for its high ability to deconjugate and growth in presence of bile acids. During experimental procedure, the strains were routinely cultured in de Man, Rogosa and Sharpe (MRS, Oxoid, UK) Agar, and incubated at 37 °C for 48 h.

5.2.2 Lactobacilli in vitro cholesterol assimilation activity

The ability of BSH-positive lactobacilli to assimilate cholesterol was tested according to the method previously described by Qayyum and co-worker (2023). Cholesterol stock solution was prepared in a 1:1 mixture of pure ethanol and Tween80 and sterilized by filtration before use. A freshly MRS broth was supplemented with 100 µg/ml of the cholesterol stock solution (MRS-CHO) and 0.3% of bile salts mixture (Oxgall, Millipore-Sigma, Germany), then 5 ml of the media was inoculated with 1% on an overnight culture of each strain and left to grown in anaerobic condition at 37 °C for 24h. the control group was represented to an inoculated MRS-CHO. Subsequently, the inoculated strains were centrifuged for 15 min at 9,000 × *g* at 4 °C, and the supernatant was collected onto sterile tubes. The *o*-phthalaldehyde (OPA) method proposed by Rudel and Morris (1973), with slight modification (Bhat et al., 2020; Qayyum et al., 2023), was assessed to determine the cholesterol residual compound. Briefly, 1 ml KOH (33%, *w*/*v*) and 2 ml of absolute ethanol were carefully mixed with 1 ml of the supernatant for 1 min and incubated at 37 °C for 15 min (including also MRS-CHO as control), Subsequently cooling at room temperature, adding 2 ml of sterile dH_2O and 3 ml of hexane, then vortexed for 1 min, place 1 ml of hexane layer into glass tube and were incubated at 65 °C and mixed using a thermal mixer until evaporation. At once, a freshly prepared OPA reagent (0.5 mg/ml in glacial acetic acid) was added into the tubes and shake for 1 min. The reaction mixture was thoroughly mixed and allowed to stand at room temperature for 10 minutes before adding 2 ml of concentrated H_2SO_4. After 10 min, the reaction mixture was measured spectrophotometrically (A_{550nm}) using 1-2 ml of the reaction

mixture. The cholesterol assimilation rate was calculated using the formula $[1 - (A_0 - A_t)/A_0] \times 100\%$, where A_0 represents the absorbance of the control group (sterile MRS-CHO medium), and A_t denotes the absorbance of the supernatant from the experimental group. The experiment was carried out in triplicate.

5.2.3 Caco-2 cell cultures

Caco-2 cells (ACC 169) were obtained from the German Collection of Microorganisms and Cell Culture (DSMZ). The human colonic cell lines were cultivated according to Hiippala and co-worker (2020) in Roswell Park Memorial Institute (RPMI) 1640 Medium (Sigma-Aldrich, USA), supplemented with 20% of heat-inactivated fetal bovine serum (FBS; 56 °C for 30 min; Gibco, USA), 1% (*v*/*v*) of nonessential amino acid (NEAA; Lonza, Belgium), 15 mM HEPES (Lonza, Belgium), 2 mM L-glutamine (Ultra-glutamine; Lonza, Belgium) and 100 U ml^{-1} penicillin/streptomycin solution (PEST). Cells were maintained at 37 °C under humidified atmosphere with 5% CO_2 and passaged upon reaching 80% confluence. TryplExpress (Lonza, Belgium) was used to detach cells starting to passage number 3 until 28, used in this experiment.

5.2.4 Adhesion ability test to Caco-2 cell

Adhesion to human epithelia Caco-2 cells was assessed by metabolically labeling bacterial cells with radioactive [^{3}H]-thymidine, followed by quantification using liquid scintillation counting, as described by Hiippala and co-worker (2022). The adherence of *L. rhamnosus* VB4, *L. rhamnosus* VB1, and *L. brevis* M3R3 to Caco-2 cell lines (seeded 14 days prior). The *L. rhamnosus* GG (ATCC

53103) was used as a reference strain in all adhesion experiments.

Briefly, Caco-2 were plated on a 96-well tissue culture plate with 12,500 cells $well^{-1}$ (Nunc), subculturing using RPMI 1640 medium supplemented with 10% of FBS and maintained at 37 °C under humidified atmosphere with 5% CO_2. For the experiment, each bacterial strain was propagated in MRS agar plates and incubated anaerobically at 37 °C for 48 hours. Colonies were inoculated in 1 ml of MRS broth supplemented with 10 µl of [6′-^{3}H]-thymidine (17.6 Ci/mmol; PerkinElmer, USA) for metabolic radiolabeling. Following overnight incubation at 37 °C (5% CO_2), the bacterial cells were harvested by centrifugation at 2,500 × *g* for 5 minutes and washed with PBS. The optical density was adjusted in RPMI 1640 supplemented with FBS at 600 nm (OD_{600nm}) to 0.25, which correspond approximately at the final concentration of 8 $\log_{10}$ CFU/ml. Caco-2 cells were washed one time with PBS, before adding 100 µl of the radiolabeled bacterial suspension to each well. The 96-well plate was incubated for 2 hours at 37 °C, and non-adherent bacteria were removed washing twice with PBS. Adherent bacteria were then lysed by adding 100 µl of lysis buffer, followed by overnight incubation at 37 °C. The lysate were transferred into vials containing 1 ml of scintillation liquid cocktail (OptiPhase HiSafe 3, Wallac, Turku, Finland) and radioactivity was measured using a liquid scintillation counter (PerkinElmer MicroBeta², Waltham, MA, USA). Bacterial adhesion was expressed as the percentage of bound bacteria relative to the radioactivity of the bacterial suspension initially added to the wells.

5.2.5 Preparation of cholesterol micellar solution

Cholesterol micelles were prepared according to the previously described methods by Hiebl and co-worker (2020), with minor modifications. Briefly, micelles were prepared in solution of chloroform:methanol 2:1 containing 0.025 mM cholesterol (Sigma-Aldrich, German), 0.1 mM L-α-lysophosphatidylcholine (Sigma-Aldrich, German), 0.15 mM oleic acid (Sigma-Aldrich, German), and 0.5 µCi/ml of [1,2-^{3}H(N)]-cholesterol (9250 KBq/ml, Revvity, USA), and carefully mixed in a glass vial, and dried under a nitrogen flow. The resulting lipid film was subsequently dissolved in free RPMI 1640 containing 1 mM of taurodeoxycholic acid, sodium salt (TDCA, Millipore, USA).

5.2.6 Caco-2 cell cholesterol uptake assay

For the cholesterol uptake test, Caco-2 cells were seeded on 96-well plate (12,500 cells per well; Nunc) and cultured for 14 days. The days before the experiment, cells were incubated in serum-free RPMI supplemented with 1% (*v*/*v*) of nonessential amino acid (NEAA; Lonza, Belgium), 15 mM HEPES (Lonza, Belgium), 2 mM L-glutamine (Ultra-glutamine; Lonza, Belgium) and 100 U ml^{-1} penicillin/streptomycin solution (PEST). The cholesterol uptake test was assessed using previously established protocol, with slight modification (Le et al., 2018; Michaels et al., 2016). In details, the 14 days Caco-2 monolayer, prepared as mentioned in section 2.3, was washed once time with PBS and seeded with 100 µl of VB1, VB4 and M3R3 strains adjusted at 0.25 OD_{600nm}. After 2 hours of incubation, 100 µl of micellar solution were added to the Caco-2 cells and incubated for 5 hours (37 °C with 5% CO_2). Following incubation, micelles were withdrawn, and the unincorporated radiolabeled

cholesterol residues were removed by washing wells twice with PBS. In both experiments, the cells were homogenized with 100 µl of lysis buffer (1%SDS-0.1 M NaOH), to easily detach cells after overnight incubation, and transferred into vials containing 1 ml of scintillation liquid cocktail (OptiPhase HiSafe 3, Wallac, Turku, Finland). Radioactivity in the cells was measured by liquid scintillation counter (PerkinElmer MicroBeta², Waltham, MA, USA), and cholesterol uptake percentage was expressed as ratio between the radioactivity detected in the cell fraction and that of the micellar solution. *L. rhamnosus* GG (ATCC 53103), was used as a reference strain.

5.2.7 Statistical analysis

Statistical analysis and graph generation were performed with GraphPad Prism 10 (GraphPad Software, La Jolla, CA, USA). The one-way ANOVA, followed by Tukey's *post*-hoc test for multiple pairwise comparisons, was applied for all analyses. A p-value < 0.05 was considered statistically significant.

5.3 Results

5.3.1 Cholesterol assimilation capability of lactobacilli strains

Data on cells cholesterol assimilation showed that the three BSH-positive lactobacilli strains resulted removed cholesterol from MRS-CHO medium after 24 h of incubation. The tested strains exhibited cholesterol assimilation efficiencies at various extent, although the obtained data are not statistically significant ($p > 0.05$) (**Figure 5.1**). The highest cholesterol assimilation was observed in *L. rhamnosus* VB1, followed to M3R3, and VB4.

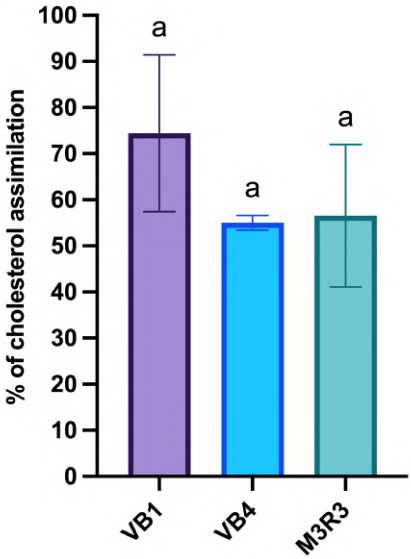

Figure 5.1 - *In vitro* cholesterol assimilation activity of *L. rhamnosus* VB1, *L. rhamnosus* VB4, *L. brevis* M3R3 in MRS-CHO media, expressed as % of cholesterol assimilation by bacterial cells

5.3.2 Adhesion to intestinal epithelial cells Caco-2

The adhesion to intestinal epithelial cells Caco-2 cells of the VB1, VB4, and M3R3 is shown in **Figure 5.2**. In accordance with the methodology described by Pino and co-worker (2024), a 1% adhesion cut-off corresponding to the level of non-specific background binding, was used to differentiate adherent from non-adherent strains. All three strains, exceeded the predefined threshold, exhibiting a good adherence to Caco-2 cells, with adhesion values of 17.34 ± 1.53 %, 11.04 ± 0.98 %, and 8.2 ± 2.26 % for VB1, VB4, and M3R3, respectively.

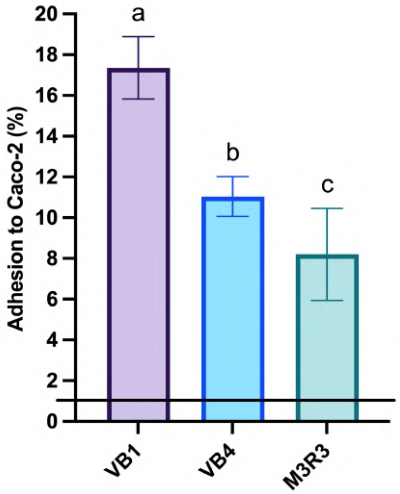

Figure 5.2 - Adhesion to human intestinal epithelium cells (Caco-2) exhibited by *L. rhamnosus* VB1, *L. rhamnosus* VB4, and *L. brevis* M3R3. Results are expressed as percentage of the added bacterial cells. Data represent the mean ± standard deviation (SD) from a representative experiment performed in six replicates. Statistical significance is indicated with letters ($p < 0.05$).

5.3.3 Cholesterol uptake by Caco-2 cells

To determine the cholesterol-lowering ability, the VB1, VB4, and M3R3 strains were pre-incubated for 2 h on a fully differentiated 14-day Caco-2 cell monolayer, followed by exposure to lipid micelles for 5 h. Prior to assessing cholesterol uptake by epithelial cell model, the three lactobacilli strains were evaluated under the same experimental conditions in the absence of Caco-2 cells, in order to verify their intrinsic ability to incorporate radiolabeled cholesterol from the micellar solution. **Figure 5.3A** showed strains' capacity to bind labeled cholesterol, demonstrating that VB4, M3R3, and L.GG

exhibited significantly higher binding capacity than VB1 ($p > 0.05$).

Following 2 h treatment of Caco-2 with bacterial strains and 5 h exposition of micellar solution, cholesterol uptake was measured in overnight Caco-2 lysate cells and compared with cells exposed to micelles without prior bacterial treatment (control). As shown in **Figure 3B**, Caco-2 cells treated with BSH-positive strains displayed a significantly reduced cholesterol micelle uptake as compared to the control. The results, expressed as percentage of cholesterol intake by Caco-2 cells, showed a statistically significant reduction compared to the control ($p < 0.05$) for all samples. Notably, VB1 exhibited higher cholesterol reduction compared with the other strains, including the reference strain *L. rhamnosus* GG.

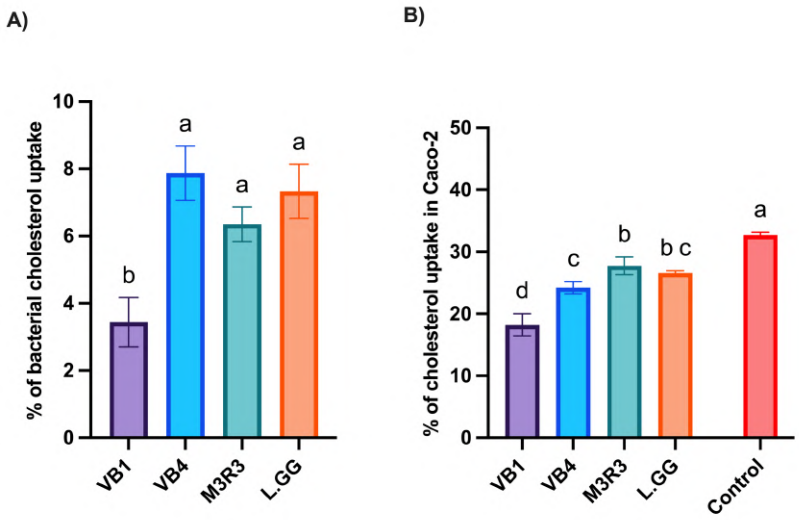

Figure 5.3 - Cholesterol uptake ability of lactobacilli strains. (A) Binding of

radiolabeled cholesterol from micellar solution in *L. rhamnosus* VB1, *L. rhamnosus* VB4, and *L. brevis* M3R3 compared with *L. rhamnosus* GG as reference strains. The results are expressed as percentage of cholesterol uptake in bacterial cells and the error bas indicated SD. (B) Cholesterol uptake in differentiated Caco-2 cells after 5 h of exposure to lipid micelles, following 2 h of pre-incubation with the tested strains (included *L. rhamnosus* GG as a reference strain) compared with Caco-2 cells without prior treatment with bacteria. Data are expressed as percentage of relative cholesterol uptake by the Caco-2 cells. All the results are expressed in mean ± SD, and statistical significance between all the samples was indicated with letters (a, b, c, d) ($p < 0.05$).

5.4 Discussion

Elevated serum cholesterol and triglyceride levels are well-recognized risk factors for CVDs (Missen et al., 2009). Recent studies have highlighted the potential of microbiota-based strategies, particularly in the use of specific probiotics which modulate lipid metabolism by reducing total cholesterol, triglycerides, and low-density lipoproteins (LDL) cholesterol, supporting their role as a natural approach to CVDs prevention (Gao & Li, 2018; Huang & Zeng, 2010).

In this study, we explored the role of three potential lactobacilli probiotic strains, from different origins, with established BSH activity. This enzymatic function is strictly connected to probiotic cholesterol-lowering ability, and to bile tolerance, improving bacterial persistence within the gastrointestinal tract (Gao & Li, 2018), features that, in turn may contribute to improved adhesion and long-term colonization capacity. Here, the BSH-positive *L. rhamnosus* VB1, *L. rhmanosus* VB4, and *L. brevis* M3R3 strains exhibited a moderate cholesterol assimilation capacity compared with numerous tested lactic acid

bacteria (LAB). The capacity to lower cholesterol levels under *in vitro* culture systems (cholesterol-supplemented MRS medium) was comparable with the cholesterol assimilation rate of *L. acidophilus* ATCC 43121, used in other studies as reference strains for its well-known high assimilation capacity by the cellular membrane (Frappier et al., 2022; Song et al., 2015). Additionally, *in vitro* cholesterol assimilation was observed in several lactobacilli which are able to deconjugate bile salts, supporting BSH potential (Kumar et al., 2012; Tsai et al., 2014). This observation providing a positive correlation between the tauro/glyco-deconjugation ability and cholesterol assimilation in the growth media, which may serve as preliminary evidence supporting the cholesterol-lowering capacity of the three BSH-positive lactobacilli. The survival and colonization of LAB in the gastrointestinal tract are critical determinants of their functional effectiveness (Lv et al., 2024). We next examined VB1, VB4, and M3R3 strains interactions with gastrointestinal epithelium, providing important into their adhesive capacity and persistence. The results are consistent compared with previous findings (Pino et al., 2022; Tuomola & Salminen, 1998), showing that VB1 exhibited the highest adhesion rate to Caco-2 cells (74.42%), followed by M3R3 (56.55%), and VB4 (55.04%). Adhesion to the intestinal epithelium represent a key trait underlying probiotic potential. Bacterial colonization not only support persistence within the gut environment but also facilitates interactions with the resident microbiota and host epithelial cells, essential for the expression of their beneficial functions, as cholesterol-lowering activity (Le et al., 2018; Tuomola et al., 1998). Notably, the strong interaction between the tested strains and Caco-2 reduced the cholesterol uptake when subsequently exposed to lipid

micelles, in agreement with other studies which verified cholesterol reduction properties (Huang et al., 2009; Le et al., 2018; Michael et al., 2016; Yoon et al., 2013), underpinning the hypothetical involvement of BSH positivity of all the tested strains.

5.5 Conclusions

The present study demonstrates that the three BSH-positive strains *L. rhamnosus* VB1, *L. rhamnosus* VB4, and *L. brevis* M3R3 exhibited promising cholesterol-lowering activity compared with the control. *In vitro* test demonstrated that they are able to assimilate cholesterol in the media and reduce the cholesterol uptake in Caco-2 during micelles exposure. Among these, VB1 displayed the highest probiotic performance, and could be considered the best strain regarding epithelial adherence and cholesterol-lowering potential. Despite these findings reinforce the relevance of bacterial BSH activity and its potential role in modulating host´s cholesterol uptake, it is important to better elucidate the molecular pathways linked to cholesterol metabolism and BSH activity, as well as exploring the interaction of these strains with host immune response and gut microbiota composition.

This work was conducted in collaboration with the University of Helsinki, under the supervision of Professor Reetta Satokari, with the contribution of Dr. Kaisa Hiippala, during a research and training period within the doctoral project at the Department of Bacteriology and Immunology, Human Microbiome Research Project (HUMI), Faculty of Medicine.

References

1. Agolino, G., Pino, A., Vaccalluzzo, A., Cristofolini, M., Solieri, L., Caggia, C., & Randazzo, C. L. (2024). Bile salt hydrolase: The complexity behind its mechanism in relation to lowering-cholesterol lactobacilli probiotics. *Journal of Functional Foods*, *120*, 106357. https://doi.org/10.1016/j.jff.2024.106357.
2. Bhat, B., & Bajaj, B. K. (2020). Multifarious cholesterol lowering potential of lactic acid bacteria equipped with desired probiotic functional attributes. *3 Biotech*, *10*(5), 200. https://doi.org/10.1007/s13205-020-02183-8.
3. Cani, P. D., & Van Hul, M. (2015). Novel opportunities for next-generation probiotics targeting metabolic syndrome. *Current opinion in biotechnology*, *32*, 21–27. https://doi.org/10.1016/j.copbio.2014.10.006
4. EFSA, E. (2023). *European food safety authority*.
5. Fontana, L., Bermudez-Brito, M., Plaza-Diaz, J., Muñoz-Quezada, S., & Gil, A. (2013). Sources, isolation, characterisation and evaluation of probiotics. *The British journal of nutrition*, *109 Suppl 2*, S35–S50. https://doi.org/10.1017/S0007114512004011.
6. Frappier, M., Auclair, J., Bouasker, S., Gunaratnam, S., Diarra, C., & Millette, M. (2022). Screening and characterization of some Lactobacillaceae for detection of cholesterol-lowering activities. *Probiotics and antimicrobial proteins*, *14*(5), 873-883. https://doi.org/10.1007/s12602-022-09959-9.
7. Hiippala, K., Barreto, G., Burrello, C., Diaz-Basabe, A., Suutarinen, M., Kainulainen, V., Bowers, J. R., Lemmer, D., Engelthaler, D. M., Eklund, K. K., Facciotti, F., & Satokari, R. (2020). Novel *Odoribacter splanchnicus* Strain and Its Outer Membrane Vesicles Exert Immunoregulatory Effects *in vitro*. *Frontiers in microbiology*, *11*, 575455. https://doi.org/10.3389/fmicb.2020.575455.
8. Gao, Y., & Li, D. (2018). Screening of lactic acid bacteria with cholesterol-lowering and triglyceride-lowering activity in vitro and evaluation of probiotic function. *Annals of Microbiology*, *68*(9), 537-545. https://doi.org/10.1007/s13213-018-1360-0.

9. Hiebl, V., Schachner, D., Ladurner, A., Heiss, E. H., Stangl, H., & Dirsch, V. M. (2020). Caco-2 Cells for Measuring Intestinal Cholesterol Transport - Possibilities and Limitations. *Biological procedures online*, *22*, 7. https://doi.org/10.1186/s12575-020-00120-w.
10. Hiippala, K., Khan, I., Ronkainen, A., Boulund, F., Vähä-Mäkilä, H., Suutarinen, M., Seifert, M., Engstrand, L., & Satokari, R. (2022). Novel strain of *Pseudoruminococcus massiliensis* possesses traits important in gut adaptation and host-microbe interactions. *Gut microbes*, *14*(1), 2013761. https://doi.org/10.1080/19490976.2021.2013761.
11. Horackova, S., Vesela, K., Klojdova, I., Bercikova, M., & Plockova, M. (2020). Bile salt hydrolase activity, growth characteristics and surface properties in Lactobacillus acidophilus. *European Food Research and Technology*, *246*(8), 1627-1636. https://doi.org/10.1007/s00217-020-03518-8.
12. Huang, Y., & Zheng, Y. (2010). The probiotic Lactobacillus acidophilus reduces cholesterol absorption through the down-regulation of Niemann-Pick C1-like 1 in Caco-2 cells. *The British journal of nutrition*, *103*(4), 473–478. https://doi.org/10.1017/S0007114509991991.
13. Ishimwe, N., Daliri, E. B., Lee, B. H., Fang, F., & Du, G. (2015). The perspective on cholesterol-lowering mechanisms of probiotics. *Molecular nutrition & food research*, *59*(1), 94–105. https://doi.org/10.1002/mnfr.201400548.
14. Jiang, J., Wu, C., Zhang, C., Zhao, J., Yu, L., Zhang, H., Narbad, A., Chen, W., & Zhai, Q. (2020). Effects of probiotic supplementation on cardiovascular risk factors in hypercholesterolemia: A systematic review and meta-analysis of randomized clinical trial. *Journal of Functional Foods*, *74*, 104177. https://doi.org/10.1016/j.jff.2020.104177.
15. Juste, C., & Gérard, P. (2021). Cholesterol-to-Coprostanol Conversion by the Gut Microbiota: What We Know, Suspect, and Ignore. *Microorganisms*, *9*(9), 1881. https://doi.org/10.3390/microorganisms9091881.
16. Khare, A., & Gaur, S. (2020). Cholesterol-Lowering Effects of Lactobacillus Species. *Current microbiology*, *77*(4), 638–644. https://doi.org/10.1007/s00284-020-01903-w.

17. Kim, G. B., Yi, S. H., & Lee, B. H. (2004). Purification and characterization of three different types of bile salt hydrolases from Bifidobacterium strains. *Journal of dairy science*, *87*(2), 258–266. https://doi.org/10.3168/jds.S0022-0302(04)73164-1.
18. Kumar, R., Grover, S., & Batish, V. K. (2012). Bile Salt Hydrolase (Bsh) Activity Screening of Lactobacilli: In Vitro Selection of Indigenous Lactobacillus Strains with Potential Bile Salt Hydrolysing and Cholesterol-Lowering Ability. *Probiotics and antimicrobial proteins*, *4*(3), 162–172. https://doi.org/10.1007/s12602-012-9101-3.
19. Le, B., & Yang, S. H. (2019). Effect of potential probiotic Leuconostoc mesenteroides FB111 in prevention of cholesterol absorption by modulating NPC1L1/PPARα/SREBP-2 pathways in epithelial Caco-2 cells. *International microbiology : the official journal of the Spanish Society for Microbiology*, *22*(2), 279–287. https://doi.org/10.1007/s10123-018-00047-z.
20. Le, B., & Yang, S. H. (2019). Identification of a Novel Potential Probiotic Lactobacillus plantarum FB003 Isolated from Salted-Fermented Shrimp and its Effect on Cholesterol Absorption by Regulation of NPC1L1 and PPARα. *Probiotics and antimicrobial proteins*, *11*(3), 785–793. https://doi.org/10.1007/s12602-018-9469-9.
21. Lv, C., Pang, X., Sun, J., Li, X., & Lu, Y. (2024). Screening of bile salt hydrolase-producing lactic acid bacteria and evaluation of cholesterol-lowering activity in vitro. *Food Bioscience*, *62*, 105338. https://doi.org/10.1016/j.fbio.2024.105338.
22. Mannarino, M. R., Ministrini, S., & Pirro, M. (2014). Nutraceuticals for the treatment of hypercholesterolemia. *European journal of internal medicine*, *25*(7), 592–599. https://doi.org/10.1016/j.ejim.2014.06.008.
23. Michael, D. R., Moss, J. W., Calvente, D. L., Garaiova, I., Plummer, S. F., & Ramji, D. P. (2016). Lactobacillus plantarum CUL66 can impact cholesterol homeostasis in Caco-2 enterocytes. *Beneficial microbes*, *7*(3), 443–451. https://doi.org/10.3920/BM2015.0146.
24. Palaniyandi, S. A., Damodharan, K., Suh, J. W., & Yang, S. H. (2020). Probiotic Characterization of Cholesterol-Lowering Lactobacillus fermentum MJM60397. *Probiotics and antimicrobial proteins*, *12*(3), 1161–1172. https://doi.org/10.1007/s12602-019-09585-y.

25. Pino, A., Hiippala, K., Ronkainen, A., Vaccalluzzo, A., Caggia, C., Satokari, R., & Randazzo, C. L. (2024). Adhesion Properties and Pathogen Inhibition of Vaginal-Derived Lactobacilli. *Probiotics and antimicrobial proteins*, 10.1007/s12602-024-10390-5. Advance online publication. https://doi.org/10.1007/s12602-024-10390-5.
26. Pino, A., Vaccalluzzo, A., Caggia, C., Balzaretti, S., Vanella, L., Sorrenti, V., Ronkainen, A., Satokari, R., & Randazzo, C. L. (2022). *Lacticaseibacillus rhamnosus*CA15 (DSM 33960) as a Candidate Probiotic Strain for Human Health. *Nutrients*, *14*(22), 4902. https://doi.org/10.3390/nu14224902.
27. Qayyum, N., Shuxuan, W., Yantin, Q., Ruiling, W., Wang, S., Ismael, M., & Lü, X. (2023). Characterization of Short-chain fatty acid-producing and cholesterol assimilation potential probiotic Lactic acid bacteria from Chinese fermented rice. *Food Bioscience*, *52*, 102404. https://doi.org/10.1016/j.fbio.2023.102404.
28. Ru, X., Zhang, C. C., Yuan, Y. H., Yue, T. L., & Guo, C. F. (2019). Bile salt hydrolase activity is present in nonintestinal lactic acid bacteria at an intermediate level. *Applied microbiology and biotechnology*, *103*(2), 893–902. https://doi.org/10.1007/s00253-018-9492-5.
29. Rudel, L. L., & Morris, M. D. (1973). Determination of cholesterol using o-phthalaldehyde. *Journal of lipid research*, *14*(3), 364–366.
30. Sharma, S., Kurpad, A. V., & Puri, S. (2016). Potential of probiotics in hypercholesterolemia: A meta-analysis. *Indian journal of public health*, *60*(4), 280–286. https://doi.org/10.4103/0019-557X.195859.
31. Sivamaruthi, B. S., Bharathi, M., Kesika, P., Suganthy, N., & Chaiyasut, C. (2021). The administration of probiotics against hypercholesterolemia: a systematic review. *Applied Sciences*, *11*(15), 6913. https://doi.org/10.3390/app11156913.
32. Song, M., Yun, B., Moon, J. H., Park, D. J., Lim, K., & Oh, S. (2015). Characterization of Selected Lactobacillus Strains for Use as Probiotics. *Korean journal for food science of animal resources*, *35*(4), 551–556. https://doi.org/10.5851/kosfa.2015.35.4.551.
33. Tsai, C. C., Lin, P. P., Hsieh, Y. M., Zhang, Z. Y., Wu, H. C., & Huang, C. C. (2014). Cholesterol-lowering potentials of lactic acid bacteria based on bile-salt hydrolase activity and effect of potent strains on

cholesterol metabolism in vitro and in vivo. *TheScientificWorldJournal*, *2014*, 690752. https://doi.org/10.1155/2014/690752.

34. Tuomola, E. M., & Salminen, S. J. (1998). Adhesion of some probiotic and dairy Lactobacillus strains to Caco-2 cell cultures. *International journal of food microbiology*, *41*(1), 45–51. https://doi.org/10.1016/s0168-1605(98)00033-6.
35. Turek, S., Rudan, I., Smolej-Narančić, N., Szirovicza, L., Čubrilo-Turek, M., Žerjavić-Hrabak, V., ... & Rudan, P. (2001). A large cross-sectional study of health attitudes, knowledge, behaviour and risks in the post-war croatian population (the first croatian health project*). *Collegium antropologicum*, *25*(1), 77-96.
36. Yoon, H. S., Ju, J. H., Kim, H. N., Park, H. J., Ji, Y., Lee, J. E., Shin, H. K., Do, M. S., & Holzapfel, W. (2013). Reduction in cholesterol absorption in Caco-2 cells through the down-regulation of Niemann-Pick C1-like 1 by the putative probiotic strains Lactobacillus rhamnosus BFE5264 and Lactobacillus plantarum NR74 from fermented foods. *International journal of food sciences and nutrition*, *64*(1), 44–52. https://doi.org/10.3109/09637486.2012.706598.
37. Zafar, H., Ain, N. U., Alshammari, A., Alghamdi, S., Raja, H., Ali, A., Siddique, A., Tahir, S. D., Akbar, S., Arif, M., Alharbi, M., & Rahman, A. (2022). *Lacticaseibacillus rhamnosus* FM9 and *Limosilactobacillus fermentum* Y57 Are as Effective as Statins at Improving Blood Lipid Profile in High Cholesterol, High-Fat Diet Model in Male Wistar Rats. *Nutrients*, *14*(8), 1654. https://doi.org/10.3390/nu14081654.

Chapter 6

6 General discussion and conclusions

Probiotic strains are live microorganisms widely recognized for their beneficial role, by supporting the microbial balance of the gastrointestinal tract (Gupta & Garg, 2009). Into practical applications, probiotic cultures are now widely incorporated into foods to develop products with health-promoting properties (Champagne & Gardner, 2005). This potential relies on multiple mechanisms, including the ability to modify both composition and function of the gut microbiota, thereby influencing host physiology and metabolism (Khare & Gaur, 2020). Growing attention has been directed toward the role of probiotics in modulating host lipid metabolism and contributing to cardiovascular health. The selection of potential probiotic strains might regulate lipid homeostasis, including cholesterol metabolism, has emerged as a promising complementary strategy alongside conventional therapies for reducing cardiovascular risk (Olas, 2020).

From this perspective, the modulation of bile acids (BAs) metabolism through microbial bile salt hydrolase (BSH) activity represent a key mechanism connecting gut microbiota homeostasis with host cholesterol regulation, has become an important criterion for probiotic selection (Dong et al., 2025).

As highlighted in the literature review (Chapter 1), the complex interplay between BAs and gut microbiota extends beyond the BSH pathway. Chapter 1 further examined the emerging evidence on various *Lactobacillus* species, isolated from human and food sources,

with demonstrated cholesterol-lowering effects, as supported by both experimental and clinical studies. Notably, BSH positive *Lactobacillus* strains exhibit considerable variability in their enzymatic activity and metabolic impact, underscoring the relevance of a rational and targeted selection of probiotic candidates. This is particularly important for probiotic strategies aimed at specific effects like cholesterol reduction.

The advent of probiogenomics has provided a powerful tool to investigate inside bacterial genome to provide functional probiotic trait, and bacterial safety (Ventura et al., 2009). Genetic approaches have greatly advanced the understanding of BSH, revealing substantial inter- and intra-species variability among lactobacilli *bsh* genes diversity and distribution (Kang et al., 2025). These insights are particularly relevant given the recent taxonomic re-classification of the *Lactobacillus* genus, emphasizing the necessity of comprehensive genomic investigations to optimize and complement phenotypic evaluations. In this context, Chapters 2 and 3 were focused on the probiogenomic and phenotypic analysis of two human-derived *Lacticaseibacillus rhamnosus* strains (VB1 and VB4), and a *Levilactobacillus brevis* strain (M3R3) isolated from sourdough, respectively. Comparative analysis highlighted genetic diversity at species level, allowing to identify the core genomes shared across all strains, as well as the accessory genomes unique to specific strains (Chen et al., 2022; Song et al., 2019). The obtained results established a connection between the *bsh* genomic profile and bile salt-associated phenotypes, demonstrating the functional importance of *bsh* gene presence associated with bacterial survival and deconjugation ability.

In line with the obtained results, all the three strains can be

considered potential probiotic candidates for their strong ability to modulate *in vitro* BAs profile. Among them, *L. rhamnosus* VB4 was selected for further analyses, as the most promising strain, characterized by a high deconjugation capacity, and notable resilience under bile salts conditions, although the unexpected reduction of the gene expression in presence of bile salt mixture.

In Chapter 4, the BSH potential of *L. rhamnosus* VB4 was extended using the SHIME® dynamic gut model. The strain showed high resistance to gastric acidity, pancreatic enzymes, and bile salts, maintaining substantial viability throughout gastrointestinal transit. Transcriptomic analysis on *bsh* gene shown active gene expression of the *bsh* gene, particularly into the small intestine, where BAs are secreted (Al-Dury & Marschall, 2018). Metabolomic profiling highlighted a clear deconjugation of conjugated bile acids in both groups: in the control group, deconjugation was attributed to the activity of the resident microbiota, whereas in the VB4-inoculated group, this effect was markedly enhanced, indicating an increased deconjugation capacity mediated by the strain. Nonetheless, these studies further studied gene expression profile in the upper GIT and colon fraction confirmed gene expression loss during the transit but confirming strain survivability and enhancement effect after microbiota interaction in the colon (T_{16h}). These results collectively reinforce the pivotal role of BSH activity as a functional trait linking probiotic colonization, and BAs metabolism. In agreement with Chapters 2-3, the in-depth characterization of *Lacticaseibacillus rhamnosus* VB4 in Chapter 4 provided robust evidence of gastrointestinal survivability, and strain-mediated modulation of BA pools under dynamic gut conditions.

In future studies, the same SHIME® workflow should be extended to *L. rhamnosus* VB1, and *L. brevis* M3R3, thereby confirming these findings within a dynamic intestinal model and enabling a more complete comparison of strain-specific probiotic potential.

The development of probiotics with BSH activity has gained considerable attention for their capacity to promote health, particularly in relation to cardiovascular through cholesterol-lowering effects. Among BSH-positive probiotics, *L. plantarum* LpLDL® represents a well-documented example, being commercially recognized for its cholesterol-lowering efficacy, which has been consistently validated by extensive experimental and clinical evidence (Keleszade et al., 2022; Zepeda-Hernàndez et al., 2025). These insights support the development of novel probiotics within a personalized therapeutic framework, optimized to specific health and clinical targets. In Chapter 5, in accordance with the previous finding this hypothesis was supported, proposing a preliminary screening to verify the cholesterol-lowering outcomes. The capacity of bacteria to interact with the intestinal epithelium represents a key determinant for sustaining probiotic functionality and maximizing their beneficial impact on the host (Ouwehand et al., 2001). The adhesion ability of VB1, VB4 and M3R3 strain combined with their BSH-positive tendency has been exploited to verify the cholesterol intake by intestinal cells. Although the obtained results are encouraging, a deeper exploration of the molecular pathways underlying these effects will be essential to consolidate and expand these findings. The observed cholesterol uptake by the strains confirms the hypocholesterolemic potential but not clarify the specific cholesterol-lowering mechanisms. As

previously outline in Chapter 1, lactobacilli can exert their hypocholesterolemic effects through multiple mechanisms. From this perspective, while all the three strains were confirmed to be BSH-positive, their capacity to reduce cholesterol absorption may also be mediated by additional pathways beyond bile salt deconjugation. To confirm the relationship, additional studies should include experimental approach, which employed the *bsh* genes knockout in lactobacilli. Wu and co-worker (2021) previously demonstrated the BSH-positive *L. plantarum* exhibited stronger adhesion to Caco-2 epithelial cells, compared to their BSH-deficient counterparts, thereby clarifying the contribution of BSH to host-microbiome interactions. Applying this approach to the investigated strains would offer a robust means of verifying whether the reduction in cholesterol uptake is directly attributable to BSH activity, to provide definitive mechanistic evidence linking BSH expression to the hypocholesterolemic effects of these strains.

Overall, this Ph.D. thesis support the potential of BSH-positive *L. rhamnosus* VB1, *L. rhamnosus* VB4, and *L. brevis* M3R3 as promising candidates for development of next-generation probiotic aimed at managing hypercholesterolemia. Beyond their biological characterization, the three strains could be considered from a translational perspective in order to expand their applicability towards the developing of a new functional food. At this regard, both human- and food-derived environments represents a valuable reservoir of microorganisms with probiotic potential, although the human gastrointestinal environment has traditionally considered the primary sources. Recently, also bacteria from fermented-food and food-associated ecosystem have gained increasing relevance for their

beneficial properties and safety, as well as a natural adaptation in processing conditions (Bernadeau et al., 2006; Terpou et al., 2022). Regulatory agencies, including EFSA and FDA, have reinforced their applicability, which recognized lactobacilli as safe for use in food application, assigning them the Qualified Presumption of Safety (QPS) and Generally Recognized as Safe (GRAS) status, respectively (O'Connel Motherway et al., 2024). In Chapters 2-3, VB4, VB1 and M3R3 were confirmed as safe according to QPS criteria. Although their origins differ, both human- and food-derived strains could be proposed for commercial use. Human-derived *L. rhamnosus* strains are well characterized, widely used in probiotic formulations, and known for their adaptability to various food matrices (Messaoudi et al., 2011; Gregoret et al., 2013; Rajoka et al., 2017). Conversely, food-derived *L. brevis* strains, in turn, may offer advantages for industrial scalability due to their natural adaptation to food environments, by improving fermentation performances, and strain-specific physiological benefits (Bao et al., 2020).

Nevertheless, further investigation will be required in the near future to better characterized these strains and verify its effectiveness particularly through: (i) *in vitro* study of the potential BSH-positive exploiting M-SHIME® model to evaluate the effect on gut microbiota and metabolome, from a fecal sample by a hypercholesterolemic donor, (ii) *in vivo* administration of BSH-positive strains as potential biotherapeutic candidates for reducing metabolic disorders, with a particular focus on mild hypercholesterolemia, (iii) technological validation in a pilot scale study could be performed, assessing strain-matrix compatibility to determine their suitability as adjunct cultures for functional food development.

References

1. Al-Dury, S., & Marschall, H. U. (2018). Ileal Bile Acid Transporter Inhibition for the Treatment of Chronic Constipation, Cholestatic Pruritus, and NASH. *Frontiers in pharmacology*, *9*, 931. https://doi.org/10.3389/fphar.2018.00931.
2. Bernardeau, M., Guguen, M., & Vernoux, J. P. (2006). Beneficial lactobacilli in food and feed: long-term use, biodiversity and proposals for specific and realistic safety assessments. *FEMS microbiology reviews*, *30*(4), 487–513. https://doi.org/10.1111/j.1574-6976.2006.00020.x.
3. Bao, W., Huang, X., Liu, J., Han, B., & Chen, J. (2020). Influence of Lactobacillus brevis on metabolite changes in bacteria-fermented sufu. *Journal of food science*, *85*(1), 165–172. https://doi.org/10.1111/1750-3841.14968.
4. Champagne, C. P., Gardner, N. J., & Roy, D. (2005). Challenges in the addition of probiotic cultures to foods. *Critical reviews in food science and nutrition*, *45*(1), 61–84. https://doi.org/10.1080/10408690590900144.
5. Chen, C., Yu, L., Tian, F., Zhao, J., & Zhai, Q. (2022). Identification of Novel Bile Salt-Tolerant Genes in *Lactobacillus* Using Comparative Genomics and Its Application in the Rapid Screening of Tolerant Strains. *Microorganisms*, *10*(12), 2371. https://doi.org/10.3390/microorganisms10122371.
6. Dong, Z., Yang, S., Tang, C., Li, D., Kan, Y., & Yao, L. (2025). New insights into microbial bile salt hydrolases: from physiological roles to potential applications. *Frontiers in microbiology*, *16*, 1513541. https://doi.org/10.3389/fmicb.2025.1513541.
7. Gregoret, V., Perezlindo, M. J., Vinderola, G., Reinheimer, J., & Binetti, A. (2013). A comprehensive approach to determine the probiotic

potential of human-derived Lactobacillus for industrial use. *Food microbiology*, *34*(1), 19–28. https://doi.org/10.1016/j.fm.2012.11.004.

8. Gupta, V., & Garg, R. (2009). Probiotics. *Indian journal of medical microbiology*, *27*(3), 202–209. https://doi.org/10.4103/0255-0857.53201.
9. Kang, M. H., Elnar, A. G., & Kim, G. B. (2025). Review on the Function, Substrate Affinity, and Potential Application of Bile Salt Hydrolase Originated from Probiotic Strains of *Lactobacillus*, *Bifidobacterium*, and *Enterococcus*. *Food science of animal resources*, *45*(2), 353–374. https://doi.org/10.5851/kosfa.2025.e1.
10. Keleszade, E., Kolida, S., & Costabile, A. (2022). The cholesterol lowering efficacy of Lactobacillus plantarum ECGC 13110402 in hypercholesterolemic adults: A double-blind, randomized, placebo controlled, pilot human intervention study. *Journal of Functional Foods*, *89*, 104939. https://doi.org/10.1016/j.jff.2022.104939.
11. Khare, A., & Gaur, S. (2020). Cholesterol-Lowering Effects of Lactobacillus Species. *Current microbiology*, *77*(4), 638–644. https://doi.org/10.1007/s00284-020-01903-w.
12. Messaoudi, M., Violle, N., Bisson, J. F., Desor, D., Javelot, H., & Rougeot, C. (2011). Beneficial psychological effects of a probiotic formulation (Lactobacillus helveticus R0052 and Bifidobacterium longum R0175) in healthy human volunteers. *Gut microbes*, *2*(4), 256–261. https://doi.org/10.4161/gmic.2.4.16108.
13. O'Connell Motherway, M., O'Connor, L., Smith, S., Bolton, D., Cormican, M., De Waal, T., Gutierrez M., Part A. M., Walsh, F., & Duffy, G. (2024). *Report of the Scientific Committee of the Food Safety Authority of Ireland on the Assessment of the safety of "probiotics" in food supplements* (Vol. 2, No. 4, p. 0050E). https://doi.org/10.2903/fr.efsa.2024.FR-0050.
14. Olas B. (2020). Probiotics, Prebiotics and Synbiotics-A Promising Strategy in Prevention and Treatment of Cardiovascular

Diseases?. *International journal of molecular sciences*, *21*(24), 9737. https://doi.org/10.3390/ijms21249737.

15. Ouwehand, A. C., Tuomola, E. M., Tölkkö, S., & Salminen, S. (2001). Assessment of adhesion properties of novel probiotic strains to human intestinal mucus. *International journal of food microbiology*, *64*(1-2), 119–126. https://doi.org/10.1016/s0168-1605(00)00440-2.
16. Rajoka, M. S. R., Mehwish, H. M., Siddiq, M., Haobin, Z., Zhu, J., Yan, L., Shao, D., Xu, X., & Shi, J. (2017). Identification, characterization, and probiotic potential of *Lactobacillus rhamnosus* isolated from human milk. *LWT*, *84*, 271-280. https://doi.org/10.1016/j.lwt.2017.05.055.
17. Song, Z., Cai, Y., Lao, X., Wang, X., Lin, X., Cui, Y., Kalavagunta, P. K., Liao, J., Jin, L., Shang, J., & Li, J. (2019). Taxonomic profiling and populational patterns of bacterial bile salt hydrolase (BSH) genes based on worldwide human gut microbiome. *Microbiome*, *7*(1), 9. https://doi.org/10.1186/s40168-019-0628-3.
18. Terpou, A., Dahiya, D., & Nigam, P. S. (2025). Evolving Dynamics of Fermented Food Microbiota and the Gut Microenvironment: Strategic Pathways to Enhance Human Health. *Foods (Basel, Switzerland)*, *14*(13), 2361. https://doi.org/10.3390/foods14132361.
19. Ventura, M., O'Flaherty, S., Claesson, M. J., Turroni, F., Klaenhammer, T. R., van Sinderen, D., & O'Toole, P. W. (2009). Genome-scale analyses of health-promoting bacteria: probiogenomics. *Nature reviews. Microbiology*, *7*(1), 61–71. https://doi.org/10.1038/nrmicro2047.
20. Wu, T., Wang, G., Tang, H., Xiong, Z., Song, X., Xia, Y., Lai, P. F., & Ai, L. (2022). Genes encoding bile salt hydrolase differentially affect adhesion of Lactiplantibacillus plantarum AR113. *Journal of the science of food and agriculture*, *102*(4), 1522–1530. https://doi.org/10.1002/jsfa.11487.
21. Zepeda-Hernández, A., Rosales-De la Cruz, M. F., Antunes-Ricardo, M., Ortega-Hernández, E., García-García, J. D., Garcia-Amezquita, L. E., &

García-Cayuela, T. (2025). Probiotic fermentation enhances the technological properties and health-promoting potential of skyr-type yogurts. *International Dairy Journal*, 106276. https://doi.org/10.1016/j.idairyj.2025.106276.

7 Annexes: Scientific Curriculum

7.1 Research and Professional Experience

- **2022-2025: Ph.D course in Agricultural, Food and Environmental Science**
  Department of Agriculture, Food and Environment (Di3A), University of Catania. Research project: "*Exploitation of probiotic strains with targeting cholesterol reduction for the formulation of functional foods*". Under the supervision of the Prof. Cinzia Lucia Randazzo
- **January 2022 – October 2022: Research grant – Associazione Italiana Contro Leucemie Linfomi e Mieloma (AIL)**
  Microbiology Laboratory, Department of Agriculture, Food and Environmental Science (Di3A), University of Catania. Project title: "Profilo immunitario e del microbioma dopo tre dosi di vaccinazione con cCovid-19 RNA nei disturbi linfoproliferativi"
- **October 2021 – December 2021: Research contract – ProBioEtna Srl**
  Microbiology Laboratory, Department of Agriculture, Food and Environmental Science (Di3A), University of Catania
- **October 2020 – March 2021: Post-graduated internship**
  Medical Molecular Microbiology and Antibiotic Resistance Laboratory (MMARLab), Department of Biomedical and Biotechnological Sciences (BIOMETEC), University of Catania

7.2 Education and Professional qualifications

- **June 2020: Professional Qualification as Senior Biologist, University of Catania**
  Membership of "Ordine dei Biologi della Regione Sicilia", Via Principe di Belmonte, 1H, Palermo (PA)
- **2017-2020: Master's degree in Health and Cellular-Molecular Biology (Curriculum Cellular and Molecular Biology) (LM-6)**
  Department of Biological, Geological and Environmental Sciences, University of Catania. Thesis: "Attività antimicrobica del Cell-Free supernatant (CFS) di *Lactobacillus* spp. verso patogeni Multi-drug Resistant". Under the supervision of Prof. Maria Santagati, Dr. Marina Scillato and Dr. Ambra Spitale
- **2013-2017: Bachelor's degree in Biological Sciences (L-13)**
- Department of Biological, Geological and Environmental Sciences, University of Catania. Thesis: "MicroRNA nel follicolo ovarico umano: caratterizzazione del loro ruolo nella regolazione della crescita e maturazione ovocitaria. Under the supervision of Prof. Cinzia Santa Di Pietro
- **2011: High School Diploma**
  Liceo Scientifico (P.N.I.) Quintino Cataudella, Scicli (RG)

7.3 Membership and Ids

- ORCID ID: https://orcid.org/my-orcid?orcid=0009-0005-1610-8811
- SCOPUS ID: 57536388400
  https://www.scopus.com/authid/detail.uri?authorId=57536388400

- ResearchGate: https://www.researchgate.net/profile/Gianluigi-Agolino?ev=hdr_xprf

7.4 Scientific contributions

- Agolino, G., Cristofolini, M., Ronsivalle, M. A., Cattivelli, A., Tagliazucchi, D., Caggia, C., Solieri, L., & Randazzo, C. L. (2025). Bile Salt Hydrolase Activity in the Food-Derived Strain Levilactobacillus brevis M3R3: Genomic and Functional Characterization. *Probiotics and antimicrobial proteins*, 10.1007/s12602-025-10810-0. Advance online publication. https://doi.org/10.1007/s12602-025-10810-0
- Vaccalluzzo, A., Agolino, G., Pino, A., Cristofolini, M., Tagliazucchi, D., Cattivelli, A., Caggia, C., Solieri, L., & Randazzo, C. L. (2025). Gastrointestinal Survivability of a BSH-Positive *Lacticaseibacillus rhamnosus* VB4 Strain and Its Effect on Bile Acid Deconjugation in a Dynamic In Vitro Gut Model. *Nutrients*, *17*(19), 3179. https://doi.org/10.3390/nu17193179
- Agolino G., Cristofolini M., Vaccalluzzo A., Tagliazucchi D., Cattivelli A., Pino A., Caggia C., Solieri L., & Randazzo C. L. (2025). Genome Mining and Characterization of Two Novel *Lacticaseibacillus rhamnosus* Probiotic Candidates with Bile Salt Hydrolase Activity. *Biomolecules*, *15*(1), 86. https://doi.org/10.3390/biom15010086
- Agolino G., Pino A., Vaccalluzzo A., Cristofolini M., Solieri L., Caggia C., & Randazzo C. L. (2024). Bile salt hydrolase: The complexity behind its mechanism in relation to lowering-

cholesterol lactobacilli probiotics. *Journal of Functional Foods*, *120*, 106357. https://doi.org/10.1016/j.jff.2024.106357

- Pino, A., Nicosia, F. D., Agolino, G., Timpanaro, N., Barbagallo, I., Ronsisvalle, S., Caggia, C., & Randazzo, C. L. (2022). Formulation of germinated brown rice fermented products functionalized by probiotics. *Innovative Food Science & Emerging Technologies*, *80*, 103076. https://doi.org/10.1016/j.ifset.2022.103076
- Pino, A., Benkaddour, B., Inturri, R., Amico, P., Vaccaro, S. C., Russo, N., Vaccalluzzo, A., Agolino, G., Caggia, C., Miloud, H., & Randazzo, C. L. (2022). Characterization of *Bifidobacterium asteroides* Isolates. *Microorganisms*, *10*(3), 655. https://doi.org/10.3390/microorganisms10030655

7.5 Conference proceedings

- Agolino G., Cristofolini M., Ronsivalle M. A., Tagliazucchi D., Cattivelli A., Solieri L., Caggia C., & Randazzo C. Genomic and functional insight into the Bile Salt Hydrolase activity of the food-derived *Levilactobacillus brevis* M3R3 strain. 8th Internation Conference on Microbial Diversity "Microbial Diversity for Empowering the Ecological Transition: Research, Innovation, and Technological Transfer". September 23-26, 2025 – Rome, Italy
- Agolino G., Vaccalluzo A., Cristofolini M., Pino A., Tagliazucchi D., Cattivelli A., Solieri L., Caggia C., & Randazzo C. Comprehensive genome profiling and characterization of Bile Salt Hydrolase activity in two promising *Lacticaseibacillus rhamnosus* probiotic strains. 8th Internation Conference on

Microbial Diversity "Microbial Diversity for Empowering the Ecological Transition: Research, Innovation, and Technological Transfer". September 23-26, 2025 – Rome, Italy Cristofolini M., Agolino G., Ronsivalle M., Cattivelli A., Tagliazucchi D., Pino A., Vaccalluzzo A., Caggia C., Solieri L., & Randazzo C. Food-derived *Levilactobacillus brevis* M3R3 as an emerging probiotic: genomic and functional study of Bile Salt Hydrolase activity. 15th National Conference on Biodiversity & 2nd International Conference on Mediterranean Biodiversity "Biodiversity in the XXI century: new paradigms for new challenges", June 3-6, 2025 – Perugia, Italy

- Montorsi A., Fochesato A., Nasuti C., Barigazzi A., Agolino G., Menghini M., Cortiello M., Bellameche F., Modica F., Baroncelli R., Collina M., Solieri L., Stefani E., & Giovanardi D. Identification and characterisation of microbial isolates from pear carposphere and their possible role in brown spot disease management. XXIX Congress SIPaV "New challenges in Plant Pathology between sustainable crop production and climate change". September 9-11, 2024 – Trieste, Italy
- Agolino G., Solieri L., Pino A., Caggia C., & Randazzo C. L. Evaluation of Bile Salt Hydrolase Activity in promising probiotic strains with potential cholesterol-lowering activity". 7th Internation Conference on Microbial Diversity "Advances in Microbial Diversity". September 26-29, 2023 – Parma, Italy
- Bosco G., Pino A., Sanfilippo R. R., Vaccalluzzo A., Agolino G., Caggia C., & Randazzo C. L. Antagonistic activity against foodborne and human pathogens, biofilm formation and antiadhesion activity from different source. 7th Internation

Conference on Microbial Diversity "Advances in Microbial Diversity". September 26-29, 2023 – Parma, Italy

7.6 Training in national or international universities and/or research institutions

I visited as a Ph.D. student two important institution within my Ph.D. research.

I have been abroad from June to December 2023 at the Laboratory of Yeast and Bacteria Biotechnology, at the Department of Life Science, University of Modena and Reggio Emilia (Italy) under the supervision of the Professor Lisa Solieri. During this part of the Ph.D. project, I significantly expanded my expertise in the selection of probiotic strains from both phenotypic and genomic perspectives. Specifically, I performed a series of assays to evaluate strain survivability under different bile salt concentrations and conducted metabolomic analyses to assess their capacity to deconjugate bile salts in the growth medium. In parallel, I applied several PCR-based techniques to investigate, at the molecular level, the presence of genes associated with bile salt hydrolase (BSH) activity. These analyses were further implemented by comparative genomics, allowing the comparison of the phylogenetic distance gene structure across different lactic acid bacteria species and supporting the interpretation of strain-specific functional traits. However, I was also involved in a second project focused on the isolation and evaluation of the antagonistic activity of bacteria and yeasts, intended for the eradication of *Stemphylium vesicarium*, a pathogenic fungus implicated in brown spot disease of Abate pears.

During my second training I spend six months (from January to

July 2025) at the University of Helsinki (Department of Bacteriology and Immunology, Human Microbial Research Program 'HUMI', Finland), under the supervision of the Professor Reetta Satokari. Specifically, I performed experimental analysis, in order to evaluate the interactions between BSH-positive strains and both human intestinal epithelial cell lines and mucosal surfaces, focusing on the strains capacity to reduce cholesterol uptake in intestinal epithelial cells, thereby providing preliminary evidence of their hypocholesterolemic potential. In addition, the strains were tested for their adhesion capacity, as a fundamental probiotic trait that supports persistence within the gastrointestinal tract.

7.7 Attended Workshop, Courses, Seminars

7.7.1 Attended Workshop

- 29th Workshop on the Developments in the Italian Ph.D. research on Food Science, Technology and Biotechnology, September 10-12, 2025
- 6th Joint Meeting of Agriculture-oriented Ph.D. Programs UniCT, UniFG and UniUD, September 30 – October 4, 2024, Lesina (FG), Italy
- 28th Workshop on the Developments in the Italian Ph.D. research on Food Science, Technology and Biotechnology, September 18-20, 2024, Catania, Italy
- 5th Joint Meeting of Agriculture-oriented Ph.D. Programs UniCT, UniFG and UniUd, September 25-28, 2023, Catania, Italy

7.7.2 Attended Courses

- "Introduction and recent trends on experimental approaches for Food Science":
  - "Introduction and recent trends on experimental approaches for Food Microbiology", held by Prof. Alessandra Pino, April 11-12, 2024
  - "The potential of agri-food by products to enhance the Food Quality", held by Prof. Lucia Parafati, May 3 and 7, 2024
- "General and Multivariate Statistical Analysis", held by Prof Maria Raimondo, March 7, 11, 14 and 18, 2024
- "Introduction to a literature review process: overview and guidelines", held by Prof. Giuseppe Antonio DI Vita, February 12 and 19, and March 18, 2024
- "Managing biological data with R: application for plants and fruit tree species", January 22-26, 2024
- "ICT for participatory methods, citizens science and disseminating, research", held by Prof. Teresa Graziano. July 10-12, 2023
- "Scientific publishing in the peer review era", held by Prof. Antonio Biondi and Michele Ricupero, June 23 and 27, 2023
- "Writing a scientific review article", held by Prof. Daniela Spina and Gaetano Chinnici, June 9 and 13, 2023
- English course for Ph.D. students, organized by C.L.A. (Centro Linguistico d'Ateneo), March 8 – May 26, 2023

7.7.3 Attended Seminars

- Summer School: "Eco-friendly Strategies for Sustainable Agriculture and Environmental Resilience: Bio-Based Products Application". June 27-28, 2024, Catania (Italy)

7.8 Teaching activities

- Didactic laboratory tutor for the course "Microbiologia dei prodotti alimentari", bachelor's degree in Catering and logistic science and technology of the Mediterranea food (L-26)
- Didactic laboratory tutor for the course "Microbiologia degli alimenti funzionali", bachelor's degree in Food science and technology (L-26)